MESOZOIC ALKALINE VOLCANISM AND MANTLE EVOLUTION OF THE SOUTHWESTERN SÃO FRANCISCO CRATON, BRAZIL.

Luiz Augusto Bizzi

Thesis presented for the degree of
DOCTOR OF PHILOSOPHY
in the Department of Geological Sciences
University of Cape Town
1995.

To my brother, Serginho.

Table of Contents

List of Figures

List of Tables

List of Abbreviations

AFFZ	-	Agulhas-Falklands/Malvinas Fault Zone
BSE	-	Bulk Silicate Earth
CFB	-	Continental Flood Basalts
CHUR	-	Chondritic Uniform Reservoir
DMM	-	Depleted Mantle Material
EMI/EMII	-	Enriched Mantle I/II
EFZ	-	Equatorial Fault Zone
GIS	-	Geographic Information System
HIMU	-	High $^{238}U/^{204}Pb$
MBL	-	Mechanical Boundary Layer
MES	-	Maximum Entropy Scaling
Mg#	-	Magnesium Number
MORB	-	Mid Ocean Ridge Basalts
MSWD	-	Mean Sum of the Weighted Deviates
NAA	-	Neutron Activation Analysis
OIB	-	Ocean Island Basalts
P & T	-	Pressure and Temperature
Pers.comm.	-	Personal Communication
PGE	-	Platinum Group Elements
HTPGE	-	High-temperature Platinum Group Elements
LTPGE	-	Low-temperature Platinum Group Elements
PREMA	-	Prevalent Mantle
REE	-	Rare Earth Elements
RGWR	-	Rio Grande-Walvis Ridge
$^{87}Sr/^{86}Sr_i$	-	Initial Isotopic Ratios
T_{CHUR}	-	Neodymium Model Age Relative to Chondritic Reservoir
T_{DM}	-	Neodymium Model Age Relative to Depleted Mantle
TBL	-	Thermal Boundary Layer
Wt%	-	Weight Percent
XRF	-	X-Ray Fluorescence

Abstract

This thesis explores the nature of the subcontinental lithosphere underlying the southwestern margin of the São Francisco craton and the relation of variations in the petrochemistry of kimberlites and related alkali igneous rocks to variations in age, thickness and thermodynamic history of their continental lithospheric hosts. The São Francisco craton is a mid- to late-Archean basement granite-greenstone terrain flanked to the west by the Proterozoic Tocantins Province (Almeida, 1977; Almeida et al., 1981). New Rb-Sr and Sm-Nd data are presented for both on- and off-craton crustal rock sequences. The ultramafic greenstone association of the Rio das Velhas Supergroup yields 3.2 Ga Rb-Sr and Sm-Nd ages, in agreement with widespread 3.2 Ga old zircons from the area. Granitic gneiss and juvenile granitoids associated with the greenstones in the Congonhas area give a Transamazonian 2128 Ma Rb-Sr age, which is in agreement with a published 2124 Ma zircon age. Further west, syntectonic granitoids and metabasalts from the Araxá Group define a 711 Ma Rb-Sr isochron. This latter age is interpreted as a Sr-isotope re-homogenization related to the development of the Brasília orogenic and foreland thrust belt. A 823 Ma Sm-Nd errorchron indicate that these rocks may be coeval to the felsic volcanism of the Araxá Group which was recently dated at 794 Ma by zircon work (Pimentel et al., 1991). Further to the west still, combined samples from the Niquelândia mafic-ultramafic igneous complex and associated granitic basement rocks yield a 1.26 Ga Rb-Sr isochron, which is best interpreted as a metamorphic age. Crystallization ages of the crustal sequences decrease and ϵ_{Nd} *values increase with increasing distance westward from the Archean craton margin. The isotopic characteristics are consistent with a model which requires that large volumes of crust, derived in the Proterozoic from mantle reservoirs similar to the sources for modern oceanic basalts, were accreted onto the pre-existing Archean nucleus during the Brasiliano orogenic event.*

The Proterozoic rocks which overly and flank the São Francisco craton margin are intruded by Cretaceous kimberlites, olivine melilitites, tuffaceous diatremes and carbonatite complexes. Eight of the freshest representatives of the alkaline magmatism are described in terms of their age and mode of emplacement, petrography and whole-rock geochemistry. Kimberlites and kimberlite-

related rocks have compositions similar to that of primary liquids derived from garnet peridotites. The kimberlite magmas are suggested to have resulted from entrainment of enriched lithosphere in plume-derived small-volume melts. The source character of the kimberlitic rocks is similar to that of carbonatites and other alkalic volcanics in the area, but is dissimilar to that of kimberlites elsewhere in the world. Compared to the source of micaceous Group II kimberlites, both the isotopically transitional kimberlites from southern Africa and the Brazilian kimberlites originated from sources with lower time-averaged Rb/Sr and Nd/Sm. Compared to the other rock types investigated, the lower time-averaged Rb/Sr, Nd/Sm and Pb/U ratios of the Brazilian kimberlites might be related to small but significant amounts of a distinctive high $^{238}U/^{204}Pb$ (HIMU) component in these kimberlites.

Major and trace elements of the alkalic rocks change with petrographic character towards more evolved compositions along liquid evolution paths indicative of shallow-level, olivine-dominated crystal fractionation. A restricted range of isotopic signatures, and the absence of any correlation between $^{87}Sr/^{86}Sr$ and 1/Sr, suggest that the shallower alkalic rocks were probably derived by melting of a light-REE enriched lithospheric mantle source rather than through crustal contamination of asthenospheric melts. Compared to the kimberlites, the other alkalic rocks studied have a greater lithospheric component. The Nd isotope characteristics of such inferred lithospheric component are compatible with an origin closely related to the evolution of the Proterozoic rocks of the Tocantins Province. The average isotope composition of the studied rift-related volcanics may be taken as an approximation of the "Enriched Mantle I" (EMI) component previously identified as an extreme composition in the Walvis ridge basalts (Richardson et al., 1982). The source of the alkaline occurrences, the source of the high-Ti basalts of the northern Paraná Basin, and the source of some Ocean Island Basalts (OIB) with Dupal signatures in the South Atlantic (viz. the Walvis Ridge basalts) are all isotopically similar to each other and closely related to this EMI-like component.

The variation in isotope composition of the Brazilian kimberlites and shallower derived alkalic rocks is proposed to represent mixing between variable amounts of deep-derived HIMU-like components and shallower, volumetrically dominant, EMI-like lithospheric mantle materials. The

HIMU-, and EMI-like signatures in particular, are envisaged to be concentrated in laterally extensive but vertically distinctive portions of the sub-continental mantle beneath the SW São Francisco craton margin. Isotope variations are complemented by a distinct range of Platinum Group Element (PGE) signatures in the studied rocks. The overall geochemical variation can be modelled by a process of physical assimilation and dilution of a PGE-rich material from the EMI-like upper mantle lithosphere by PGE-poor small volume melts with HIMU-like characteristics.

The geochemical similarities of the source of the Mesozoic Minas Gerais alkalic volcanics to the source of the HTZ Paraná basalts emplaced along the craton margin are credited to enriched to EMI-like lithospheric mantle materials which were involved in the generation of both rock sequences and, to a lesser extent, in the generation of the Minas Gerais kimberlites. Whilst the isotope evidence provide further evidence that discrete large-scale geochemical domains existed in Southern Gondwana, it is here suggested that such domains were not necessarily related to ancient lithospheric chemical heterogeneities or bound by ancient structural features, but rather that these domains reflect mixing processes that can be ascribed to specific geodynamic mechanisms. The similarity of the inferred source of the studied occurrences to the source of some OIB with Dupal signatures in the South Atlantic is ascribed to mantle processes during which overthickened Brazilian lithosphere was delaminated and contaminated a belt of South Atlantic asthenosphere which is now erupting at hotspot islands and which, in turn, may contaminate nearby sections of the Mid-Atlantic ridge.

Peaks of Mesozoic magmatism along the southwestern margin of the São Francisco craton were contemporaneous with changes in plate vectors during the opening of the South Atlantic. It is suggested that changes in within-plate stress fields and associated fault reactivation along old lithospheric shear zones were the main control of sites of intraplate alkaline magmatism such as that along the southwestern São Francisco craton margin.

Preface

This thesis was part of a project conceived to assess the nature of the subcontinental lithosphere underlying the southwestern margin of the São Francisco craton. This was attempted by integrating the source character of Cretaceous kimberlites and related igneous rocks of that region with the isotope characteristics of the local continental crust, both on- and off-craton; and by evaluating the thermo-tectonic evolution of the craton margin (which is the major focus of a companion thesis being prepared by Franciscus Baars). The economic rational of the project is rooted in the recovery of large diamonds in the Minas Gerais state of Brazil for over two centuries. The stones are normally associated with sediments (Tompkins & Gonzaga, 1989), and it has been more than a hundred years since Campos (1891) first suggested that a primary kimberlitic source should exist in the southern São Francisco craton. Hundreds of kimberlites and kimberlite-related rocks have now been found in the area (e.g. Bizzi et al., 1993) but, to date, the inferred primary source for the diamonds has still not been located.

The main objective of this thesis was to investigate the source characteristics of both kimberlites and the upper-Cretaceous Mata da Corda alkaline volcanics using whole-rock isotope geochemistry. The close resemblance of some of these volcanics to kimberlites has been the subject of debate for almost 100 years, since it was first pointed out by Hussak (1894); and whole-rock isotope work has never been attempted before on Brazilian kimberlites. Once the kinship of kimberlites and the Mata da Corda volcanics was verified, I *first* wanted to investigate what processes could have generated the different rock types. *Secondly*, I wanted to see what sort of isotopic variations occur along the craton margin; and what the relation between the crust and the underlying sub-continental lithosphere along the craton margin might be. *Thirdly*, I wanted to investigate the possible relationship of the upper-Cretaceous volcanics to the Jurassic volcanics of the Paraná basin, and how, on a bigger scale, these volcanic sequences might reflect geodynamic processes related to the opening of the South Atlantic.

During the first nine months of 1989 I selected and visited forty-two kimberlite or kimberlite-related occurrences distributed along the western margin of the craton. From these, eight localities representing the freshest possible material from a range of different alkalic ultrabasic rock types were chosen and studied in detail. In July 1989 Dr. Craig Smith (of the Bernard Price Institute of Geophysics of the University of the Witwatersrand) visited the selected localities, and complementary sampling for isotope work took place. The study of these intrusives, which are distributed along a 200 km E-W traverse roughly perpendicular to the western São Francisco craton margin, was accompanied by a series of regional scale E-W traverses in which the major tectonic and structural features were analyzed. These traverses were supplemented in March-August 1991 during field work with Franciscus Baars and Prof. Maarten J. de Wit (of the Department of Geological Sciences of the University of Cape Town), when sampling of the crustal sequences was carried out for the isotope work.

Analytical work started in September 1989. Isotope analysis of the alkalic rocks was carried out at both the Bernard Price Institute of Geophysics, University of the Witwatersrand (Rb-Sr dating of mica separates, and Rb-Sr and Sm-Nd on whole rock samples); and at the Radiogenic Isotope Facility of the University of Cape Town (U-Pb and Pb-Pb on whole-rock samples). The same powdered samples were used for X-Ray Fluorescence (XRF) at the University of Cape Town; and Neutron Activation Analysis (NAA) at the Schonland Centre for Nuclear Research, University of the Witwatersrand. Noble metal concentrations were determined by submitting the same rock powders to combined nickel sulphide fire-assay and NAA at the Schonland Centre for Nuclear Research, University of the Witwatersrand. This NAA work was performed in cooperation with Iain McDonald and some of the results of that have also been presented in his PhD thesis which was completed in 1994. Isotope analysis of the rocks from the crustal sequences (Rb-Sr and Sm-Nd on whole-rock samples) was performed at the Radiogenic Isotope Facility of the University of Cape Town. Electron microprobe work was undertaken at the University of Cape Town on polished thin sections prepared by the Anglo American Research Laboratories in Johannesburg. Samples of the crustal sequences were prepared for single zircon work by the SHRIMP (Secondary High Resolution Ion Micro Probe) in Canberra, but the analyses were not completed in time for inclusion in this thesis. Computer laboratory work was

carried out at the Remote Sensing Unit of Anglo American Corporation, in Johannesburg (imagery interpretation of TM-Landsat on a VAX-Mainframe Network); and at the Centre for Interactive Graphical Computing of the University of Cape Town (GIS and computer graphics on Unix-based workstations).

This thesis has been organized in five chapters. In the **first chapter**, an overview of the tectonic framework of the São Francisco craton and the Tocantins Province is provided, together with comments on the geology of selected areas. New Sr and Nd data on crystalline basement rocks situated both on- and off-craton are presented. The source characteristics of the crustal sequences were tentatively categorized in a framework of the lithospheric evolution of the craton and its western margin and integrated with existing geologic information in an attempt to delineate chrono-tectonic provinces. The preliminary Nd isotope evolution models attempted for this segment of continental crust, however, have been severely restricted by the lack of reliable age control and will have to be reviewed when the U/Pb zircon age data in preparation becomes available. The main objective of this chapter is to provide an overview of the basement characteristics into which the Mesozoic alkaline rocks, described and discussed in the next two chapters, were emplaced.

The **second chapter** deals with the petrography, age and mode of emplacement, bulk composition and isotope geochemistry of the selected kimberlites and Mesozoic alkaline volcanics which intruded the western margin of the São Francisco craton. In this chapter I present evidence that a common enriched lithospheric source was involved in the generation of all the different rock types in the area; and that the source of the Brazilian kimberlites and alkaline volcanics represented in this study is dissimilar to the sources of kimberlites elsewhere in the world.

The focus of the **third chapter** is on the isotopic and Platinum-Group-Elements (PGE) variation of the alkalic volcanics. Source characteristics of the alkalic rock types are contrasted with evidence for fractionation and interaction with the enriched sub-continental lithosphere. Despite evidence for mantle mixing, the definitive geochemical characterization of end-members involved

in the mixing process remains ambiguous because of the relatively restricted range of isotopic signatures of the rocks.

The first three chapters incorporate discussions of large-scale mantle processes, hot-spot activity and heat flux of continental-scale significance during the late Mesozoic. In the **penultimate chapter**, a geotectonic overview is attempted in order to evaluate the significance of the Brazilian data at a larger scale. Some comparisons are made with the Kaapvaal craton of Southern Africa. Aspects that may shed some light onto the significance of the similar isotope characteristics of the source of the alkaline occurrences emplaced along the southwestern margin of the São Francisco craton, the source of the high-Ti basalts of the northern Paraná basin, the source of kimberlites and carbonatites emplaced along marginally cratonic settings, and the source of some OIB with Dupal signatures in the South Atlantic are discussed.

Concluding remarks are presented at the end of each chapter in an attempt to review and interrelate several of the ideas which have been developed. A summary of conclusions is presented in **chapter five**.

Acknowledgements

I am indebted to Prof. Maarten J. de Wit from the Department of Geological Sciences of the University of Cape Town; and Dr. Craig Smith from the Bernard Price Institute of Geophysics, University of the Witwatersrand, my co-supervisors, who provided an excellent and uniquely inspiring blend of advisory support throughout the Project. Both were always available for discussion and comment, and were undoubtly a most important factor in this work. Both visited the field area in Brazil, and both painstakingly and critically reviewed the manuscript for science and English grammar a number of times. I am specially thankful to Maarten for allowing me to use some preprints and unpublished diagrams in Chapter IV.

Anglo American Corporation provided full financial and logistical support. For this opportunity, and for their support at various times, I would like to acknowledge Mr. Roy Edwards, Dr. Roger Clement and Mr. Gus Edwards, consulting geologists for diamonds; and Mr. Jeffrey M. Watkins, managing director for Sopemi in Brazil. Mr. John Oglesby, former managing director for Sopemi, is gratefully acknowledged for his input in the early stages of this project. Mr.Osvaldo França and Mr.Milton França (Sopemi) are thanked for their help in the initial stages of the field work; and Mr.Luis C. de Assis and Manfred Baecker from Mineração Catalão are thanked for providing fresh drill-core samples and for a crash-course in carbonatite geology. Members of the Diamond Research Group in the Anglo American Research Laboratories Pty and of the Remote Sensing Unit of Anglo American Corporation are acknowledged for their technical support. Special thanks go to Mr. Mike Skinner, Dr. John Bristow, Dr. Jock Robey, Dr. Chris Hatton, Mr. Mathew Fields, Dr. Lilo de Gasparis, Dr. Michael Brown and Dr. Barbara S. Smith. Bill McKechnie and his staff in De Beers, Kimberley, are thanked for their efficient logistical support.

A number of students and Faculty members from the Department of Geological Sciences at the University of Cape Town were instrumental in bringing this PhD to fruition. I am indebted to

Dr. Richard Armstrong for his advice during the isotope work and for his continuous support from the very beginning of the project. The close collaboration with the PhD students Mr. Franciscus Baars and Dr. Iain McDonald proved to be one of the highlights in this project. I am most thankful to both of them for fruitful discussions and camaraderie, for providing samples for analyses (Frankie), and for the analysis of PGE (Iain). Mr.Russel Herbert and Ms. Erminia Vitali from the Centre for Interactive Graphics are thanked for their skillful advice and help in computers while thoroughly crash-testing Intergraph to produce the color plots in this thesis. The development of the ideas has been aided by conversations with many of the staff members of UCT. Special thanks go to Dr. Marian Tredoux for reviewing a draft written on the PGE data. Prof. Anton LeRoex and Dr. Dave Reid are thanked for reviewing and discussing manuscripts submitted for publication and the external examiners are thanked for constructively criticizing an earlier version of this thesis.

My best friend and wife has had a tremendous impact on the successful completion of this Project. During the approximately three years spent in South Africa, Edi not only managed and organized most aspects of life not related to the preparation of the manuscript but also did a superb job developing, from scratch, the graphics and GIS images used in this thesis. I would like to thank her, my parents Augusto and Annayr, and my brother Serginho for inspiration and support.

Chapter I

Aspects of the geologic evolution of the SW São Francisco craton.

I.1 - INTRODUCTION

The São Francisco craton (Almeida, 1977) is a mid- to late-Archean granite-gneiss and granite-greenstone terrain. This craton, arguably, represents only a remnant of a larger Archean crustal block called the Paramirin craton (Almeida et al., 1981), which has also been defined by gravity data (e.g. Haralyi and Hasui, 1982). The southern boundary of the São Francisco craton is marked by a steep, seismically active, strike-slip fault system. Its western margin is overprinted by Brasiliano-age (~ 0.5 - 0.8 Ga) tectonism and is overlain by a thin-skinned folded thrust belt of allochthonous to para-allochtonous units. The thin-skinned fold and thrust belt (the Brasília belt) is coupled to an external Proterozoic orogenic zone (the Uruaçu belt) of metasediments, orthogneisses, metavolcanic and metaplutonic assemblages of various ages (see Figure I.1).

Further to the west lies the Goiás Median massif, which comprises a complex and still poorly understood association of crystalline rocks of various ages. Recent geochronological data have been used to delineate several sub-provinces in this massif, ranging from Archean to NeoProterozoic (Pimentel et al., 1991; Fuck et al., 1987). The complex may thus represent a collage of crustal segments of various ages which collided during the Brasiliano orogenesis (Marini et al., 1984). The western Goiás area is characterized by a metamorphic basement composed largely of volcano-sedimentary arc assemblages and orthogneisses (Pimentel et al., 1991; and references therein). The Brasiliano age orogenic zone in the western Goiás area is linked with the southern segment of the Uruaçu and Brasília fold belts (Figure I.1), which represents a NeoProterozoic fold and thrust belt - foreland basin association formed along the craton margin. The entire Proterozoic orogenic zone to the west of the São Francisco craton has been collectively named the Tocantins Province by Almeida et al. (1981).

Kimberlite diatremes intruded along the southwestern margin of the São Francisco craton contain mantle, lower crustal and upper crustal xenoliths (chapter II). Geothermobarometry of these xenoliths yields fossil geotherms that are relatively cool and indicate an underlying mantle source that transfers heat by conduction, not convection. Some of the kimberlites in the study area are diamondiferous (e.g. Gonzaga & Tompkins, 1991). The presence of diamonds may indicate that at least some stones formed early in the development of the lithosphere were able to survive in the mantle beneath the craton margin until being "sampled" by the Mesozoic kimberlite magmas. Such preservation of the diamonds is possible only if the refractive, relatively cool and low-density mantle root attached to the craton remained unaffected by later re-heating and excessive tectonic reworking during the Brasiliano/Pan-African orogeny. At surface, however, the area intruded by the kimberlites has been extensively overprinted by Brasiliano-age thin-skinned tectonism. The allochthonous to para-allochthonous terrains are believed to cover extensive parts of the western São Francisco craton (Baars, in prep.). The cratonic domain may thus extend further to the west beneath these "thin skinned" tectonic terrains than recognized from surface features. Gravity and magnetic observation indicate that this may indeed be so (Haralyi & Hasui, 1982; Pires, 1986). The nature and extent of the buried marginally cratonic areas, however, have not yet been well constrained because of the lack of geochronological data. U-Pb single zircon isotopic data is available for a number of localities from the southern portion of the craton, but the coverage is still very sparse.

The evolution of the São Francisco craton margin can be best understood in a framework of continental growth, reworking and partial destruction. It is generally accepted that continents grow through a combination of subduction-related additions of new materials from the mantle and amalgamation of pre-existing lithospheric fragments (e.g. de Wit et al., 1992; and references therein). During such major episodes of orogenic compression, volcanism along the continental margins and, to a much lesser extent, along continental rifts, generates buoyant refractory mantle which is resistant to convective recycling. Lateral accretion of this material above subduction zones or by diapirism above descending slabs provides a mechanism for thickening of continental areas by addition of mantle lithosphere (e.g. Jordan et al., 1989). Competing against these constructive processes, however, are destructive processes and instabilities associated with

extension and heating during subsequent orogenic cycles. Thinning of the continental areas can be attained during continental extension which may, eventually, allow for convective disruption and thermal erosion of the mantle lithosphere. The "diamond fertility" of any refractory keel attached to old cratonic blocks like the São Francisco craton will depend on the balance of these two processes at a given geologic time when the lithospheric section is cross-cut by deeply derived melts.

The aim of this chapter is to better understand the thermo-tectonic evolution of the western margin of the São Francisco craton in order to access its role in the genesis of Mesozoic mantle-derived magmas and in the preservation of diamonds through the Brasiliano tectono-thermal event. New whole-rock Nd data obtained from samples collected for U/Pb zircon determinations have tentatively been incorporated into models of crustal evolution. Strictly speaking, this exercise would only be valid once the emplacement ages have been constrained by the zircon data, which is still outstanding. In the absence of these ages, subsets of the Sr and Nd data were used in combination with field relations to roughly establish the possible correlation of the studied rock sequences to zircon age data already available in the literature. It must be emphasized that the "ages" determined in this Rb-Sr and Sm-Nd whole rock study are considered to have almost no geochronological value by themselves, but that those considered in the exercise are supported by U/Pb zircon ages published elsewhere.

I.2 - REGIONAL GEOLOGY, TECTONIC SETTING AND ISOTOPIC AGES

In this chapter, four areas will be discussed in some detail. First, the greenstone belts and associated granitoids of the southern São Francisco cratonic core are dealt with. The other three areas, all of which are part of the Tocantins Province, are the Arai Group rhyolites and associated granitic intrusions; the NeoProterozoic gneiss and metavolcanics in western Goias and western Minas Gerais regions; and the Niquelandia mafic-ultramafic igneous complex. The distribution of tectonic elements and the location of those areas to be discussed in the text are summarized in Figure I.1.

Figure I.1 - Tectonic framework of the São Francisco craton and the Tocantins Province with indication of regions discussed in the text. Geology, craton boundaries and domain boundaries within the Tocantins Province after Schobbenhaus et al. (1984). The thin-skinned fold and thrust Brasilia belt is coupled to the Uruaçu belt, an external Proterozoic orogenic zone comprised of metasediments, orthogneisses, metavolcanic and metaplutonic assemblages of various ages. The Goiás Massif comprises an association of crystalline rocks of various ages. Those three orogenic zones (numbers 6, 4 and 2 in the inset) are collectively denominated the Tocantins Province (Almeida et al., 1981). The limits of the Brasiliano-age (0.8 - 0.5 Ga) tectonism along the western cratonic margin also mark a distinct change in age of basement from >2.0 Ga to <2.0 Ga from southern São Francisco craton to southern Tocantins domains. Note also the extension of Mesozoic covers and the relative position of basement inliers.

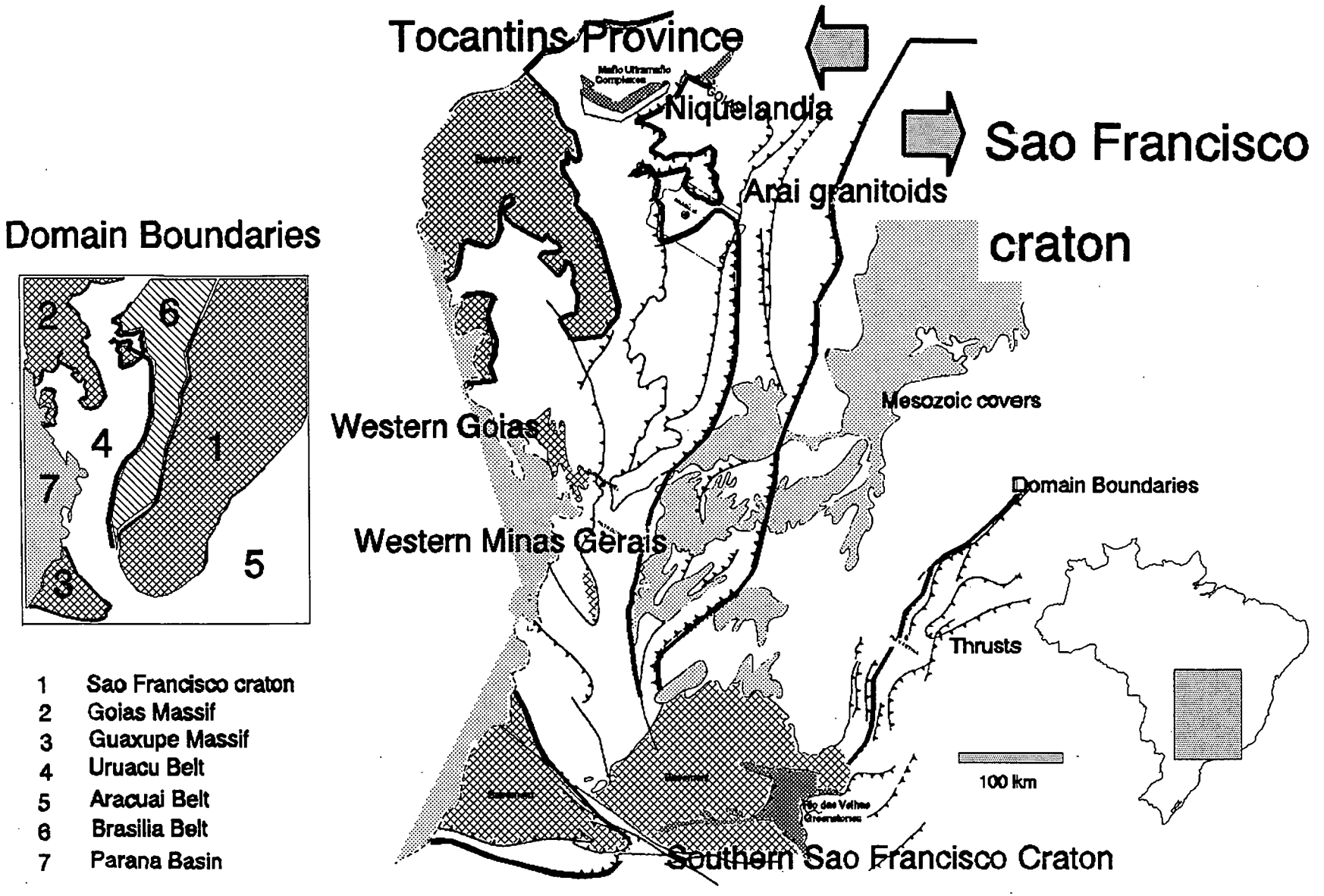
Domain Boundaries
2
6
4
1
7
5
3
1 Sao Francisco craton
2 Goias Massif
3 Guaxupe Massif
4 Uruacu Belt
5 Aracuai Belt
6 Brasilia Belt
7 Parana Basin
Tocantins Province
Niquelandia
Sao Francisco craton
Arai granitoids
Western Goias
Western Minas Gerais
Mesozoic covers
Domain Boundaries
Thrusts
100 km
Southern Sao Francisco Craton

I.2.1 - The southern São Francisco craton

The Archean basement in the southern portion of the São Francisco craton constitutes a nucleus of about 10 000 km^2 (Teixeira et al., 1987). Rb-Sr, K-Ar and Pb-Pb isotopic data (Teixeira, 1982; Teixeira et al., 1987; and references therein) indicate that episodes of crustal formation were dominant during mid- to late-Archean (3.3-2.6 Ga) and ProtoProterozoic (2.4-2.1 Ga). Episodic orogenesis in the periods 2.2-1.7, 1.3-1.1 and 0.9-0.45 Ga are termed the Transamazonian, Uruaçuano and Brasiliano thermo-tectonic cycles, respectively. Final cooling below 100°C has been established by apatite fission track dating to 850 Ma and 550 Ma in the internal areas and along the southwestern margin of the craton, respectively (Teixeira et al., 1985). Meso- to NeoProterozoic extensional tectonics produced broad asymmetrical extended basins along the western margin of the craton. The NeoProterozoic Macaúbas and basal portion of the Bambuí Groups were deposited during an extensional regime, whereas the overlying Tres Marias Formation reflects later inversion of the tectonic stresses during the Brasiliano cycle (e.g. Kiang et al., 1988).

i) Mid-Archean basement granitoids

Basement rocks in the cratonic area are predominantly composed of medium grade granitic gneisses and amphibolites. Inherited zircon ages indicate that the basement of the Moeda Complex in the Bonfim area (see Figure I.2) is at least as old as 3.32 Ga (Carneiro et al., in press). Magmatic zircon grains from felsic volcanics from Caeté (about 40 km NE from the Bonfim area) give an age of 3.03 Ga (Machado et al., 1989); and inherited zircons from the felsic volcanics of the Nova Lima Group in Piedade do Paraopeba (about 15 km north from the Bonfim area) yield ages of 2.9 Ga (Machado et al., 1989).

In the Barbacena area (about 110 km south from the Bonfim area; Figure I.2), U-Pb single zircons analyzed from two different portions of an heterogeneous migmatitic gneiss (samples AM147 and AM149 from Delhal & Demaiffe, 1985) yield a recalculated age of 3155 $\pm$ 2.6 My. Zircon data from an adamelitic gneiss (sample JD144 from Delhal & Demaiffe, op.cit.) further south, in the Juiz de Fora area, were also recalculated and yield an age of 3092 $\pm$ 16 My. These recalculated isotopic ages are more likely to have geological significance then the ones originally

calculated by Delhal & Demaiffe, because they were recalculated using data of samples representing only single outcrops; and because there is uncertainty about the origin of the sphenes (in this case not included) in such a high-grade metamorphic environment. Lower intercepts were recalculated by me at 1317 Ma and 1231 Ma for the samples from the Barbacena and Juiz de Fora areas, respectively.

ii) Mid- to late-Archean greenstone belts and associated granitoids

A major geological feature of the southern sector of the São Francisco craton is the Rio das Velhas greenstone belt. This belt is exposed mainly in the Quadrilátero Ferrífero area but extends northwestward up to the Pará de Minas area and southwestward in the Congonhas and Conselheiro Lafaiete areas, and up to Lavras (Figure I.2). The evolution of the Rio das Velhas greenstone belt includes regional anatexis and plutonism of granitic-gneisses and large-scale crustal deformation extending into the early Proterozoic (see discussion below).

The rocks of the Rio das Velhas Supergroup comprise a greenstone belt sequence which has been divided into three Groups (Schorscher et al., 1982; and references therein). The lower Quebra Osso Group comprises mainly mafic-ultramafic sequences (including spinifex textured komatiites), banded iron formations and metacherts. The middle Nova Lima Group is particularly thick (>4000 meters), and composed dominantly of schists which represent a variety of volcanic and sedimentary rocks, including volcanic flows, pyroclastics, immature volcanogenic and chemical sediments (cherts), together with dolomites, banded iron formations and manganesiferous formations. The upper Maquiné Group is composed of schists and quartzites, occasionally with intraformational lenses of meta-conglomerate. The age of the Rio das Velhas Supergroup is constrained by zircon ages of 2.77 Ga obtained from the felsic volcanics of the lower portion of the Nova Lima Group in the Piedade do Paraopeba area; and 2.78 Ga for both granitoids and acid volcanics of the Nova Lima Group in the Caeté area (Machado et al., 1989).

The events of felsic volcanism in the southern São Francisco craton during the Archean are relatively well constrained. On the basis of U-Pb zircon and sphene dating Delhal & Demaiffe

(1985) indicate that 2.82 Ga should be considered a minimum age for the Bação complex. The younger zircon ages of 2.78 Ga reported for granitoids and felsic volcanics in the Caeté area (Machado et al., 1989) compare favorably with the 2.78 Ga zircon age for emplacement of the Alberto Flores tonalite in the Bonfim area (Carneiro et al., in press) and indicate a second event with widespread granitegenesis and felsic volcanism in the Quadrilátero Ferrífero domain at this time. Zircon ages of 2.76 and 2.74 Ga have been obtained for the Mateus Leme and Caio Martins granitoids, respectively (Romano, 1989); and a zircon age of 2.73 Ga was obtained for the Moeda granitoid (Machado et al., 1989).

The Piunhi massif, about 180 km west of the Quadrilátero Ferrífero area, has been described as a greenstone belt by Schrank (1982), who divided the complex into three Groups. The lower Araras Group comprises mainly komatiitic rocks with spinifex textures associated with a thick volcanosedimentary sequence. This section is tectonically overlain by the Paciência Group which comprises platform sediments, turbidites and sparse mafic and felsic intrusives. The Paciência Group is tectonically overlain by schists, clastic sediments, banded iron formations and mafic-ultramafic bodies and chromitites of the Lavapés Group. Zircon grains extracted from sills intruded into the lower portion of the Araras Group have been dated at 3.12 Ga, whilst a rhyodacytic dome also intrusive into the Araras Group produced ages of 3.00 Ga (Machado and Schrank,1989). In addition, zircon grains from sheared granites in tectonic contact with the Araras Group were dated at 726 Ma (minimum age) and porphyritic trachytes intruded into the Paciência Group produced zircons which have been dated at 635 Ma (Machado & Schrank, op.cit.) indicating that the Piumhi massif has been extensively affected by the Brasiliano tectono-thermal event.

It is evident, therefore, that large portions of the southern São Francisco craton comprises Archean areas which were episodically rehomogenized, and that tectonic remnants with deformed Archean basement exist westward, beyond the craton limits indicated in Figure I.1. Whole-rock Rb-Sr ages in the interval 2.8 - 2.6 Ga are widespread in the southern sector of the craton (e.g. Teixeira et al., 1987) and these ages have been suggested to represent the final stabilization of an Archean continent. The original dimensions of this early part of the Sao Francisco craton

remain uncertain, since it also extends under the NeoProterozoic Bambuí cover (Teixeira & Figueiredo, 1991).

iii) Proterozoic supracrustal sequences and tectono-thermal rejuvenation events

Following the late Archean continental stabilization, ProtoProterozoic crustal rifting took place and intracratonic and marginal basins were formed. In the southern sector of the craton these events are represented by platform sequences of the Minas Supergroup (e.g. Pflug & Renger, 1973; Pflug & Scholl, 1975; Marshak & Alkmin, 1989). Its present areal distribution is restricted (Figure I.2) and probably only represents an erosional remnant of a much wider distribution. It has been suggested, for example, (Queménéur, 1987; Teixeira & Figueiredo, 1991) that the Bon-sucesso ridge is likely a southward extension of the Minas Supergroup. The age of deposition of the Minas Supergroup is constrained by the 2420 Ma age of carbonates from the Gandarela Formation (Pb-Pb work on whole rock samples by Babinski et al., 1991) and by a detrital zircon age of 2125 Ma for the Sabará Formation (Machado et al., 1989).

The ProtoProterozoic Transamazonian tectono-thermal processes represent a major event in the evolution of the craton. Isotope analysis have shown that both juvenile crust formation and extensive reworking of older rocks have occurred (e.g. Teixeira et al., 1987). Apparently many of the Archean granitic and gneissic complexes were partially remobilized during this episode. For example, in the 2.8 Ga Bação Complex, titanite and monazite grains produce U-Pb ages of 2.06 and 2.03 Ga, respectively, (Machado et al., 1989); and granitic dykes intruded into the Bonfim complex yield 2.1 Ga old zircons (Carneiro et al., in press.). This tectono-thermal event also affected rutiles in the Archean Caeté granitoid complex at 2.0-2.2 Ga (Machado et al., op.cit.) and almost completely reset the Rb-Sr system (2.25-2.13 Ga; Oliveira & Teixeira, 1990).

A complex history of Proterozoic deformation has been documented along the southern parts of the craton, where the development of planar fabrics and isotopic rejuvenation on a regional scale are conspicuous (Teixeira & Figueiredo, 1991; and references therein). The domal structures of the central part of the craton grade into planar structures imposed on gneissic and migmatitic

rocks metamorphosed at amphibolite and granulite facies. These planar structures control juvenile granitic intrusives, alkaline rocks and pegmatoids which have whole-rock Rb-Sr isotopic ages between 2.2 - 1.9 Ga (Teixeira et al., 1987; Teixeira & Figueiredo, 1991). Mafic dike swarms in the Pará de Minas and Lavras areas, which are probably related to the ProtoProterozoic tensional episodes, may have undergone partial rejuvenation during NeoProterozoic compressional events (Teixeira et al., 1988).

MesoProterozoic extensional tectonics produced broad asymmetrical basins along both the eastern and western margins of the craton. These basins have been overprinted by Brasiliano-age fold and thrust tectonism of the Araçuaí and Brasília belts, along the eastern and western margins of the craton, respectively (see Figure I.1). The tectonic elements described are comparable to those found in fold and thrust belts, and foreland basins elsewhere (e.g. Kiang et al., 1988; Pimentel et al., 1991; Baars, thesis in preparation). According to these and other authors, the NeoProterozoic Araxá, Paranoá and Macaúbas Groups, and the basal portion of the Bambuí Group were deposited during the MesoProterozoic extensional regime, whereas the overlying Tres Marias Formation of the Bambuí Group reflects foreland basin sedimentation during the NeoProterozoic inversion on the tectonic stresses. The age of deposition of the basal portion of the Bambuí Group (the Paraopeba Formation) has been estimated to be 640 $\pm$ 15 Ma and the age of the Tres Marias Formation to be 620 $\pm$ 40 Ma by Couto et al. (1981) on the basis of Rb-Sr isotopes on undeformed whole rock samples and Pb-Pb determinations on galena separates. It is also possible, however, that these ages could represent regional foreland basinal fluid migration during the late stages of foreland thrusting (c.f. Duane and de Wit, 1988; M. de Wit, pers. comm., 1993).

The presence of a Brasiliano overprint within the craton limits is well established. The extent of Brasiliano-age deformation within stable "on-craton" environments, however, is the subject of intense debate (Baars, thesis in preparation). Concordant $^{206}Pb/^{238}U$ and $^{207}Pb/^{235}U$ sphene ages at *ca* 600 Ma reported by Delhal & Demaiffe (1985) for the Barbacena and Juiz de Fora areas may indicate the crystallization or recrystallization of this mineral and attest to the influence of the Brasiliano orogeny along the southern margin of the craton. A lower intercept at 760 Ma on

rocks of the Bação Complex was related to episodic Pb loss during the Brasiliano event (Delhal & Demaiffe, 1985). Zircon grains from the Caeté granitoids and acid volcanics have lower intercepts at 453 and 447 Ma (Machado et al., 1989). Zircons from the Mateus Leme and Caio Martins granitoids have lower intercepts at 517 and 411 Ma respectively, (Romano, 1989). Moreover, Teixeira and coworkers (e.g. Teixeira et al., 1987; Teixeira & Figueiredo, 1991; and references therein) have been arguing for a long time that the abundant K-Ar ages ranging from 1.5 to 0.75 Ga in the southern portion of the craton may reflect partial loss of argon during the Brasiliano orogeny; and that the geographic distribution of K-Ar age patterns suggests that associated thermal events might also have affected the eastern and southern portions of the "stable" cratonic area.

I.2.2 - The Tocantins province

The distribution of the major geological subdomains in the Tocantins Province (Almeida et al., 1981) is shown in Figure I.1. Reliable geochronological data for the Province is sparse, and almost non existent in its southern sector. New isotopic data recently produced in two areas in the northern and western portions of the province (see Figures I.1, I.3 and I.4) are here used to constrain the possible crustal evolution of the southern Tocantins province and its relation to the mid- to late-Archean craton.

i) Araí Group rhyolites and associated granitic intrusions

The Araí Group comprises mainly a thick (up to 1200 m) sequence of MesoProterozoic continental sediments, which covers large portions of the northeastern Uruaçu belt. Coarse grained sediments of the Arraias Formation (the lower portion of the sedimentary sequence) are interlayered with a thick rhyolitic unit which, in turn, is associated with alkali-rich, tin-bearing granitic rocks. No intrusive relationships have been found between the granites and the sediments of the Araí Group (Marini & Botelho, 1986).

The geochronology of the Araí rhyolites has recently been constrained by U-Pb zircon data and supports a genetic association of the intrusive granites and the extrusive silicic rocks as first suggested by Marini and Botelho (1986). Pimentel et al., (1991) indicated that the zircon ages

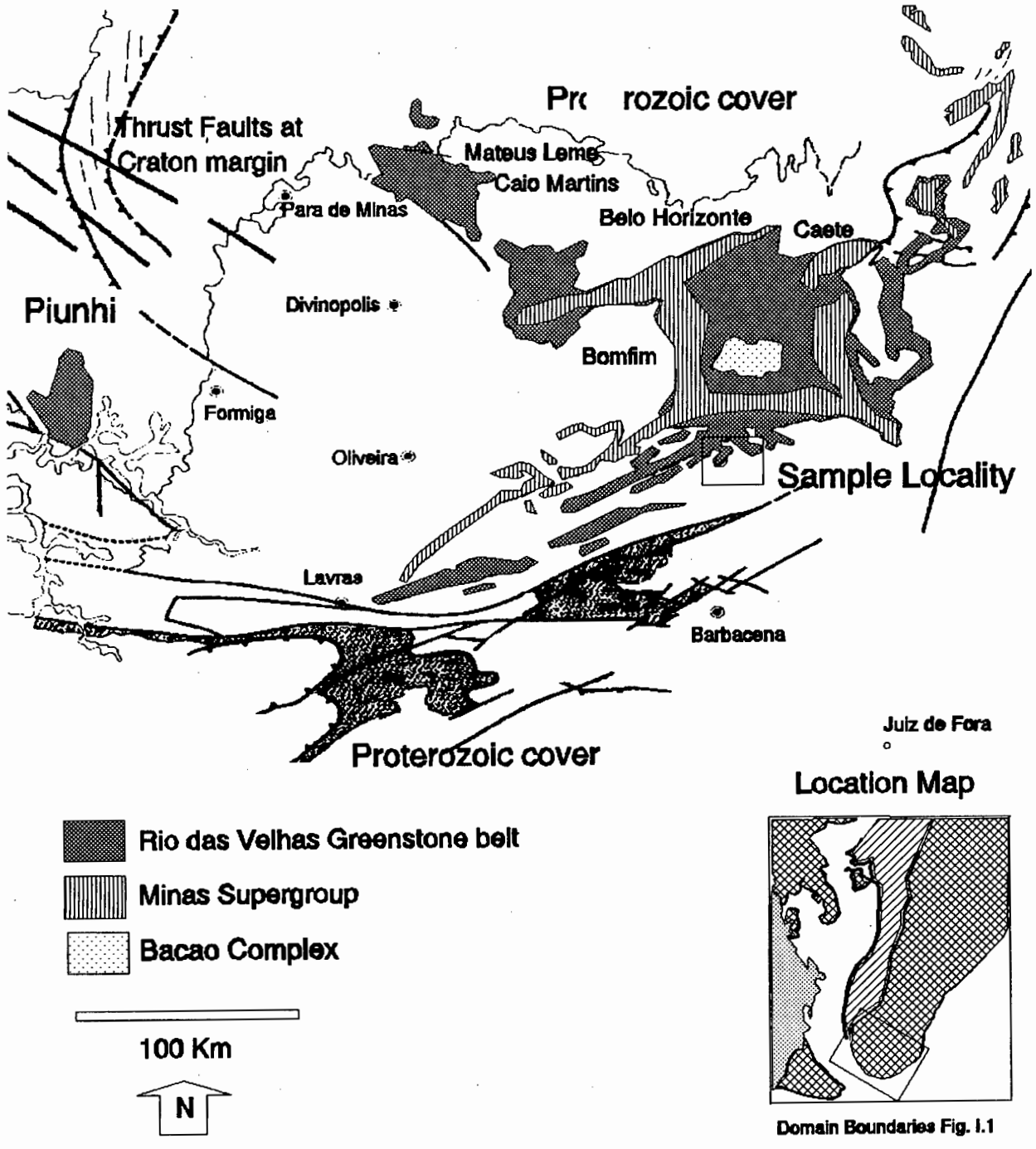

Figure I.2 - Geological setting of the Southern São Francisco craton and the Congonhas do Campo region (the study area) after Shobbenhaus et al. (1984). Note the extension of the mid to late Archean Rio das Velhas greenstone belt and associated granitoids and the location of the Piunhi Massif. Whole-rock Rb-Sr ages in the interval 2.8 - 2.6 Ga are widespread in this sector of the craton (e.g. Teixeira et al., 1987) and have been suggested to indicate the final stabilization of an Archean continent. The present areal distribution of platform sequences of the Minas Supergroup probably represents an erosional remnant of a much greater distribution.

Figure I.3 - Geological setting of the Arai rhyolites and associated granitoids (after Pimentel et al., 1991). Zircon ages from the Rio Paranã sub-Province (RPS: So = Soledade, PB = Pedra Branca, Su = Sucurí, Mo = Mocambo, Ma = Mangabeira, SM = Serra do Mendes and Ba = Banhado) are indistinguishable from the ages of the Arai Group (i.e. 1.77 Ga); whereas zircons from the Rio Tocantins sub-Province (RTS: SD = Serra Dourada, SE = Serra do Encosto, SB = Serra Branca, SM = Serra da Mesa, Pi = Pirapitinga, SR = São Roque, Ra = Raizaminha, and SC = Serra da Cangalha) and from the Serra da Mesa Group reveal a distinct 1.6 Ga episode of acid magmatism.

Geology of Central-eastern Goias

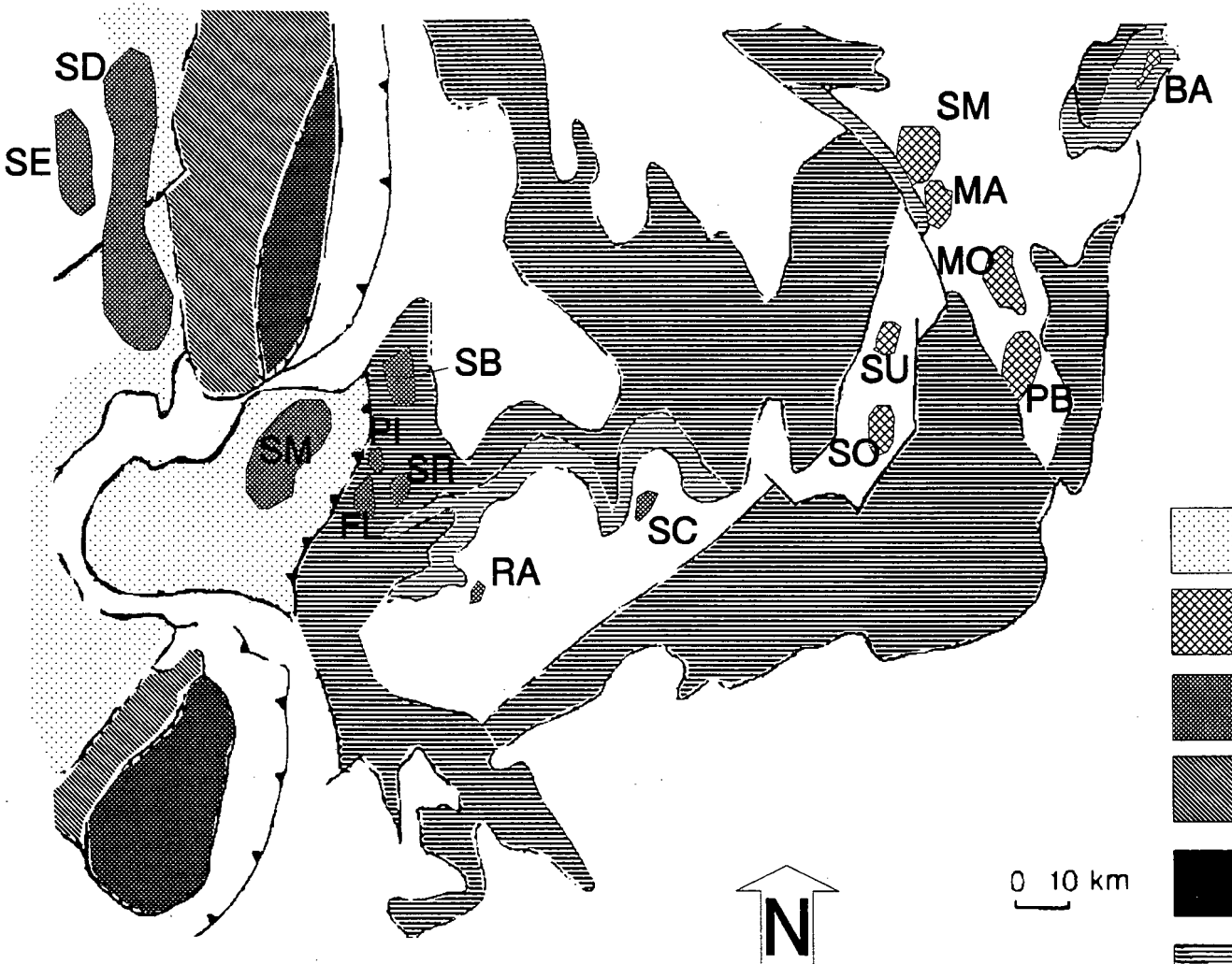

Location Map

Domain Boundaries Fig. I.1

Serra da Mesa Group

RPS granitoids-1.77Ga

RTS granitoids-1.6Ga

Volc-Sed.Sequences

Maf-Umaf.Complexes

Arai Group

of granites in the Rio Paranã sub-Province (see Figure I.3) are indistinguishable from the zircon ages of rhyolitic lavas (1771 ± 2 Ma); whereas zircons from the Serra da Mesa granites in the western Rio Tocantins sub-Province (about 100 km further to the west; see Figure I.3) revealed a distinct episode of MesoProterozoic continental acid magmatism at *ca.* 1600 Ma ago.

The inheritance pattern reported for the zircons from the Araí rhyolite suggests that the sialic basement may include a ProtoProterozoic (*ca.* 2.2 Ga) component, whereas an older Archean (*ca.* 3.3 Ga) inheritance has been recorded for zircons from the Sucurí granite (Pimentel et al., 1991). Lower intercept ages at *ca.* 650 Ma reported by these authors indicate an event of Pb loss during a heating event at the end of the Proterozoic (Pimentel et al., 1991). This thermal disturbance has also been recognized in the Rb-Sr and K-Ar whole-rock isotopic analysis (e.g. Reis Neto & Cordani, 1984; and many other references in Pimentel et al., 1991). No Sm/Nd data are available for the area.

ii) NeoProterozoic gneiss and metavolcanics in western Goiás

Recent detailed field work combined with Rb-Sr, Sm-Nd and U-Pb geochronological studies in the western and southern Goiás area (Figure I.4) have detected the presence of several NeoProterozoic metavolcanic and metaplutonic assemblages (Pimentel et al., 1991; Pimentel & Fuck, 1992). For example, orthogneisses in the Arenópolis, Matrinxã and Sanclerlândia areas of western Goiás (see Figure I.4) are calcic to calc-alkalic volcanic-arc granitoids, with U-Pb and Rb-Sr emplacement ages of 940 to 895 Ma. Concordant sphene analysis indicate a metamorphic recrystallization of these rocks at *ca.* 637 Ma (Pimentel et al., 1991). Metavolcanic assemblages in the same region (part of the Bom Jardim, Arenópolis, Iporá and Jaupaci sequences), ranging from tholeiitic basalts to K_2O-rich rhyolites, yield U-Pb and Rb-Sr ages ranging from 930 to 587 Ma. Upper intercept zircon ages from the Arenópolis and Jaupaci meta-rhyolites at 929 Ma and 764 Ma, respectively, suggest that two periods of arc magmatism may have preceded the Brasiliano tectono-metamorphic event in the southwestern Goiás (Pimentel & Fuck, 1992).

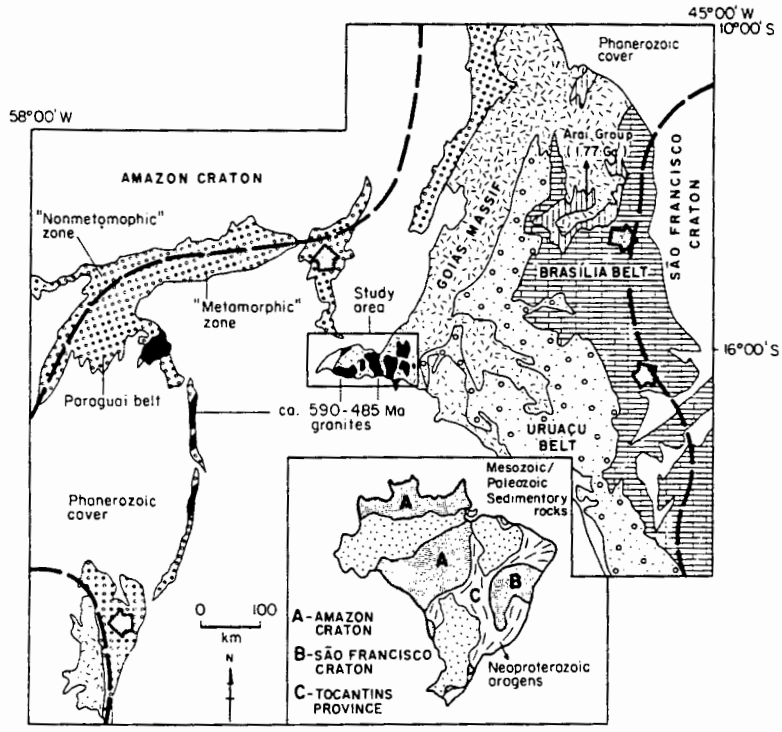

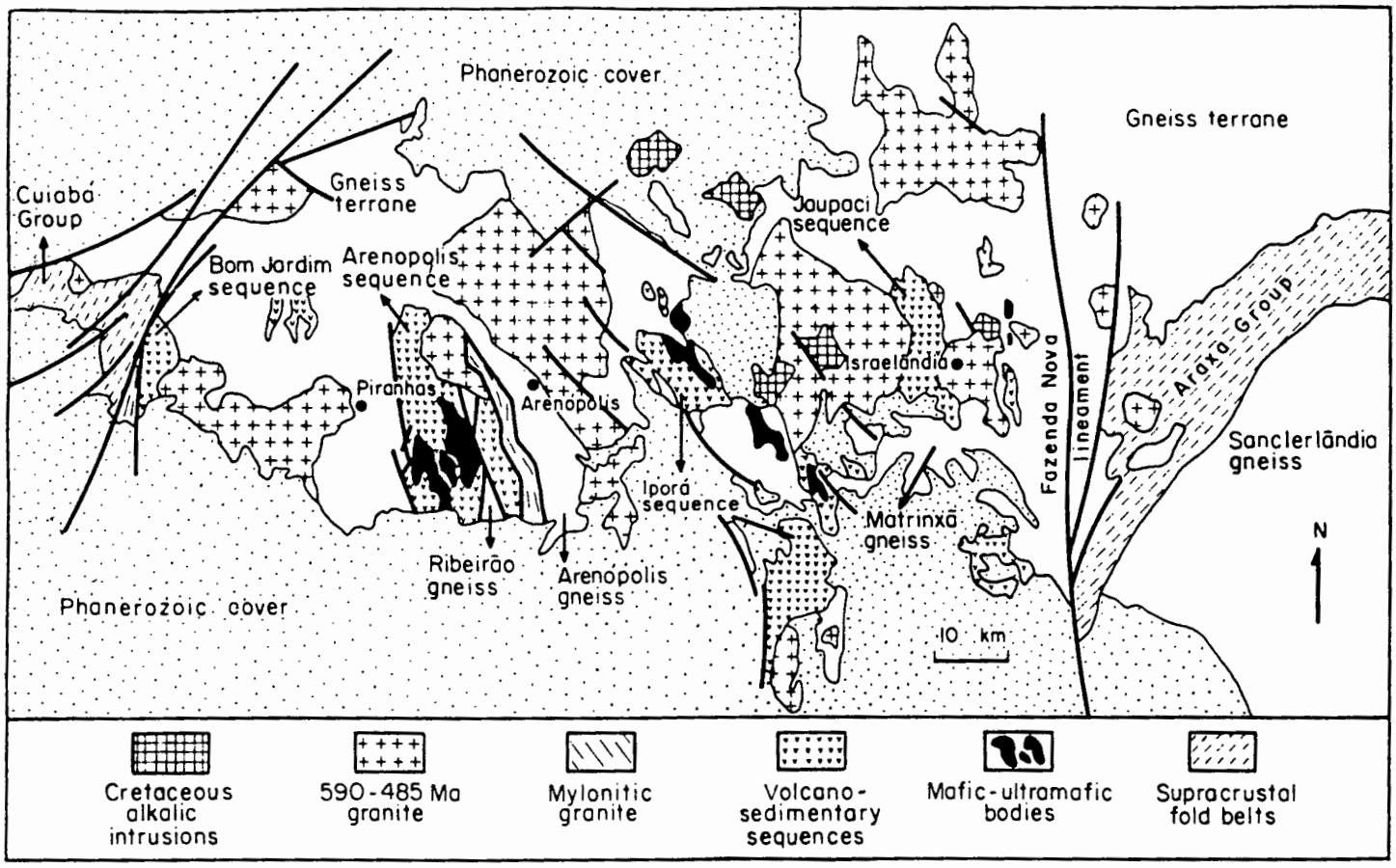

Figure I.4 - Geological setting of the western Goiás area (from Pimentel et al., 1991).

Sphenes extracted from rhyolites of the Arenópolis sequence yielded metamorphic recrystallization ages of 764 Ma and 594 Ma, which probably reflect the development of steep-dipping strike slip shear zones in the area (Pimentel et al., 1991). These metamorphic recrystallization ages were accompanied by resetting of the Rb-Sr whole-rock isotopic system in mylonitic rocks *ca.* 600 Ma, and by resetting of the K-Ar isotopic system on a regional scale (Marini et al., 1984 and references therein). Several large, late- to post-orogenic granitoid intrusions (ranging in composition from early calc-alkalic, I-type rocks, to younger alkali-rich A-type rocks with metaluminous to slightly peraluminous compositions) were emplaced between 590 and 485 Ma (Pimentel & Fuck, 1987 and 1992).

Further east, in the Pires do Rio area, U-Pb analysis in zircon grains extracted from meta-rhyolites of the Maratá sequence (Araxá Group) indicate a *ca.* 2.0 Ga old inherited component; and a 794 Ma age for crystallization of the volcanic protolith (Pimentel et al., 1991). Pimentel et al. (1991) also reported Rb-Sr isochrons of 829 Ma (initial $^{87}Sr/^{86}Sr$ of 0.7057) and 691 Ma (initial $^{87}Sr/^{86}Sr$ of 0.7337). The latter isochron was interpreted as representing a Sr-isotopic re-homogenization episode associated with the Brasiliano tectonothermal event. Sm-Nd data yielded ϵ_{Nd} values in the range of -6.1 to -9.5 (at 794 Ma).

iii) The Niquelândia mafic-ultramafic complex

The Niquelândia complex is part of a 350 km long belt formed by three individual complexes (i.e. the Barro Alto, Niquelândia and Cana Brava complexes) composed of layered sequences which are partly metamorphosed at granulite grade. Danni et al. (1982) indicated these complexes, and Niquelândia in particular, to be representative of an Archean proto-ophiolitic sequence (the lower zone of granulite facies peridotite) tectonically overlain by amphibolites and an amphibolite facies gabbro-anorthositic sequence which they interpreted as metamorphosed ocean-floor basalts. Petrochemical studies in the Juscelândia (Danni & Kuijmjian, 1984) and Palmeirópolis (Araújo & Nilson, 1987) metamorphic volcanic-sedimentary sequences along the western border of the complexes have been used to interpret these rocks as being ocean floor basalts. Girardi et al. (1986), however, interpreted the Niquelândia complex as a layered complex similar to Bushveld and Stillwater, with fractionation trends related to different *liquidus*

phases. More recently, Ferreira Filho et al. (1993) considered the Niquelândia complex as a single major stratiform mafic-ultramafic complex which subsequently underwent tectonism with associated high-grade metamorphism.

Although these mafic-ultramafic complexes have been considered (e.g. Danni et al., 1982) as Archean (granulitic part) and ProtoProterozoic (amphibolites); no reliable geochronological data have yet been presented. A Rb-Sr geochronologic investigation on felsic rocks from the granulite belt and gneisses of the Juscelândia sequence defined an isochron at 1266 Ma (initial $^{87}Sr/^{86}Sr$ of 0.73473) which has been interpreted as Sr-isotopic re-homogenization during high-grade metamorphic conditions (Fuck et al., 1988).

I.3 - ISOTOPE SYSTEMATICS OF SELECTED AREAS

A number of samples among those collected for zircon work were selected during this study for Rb-Sr and Sm-Nd isotopic analysis. The geological framework of these samples is illustrated in Figures I.1 to I.5 and I.7. The strategy was to select samples from a broad geographic area and to include samples representative of a broad region around each sample locality. In the absence of emplacement ages constrained by the zircon data in preparation, subsets of the Sr and Nd data were used, in combination with field relations, to roughly establish the possible correlation of the studied rock sequences to sequences for which independent age control is available. It is emphasized, however, that the "ages" determined in this Rb-Sr and Sm-Nd whole rock study are considered to have almost no geochronological value until they can be supported by U/Pb zircon ages.

I.3.1 - The Congonhas Lineament

The Congonhas Lineament (the study area indicated in Figures I.2 and I.5) is one of a series of regionally significant lineaments which cross-cut the southern São Francisco craton and display evidence for episodic reactivation from at least the ProtoProterozoic through to the Cretaceous. Voluminous, syntectonic, juvenile granitoids intrude deformed metavolcano sedimentary rocks of the Rio das Velhas greenstone association along this lineament. Previous work in the area has

been reported in Seixas (1988) and Seixas & Baars (1991).

Seven rock samples from the area were analyzed for Rb-Sr and Sm-Nd. Zircon grains have been extracted from two of them (the Lobo Leite metagabbro and the Vila Matias Gneiss) and are awaiting U/Pb analysis. Results of the zircon work on these two samples, as well as detailed mapping, petrographic description and micro-probe work on the samples whose Rb-Sr and Sm-Nd isotopic compositions are being reported here will be discussed in detail by Franciscus Baars (thesis in preparation). The whole-rock Rb-Sr and Sm-Nd analytical results obtained are shown in Table I.1; and the approximate location of the studied samples is indicated in Figure I.5.

i) Greenstone association

Three localities representing the greenstone association in the area were sampled and analyzed. The "Lobo Leite metagabbro" (LLG) comprises a medium- to coarse-grained, upper greenshist facies metagabbro from the base of a serpentinized komatiite sequence of the Rio das Velhas Supergroup. The "Alto da Varginha komatiitic metaperidotite" (AVK) comprises serpentinised metakomatiite with a pseudomorphed spinifex-like texture of chlorite, serpentine and tremolite. The rock samples from this locality (the Chuel Mineração Dimension Stone Quarry) have not been affected by the shearing that is so pervasive throughout the lineament. The "Alto da Varginha massive metaperidotite" (AVM) is volumetrically the most abundant meta-ultramafic rock of the Rio das Velhas Supergroup in the lineament. Samples chosen for analysis are also from the Chuel Mineração Quarry and occur in gradational contact with the above mentioned komatiitic metaperidotites. Whole-rock major and Rare Earth Element (REE) compositions suggest a cogenetic relation of these two rock types by fractionation from a single komatiitic liquid (Seixas, 1988).

The Rb-Sr data obtained for the samples from these three localities define an errorchron at 3224 $\pm$ 82 Ma (initial $^{87}Sr/^{86}Sr$ of 0.7062; Figure I.6). The Sm-Nd data obtained are concordant with those obtained from the basement and juvenile granitoids in the area (see discussion below), and an errorchron of 3194 $\pm$ 127 Ma (initial $^{143}Nd/^{144}Nd$ of 0.5091, which corresponds to an epsilon value of 11 $\pm$ 2.2) is obtained when all the six samples from the Congonhas Lineament are

combined (Figure I.6). Caution is deemed necessary in assigning any geochronological significance to these numbers because (a) there is a limited number of samples; (b) there is a large scatter in the data shown in Figure I.6; and (c) the distinct nature of rocks types combined together on the Sm-Nd diagram, which might not be cogenetic. In addition, the initial epsilon neodymium value of +11 at 3.2 Ga plots well above the mantle evolution curve, which strongly suggests that the age is incorrect and that there might have been Sm-Nd fractionation during the evolution of those rocks. However, because the analysis by the two isotopic systems give similar results, and because of the widespread occurrence of 3.2 Ga zircon ages in the areas nearby. It is speculated that the errorchrons may represent the time at which the ultramafic units of the Rio das Velhas greenstone association separated from a depleted upper-mantle reservoir. The real geological significance of these numbers will have to await completion of the U/Pb zircon analysis ages from the Lobo Leite metagrabbro. If the zircon ages reveal comparable results, the early stages of development of the Rio das Velhas Supergroup must have started in the mid-Archean, which is earlier than previously believed, but which is considered to be one of the most important crustal formation episodes of the southern São Francisco craton according to Teixeira and co-workers.

ii) Basement and juvenile granitoids

Three samples from two localities 4 km apart were included in this study. The "Vila Matias gneiss" (VMG) is a fine grained, banded gneiss that only sporadically outcrops as possible inliers of basement to the greenstone metavolcanosedimentary sequence. Field evidence indicates that this gneiss is equivalent to the basement of the Moeda Complex in the Bonfim area, which has yielded 3.32 Ga inherited zircon ages, and for which metamorphic imprints at 3.0 and 2.7 Ga have been reported (Carneiro et al., in press). The "Alto Maranhão foliated tonalite" (AMT) contains xenoliths of dacitic and rhyolitic materials that are resorbed and oriented parallel to the foliation. This tonalite is representative of the larger complex of syntectonic tonalitic batholiths, intrusive into the supracrustal sequence. An age of 2124 $\pm$ 12 Ma has been recently determined by U/Pb on magmatic zircons extracted from samples from the same outcrop (F.Baars, pers. comm., 1992). The "Alto Maranhão Dioritic dike" (AMD) samples comprise fine-grained diorite which cross-cut the foliation of the tonalite.

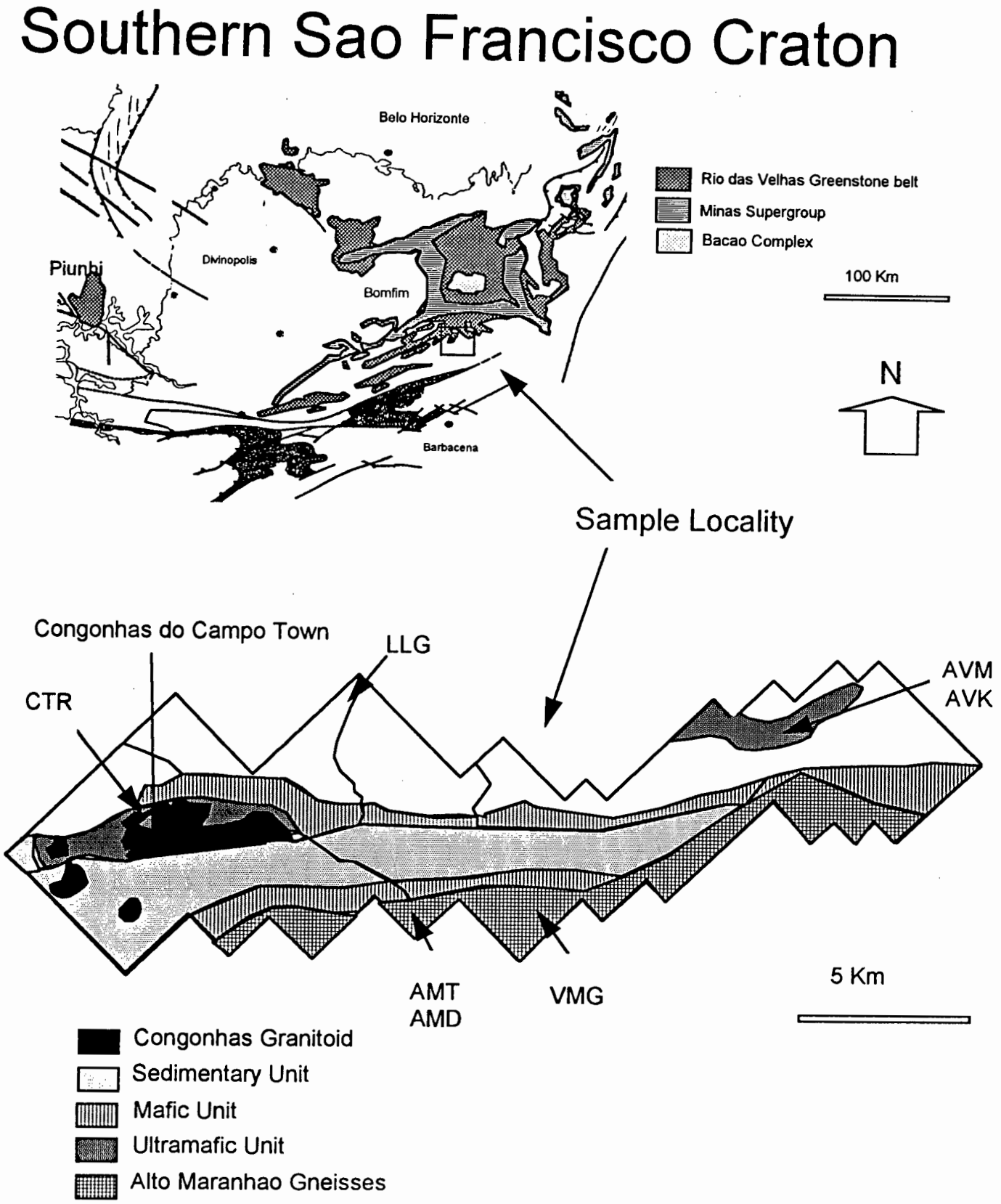

Figure I.5 - The Congonhas do Campo area comprises of voluminous syntectonic juvenile granitoids intruding deformed metavolcanosedimentary rocks of the Rio das Velhas greenstone belt. Location of rock samples from both the greenstone association and the basement and juvenile granitoids indicated as in the text.

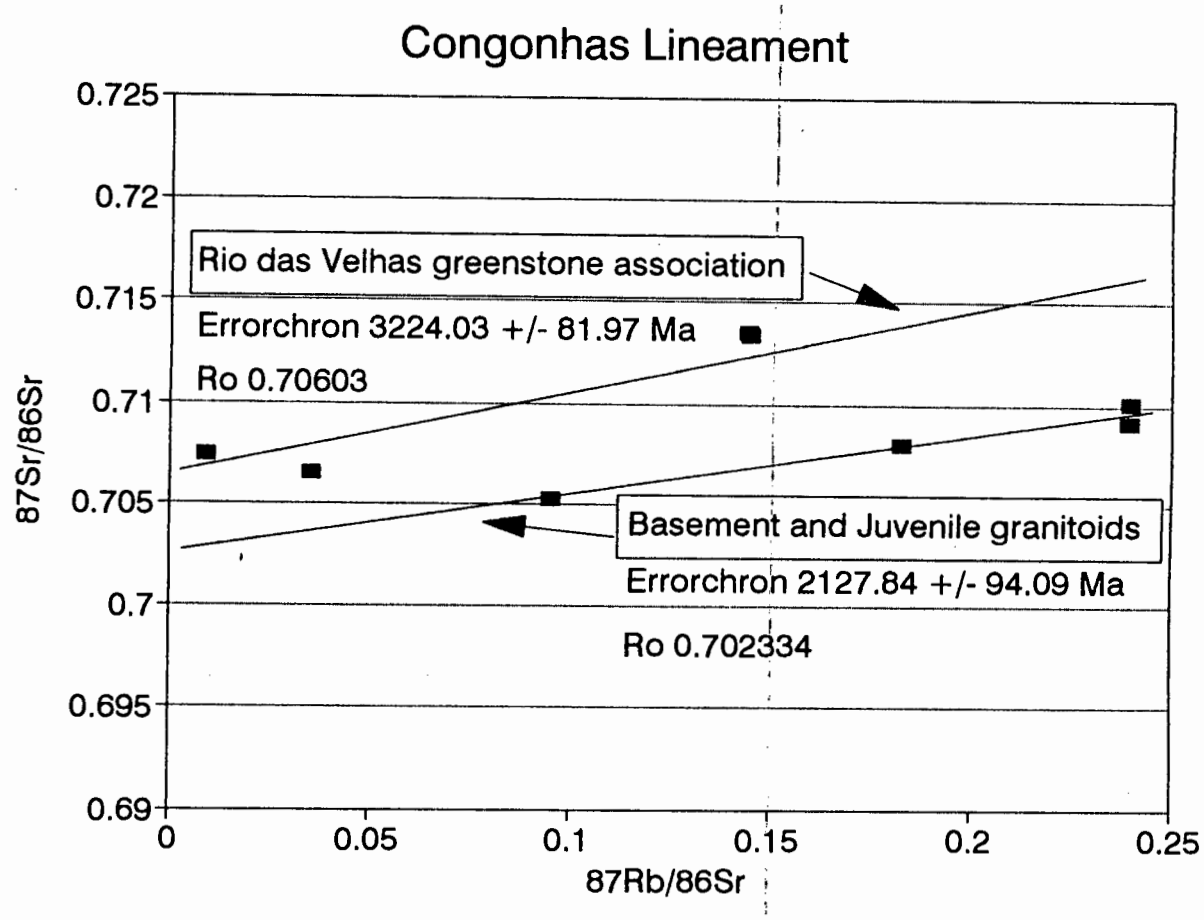

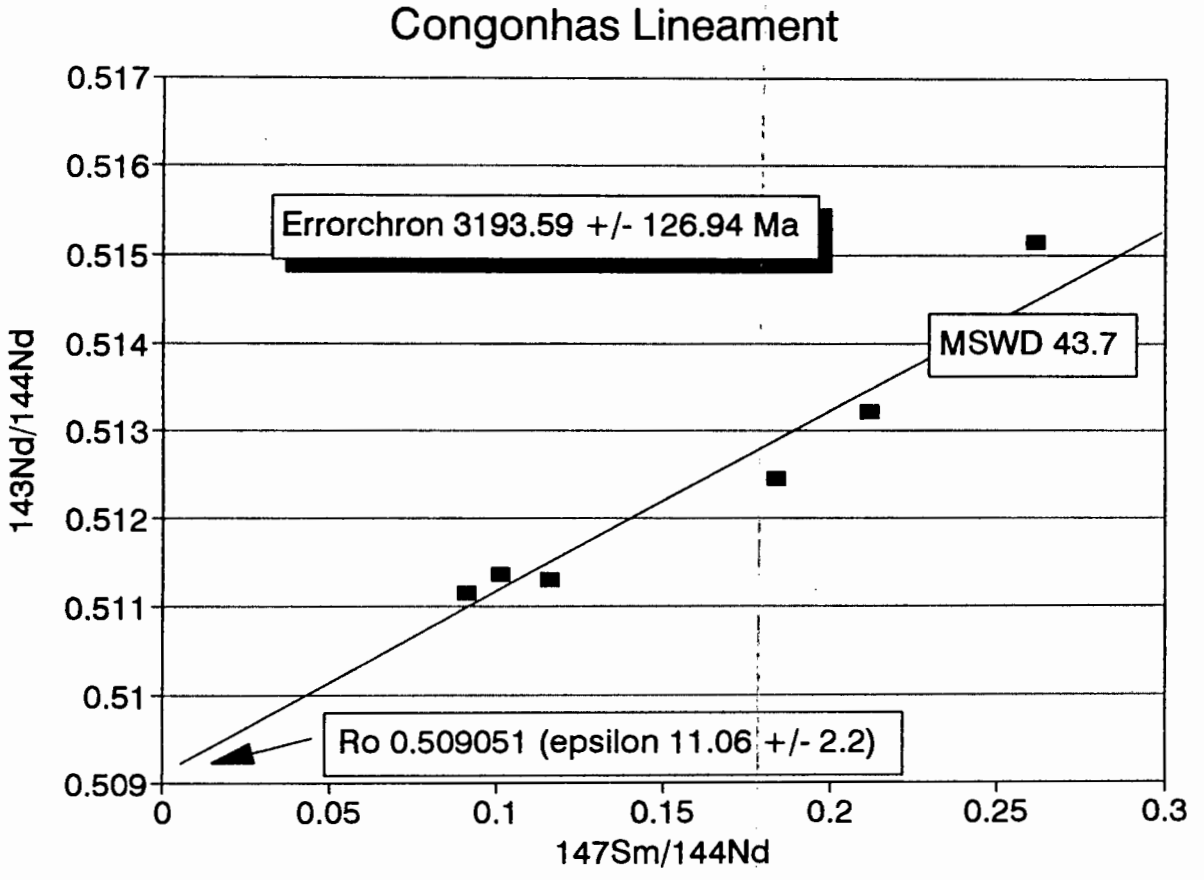

Figure I.6 - Rb-Sr and Sm-Nd isotopes diagrams for the greenstone association and granitoids in the Congonhas do campo area. Decay constants used = 1.42000E-11 and 6.54000E-12, respectively. Sample uncertainties are 1 sigma. Confidence limits 95%. Determinations were made using Geodate V.2.1 (12.11.90) at the UCT radiogenic isotopes facility.

The Rb-Sr data obtained delineate a 2128 ± 94 Ma (initial $^{87}Sr/^{86}Sr$ of 0.70233; see Figure I.6) errorchron which is in excellent agreement with the U/Pb zircon age defined for samples from the same outcrop. In the light of field observations, the coherent behavior of the VMG sample could represent Sr-isotope re-homogenization in the basement gneisses during the Transamazonian event. The Sm-Nd data for these rocks is concordant with the signatures obtained from the ultramafic rocks of greenstone association discussed earlier. The behavior of the REE suggests that both the peridotites of the greenstone association and the Vila Matias gneisses could have been extracted (in the mid-Archean?) from a light-REE depleted source, whereas the Alto Maranhão tonalites would be derived from a light-REE enriched source (ϵ_{Nd} - 4.1 at 2.1 Ga) in the ProtoProterozoic. Because of the affinity of the isotopic signatures, it is tempting to suggest that the mafic-ultramafic rocks were all extracted from the same source, and that the Alto Maranhão tonalites were largely the product of remelting of this Archean crustal material, as has been suggested for granite-greenstone terrains in many places elsewhere (c.f. Martin, 1993). Such interpretation, however, does not explain the initial $^{87}Sr/^{86}Sr$ ratio of the obtained isochron, which is low for a billion years of crustal residence; and does not fit the model ages obtained (T_{CHUR} averaging 2.25 Ga and T_{DM} averaging 2.48 Ga). From that aspect these rocks are more likely juvenile (i.e. mantle-derived, either directly or from crustal protolith of immediate mantle derivation) at about 2.1 Ga. With the information available at the moment choosing between the two alternatives is premature.

The above results represent only a very preliminary stage towards integrating isotope studies with geology and understanding the crustal evolution of the area near Congonhas do Campo. It is clear, however, that 2.1 Ga is the minimum age of the Congonhas lineament. The possible tectonic significance of the lineament and its continuation through the Pará de Minas region will be addressed by Franciscus Baars (thesis in preparation).

I.3.2 - The Brasília orogenic and foreland thrust belt

To date, very little reliable geochronologic data have been produced from the rocks in the vicinities of the Mesozoic intrusives to be discussed in chapters II and III. Five rock samples from this region were therefore selected and analyzed for Rb-Sr and Sm-Nd isotopes. Zircons

were extracted from three of them (the Perdizes diorite, the Ribeirão Areado granodiorite, and the Monte Carmelo porphyritic granite). Results of the zircon analysis, together with detailed petrography and micro-probe work on the samples will be reported by Franciscus Baars (in preparation). The whole-rock Rb-Sr and Sm-Nd analytical results are shown in Table I.1; and the location of the studied samples is indicated in Figure I.7.

Three samples, from one single outcrop about 10 km south of Abadia dos Dourados, have been included in this project. These rocks are representative of a suite of syntectonic (Brasiliano-age) granitoids which occur in the far western orogenic portion of the Brasília belt. The "Perdizes diorite" (PDD) is a medium-grained member of the suite of syntectonic granitoids intrusive into NeoProterozoic metavolcanosediments. The "Ribeirão Areado granodiorite" (RAG) is a late-stage, shallow level, sheet-like intrusive with amphibolitic xenoliths and a late-stage pegmatitic veins system. A foliated amphibolite xenolith enclosed and partly resorbed by the Ribeirão Areado granodiorite (RAX) has also been analyzed because it may represent a significant subcrustal contaminant in the granitic intrusives.

The "Monte Carmelo porphyritic granite" (MCG) samples are representative of the granitoids which occur near the southern intrusive boundary of the granitic complex in the vicinities of Monte Carmelo. It is a poorly-foliated and xenolith-free medium- to coarse-grained rock with K-feldspar phenocrysts. Rb-Sr and Sm-Nd analyses of these samples were completed to support the zircon work. The "Abadia Metabasalt" (AMB) is a fine-grained, intensely foliated metabasalt from the supracrustal Araxá Group in the vicinity of Abadia dos Dourados. These rocks are associated with a 794 Ma bimodal volcanic sequence (Pimentel et al., 1991).

The sparse Rb-Sr data obtained suggest that the granitoids (PDD and RAG samples) might not have been in isotopic equilibrium with the amphibolitic xenoliths (RAX samples). On a $^{87}Sr/^{86}Sr$ *versus* $^{87}Rb/^{86}Sr$ plot (Figure I.8) the granitoid samples align sub-parallel to the 720 Ma reference line. A three point isochron can be defined for the PDD, RAG and AMB samples at 711 $\pm$ 17 Ma (MSWD = 0.8; initial $^{87}Sr/^{86}Sr$ of 0.71188). This whole-rock Rb-Sr age is comparable to the Rb-Sr isochrons reported by Pimentel et al. (1991) for the Araxá Group volcanics

Western Minas Gerais Area

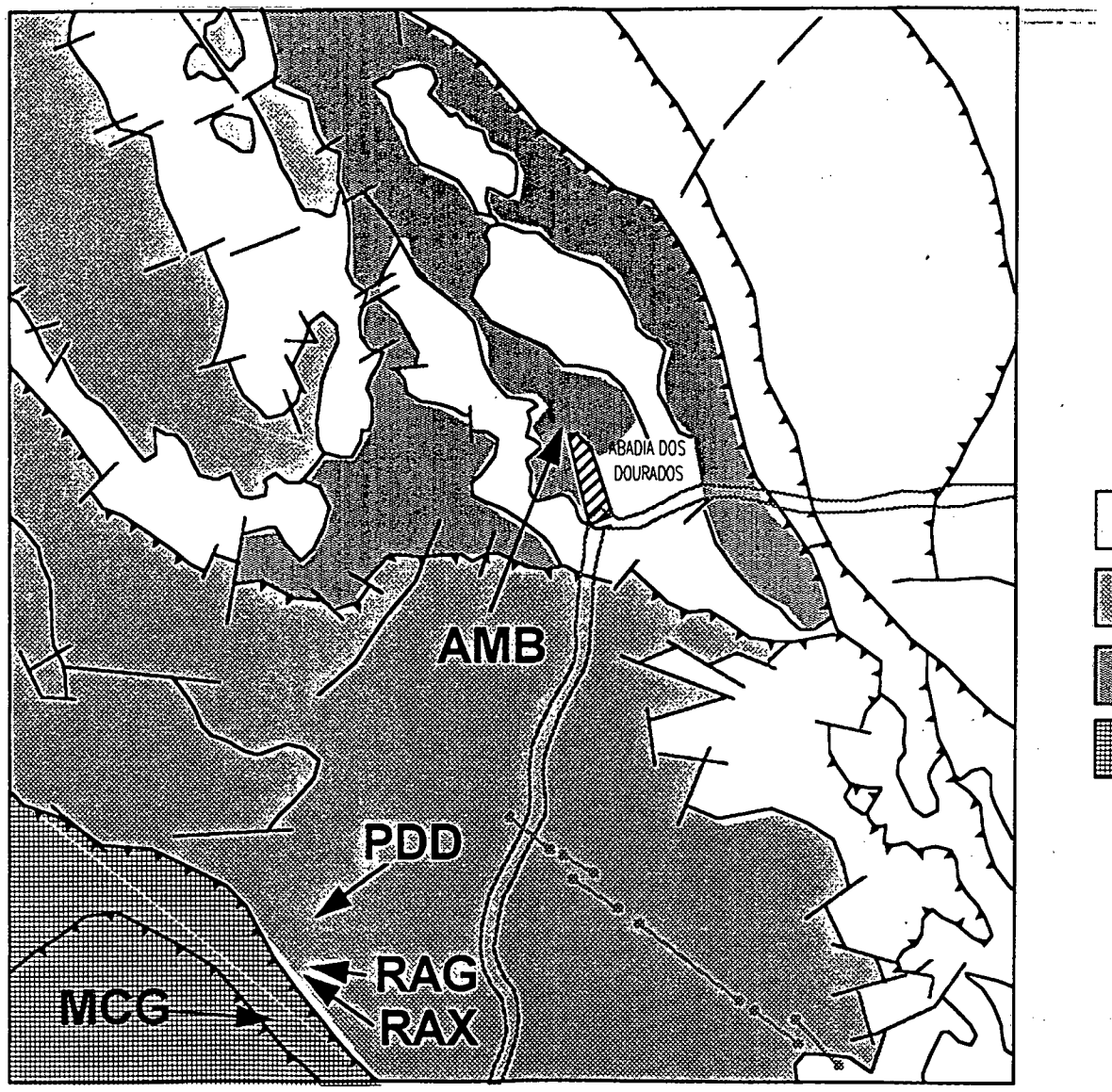

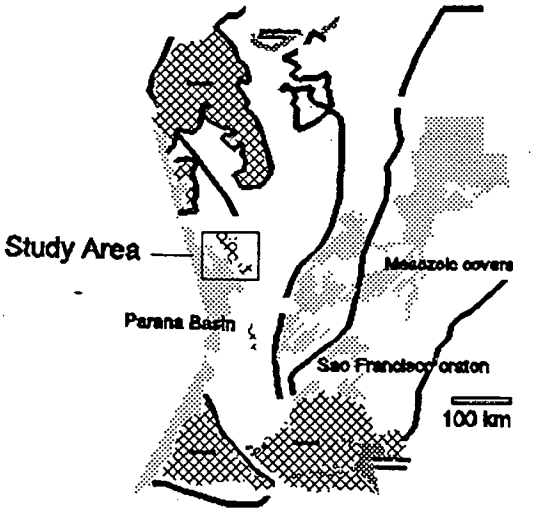

Araxá metasediments

Syn-tectonic granites

Araxá Metabasics

Basement Granitoids

10 Km

Figure I.7 - The geological setting of the western Minas Gerais area is conditioned by the Brasilia orogenic and foreland thrust belt. Location of the rock samples analyzed for Rb-Sr and Sm-Nd isotopes indicated as in the text. Inset illustrate approximate location and relative size of this study-area in the context of Figure I.1.

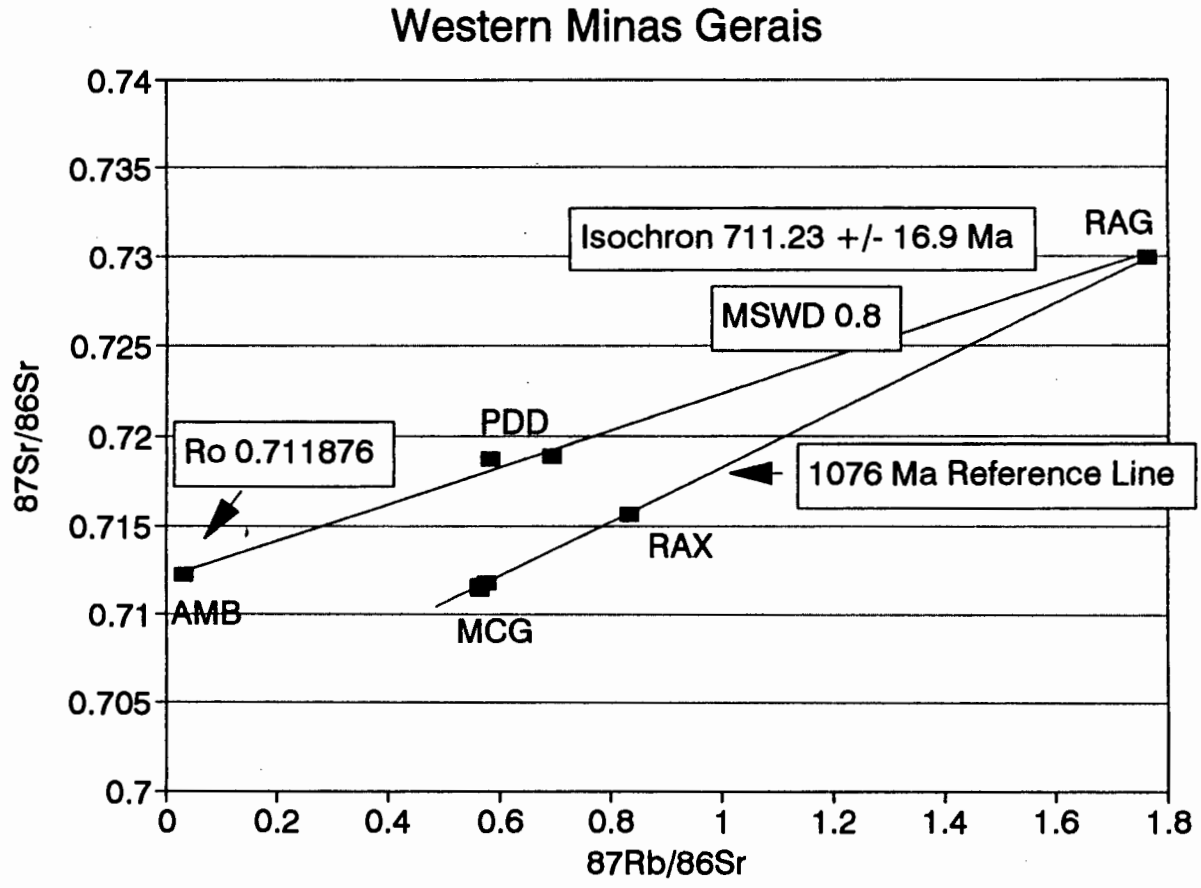

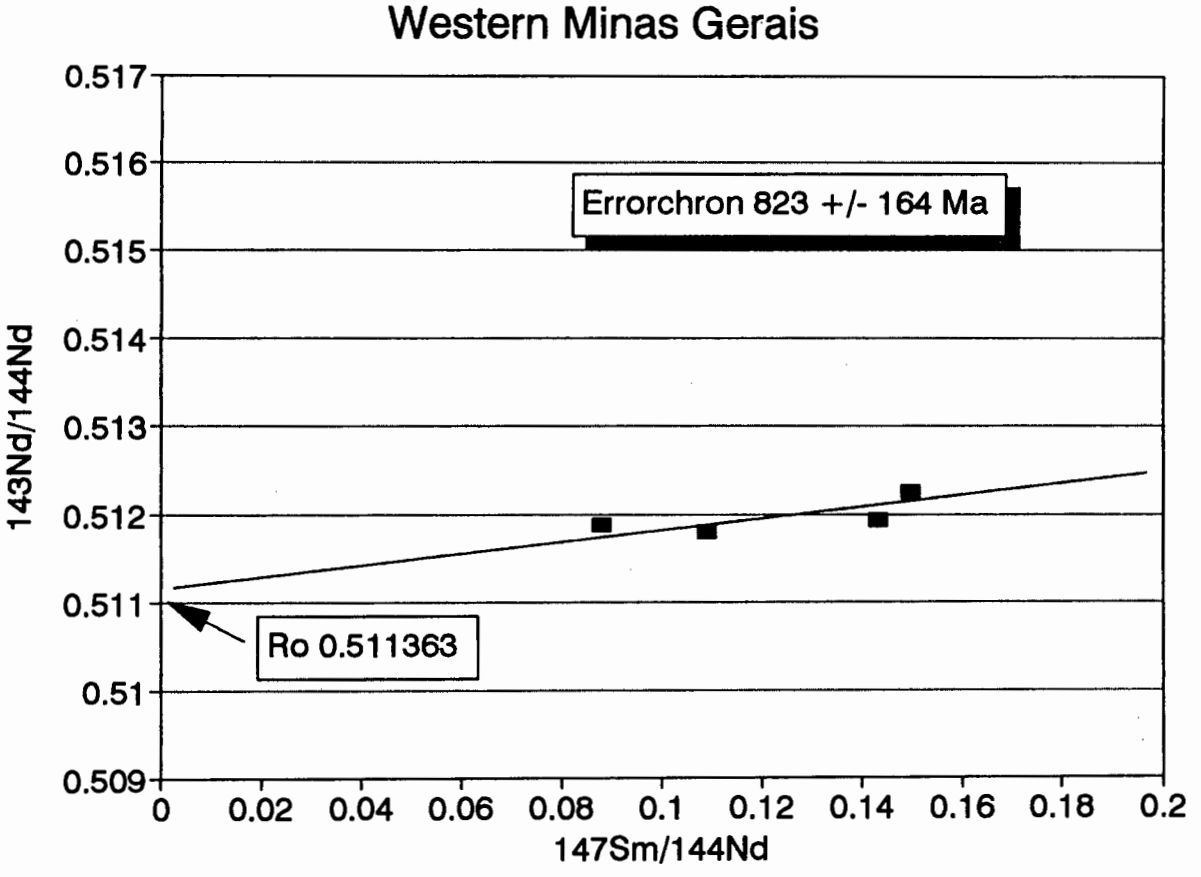

Figure I.8 - Rb-Sr and Sm-Nd isotopes diagrams for granitoids in the western Minas Gerais area. Decay constants used = 1.42000E-11 and 6.54000E-12, respectively. Sample uncertainties are 1 sigma. Confidence limits 95%. Determinations were made using Geodate V.2.1 (12.11.90) at the UCT radiogenic isotopes facility.

outcropping 100 km northwest from the sample locality. Therefore, despite the small scatter in $^{87}Rb/^{86}Sr$ (0.031 to 1.763) of these samples, and despite the fact that only three samples are included on the same regression line, it is possible that the isotopic age obtained has geological significance. Because of the relatively high initial $^{87}Sr/^{86}Sr$ ratio this age could be related to a large scale Sr-isotope re-homogenization episode during the intense deformation and metamorphism of the Brasiliano tectono-thermal event in the area. In addition, the rocks from this sample locality define a whole-rock $^{143}Nd/^{144}Nd$ *versus* $^{147}Sm/^{144}Nd$ errorchron at 823 $\pm$ 164 Ma (Figure I.8). It is speculated, therefore, that this suite of granitoids may be coeval to the felsic volcanism in the Araxá Group. Again, these numbers need to be tested by the pending U/Pb zircon work.

The samples from the Monte Carmelo granite have Sr-Nd signatures which are clearly distinctive from the granitoids in the Abadia dos Dourados area, and yield much older Nd model ages. The samples from the Ribeirão Areado and the included xenoliths, however, define a Rb-Sr mixing line which extends into the samples of the Monte Carmelo granite. The trend defined by the RAG, RAX and MCG samples align about a 1076 $\pm$ 46 Ma errorchron which probably has no geologic significance. If anything, this mixing line may be related to the process of entrainment of older basement country rock by the syntectonic Brasiliano-age granitoids.

I.3.3 - The Niquelândia mafic-ultramafic complex

The Niquelândia complex within the Goiás Massif Domain (Figure I.1) is one of a series of basement windows of deep crustal layered mafic-ultramafic rocks which protrude through their tectonic cover of the Paranoá Group. Four samples from the layered sequence and its basement have been analyzed for Rb-Sr and Sm-Nd isotopes. Results obtained are shown in Table I.1.

Samples were taken from a K-feldspar porphyritic augen granite gneiss (NIQ2) which occurs structurally below the mylonitic gabbros of the complex but structurally above the supracrustal rocks of the Paranoá Group. Samples of foliated meta-websterite (NIQ4) were selected as representatives of the peridotitic ultramafic rocks at the base of the sequence. Samples of a small sheet of metaluminous granodiorite (NIQ13) within the centre of the complex were also

analyzed, as was one sample from an anorthosite of the upper part of the Complex (NIQ15).

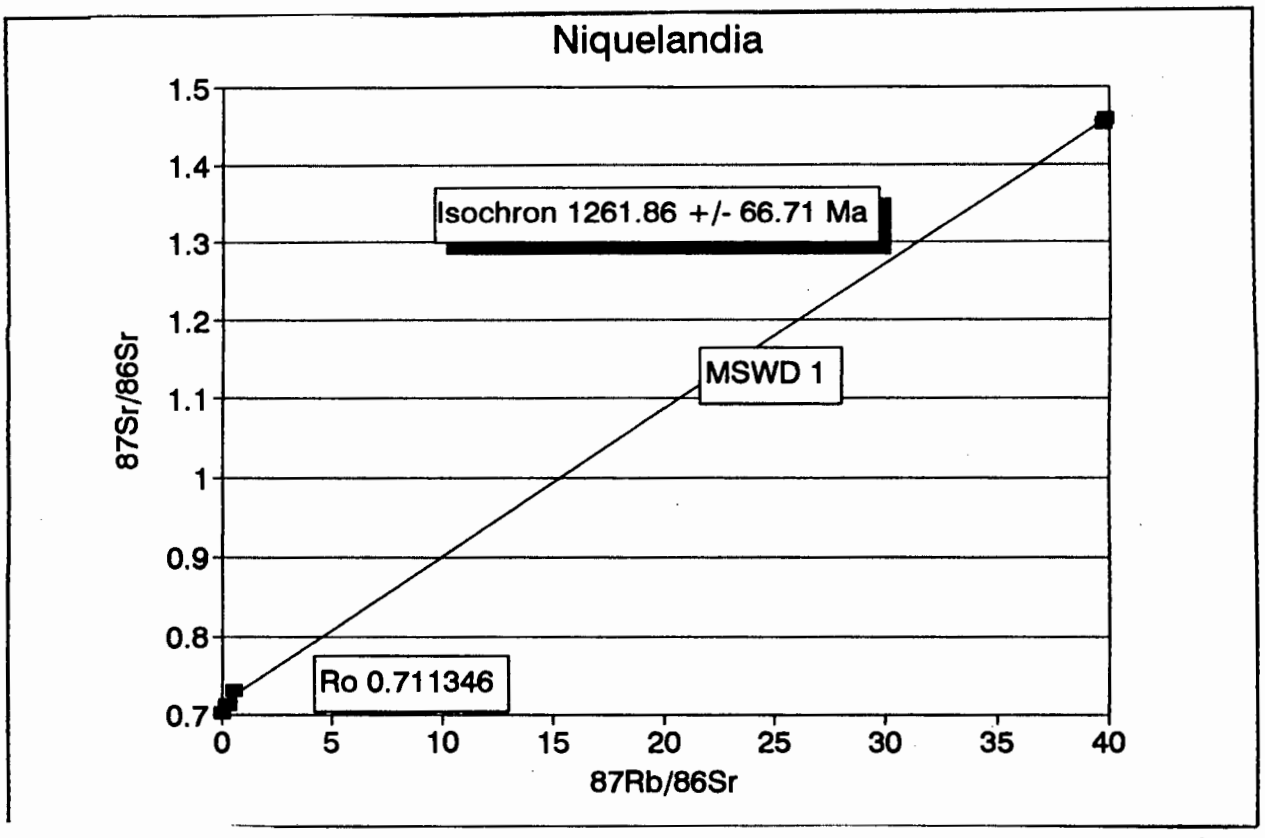

Figure I.9 - Rb Sr isotopes diagram for samples from the Niquelândia Complex. Decay constant used 1.42000E-11. Sample uncertainty 1 sigma. Confidence limits 95%. Determination was made using Geodate V.2.1 (12.11.90) at the UCT radiogenic isotopes facility.

Rb-Sr data from all the above samples of the complex yield a nine points isochron at 1262 ± 67 Ma (initial $^{87}Sr/^{86}Sr$ of 0.71135; Figure I.9), in good agreement with the 1266 ± 17 Ma isochron obtained by Fuck et al. (1988) for the Serra da Gameleira samples of the nearby Barro Alto mafic-ultramafic complex. Fuck et al. (1988) interpreted their age as a homogenization event during high-grade metamorphism. The initial ratio reported here is significantly lower than the 0.73473 reported by Fuck et al. (*op.cit.*), but can still be similarly interpreted to indicate that the protoliths were incorporated into the crust long before the metamorphic event. Moreover, model ages for assumed initial ratios of 0.705 and 0.710 are about 1300 Ma and comparable to the Serra da Gameleira samples.

When the three samples from the igneous complex only (i.e. NIQ4, NIQ13 and NIQ15) are

considered, an errorchron of 3418 ± 65 Ma (initial $^{87}Sr/^{86}Sr$ of 0.70143) is produced. The geologic meaning of this age is suspect, however, because of the very small spread of $^{87}Rb/^{86}Sr$ ratios on which it is based, and because of the implied assumptions of a cogenetic origin for the rocks across the compositional range peridotite to anorthosite. Furthermore, this age would imply that the granulite facies metamorphic overprint did not cause wholescale Sr-isotopic rehomogeneization. Nd isotopic signatures of these samples are very heterogeneous, and no coherence has been observed in the $^{143}Nd/^{144}Nd$ *versus* $^{147}Sm/^{144}Nd$ plots. Nevertheless, epsilon values calculated at 3.4 Ga for the different granodiorite samples range between 12 and 13; which indicates that, if the *circa* 3.4 Ga age has any geologic significance, the source character of the complex is compatible with a depleted mantle derivation. However, few types of materials other than some possible eclogite samples are known to be this depleted this early in the Earth.

I.4 - A PRELIMINARY MODEL FOR THE EVOLUTION OF THE CRATON MARGIN

Neodymium model ages (T_{DM}) calculate the time when a sample had an isotopic composition identical to that of the depleted mantle reservoir source (c.f. DePaolo, 1988). The accuracy and significance of T_{DM} ages depends on how well the evolution of the source of the rocks is known. Main assumptions inherent in this approach include: (*i*) knowledge of the isotopic evolution of the mantle; (*ii*) the emplacement in the continental crust and the acquisition of the Sm-Nd ratio are separated by a very short period of time; and (*iii*) the Sm/Nd of the sample has not been modified by subsequent crustal events (e.g. DePaolo, 1988; and references therein).

For a Nd model age to "date" a crust-formation event, the Sm/Nd ratio in the sample must not have been modified since extraction of the protolith from the mantle; i.e. a single stage evolution must be aplicable. Many of the samples reported in this thesis are likely to be a mixture of materials derived from the mantle at different times. Granitic magmas were probably formed mainly through melting of pre-existing crustal rocks, and their initial ϵ_{Nd} values should, therefore, cluster at a value for the average crustal rock. Therefore, the Sm-Nd systematics in these rocks can provide only an estimate of the average time that the material in the sample has been resident in the continental crust. Moreover, Pimentel & Charnley (1991) have reported cases of highly evolved granitic rocks from the Tocantins province in which

variable Sm-Nd fractionation resulted in large deviations in Nd model age values. This demonstrates that, in many cases, calculated Nd model age values were affected by intracrustal magmatic processes. Because of these limitations, in this work the crust formation ages of the provinces are distinguished using Nd isotopic evolution paths established on the basis of "standard" $f_{Sm/Nd}$ in crustal rocks (c.f. DePaolo, 1988) rather than relying purely on the Nd model ages.

Samarium-neodymium isotopic data obtained in this work, together with other published geologic and geochronological information can be combined to evaluate the history of crust-mantle segregation and continental growth of the southwestern margin of the São Francisco craton. In Figure I.10, ϵ_{Nd} values for samples from both the southern São Francisco craton area and from the southwestern margin of the craton area, within the Tocantins Province, are plotted against crystallization ages and used to define distinct and subparallel isotopic evolution paths with average $f_{Sm/Nd}$ crustal values. The rocks related to the on-craton greenstone sequences and some of the granites intruded through the Tocantins Province have initial ϵ_{Nd} values approximating that of the mantle at the time of their presumed formation. The initial ϵ_{Nd} values of most of the crustal sequences, however, define a region extending to substantially negative values. Following Bennet & DePaolo (1987), the initial ϵ_{Nd} and crystallization ages of the studied rock samples are used to define evolutionary paths for the crust in the area. Such paths start from the mantle evolution curve (DePaolo, 1981) and progress linearly away from this curve with time. The data suggest that most of the post-orogenic granites intruded through the Tocantins Province were formed by melting of Proterozoic arc-related magmas (Pimentel et al., 1991). This situation is similar to that found for rocks in the western United States. The data set from the São Francisco craton and its margins, however, is not large enough yet to characterize discontinuities such as those observed in central Nevada and western Utah (Bennett & DePaolo, 1987; Farmer & DePaolo, 1983 and 1984; Nelson & DePaolo, 1984 and 1985; and DePaolo, 1988).

From Figure I.10, a T_{DM} age discontinuity is inferred to exist between the Archean cratonic nucleus and the Proterozoic Tocantins Province. The contrast in Nd isotope characteristics across the craton margin parallels a consistent pattern of decreasing crystallization ages with increasing

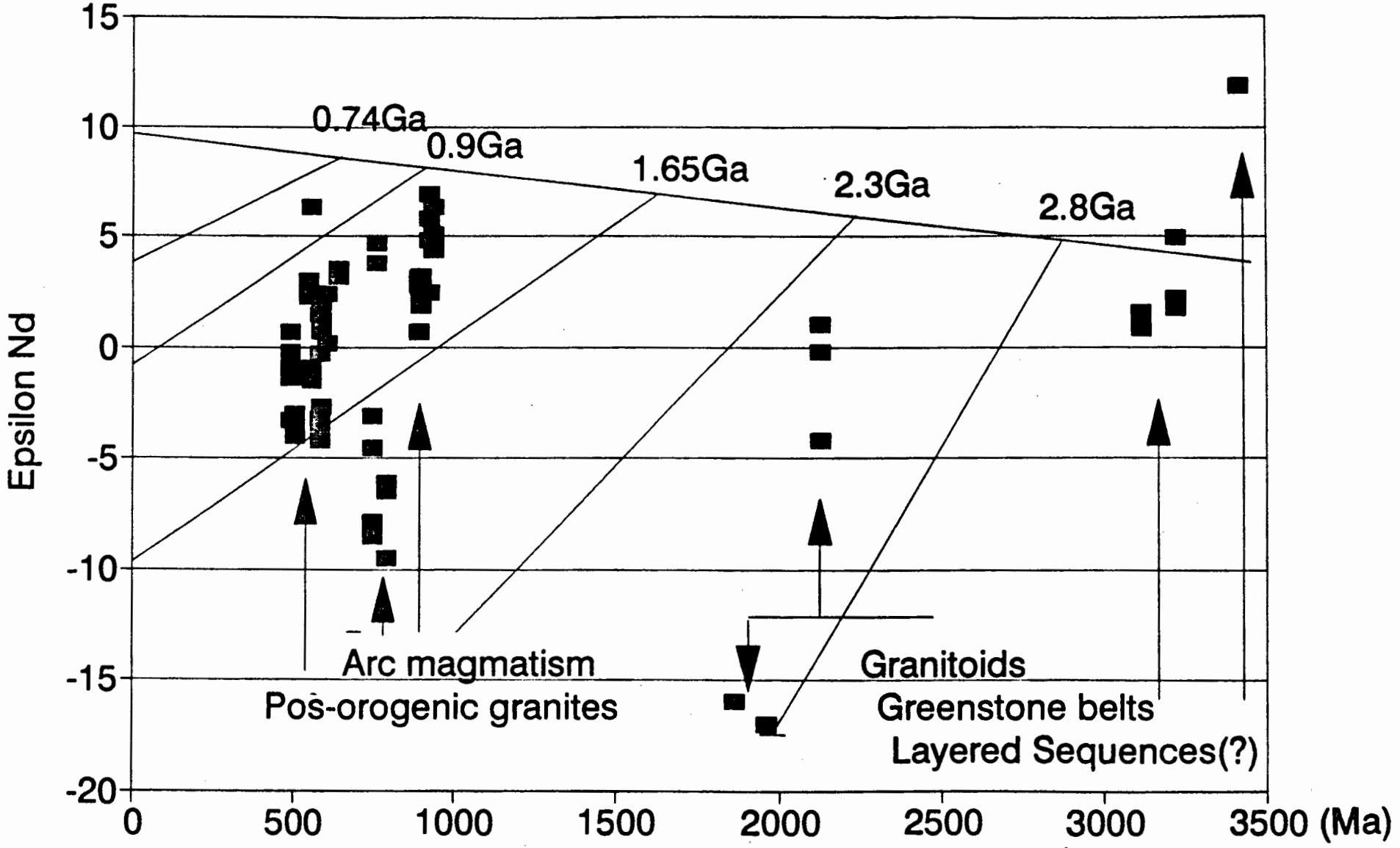

Figure I.10 - Epsilon Neodymium versus time of emplacement. Initial Nd signatures and crystallization ages are used to define evolutionary paths for the crust in the area. Paths start from the mantle evolution curve and progress linearly with time following average fSm/Nd crustal values. Most of the post-orogenic granites intruded through the Tocantins Province were formed by melting of arc-related magmas. TDM ages within the craton limits are greater than 2.7 Ga whereas in the Tocantins Province TDM ages tend to be Proterozoic, what would be consistent with the formation of new crust by accretion of magmatic arcs at the edge of the Archean craton.

distance westward from the craton margin. Both the large range in ϵ_{Nd} values and the corresponding restricted range in T_{DM} values observed in the Tocantins Province (Figure I.10) indicate that widespread crustal recycling and mixing of different isotope reservoirs must have occurred in the Proterozoic. Pre-existing crust was probably being extensively reworked whilst new crust was also accreted to the cratonic nucleus in the Proterozoic.

A number of models can explain the variations of T_{DM} and ϵ_{Nd} values along the craton margin. Possible scenarios include (*i*) the massive injection of mantle-derived magmas; (*ii*) the juxtaposition of two different age terrains along faults or sutures; (*iii*) intense reworking and "dilution" of Archean materials during the Proterozoic; or a combination of all three.

Both the average ϵ_{Nd} value and the average $f_{Sm/Nd}$ value of the crust should increase if a significant amount of mantle-derived magma was injected into the crust during the Transamazonian episode. A discontinuity in the crustal evolution path should then have resulted, provided no significant amount of mantle derived magma interacted with the pre-existing continental crust within the cratonic domains. Such a model would assume that the cratonic area remained undisturbed, thereby enhancing the isotopic contrast along the pericratonic transition zone. One of the mechanisms which could account for the isotopic variations recorded at the craton boundary zone would be the intrusion of dikes and sills and Proterozoic intraplate mantle magmas of high ϵ_{Nd} values into an overlying crust which was dominated by low ϵ_{Nd} value Archean rocks.

Alternatively, the transition zone between the craton and the Tocantins Province could represent the juxtaposition of two different age terrains along steep faults or sutures. If this transition zone was associated with a subduction zone, then there should have been sufficient mantle magma introduced into the overlying crust for it to have become noticeably modified (Farmer & DePaolo, 1984; DePaolo, 1988). In that case, most of the isotopic characteristics of the Tocantins Province would have been generated by newly forming crust in an island arc or Andean-like setting which incorporated Archean material. Pimentel et al. (1991) have proposed that such a model best explains observations in the western Goias areas. The paucity of calc-

alkaline igneous activity at what is conventionally called the craton margin, however, seems to indicate that subduction zones and juvenile arc magmatism were largely absent, and probably restricted only to the areas more to the west (M.Pimentel, pers. comm., 1992). Further discussion of the nature of the magmatism along the craton margin area, including major and trace element geochemistry of the samples for which Sr and Nd isotopes are being reported here, will be presented by Franciscus Baars (thesis in preparation).

Whilst contamination by Archean crust cannot be completely discounted, the Brasiliano age magmas emplaced along the southern Tocantins province have a coherent Nd geochemistry, and no inherited Archean zircons have been recorded. This suggests that the protolith had a history no longer than about 1 Ga; and that large scale assimilation of Archean crust is unlikely to have been of major importance. The mantle-like characteristics of arc suites in western Goiás and in the Uruaçuano and Brasília mobile belts do not support ensialic models for the Tocantins Province (Pimentel & Fuck, 1992), and both the Transamazonian and the Brasiliano tectono-thermal events were major events of juvenile crustal accretion from mantle sources. The majority of the presently exposed area of the southern Tocantins province consists of new mantle derived material added during the Proterozoic. Pimentel & Fuck (1992), have suggested that changes in the geochemical composition of volcanic rocks with decreasing age may indicate gradual thickening of the continental crust, probably with larger degrees of reworking and involvement of newly formed crustal material. Such a long term process would culminate in final stabilization and cratonization. Along the margins of the São Francisco craton this process probably followed basin closure and continental collision at *circa* 600 Ma.

I.5 - CONCLUDING REMARKS

Isotopic data indicate that continental crust (i.e. material derived from and chemically fractionated with respect to the upper mantle) has been forming or been reworked within and around the São Francisco craton over the past 3.3 Ga. The São Francisco craton can be envisaged as made up of a mosaic of relatively large lithospheric blocks of Archean age, assembled during the ProtoProterozoic Transamazonian orogeny. Although the ProtoProterozoic

domains display conspicuous linear structures on a regional scale (e.g. Teixeira & Figueiredo, 1991; Baars, thesis in preparation) the precise delineation of the boundaries of the Archean fragments is difficult because multiple episodes of metamorphism and deformation have destroyed the original relationships among the tectonic domains; and because the crystallization ages have been overprinted or obscured by later geologic events. The similar range of isotopic ages in the different blocks does not necessarily mean that these terrains were continuous or directly attached to each other before the Transamazonian orogeny. A detailed terrain characterization of the southern São Francisco craton on the basis of structural criteria will be presented by Baars (thesis in preparation).

Though some major Archean blocks have been recognized beyond the western margin of the São Francisco craton (e.g. the Piumhi massif; Figure I.2), to date the geochronological information available indicates that pristine Archean materials constitute only a minority component within the Tocantins Province. The evolution of the southwestern margin of the craton can be best viewed at present as due to continental growth through a combination of subduction-related additions of new materials from the mantle, and amalgamation of pre-existing lithospheric fragments throughout the Proterozoic. The continental growth in the Tocantins Province during the Proterozoic is envisaged as a semi-continuous process during which new crust was built outward from the craton and contributions of Archean material to the newly forming crust were progressively "screened" in a such a way that the more distal regions away from the cratonic nucleus were derived almost entirely from Proterozoic materials.

Table I.4 - Whole-rock isotope compositions.

Ref	PDD(B)	PDD(B)	RAG(B)	RAX(B)	MCG(B)	MCG(B)	MCG(B)	AMB(B)	LLG(C^1)	AVK(C^1)	AVM(C^1)
$^{87}Sr/^{86}Sr$	0.71885	0.71872	0.72994	0.71565	0.71161	0.71179	0.71138	0.71220	0.70654	0.70744	0.71349
$^{87}Rb/^{86}Sr$	0.6943	0.5838	1.7632	0.8330	0.5664	0.5780	0.5654	0.0312	0.0353	0.0091	0.1446
Sr	767	924	341	390	506	501	507	168	114	74	4.9
Rb	183.9	186.2	207.7	112.1	99.0	100.1	99.0	1.8	1.4	0.2	0.2
Ro	0.71142	0.71247	0.71106	0.70673	0.70555	0.70560	0.70536	0.71186	0.70590	0.70701	0.70672
$^{147}Sm/^{144}Nd$	0.0881	nd	0.1093	0.1498	nd	nd	nd	0.1434	0.1838	0.2116	0.2613
$^{143}Nd/^{144}Nd$	0.51187	nd	0.51181	0.51225	0.51221	nd	nd	0.51194	0.51245	0.51321	0.51515
Sm	12.6	nd	10.8	4.5	nd	nd	nd	4.1	3.8	0.7	0.15
Nd	86.2	nd	59.9	18.2	29.3	nd	nd	17.4	12.4	2.1	0.34
Ro	0.51144	nd	0.51127	0.51151	nd	nd	nd	0.51124	0.50854	0.50870	0.50958
T_{DM}(Ma)	1428.8	nd	1825.0	1934.4	nd	nd	nd	2463.8	3636.4	4481.1	5449.4

Ref	AVM(C^1)	VMG(C^2)	AMT(C^2)	AMD(C^2)	NIQ4(N)	NIQ4(N)	NIQ4(N)	NIQ13(N)	NIQ13(N)	NIQ15(N)	NIQ2(N)	NIQ2(N)
$^{87}Sr/^{86}Sr$	0.71339	0.70527	0.71009	0.70801	0.71229	0.71229	0.71229	0.73114	0.73111	0.70231	1.45906	1.45346
$^{87}Rb/^{86}Sr$	0.1447	0.0954	0.2399	0.1828	0.2338	0.3186	0.2905	0.5809	0.5819	0.0173	39.8437	39.7402
Sr	4.9	1158	842	842	0.36	0.36	0.36	214	214	222.8	36.84	37.08
Rb	0.25	38.2	69.8	53.3	0.03	0.04	0.04	43	43	1.33	472.66	474.68
Ro	0.70662	0.70233	0.70269	0.70237	0.70069	0.69645	0.69785	0.70225	0.70217	0.70145	0.52250	0.52295
Ro*					0.70795	0.70636	0.70688	0.72032	0.72027	0.70199	0.71671	0.71305
$^{147}Sm/^{144}Nd$	nd	0.1016	0.1164	0.0915	0.4459	nd	nd	0.1329	0.1359	0.0680	0.0006	nd
$^{143}Nd/^{144}Nd$	nd	0.51135	0.51129	0.51115	nd	nd	nd	0.51187	0.51187	0.51228	0.51163	nd
Sm	nd	5.1	5.7	4.6	2.7	nd	nd	4.3	4.4	0.44	0.017	nd
Nd	nd	30.2	29.6	30.4	nd	nd	nd	19.5	19.4	3.90	17.933	nd
Ro	nd	0.50992	0.50965	0.50986	nd	nd	nd	0.50888	0.50881	0.51125	0.51162	nd
T_{DM}	nd	2336.2	2819.6	2401.8	nd	nd	nd	nd	nd	nd	nd	nd

Key: PDD = Perdizes Diorite; RAG = Ribeirão Areado Granodiorite; RAX = Ribeirão Areado Granodiorite Amphibolite Xenolith; MCG = Monte Carmelo Porphyritic Granite; AMB = Abadia Metabasalt of the Araxá Group; LLG = Lobo Leite Metagabbro at the base of the Rio das Velhas Supergroup; AVK = Alto da Varginha Komatiitic Metaperidotite; AVM = Alto da Varginha Massive Metaperidotite; VMG = Vila Matias Gneiss; CTR = Congonhas Trondjemite; AMT = Alto Maranhão Tonalite; AMD = Alto Maranhão Diorite Dyke; NIQ2= Granitic Gneiss at the base of the Niquelandia Complex; NIQ4= Websterite; NIQ13 = Granodiorite; NIQ15 = Anorthosite. (B)=Brasília orogenic and foreland thrust belt, (C)=Congonhas lineament and (N)=Niquelandia mafic-ultramafic complex). $^{143}Nd/^{144}Nd$ reported relative to 0.51264 in BCR/1 and $^{87}Sr/^{86}Sr$ reported relative to 0.7080 in EnA Sr standard. Initial ratios calculated for 750 Ma (B), 3224 Ma (C^1), 2140 Ma (C^2), 3140 Ma (N) and 1300 Ma (Ro*). Decay Constants 1.42000E-11 and 6.54000E-12 for Sr and Nd, respectively

Chapter II

Kimberlites and alkalic rocks of the southwestern São Francisco craton

II.1 - INTRODUCTION

Kimberlite pipes in the Mata da Corda region of western Minas Gerais state of Brazil were first referred to by Rimann (1917). These rocks were later considered not to be true kimberlites, but varieties of ultrabasic alkaline rocks (Guimarães, 1932). Barbosa et al. (1976) maintain that the discovery of the first kimberlite in the Coromandel area was in 1969. Since then many others have been identified (e.g. Svisero et al., 1984), all of them believed to be upper-Cretaceous in age (Shobbenhaus et al., 1981 and 1984; Tompkins and Gonzaga, 1989). Leonardos and Ülbrich (1987) reported the discovery of madupitic lamproites in the Presidente Olegário area. A systematic prospecting program for kimberlites was started by Sopemi S.A./BRGM in 1967 and so far has resulted in the location of more than 300 "kimberlite-type" (*sensu latu*) bodies in the districts of Coromandel, Monte Carmelo, Estrela do Sul, Douradoquara, Patrocínio and Patos de Minas. However, detailed petrography indicates that only a few of them are "true kimberlites" (*sensu strictu*). None of them contain economic concentrations of diamonds.

Alluvial diamonds have been known to occur in the southern portion of the São Francisco Craton since the early 1700's. The origin of these diamond occurrences and the age and location of their primary sources has been long debated (e.g. Gonzaga & Tompkins, 1991; and references therein). The existence of a Proterozoic or older primary source(s) is attested by MesoProterozoic diamond-bearing conglomerates of the Sopa-Brumadinho Formation (Espinhaço Supergroup), which have supported extensive diamond mining activities in the Diamantina area. Fluvial transport directions suggest that the central São Francisco Craton was the source of these shallow epicontinental sediments (e.g. Dossin et al., 1985). A nearby Cretaceous primary source

for the diamonds from upper-Cretaceous diamond-bearing polymictic conglomerates in the Romaria mine has been suggested on the basis of heavy mineral characteristics (Svisero 1979; Svisero and Meyer, 1981). Except for the established mines in these two areas, all the other numerous small scale-diamond mining activities in the southern São Francisco Craton area are restricted to recent alluvial deposits. Tompkins and Gonzaga (1989) postulate Precambrian primary source(s) for the large diamonds (>100 ct), and suggest that the distribution of the majority of the diamonds in the area can be correlated with *(a)* the NeoProterozoic Jequitaí glacial deposits; *(b)* the Cambrian Santa Fé glacial deposits; and *(c)* reconcentration of *(a+b)* into more recent deposits. They further speculate that the upper Cretaceous kimberlites in the marginally cratonic Coromandel area are non-economic with respect to diamonds because of inferred lithospheric thinning during the Brasiliano orogeny.

On a regional scale, the petrographic characteristics and distribution of alkaline igneous activity along the São Francisco craton margin are comparable to those in southern Africa (e.g. the olivine melilitite-carbonatite suite related to kimberlites in the NE of Namaqualand, South Africa), southwestern Uganda and Montana. By analogy with southern Africa (e.g. Gurney et al., 1991), diamondiferous kimberlite provinces should be found "on-craton", and accompanied towards and beyond the margin of the craton by non-diamondiferous kimberlites, alkaline complexes, carbonatites, lamprophyres and other intrusive and extrusive rocks of diverse character, often containing silica-deficient minerals such as melilite, monticellite, nepheline, leucite and perovskite. In other parts of the world, however, diamonds also occur in kimberlites and olivine lamproites emplaced beyond the craton margin. Examples are along the Wyoming craton in the western U.S.A, and along the Pilbara craton in northwestern Australia (e.g. Mitchell and Bergman, 1991).

In this chapter, the first whole-rock isotopic analyses of Brazilian kimberlites and related rocks are presented. Isotopic signatures of kimberlitic rocks in the Coromandel area of the Minas Gerais state of Brazil, together with mineralogy, major and trace element compositions, are compared to those of related alkalic rocks in the same area and to those of South African kimberlites. A number of research groups from other institutions have been investigating the

same occurrences in terms of petrography and mineral chemistry. Their work is referred to in section II.2.

Exploration by the Brazilian Geological Survey reported average platinum grades of 2 g/ton for the tuffs of Patos, Coromandel and Carmo do Paranaíba, but there are no known platinum deposits in the area. Leonardos et al. (1991) have described platinum-copper-nickel sulphide minerals dispersed in magnetite crystals in the Mata da Corda volcanics near Presidente Olegário, and suggested that these sulphides may have been the origin of the secondary platinum nuggets which are occasionally recovered in heavy mineral concentrates in the area. The platinum-group-element (PGE) and gold contents of the volcanic tuffs of the Mata da Corda Formation, of the kimberlites, and of the "kimberlite-related" rock-types in the southwestern Minas Gerais area have also been investigated in this project and are reported in section II.3.

II.1.1 - Geological setting

Important tectonic movements have taken place along the western margin of the São Francisco craton since its final stabilization at the end of the Brasiliano orogeny. The northern limits of early Paleozoic transgressive marine formations (Paraná Group) which were succeeded by Devonian-Carboniferous glacial and post-glacial sequences (Tubarão and Passa Dois Groups); and Mesozoic continental sequences (São Bento Group) are delineated by the Goiânia flexure. Deposition of the late Jurassic and early Cretaceous eolian sedimentary rocks and Serra Geral flood basalts of the Paraná Province were contemporaneous with the development of a tectonic uplift named the Alto Paranaíba uplift (Brito Neves et al., 1984). The most important foci of Mesozoic alkalic magmatic activity (upper Cretaceous kimberlites, olivine melilitites, tuffaceous and breccia filled diatremes, and carbonatite complexes) occurred in the Alto Paranaíba area over a period of about 40 Ma (i.e. from 80 to 120 Ma), concomitant with an early Cretaceous continental extension and the deposition of the Cretaceous volcanics comprising the Mata da Corda Formation (Figures II.1 to II.3). These alkaline intrusions are part of an approximately 1500 km-long NW-SE lineament (named Lineament 125 AZ by Bardet, 1977) defined by alkaline intrusives and most of the known Brazilian kimberlites (Schobbenhaus et al., 1981 and 1984; Tompkins and Gonzaga, 1989; Tompkins, 1991; Almeida and Svisero, 1991).

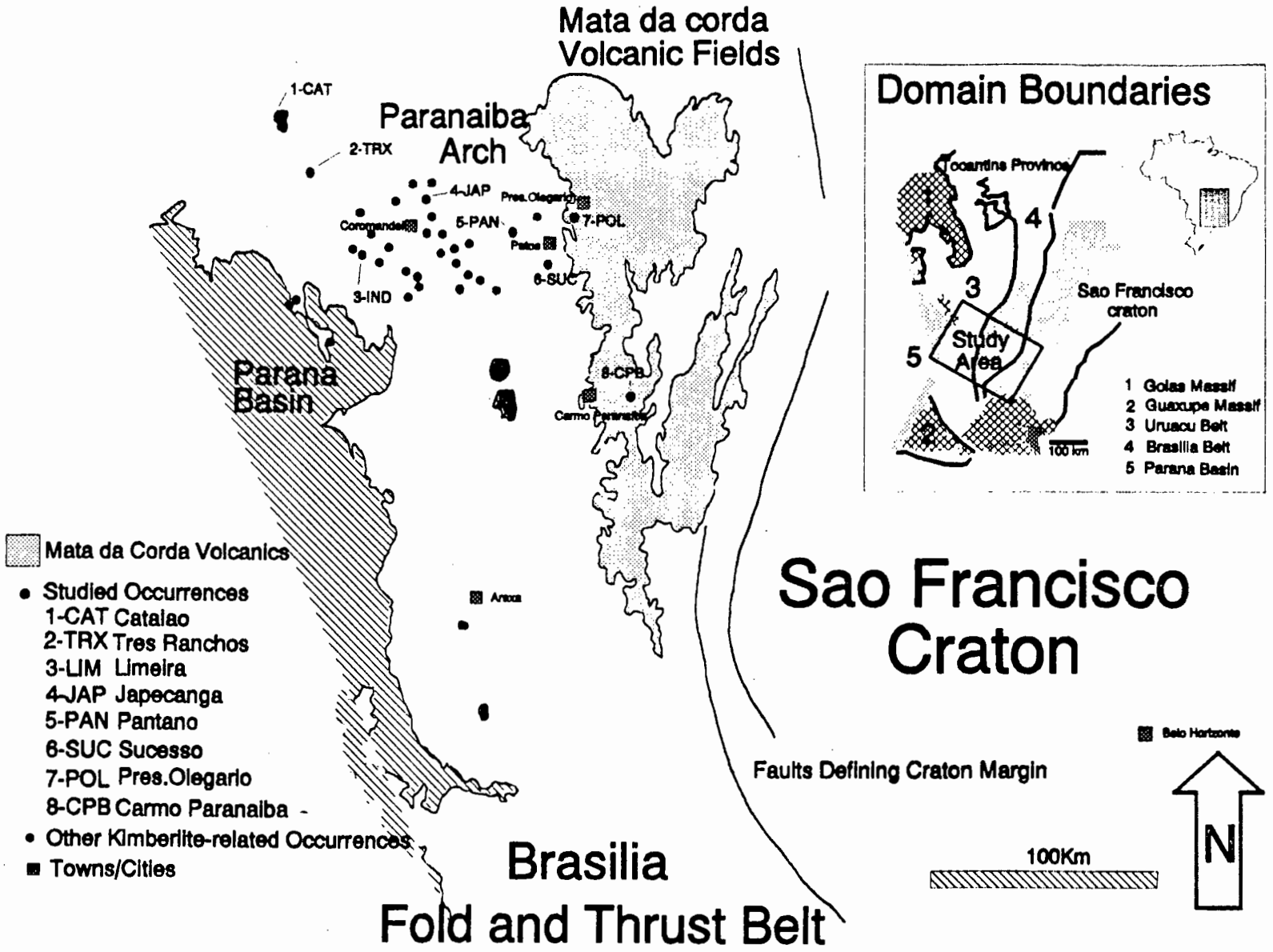

Figure II.1 - Geological setting and location of studied occurrences (numbered 1 to 8). The Goiânia flexure controlled the northern extension of the Mesozoic continental sequences and was replaced by the late-Jurassic to late-Cretaceous Alto Paranaíba arch. Repeated tectonic uplift along the arch and reactivation of old NW-SE lineaments provided structural controls for alkalic magmatic activity and for exposure of deep erosion levels. Note the high concentration of kimberlite-related intrusives in the Alto Paranaíba region and the distribution of the intrusives selected for this study along a 200 km traverse which is roughly perpendicular to the western margin of the craton.

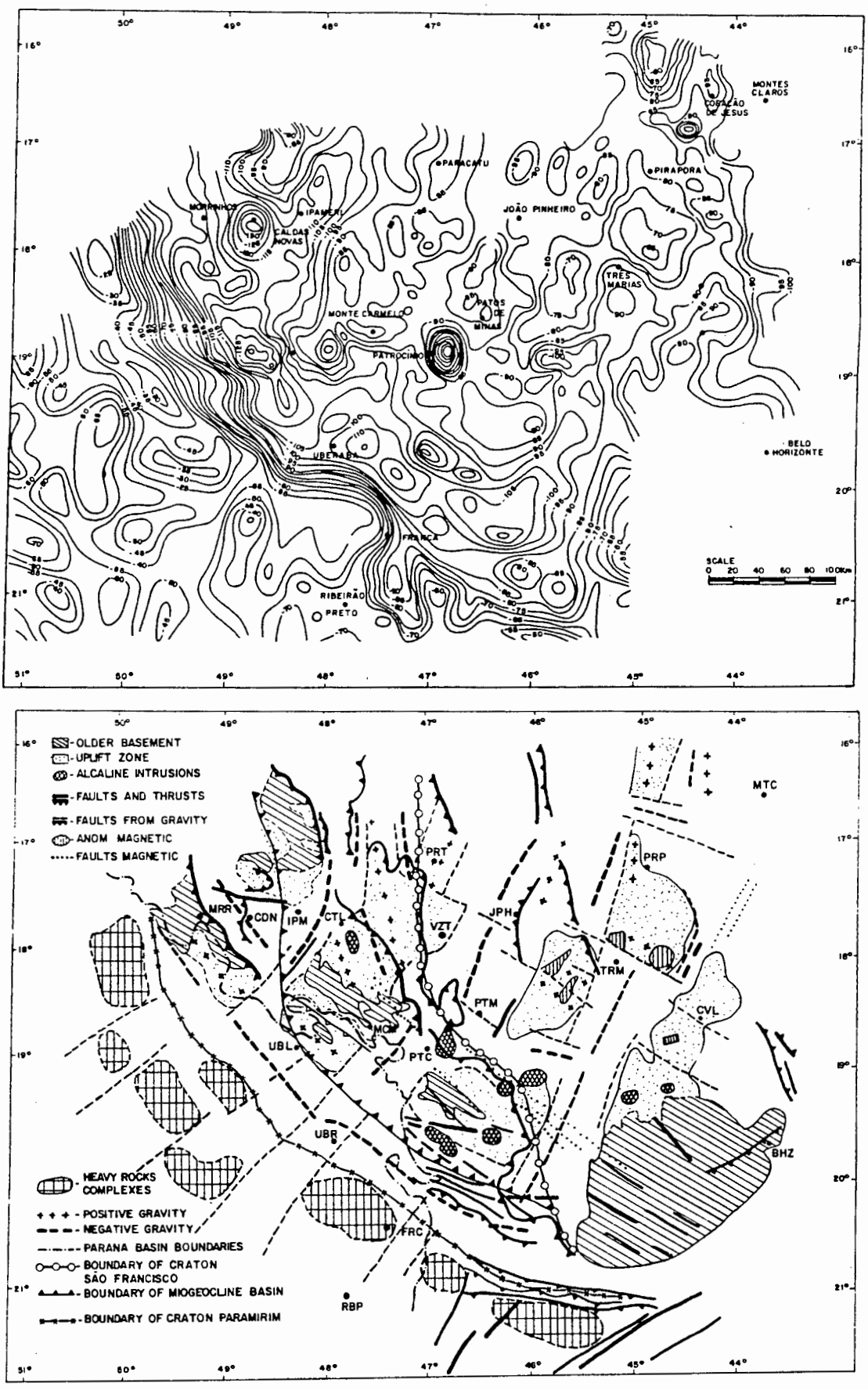

Figure II.2 - Bouguer anomaly map and interpretative structural map of SW Minas Gerais.

The Mesozoic alkalic volcanic fields along the southwestern margin of the São Francisco Craton occur largely on tectonically uplifted blocks, or are preserved in the graben zones between these uplifted blocks. The area has experienced several periods of uplift during the Phanerozoic, particularly during the end of the Jurassic to the Cretaceous when the Wealdenian reactivation of the South American Platform took place in the Triângulo Mineiro, Alto Paranaíba and southeastern Goiás (e.g. Hasui et al., 1977). Sedimentation and volcanic activity apparently broadly coincided with increased rates of uplift. Exposure of both Proterozoic meta-sediments and Mesozoic volcanic and non-volcanic sediments display increasingly deeper erosion levels to the west; the greatest erosion (a minimum of 1000 meters; F.Baars, pers.comm., 1992) having occurred in the regions which today mark the northern limits of the Paraná Basin. Tertiary to recent river terraces indicate that neotectonic uplift is continuing, and Cenozoic reactivation of older lineaments has also been documented (A. Saadi, pers. comm. 1991).

The main carbonatite complexes in the area are Araxá, Tapira, Salitre, Serra Negra and Catalão I and II (Figure II.1). Most complexes are characterized by an early ultramafic stage of mica peridotite and pyroxenite; an intermediate carbonatitic stage represented by phoscorites, sovites, berforsites; and a late hydrothermal stage with remobilized calcite, sulphides, barite and quartz. In the Serra Negra and Salitre complexes apatite and calcite were broken down by lateritic weathering; and supergene anatase was formed in economic concentrations following decalcification of perovskite (e.g. Mariano & Marchetto, 1991). In the Catalão complexes supergene and residual deposits of apatite, Ba-pyrochlore, vermiculite, anatase, REE carbonates and phosphates are present in abundance (e.g. Danni et al., 1991).

II.1.2 - Remote Sensing and GIS

The Thematic Mapping (TM) imagery of the area between approximately 18°S & 19°30'S and 46°25'W & 48°W has been studied in close detail. Color composites 742 (vegetation green) and 752 (vegetation suppressed) are able to produce strong contrast between country rocks of volcanosedimentary origin (brown and blue tones) and basement or intrusive granitic and gneissic rocks (white tones) and illustrate the distinctive reflective properties and textures of the different lithologies in the area (see photographs in Figure II.4).

Large-scale structural relationships are visible on TM imagery. Fault traces normally appear as non-reflective or vegetated lineaments and are best viewed on false color composites in bands 752 or 751. There is a distinct association between known alkaline occurrences and faults bounding graben-horst structures. Such a structural setting applies to the Limeira, Japecanga, Pântano, Sucesso and Presidente Olegário bodies (localities 3 to 7, respectively, in Figure II.1). The Pântano body (locality 5 in Figure II.1) is associated with a vegetation species that is more reflective in bands 4 and 2 than the regional vegetation. A similar feature is seen on the volcanic cone of the Presidente Olegário body (locality 7). Limeira (locality 3) and, to a lesser extent, Sucesso (locality,6) are marked by a marginally darker exposure in band 7. These two localities would be extremely difficult to recognize without adequate ground control.

The Serra Negra complex is associated with a fenitization halo which is expressed on the "clay-iron-prediction" composite as a negative anomaly (see photographs in Figure II.4). This indicates that the halo is not associated with hydrous minerals and that the fenitizing fluid species were water-poor. Field observations confirm that the fenite aureole is composed dominantly of carbonate.

Field observations obtained during regional scale E-W traverses were combined with information obtained during the remote sensing imagery interpretation and overlaid on pre-existing maps of the area (the "Carta Metalogenética Patos de Minas" and the maps from the "Projeto Chaminés - Geologia do Triângulo Mineiro"), and assembled in Figure II.3 using Geographic Information System (GIS) technology. In this process, the compiled map was digitized and various elements were digitally classified to allow for separate manipulation based on gechronological, igneous, metamorphic and structural data. With this information, complex enquiries and demands can now be made to test possible relationships between the different data sets.

Figure II.3 - Set of maps digitized from 1:250000 scale geology maps ("Carta Metalogenética Patos de Minas" and "Geologia do Triângulo Mineiro - Projeto Chaminés"), remote sensing interpretation both on screen and on 1:100000 hard-copy images, and field data compiled using GIS technology. The digital data sets were produced and manipulated using an Intergraph workstation. A map with the geology of the study area in the southwestern São Francisco craton (copy plotted in a bigger scale available in the back cover) was generated to illustrate the geological information available. Overlays with the hydrography (digitized by Sopemi S.A. from 1:50000 topographic maps) and major lineaments are also shown. The exact location of the studied alkalic occurrences (key for the occurrences as in Table II.1) and major roads have been included in a "location map". The "graphical representation of Brazil database" illustrates the location of all data cells available at the moment. Those elements can be digitally classified to allow for separate manipulation based on geochronological, petrological or structural data and complex enquiries and demands can now be made to test possible relationships between the data sets.

GEOLOGY OF SOUTH WESTERN SAO FRANCISCO CRATON

Produced using GIS Technology

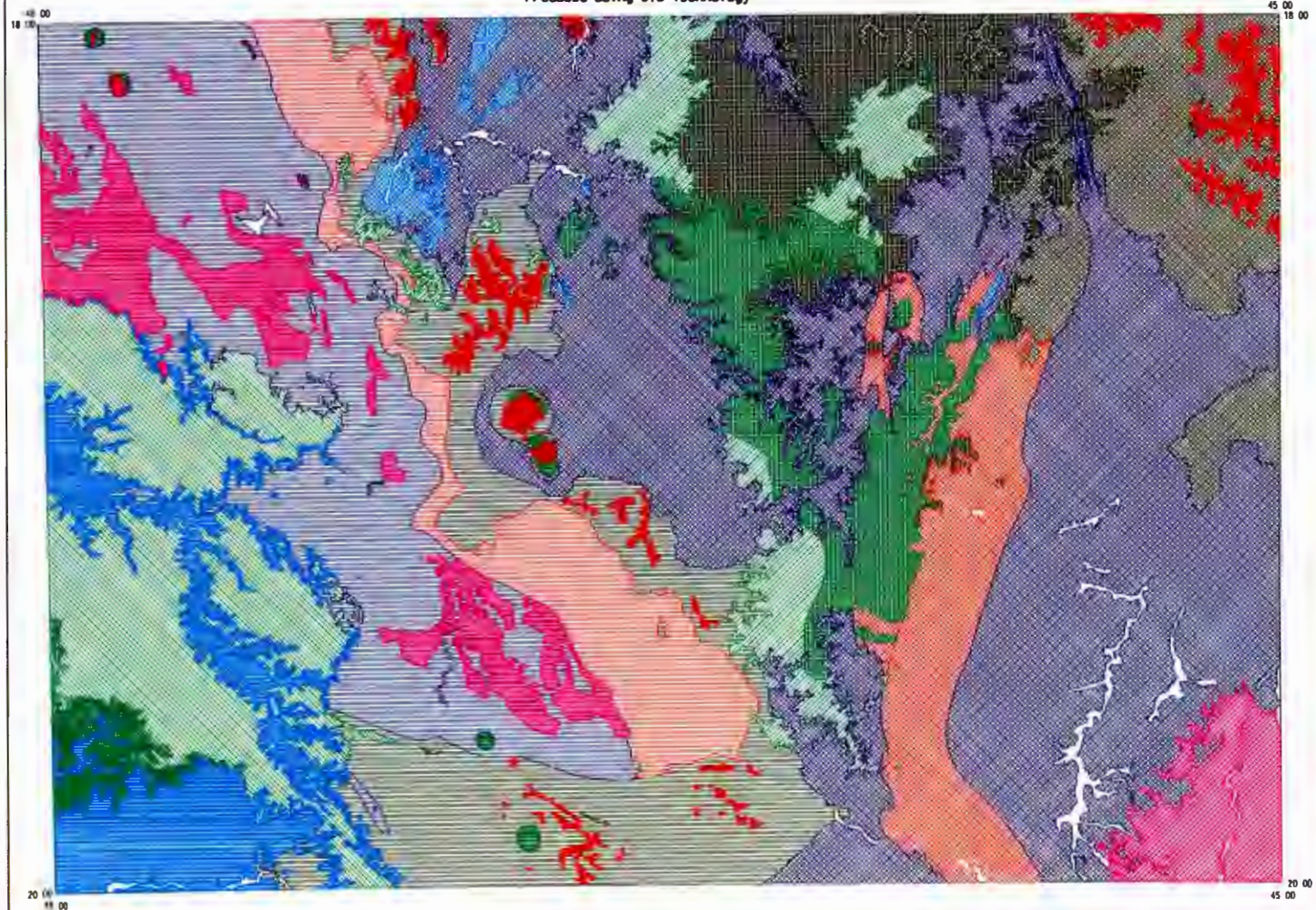

LEGEND

QUATERNARY

- Alluvial Sands

TERTIARY

- Laterites

CRETACEOUS

- Alkaline Complexes
- Mata da Corda Sandstones
- Mata da Corda Tuffs
- Bauru Sandstones
- Bauru Tuffs
- Areado Sandstones
- Serra Geral Volcanics

UPPER TO MIDDLE PROTEROZOIC

- Bambui Arkoses
- Bambui Limestones
- Bambui Siltstones
- Bambui Metapelites
- Ibia Quartzites
- Araxa Schists and Amphibolites
- Canastra Schists and Quartzites

LOWER PROTEROZOIC TO ARCHEAN

- Granite-gneiss (mainly Proterozoic)
- Granite-gneiss (mainly Archean)

N

Kilometers

0 10 50 100

HYDROGRAPHY

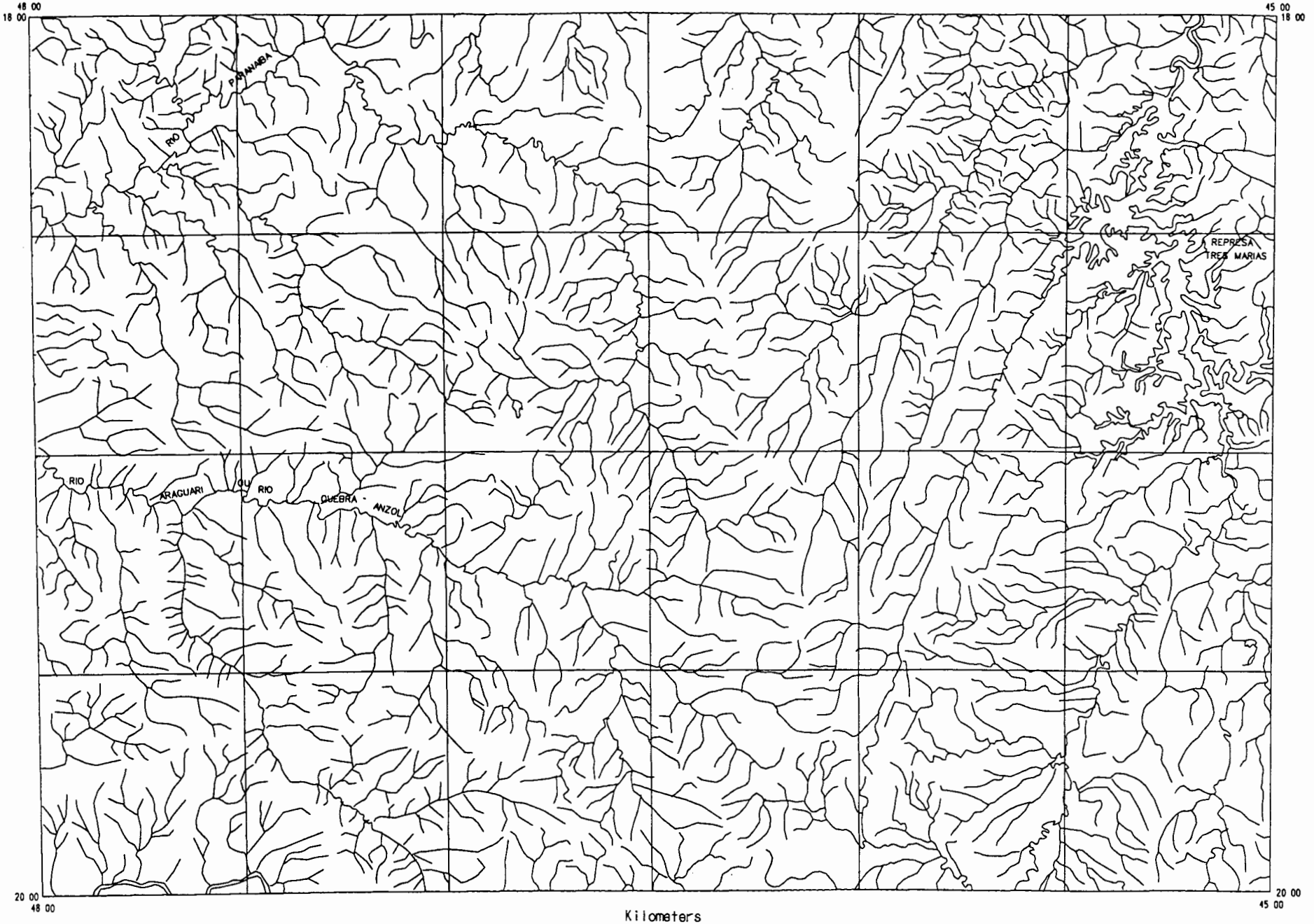

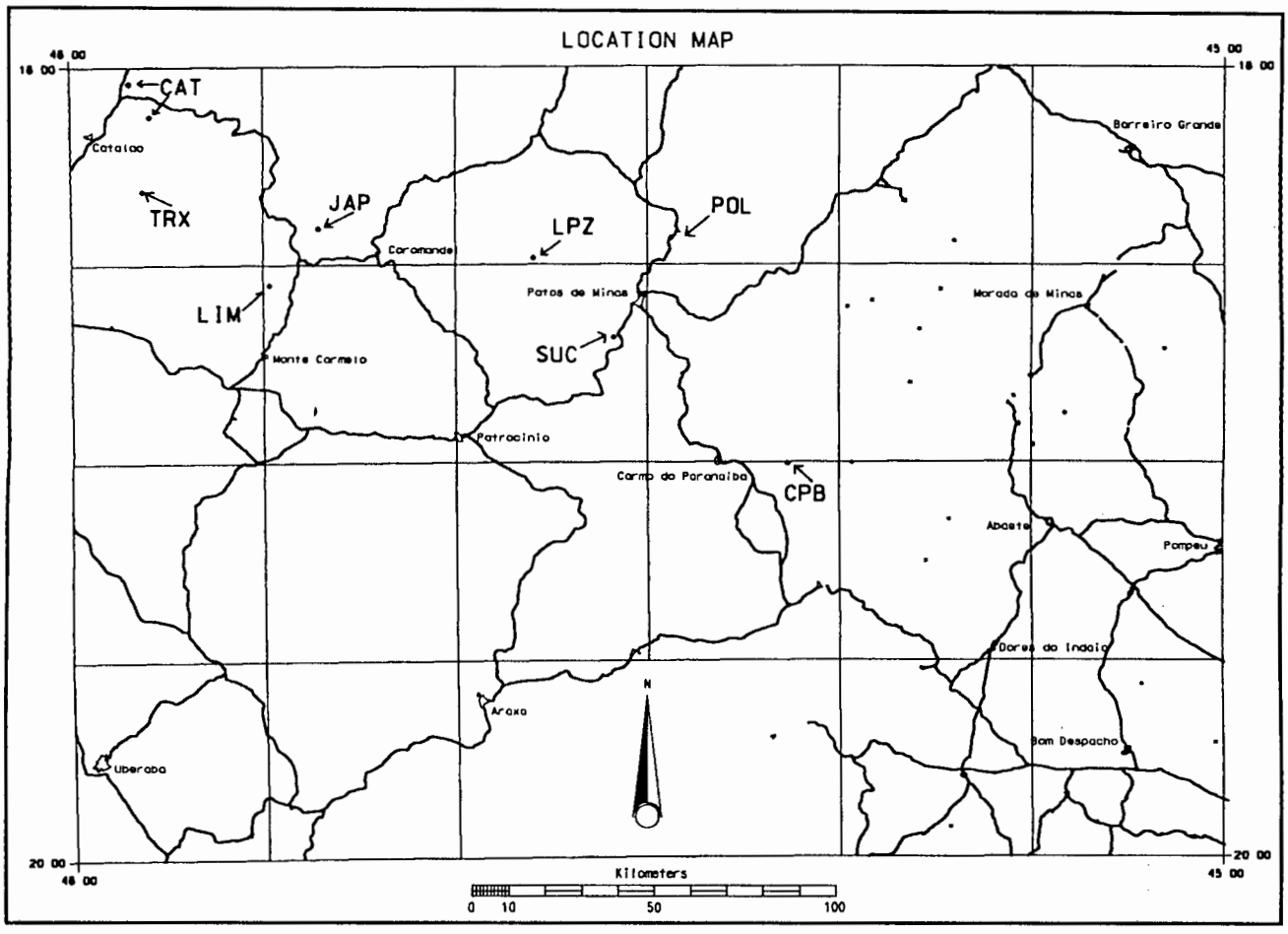
LOCATION MAP
48 00
18 00
45 00
18 00
CAT
Cataloo
TRX
JAP
LPZ
POL
Barreiro Grande
Coromande
Patos de Minas
Morada de Minas
LIM
SUC
Monte Carmelo
Patrocinio
Carmo do Paranaiba
CPB
Abaete
Pompeu
Dores do Indaia
Araxa
Bom Despacho
Uberaba
N
20 00
48 00
20 00
45 00
Kilometers
0 10 50 100

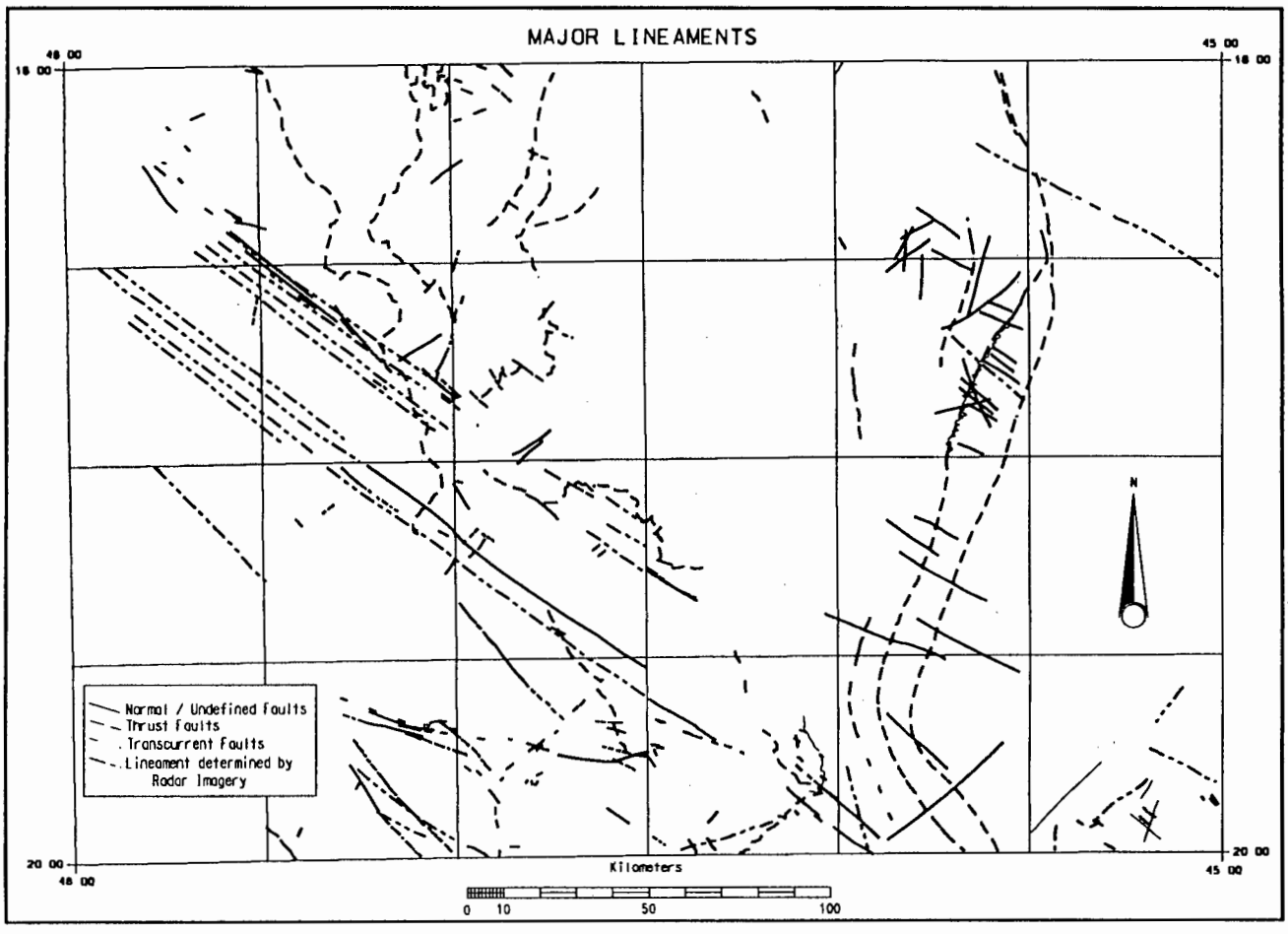
MAJOR LINEAMENTS
48 00
18 00
45 00
18 00
Normal / Undefined Faults
Thrust Faults
Transcurrent Faults
Lineament determined by Radar Imagery
N
20 00
48 00
20 00
45 00
Kilometers
0 10 50 100

GRAPHICAL REPRESENTATION OF BRAZIL DATABASE

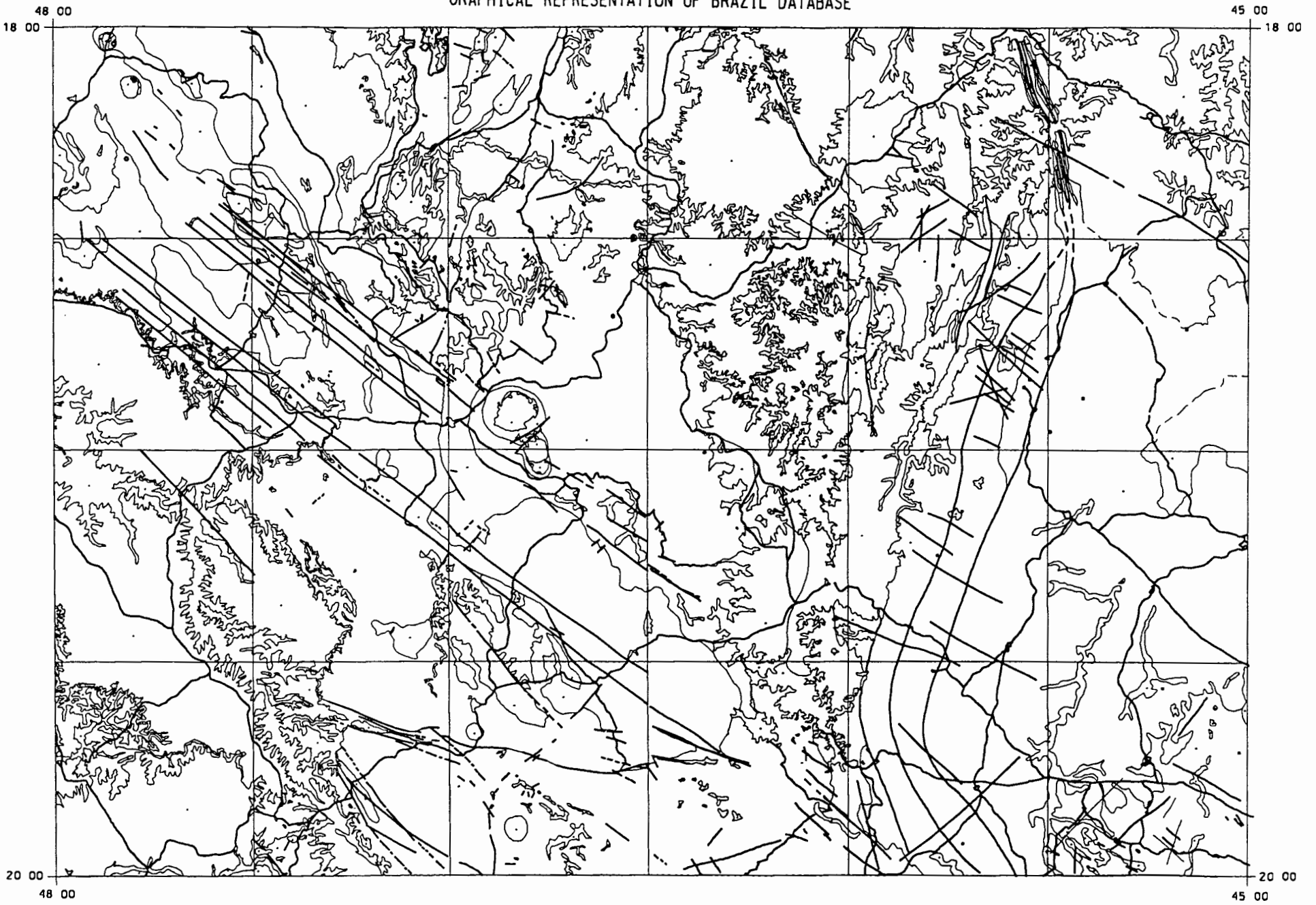

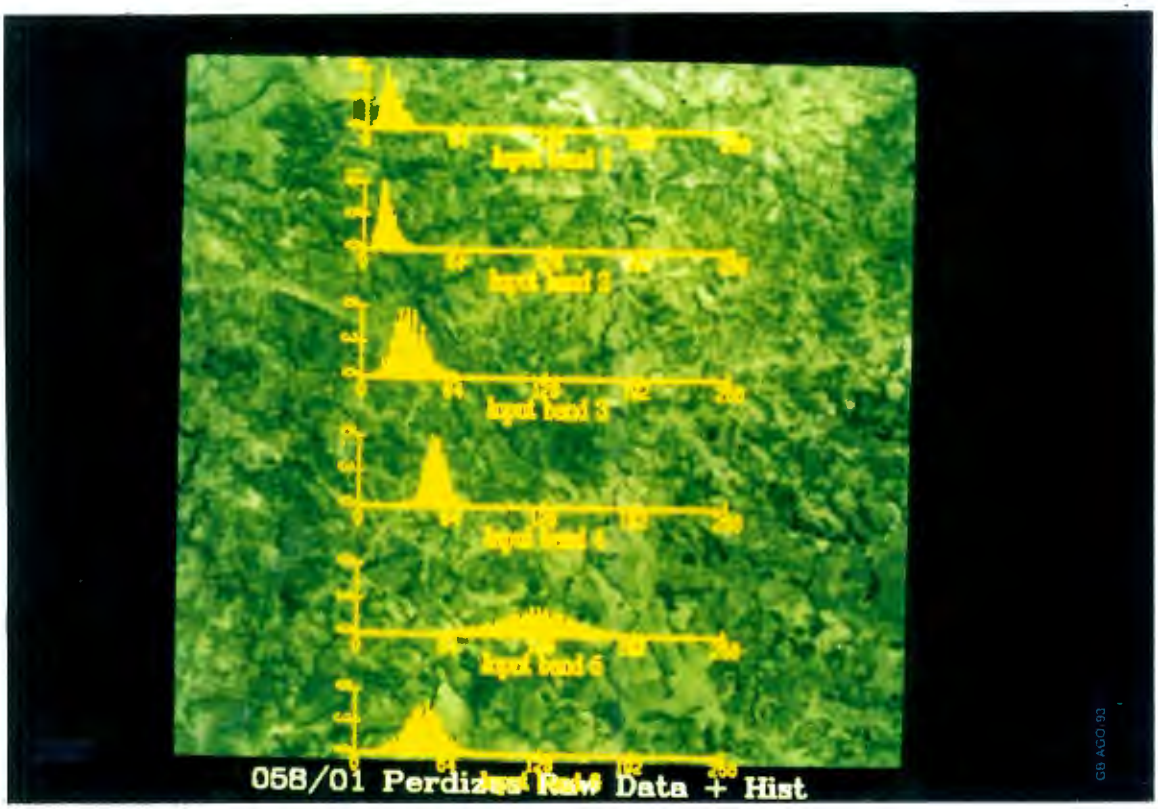

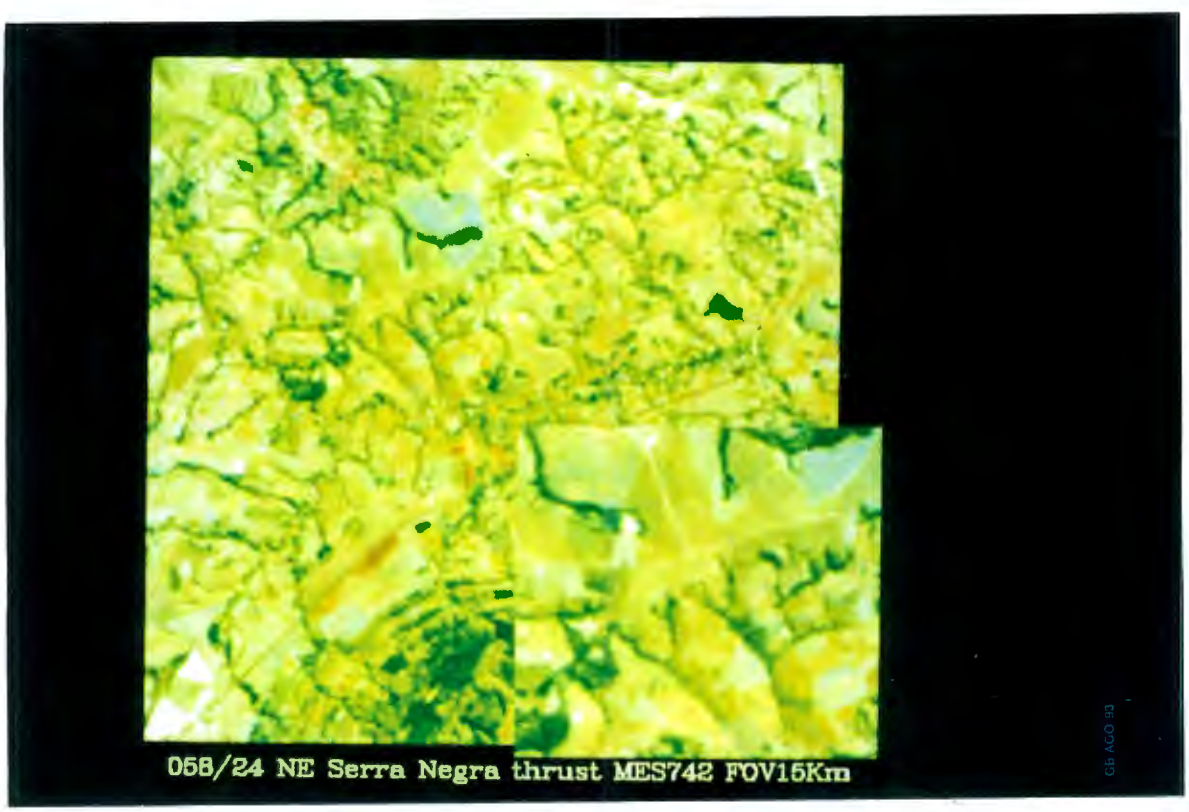

Figure II.4 - Photographs illustrating the use of thematic mapping (TM) imagery in this thesis. Photograph 058/01, covering the area in the vicinities of the Perdizes river, illustrates raw data and histogram for the distribution of reflectance in bands 1 to 7 before the Maximum Entropy Scaling (MES) technique was used. Photograph 058/24 illustrates thrust faults NE of the Serra Negra Complex (field of view 15 km and inset 5 km) using a color composite 742 produced after MES. Note the clear identification of fault traces using the image and the evidence for recent river capture. Photograph 058/22 illustrates the Serra Negra Complex (location shown in Figures II.1 to II.3; field of view 15 km) divided in two halves: left = MES color composite 742 (vegetation green); and right = clay iron prediction composite. It indicates that the halo is not associated with hydrous minerals and that the fenitizing fluid species were water-poor. Photograph 058/28 illustrates the contrasting reflective properties of basement or intrusive granitic and gneissic rocks (white tones) and the Araxá Group volcanosedimentary units in the vicinities of Monte Carmelo. Field of view 15 km. Again, left = MES color composite 742 (vegetation green); and right = clay iron prediction composite.

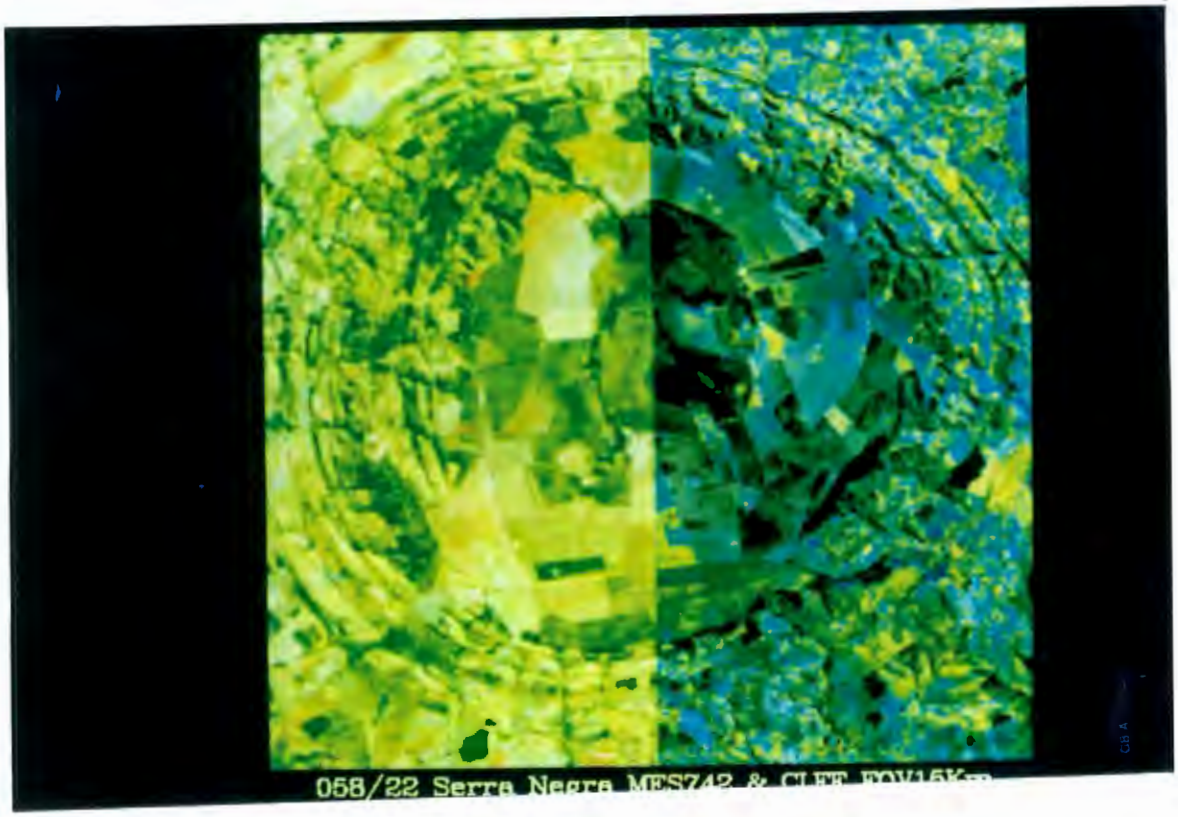
058/22 Serra Negra MES742 &

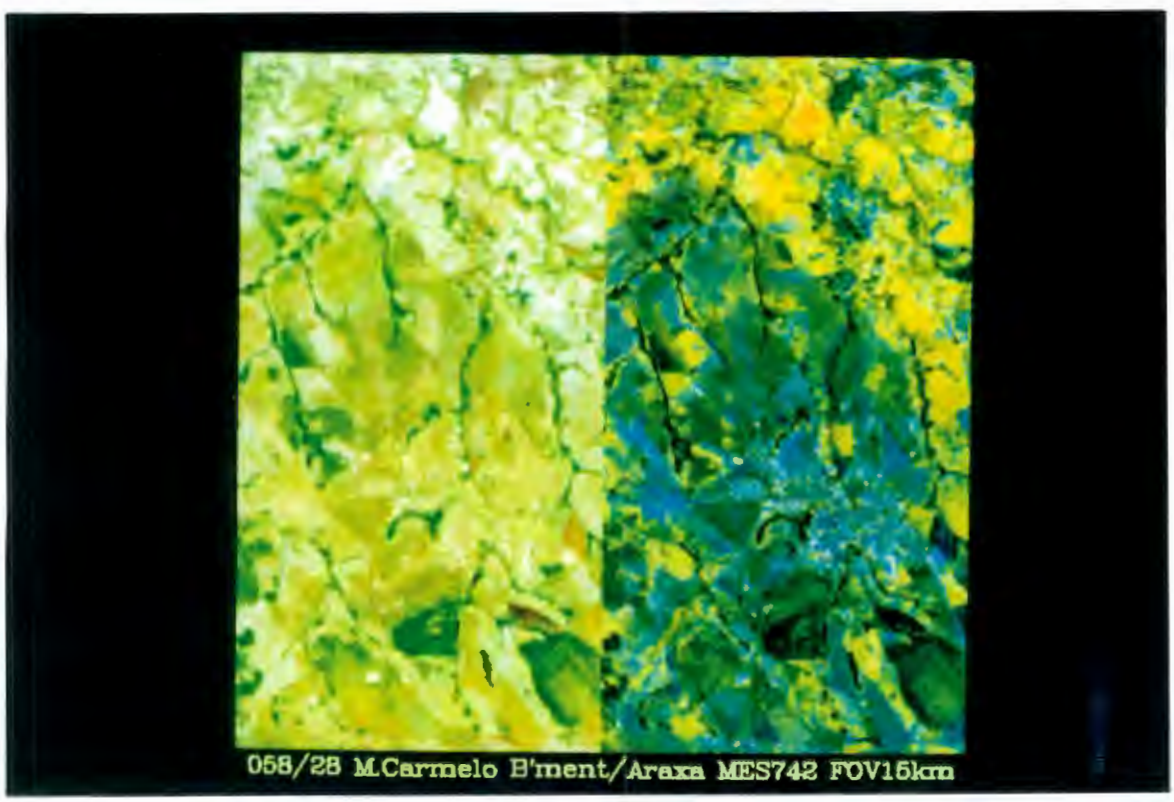
058/28 M.Carmelo B'rnent/Araxa MES742 FOV15km

II.1.3 - Selection and sampling of occurrences

Most of the "kimberlite-type" rocks thus far identified in the study area are intensely weathered at the surface or concealed by thick (and similarly altered) crater or diatreme facies material. The thick weathering profile throughout Brazil is in part the reason for the relative late discovery of kimberlites in this country. In addition, the intense alteration limits dramatically the range of rocks suitable for isotope analysis or other geochemical work.

During a first stage of field-work, forty-two kimberlite or "kimberlite-related" occurrences were selected and visited. From the initial forty-two, eight localities were chosen in such a way that samples selected for the geochemical analysis are the freshest possible material, and that these samples represent a substantial range of different alkalic ultrabasic rock types in the Coromandel area. In addition, the selected intrusions are distributed along a 200 km E-W traverse, roughly perpendicular to the western margin of the São Francisco Craton. The locations of the studied occurrences are indicated in Figures II.1 and II.3. Heavy-mineral concentrates were collected (two 100-litre sample volumes for each locality; one from saprolite and one from alluvium immediately downstream from the sample locality) and analyzed for garnets, pyroxenes and mantle oxide-minerals. The recovered mineral-grains are listed in Table II.1. Because of the very low incidence (virtual absence in most cases) of garnets and chromium spinels in most of the selected occurrences, the micro-probe study of these populations has been postponed until more mineral grains become available for analysis.

II.2 - GEOLOGY OF SELECTED OCCURRENCES

II.2.1 - Terminology and classification

There is no general agreement regarding the nomenclature and classification of the alkaline rocks in the study area. The isotopic resemblance of the Minas Gerais kimberlites to carbonatites (see below) and the rather unusual mineral compositions of the intrusives in the area (e.g. Danni et al., 1991) have provoked different and controversial interpretations and nomenclature for the same occurrences. For example, Svisero et al. (1984) referred to most of the occurrences

discussed in this work as kimberlites. The volcanics outcropping south of Presidente Olegário were denoted lamproites by Leonardos and Ulbrich (1987). Bizzi et al. (1990, 1991 and 1993) indicated that the alkaline province encompass both kimberlites and high-level volcanics of kamafugitic affinity; whereas Mitchell and Bergman (1991) indicated a lamproitic character for the province.

Six of the eight intrusives selected for this work have been visited by many participants during the Fifth International Kimberlite Conference held in Brazil in 1991. The matter of nomenclature was extensively discussed among the different geoscientists involved in studying these rocks, but no consensus was reached. Some of the rocks which have petrography and whole-rock geochemistry similar to South African kimberlites, have micas with compositions which resemble those of lamproites. Some others, which in many thin sections are petrographically similar to lamproites and have micas with compositions similar to those of lamproites, have a whole-rock geochemistry similar to kamafugites. Moreover, in the Limeira and Presidente Olegário localities at least, lateral variation is such that kimberlite-like and lamproite-like features and mineralogy are restricted to part of the magmatic material only. This nomenclature debate is an important problem deserving of serious analysis, but the detailed study and discussion of all petrographic variations in each one of the studied localities are beyond the objectives of this thesis. My objective in this section is simply to document the main characteristics of the rock samples used for isotope work and to place them in the context of the intrusive as a whole.

For the sake of simplicity, in his thesis the studied rocks have been categorized into four groups viz. kimberlites, alkalic rocks of kimberlitic affinity, rift-related alkalic rocks (related either to the Paraná volcanism or to the Mata da Corda Formation) and carbonatites. The explanation and justification for this classification scheme and of the names adopted in this thesis are described below.

The "true-kimberlites" discussed here are the localities 2 and 3 in Figure II.1, designated Tres Ranchos and Limeira kimberlites, respectively. Chemical, petrographic and mineralogic distinctions between them and the South African Group I kimberlites are no greater than the

distinction between Group I kimberlites and the South African "transitional kimberlites" of Clark et al. (1991). In consideration of contrasting opinions of other authors (see also Meyer & Svisero, 1991; Meyer et al., 1991 and 1993) the term kimberlite *(sensu strictu)* has been avoided in this thesis. I have prefixed the closest petrographic rock type with the geographic locality (viz. "Brazilian kimberlite"), and I suggest this nomenclature should be adopted until a consensus is reached on the controversial issue of giving these rocks a name.

The nomenclature of the rocks grouped under "alkalic rocks with kimberlitic affinity" is even more contentious. These diatremes and plugs carry high-Mg/low-Cr ilmenites and garnets of various compositions. Their hypabysal phases have both chemical, mineralogical and petrographic similarities to the above mentioned "true-kimberlites" (e.g. two generations of olivine and matrix mineralogy) that suggest a kimberlitic affinity for these rocks. The studied samples from the localities designated Japecanga and Pântano are textually similar to hypabysal aphanitic kimberlites but differ in the shape of olivine phenocrysts which tend to be more elongated, the presence of dolomite phenocrysts(?) and the relative abundance of perovskite grains. In this respect these two occurrences have rather stronger affinities with shallower derived melts (e.g. olivine melilitites and mildly alkalic ultrabasic rocks related to kamafugites). For the purpose of this work, these two localities (numbered 4 and 5 in Figure II.1) are referred to as "mica peridotites". This name, which has no genetic implications, has been used by other authors working on these intrusives (e.g. Meyer et al., 1991) and is used here to denote a rock that in most aspects looks like a kimberlite, but in some aspects is anomalous and as such are "ambiguous" kimberlites.

The volcanic fields within the Mata da Corda Formation have a well preserved record of lava flows, volcanic breccias, ashes and volcanic and non-volcanic sediments (e.g. Seer and Moraes, 1988; Seer et al., 1989; Leonardos and Ulbrich, 1987; Leonardos et al., 1991). Sediment- and breccia-filled maars (or diatremes) of alkalic affinity ranging from 50 to 500 m or more in diameter are widespread in the regions of Carmo do Paranaíba, Patos de Minas and Presidente Olegário. The Cretaceous volcanic and sedimentary stratigraphy of the Mata da Corda and Areado Formations have been affected by large-scale syn-volcanic listric normal faults, and there

is clear evidence, both in the field and in satellite imagery, for tectonic control of these extrusives along major NNE-SSW oriented extension structures. Three localities (numbered 6, 7 and 8 in Figure II.1) have also been selected for isotopic study and are here designated as "rift-related alkalic rocks". Radiometric determination of emplacement ages (see discussion below) indicate a significant age gap between the rocks previously believed to be part of the same geologic sequence (i.e. the Mata da Corda Formation). As a result, the locality denominated Sucesso (number 6) is now believed to represent late-stage alkaline activity related to the Jurassic Paraná volcanism. Emplacement ages and general characteristics of the localities Presidente Olegário (number 7) and Carmo do Paranaíba (number 8) confirm they are integral parts of the upper Cretaceous (Hasui and Cordani, 1968) Mata da Corda Formation.

The main petrographic and mineralogical characteristics of the various rock types used in the isotope work, with details for each occurrence, including heavy mineral abundance recovered from soil samples, are presented below and summarized in Table II.1.

II.2.2 - Brazilian kimberlites

The kimberlitic rocks selected from the localities of Tres Ranchos (also known as the Fazenda Alagoinha intrusion; Danni et al., 1991) and Limeira (referred to as Limeira I by Meyer and Svisero, 1991) intrude granite-gneissic basement rocks. The Tres Ranchos kimberlite occurs as a 150 x 350 meter long blow, striking about N40W. This kimberlite is spatially associated with a dolerite dike which, although not dated, is almost certainly related to the Paraná basalts on the basis of field criteria. This association indicates that locally both events (i.e. the Jurassic dikes related to the Paraná volcanism and the upper Cretaceous kimberlites) may have exploited similar structural guides to the surface. The Limeira kimberlite occurs as a circular pipe about 200 meters in diameter at the present level of erosion. Chemically, petrographically and mineralogically, these kimberlites are similar to the South African Group I kimberlites (i.e. hypabysal calcite-monticellite types, with uniformly distributed groundmass minerals). However, the peculiar composition of micas and other matrix minerals (e.g. spinels) in these kimberlites (see Figure II.9), together with their distinct isotope compositions (Table II.5), characterizes the Brazilian group of kimberlites as being a "clan" distinct to kimberlites from elsewhere (Bizzi et

al., 1993).

The Tres Ranchos kimberlite pipe (locality 2 in Figure II.1) mineralogy comprises macrocrysts and phenocrysts of olivine (10 to 0.2 mm) and phlogopite (3 to <0.1 mm) set in a matrix of serpentinized monticellite, phlogopite, opaque minerals, apatite, perovskite, serpentine and calcite. Significantly, ilmenites have not been recovered from the mineral concentrates nor identified in thin sections. Consistent accurate petrographic distinction between olivine phenocrysts and xenocrysts is not possible. In most cases the olivines (usually with compositions Fo_{90-92}, occasionally with Mg as low as Fo_{85}) are partly replaced by serpentine, steatite or clay, and associated to mica (phlogopite and/or vermiculite). Phlogopite has been identified both as megacrysts and phenocrysts. Danni et al. (1991) have recognized three different compositional groups of micas in this intrusive and attributed variations in TiO_2 and Al_2O_3 among the different groups to changes in the fluid composition during late-stage crystallization. These authors indicate that the carbonatitic/lamproitic-like composition of such late-stage fluids could possibly be related to the evolved compositions of mantle spinels (which plot inside the lamproite field of Mitchell, 1985; or in between the kimberlite and the lamproite compositional fields). Rounded to sub-angular crustal and mantle derived xenolithic fragments (up to 10 cm) have been replaced by calcite, serpentine, phlogopite, opaque minerals, clay minerals and minor clinopyroxene (see Figure II.5). A few of the xenoliths are carbonatized basalts with relics of ophitic and sub-ophitic textures.

The Limeira kimberlite pipe (locality 3 in Figure II.1) comprises macrocrysts and phenocrysts of olivine (8 to 0.3 mm), phlogopite (2 to 0.1 mm) and ilmenite (up to 2 mm) set in a matrix of serpentine, monticellite, apatite, perovskite and opaque minerals. A range between Fo_{92} and Fo_{84} (accompanied by increasing TiO_2 contents up to 0.07 wt.%) has been reported for the olivines (Meyer and Svisero, 1991; Meyer et al., 1993). In some cases phenocrysts partially or wholly enclose euhedral groundmass spinels in their outer margins, indicating contemporaneous crystallization of these minerals. In Figure II.9 spinel and mica compositions from the Limeira kimberlite are compared to those of the Tres Ranchos kimberlite. Further mineral chemistry, petrography and compositional variations within the Limeira kimberlite have

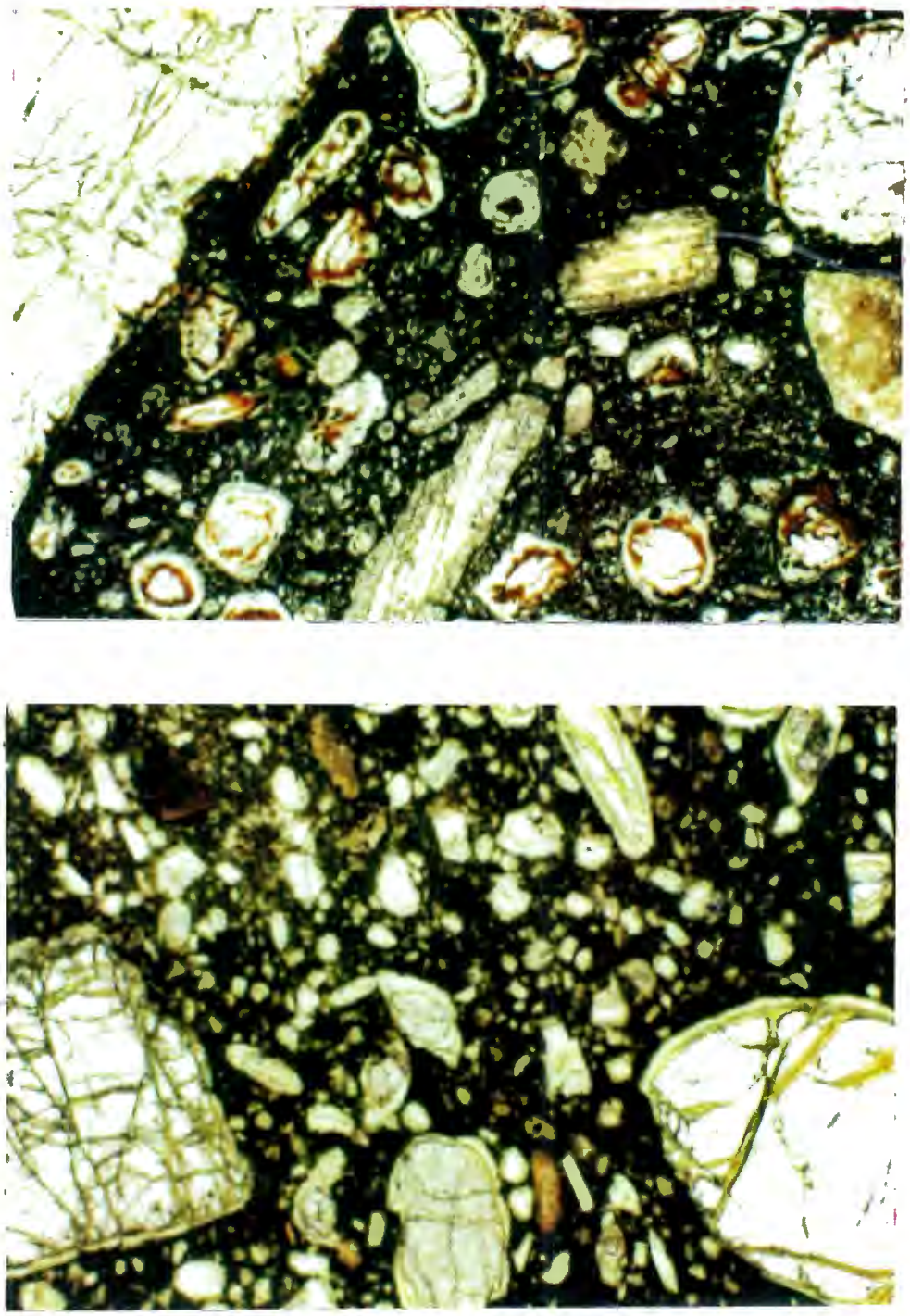

Figure II.5 - Photomicrographs of kimberlitic rocks (Três Ranchos at the top and Limeira at the bottom)in plane-polarized light. Those rocks are typical hypabbysal calcite-monticellite kimberlites with uniformly distributed matrix minerals of serpentine, phlogopite, apatite, perovskite, calcite and opaque minerals. Textural disequilibrium features (e.g. extensive resorption of olivine macrocrysts and partial replacement of phlogopite macrocrysts by olivine) are abundant in Tres Ranchos whether in Limeira examples of both textural disequilibrium and equilibrium normally occur in the same thin section. Width of field = 12 mm.

been reported in some detail in Meyer et al. (1991 and 1993). One major difference between Limeira and Tres Ranchos is the amount of carbonate. In the Limeira kimberlite, calcite is only a minor phase present in the groundmass or as small clasts (< 10 mm), and xenolithic materials are almost unaffected by deuteric alteration. Conversely, the Tres Ranchos kimberlite contains abundant groundmass calcite as a late crystallizing phase (in some sections comprising up to 30% in volume), and abundant secondary dolomite accompanies xenoliths which are completely carbonatized.

Rounded xenolithic fragments (up to 3,5 cm) of spinel lherzolite, harzburgite and dunite are common in the Limeira kimberlite, and display evidence of spinel and phlogopite metasomatism similar to that observed in xenoliths found in South African kimberlites. Geothermobarometric investigations indicate that the xenoliths from the Limeira kimberlite probably equilibrated at relatively low pressures (circa 27 kb) within the subcontinental lithosphere (H.O.A. Meyer, pers. comm., 1989), and to date only spinel-bearing xenoliths have been found. "... no garnet bearing ones have been discovered" (Meyer and Svisero, 1991). The general lack of high-pressure xenolith populations (i.e. garnet peridotites and diamonds) in these rocks compared to kimberlites elsewhere in the world points to a shallow lithospheric source for the xenoliths sampled by these alkalic magmas. It is not clear at the moment if the dominance of spinel lherzolite xenoliths in the area is a sampling problem, or is due to thin lithosphere. Unfortunately, seismic tomography data are not available for the area of this Project.

II.2.3 - Alkalic Rocks of Kimberlitic Affinity

The Japecanga "mica-peridotite" (locality 4 in Figure II.1) occurs as an approximately 2 km^2 sediment and tuffisitic breccia-filled crater. The pipe is intrusive into metasediments of the NeoProterozoic Araxá Group. Volcaniclastic fine-grained material and magmatic dykes recovered in drill-core samples (bore-hole BH61 by Sopemi Pesquisa e Exploração S.A.; samples from 60 and 65 meters depth) comprise sporadic olivine macrocrysts and abundant phenocrysts of olivine and lesser phlogopite set in a sometimes unusually "glassy" matrix of serpentine, serpentinized monticellite, phlogopite, clinopyroxene, amphibole, opaque minerals, apatite, spinel, perovskite and clay minerals. Two generations of olivine are present, although

it is not possible petrographically to assign every grain to one or another olivine population. Anhedral olivine macrocrysts (up to 6 mm) occur as corroded grains frequently strained, exhibiting undulose extinction or containing marginal and/or internal zones of mosaic-textured recrystallized olivines. There is a size overlap between these "macrocrystic-type" olivines and the euhedral to subhedral olivine phenocrysts which occur as single crystals (frequently skeletal and in some cases corroded) or as multiple growth aggregates. It is not possible to distinguish the two olivine types on the basis of chemical composition (Fo_{84} to Fo_{93}). Small (0.2 mm or less) euhedral crystals in the matrix were identified by microprobe as being dolomite.

The crater facies materials from Japecanga consist of altered and monotonous, very fine grained pale blue tuffaceous sediments. Diatreme facies breccia outcropping at the western margin of the pipe comprises of clinopyroxene, serpentine and spinels in an altered clay matrix (Tompkins, 1991; and references therein). The Pântano "mica-peridotite" (locality 5 in Figure II.1) plug intrudes meta-sediments of the MesoProterozoic Canastra Group. At the present level of erosion this intrusion outcrops as an ellipsoidal pipe about 250 x 700 meters. The rock comprises macrocrysts and phenocrysts of olivine (up to 7 mm) set in a matrix of monticellite, diopside, perovskite, apatite, opaque minerals and minor phlogopite and spinel within serpentine and clay minerals. The olivines are generally fresh but have thin alteration rims; and a few are completely altered to serpentine. Olivine, spinel, phlogopite and perovskite crystallization around olivine megacrysts is common (Figure II.6). Olivine macrocrysts have a higher Fo content than the microphenocrysts (Fo_{89-92} and Fo_{84-87}, respectively; Meyer et al., 1993). Phlogopites occur as euhedral to subhedral single grains or as multiple crystal-aggregates, and two perovskite populations with complex twining and zoning are distinguished optically. Meyer et al. (1993) classified the phlogopites into four distinct types that they referred to as *i)* macroliths; *ii)* macrocrysts; *iii)* mantled phenocrysts; and *iv)* groundmass poikilitic plates. Contrasting compositions of the different phlogopites from Pântano are illustrated in Figure II.9. Diopsides have been reported to have lower TiO_2 (0.6 - 1.4 wt%), Al_2O_3 (<0.3 wt%) and Na_2O (0.4 - 1.3 wt%) compared to the Limeira kimberlite. Further mineral chemistry, petrography and compositional variations within this intrusive have been reported in Meyer et al.(1991) and Meyer et al. (1993).

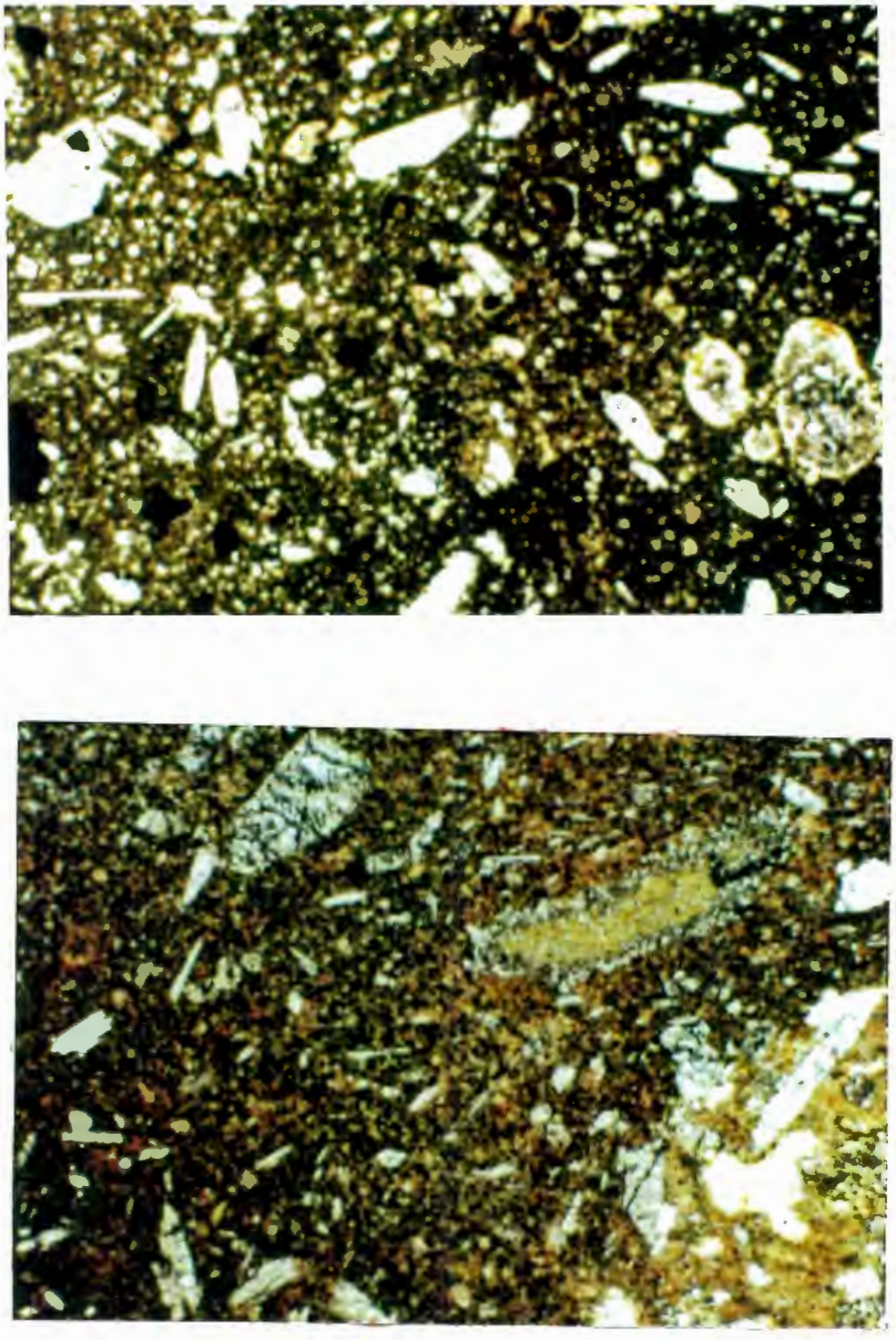

Figure II.6 - Photomicrographs of alkalic rocks of kimberlitic affinity (Japecanga at the top and Pântano at the bottom) in plane polarized-light. The Japecanga mineralogy comprise olivine macrocrysts and phenocrysts and phlogopite set in serpentine, phlogopite, clinopyroxene, amphibole, opaque minerals, apatite, spinel, perovskite and clay minerals. The Pântano intrusive is characterized by macro and phenocrysts of olivine set in a matrix of phlogopite, monticellite, diopside, perovskite, apatite, opaque minerals, serpentine and clay minerals. In some cases pervasive phlogopite replacement is followed by serpentinization; in others primary phlogopite macrocrysts are contained between olivine neoblasts. Width of field = 12 mm.

II.2.4 - Rift-related Alkalic Rocks

One occurrence of basalt breccia and composite lava flows, named Sucesso (locality 6 on Figure II.1), was included in the present study. Angular to rounded nodules, mineralogically similar to matrix material, with clinopyroxene, opaque minerals, perovskite, altered olivine, ghost relics of feldspar and rare leucite, phlogopite and apatite are set in a matrix of secondary clay, chlorite and serpentine. Significant compositional variations have been recognized in samples from this locality as illustrated by the analyses of samples SUC-G and SUC-R shown in Tables II.2 and II.3.

Volcanic and non-volcanic sediments of the Mata da Corda Formation are intercalated with lava flows and base-surge deposits continuously exposed for 1.2 km southward from Presidente Olegário (locality 7 on Figure II.1). The sequences conformably overlie cross-bedded sandstones of the Areado Formation which display sin-depositional listric block rotation. The lava-flows comprise serpentinized olivine phenocrysts set in a groundmass of clinopyroxene, Ti-rich phlogopite, leucite, apatite, melilite relics (?), opaque minerals, perovskite and clay minerals. Sparse pink amphibole (potassium richterite; Leonardos et al., 1991) occurs as an accessory phase. General petrographic characteristics of the lavas led Leonardos & Ülbrich (1987) to classify these rocks as madupitic lamproites. These authors, however, later indicated that though "... with some characteristics common to madupitic lamproites [there is] petrographic and chemical convergence towards the kamafugitic-kimberlitic clan" (Leonardos et al., 1991). Interestingly, the variation of Al_2O_3 *versus* TiO_2 for the Presidente Olegário phlogopites contrasts markedly with that of the other studied rocks and plot well within the high-Ti lamproite field of Mitchel and Bergman (1991; page 215) as illustrated in Figure II.9.

Lapilli-size pyroclastic blocks within the surge deposits contain abundant matrix opaques and altered laths of melilite. Coarse fragments of mela-syenite and pyroxenite (bebedourite) with variable proportions of pyroxene, andradite garnet, Ti-poor Fe-rich biotite, Ba-orthoclase (up to 7 wt% BaO), apatite, perovskite and magnetite reflect strong magmatic layering (Leonardos et al., 1991). Xenoliths (up to 10 cm large) are restricted to spinel-peridotite or cumulus peridotite nodules presumed to be of cognate origin (with perovskite and olivine which alternate

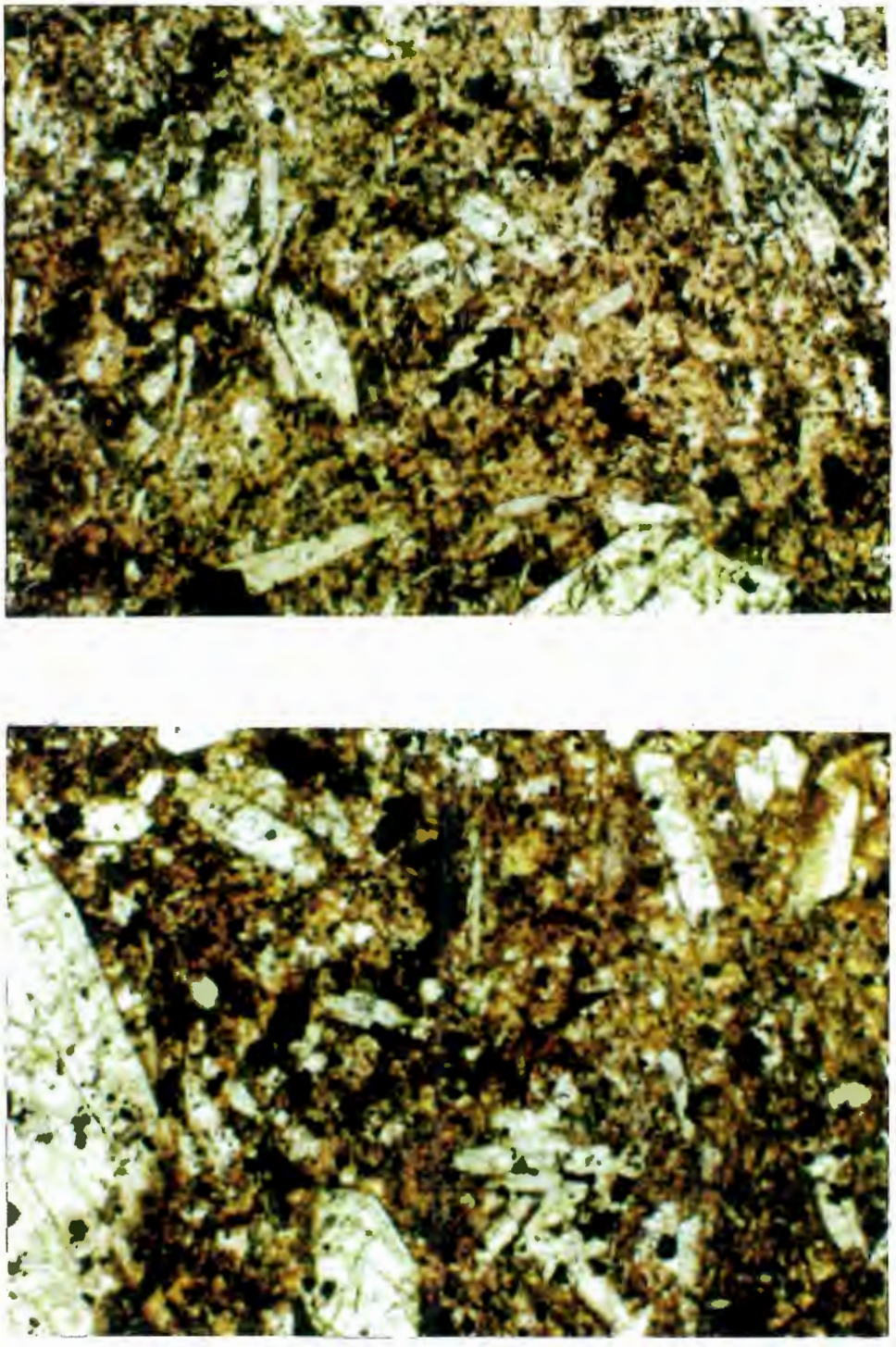

Figure II.7 - Photomicrographs of rift-related alkalic rocks (Carmo do Paranaíba at the top and Presidente Olegário at the bottom) in plane-polarized light. Serpentinized macro and phenocrysts of olivine set in a groundmass of clinopyroxene, phlogopite, apatite, melilite relicts (?) opaque minerals, perovskite and clay minerals. Note the predominance of euhedral to subhedral olivine phenocrysts occurring as single crystals or as multiple growth aggregates. Those forms, rare in the "alkalic rocks of kimberlitic affinity" and virtually absent in the kimberlites, may be related to magmatic processes at shallow levels (J.Robey, pers. comm., 1987). Width of field = 8 mm.

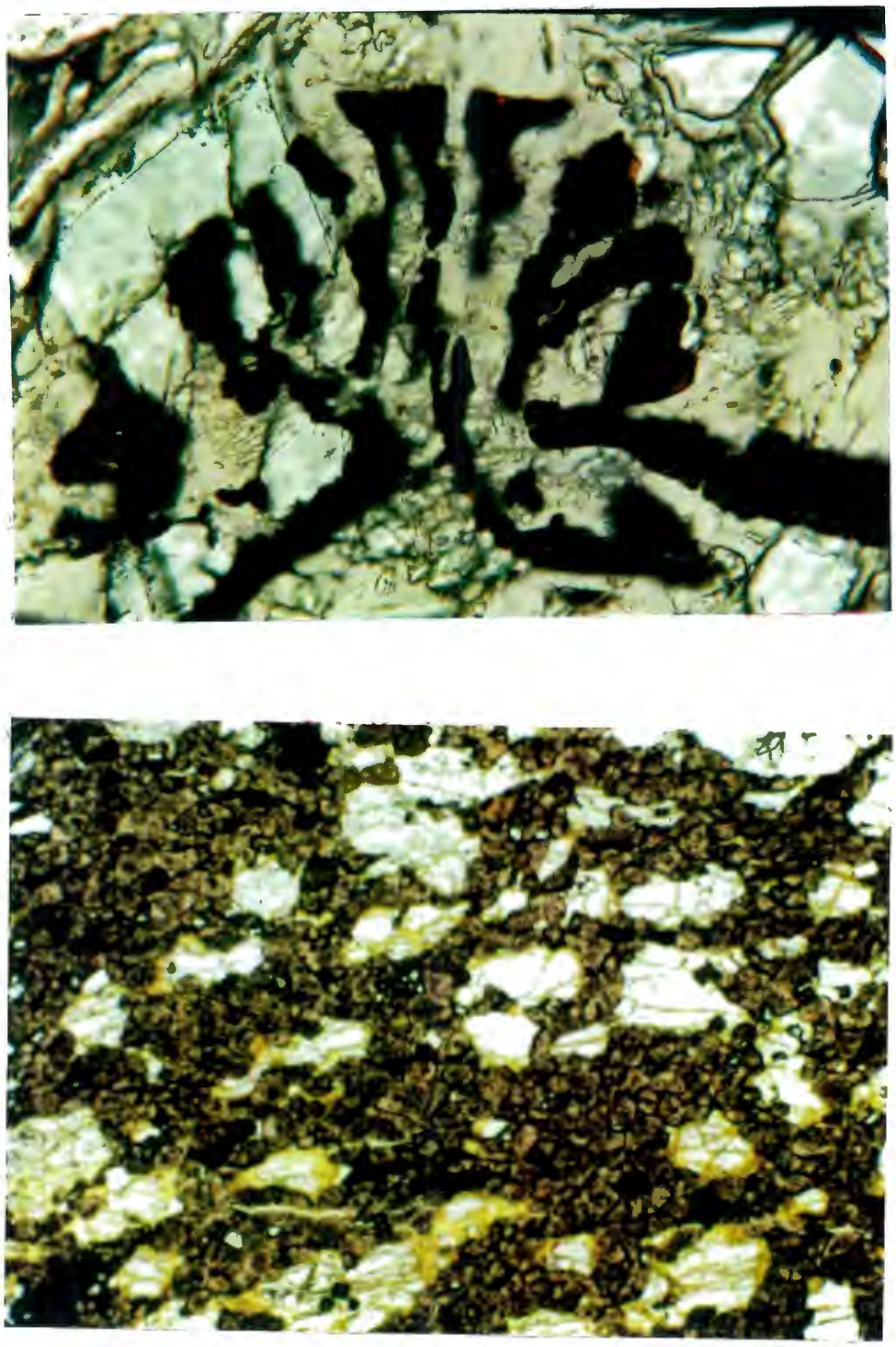

Figure II.8 - Photomicrographs of xenolith materials in plane polarized light. At the top, bleb of spinel and green diopside overgrown in veined phlogopite lherzolite from the Limeira kimberlite. Those features are not rare, but vein-like or stockwork metasomatism in the kimberlites is in fact dominated by phlogopite relative to diopside. Width of field 4 mm. At the bottom, cognate cumulus peridotite nodules with perovskite and olivine (which alternate as the dominant phases) from Presidente Olegário. Those cognate nodules are found to be indicative of re-equilibration within temperature-zoned reservoirs. Width of field = 12 mm.

as cumulus and adcumulus phases; and minor magnetite and pyroxene as intercumulus; see Figure II.8).

The extrusive rocks from Carmo do Paranaíba (locality 8 in Figure II.1) included in this study are petrographically and mineralogically equivalent to the Presidente Olegário occurrences. The occurrence actually comprises two volcanic pipes with inter-digitized lava-flows and pyroclastics. Description of the mode of emplacement and mineralogical and petrographic variations of the Mata da Corda volcanics in this area have been presented in detail by Seer et al. (1989). In previous studies Moraes et al. (1986 and 1987) have provided descriptions and chemical analyses and concluded that these rocks have strong affinity with kamafugitic types.

A review on the general characteristics and historical background of the Mata da Corda volcanics in general is provided by Leonardos et al. (1991) and other references therein. Petrographically, the alkalic suite as a whole resemble the alkaline volcanics in Uganda and in Montana, where individual potassic rocks commonly strongly resemble lamproites (B.Scott-Smith, pers.comm., 1991).

II.2.5 - Carbonatite Complexes

The two carbonatite complexes of Catalão I and II (locality 1 in Figure II.1) intrude metasediments of the MesoProterozoic Araxá Group. Metasomatised magnetite and mica peridotites and pyroxenites of an early stage are associated with five other late-stage magmatic carbonatites and late hydrothermal activity represented by foscorite, sovite, cryptocrystalline berforsite, glimmerite and lamprophyre (Baeker, 1983). The metasomatic equilibration of magnetite pyroxenites and peridotites detected in the centre of the dome (up to 6 km in diameter) is accompanied by pervasive phlogopitization and exsolution of oxides. The subsequent magmatic carbonatitic phases, especially the foscorite stage, introduced magnetite, phlogopite, apatite and pyroclore, resulting in an enrichment of incompatible elements. More detailed description is available in Danni et al. (1991) and in other references therein. Drill-core samples of foscorite, sovite and lamprophyre from the Catalão II carbonatite supplied by Mineracao Catalao were selected for analyses.

II.3 - WHOLE ROCK GEOCHEMISTRY

Bulk rock samples of all the occurrences selected for the project have been analyzed by X-ray fluorescence (XRF) and Neutron Activation Analysis (NAA). The compositions of the samples used in the isotopic analysis are presented in Tables II.2 and II.3. Volatile-free compositions have been used in the plots presented herewith. Analytical methods and confidence limits of the analyses are described in the Appendix.

II.3.1 - Contamination

Petrographic examination of the samples indicates that large-scale contamination can be discounted, and that the compositions of the samples used in this study may be regarded as representative of the magmas prior to any significant alteration. The only possible exceptions are the samples selected to represent Japecanga, which represent a petrographic type that is volumetrically insignificant at the present level of erosion (e.g. Tompkins, 1991).

The intrusions contain variable proportions of lower crust and mantle-derived xenoliths that are completely carbonatized (in the Tres Ranchos kimberlite) or contain pronounced reaction rims (in the Limeira kimberlite; and in the Presidente Olegário and Carmo do Paranaíba volcanics). Contamination is, therefore, at least a potential problem. With that in mind, fresh samples used for the analyses were initially crushed into small (1 cm or less) fragments and xenolith-free portions were carefully selected under a 20x stereo microscope before being powdered in pre-contaminated agate mills (see Appendix).

The lack of correlation between $^{87}Sr/^{86}Sr$ and 1/Sr argues against large-scale contamination processes. Also, Sr and Nd contents of the studied rocks (537-13346 ppm and 19-439 ppm, respectively) are significantly higher than average upper-crust (260-500 ppm Sr and 16-23 ppm Nd; Weaver and Tarney, 1984). It is assumed, therefore, that, in spite of the presence of lithic fragments in the studied rock samples, significant crustal contamination can be discounted. Serpentine, which occurs both as a groundmass mineral and as a deuteric alteration product of

olivine macrocrysts and phenocrysts, probably accounts for the higher LOI (Loss-On-Ignition) of the kimberlitic rocks compared to the other rock types. Other possibilities such as interaction with groundwater causing high LOI in the studied rocks may also be ruled out as there is a negative relationship between LOI and elements like Ba and Sr which tend to be readily leached during weathering and percolation of ground water. Plots of isotope ratios *versus* strontium contents (Figure II.10) display a slight positive correlation which mirrors the overall relationship between isotopic signatures and fractionation indexes (see discussion below). Contamination indices have been calculated and these support an absence of extensive crustal contamination in the analyzed samples.

Disruption and digestion of olivine-rich mantle xenoliths (or digestion of xenocrystic olivines) could have increased MgO, Ni and possibly Cr in the host rocks. This process, however, should not significantly have affected incompatible element content or isotopic composition of the rocks. One sample from a dolerite dike associated with the Tres Ranchos kimberlite was analyzed for major and trace elements and isotope compositions (referred to as TRX.Dk in Tables II.1, II.2 and II.5). A close examination of the geochemistry of both the diabase dike and the cross-cutting Tres Ranchos kimberlite indicate that each rock-type preserved its own chemical characteristics, and that neither mantle nor crustal contamination processes were of major significance.

II.3.2 - Major elements and compatible trace elements

Major elements and compatible trace element compositions are listed in Table II.2. The studied rocks are ultrabasic (SiO_2 contents normally lower than 40 wt%) and plot in the highly alkalic field in a silica *versus* total alkalies diagram (Figure II.10). The kimberlites and related rocks are ultrapotassic ($K_2O/Na_2O > 3$) and, on the basis of chemical signatures (e.g. SiO_2, Al_2O_3, CaO, MgO and Na_2O), just a few of the rift-related intrusions plot within the field of kamafugites (c.f. Foley et al. 1987).

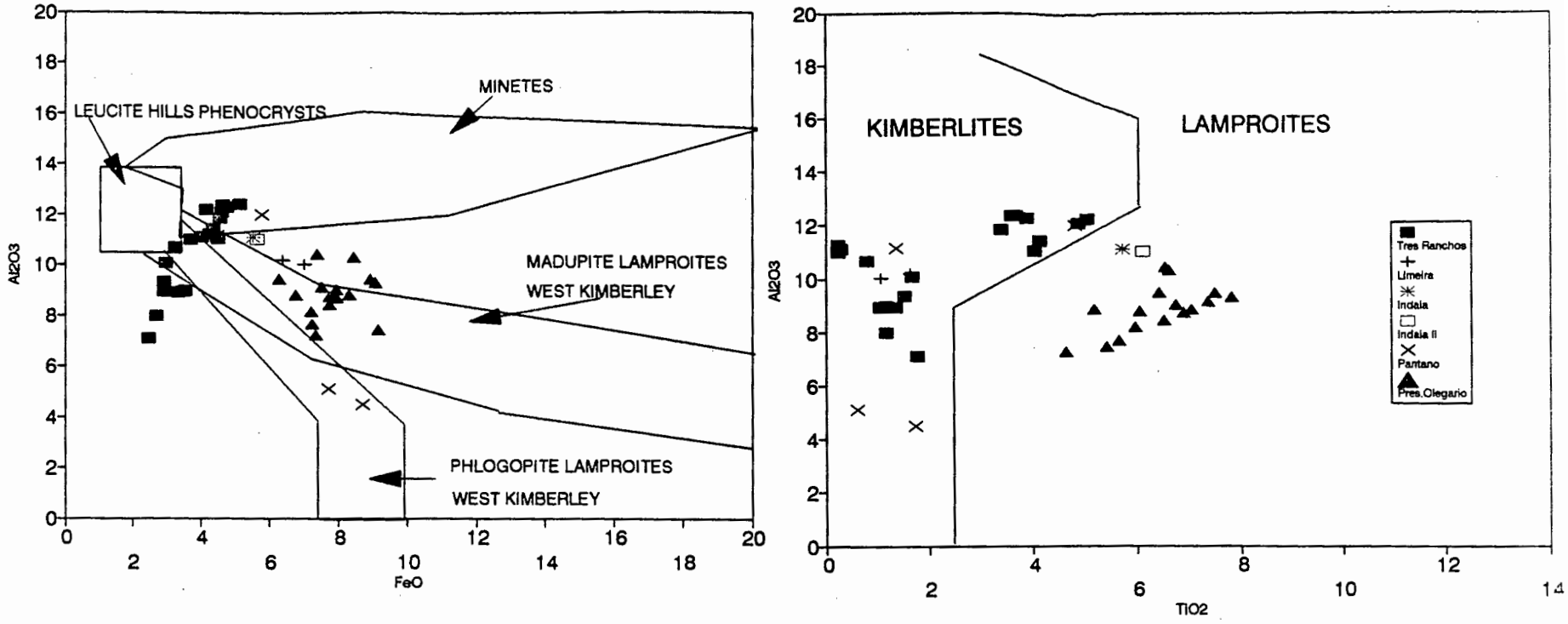

Figure II.9 - Spinel and mica compositions of Brazilian kimberlites and related rocks. Note, on top, the spreading of micas in terms of Al_2O_3 versus FeO and TiO_2 (fields after Mitchell and Bergman, 1991). Trends shown by chrome-spinels from Limeira and Indaia are typically kimberlitic, whether the Cr-Al-($Ti+Fe^3$) composition of the Tres Ranchos spinels is anomalous (see text).

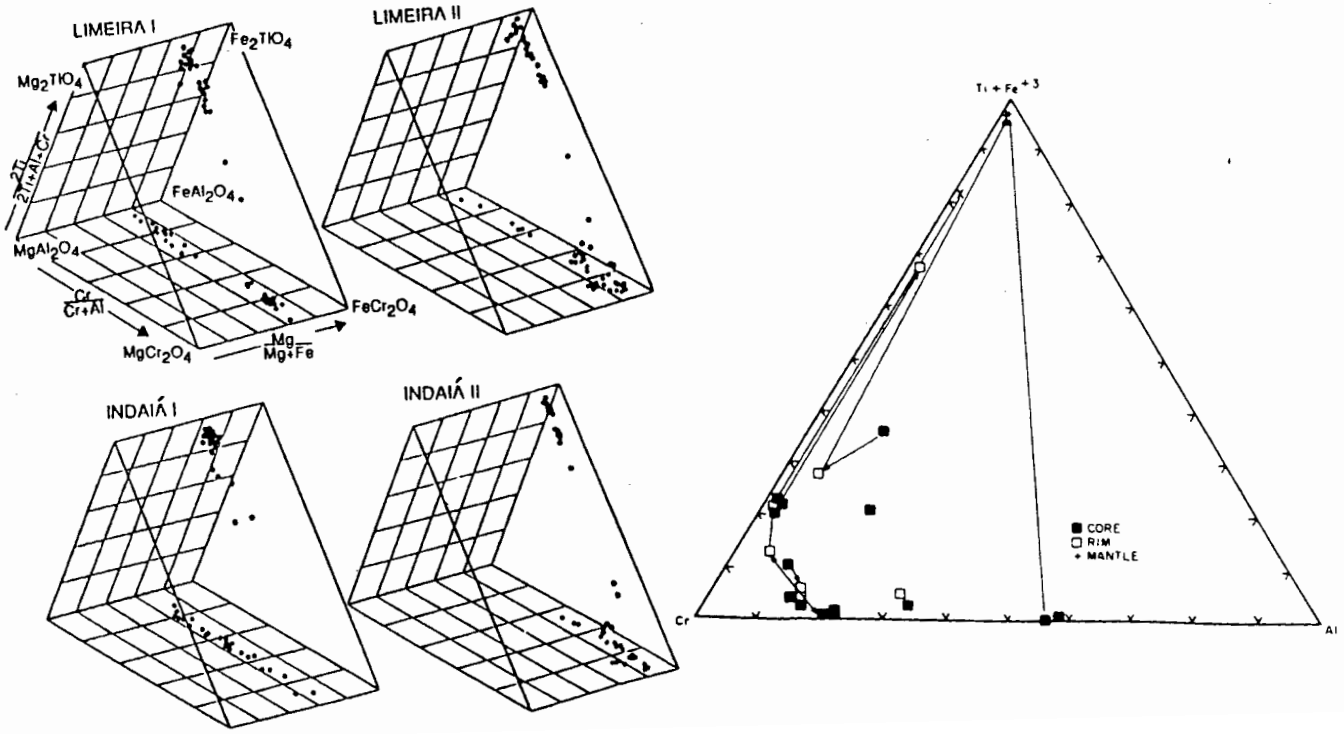

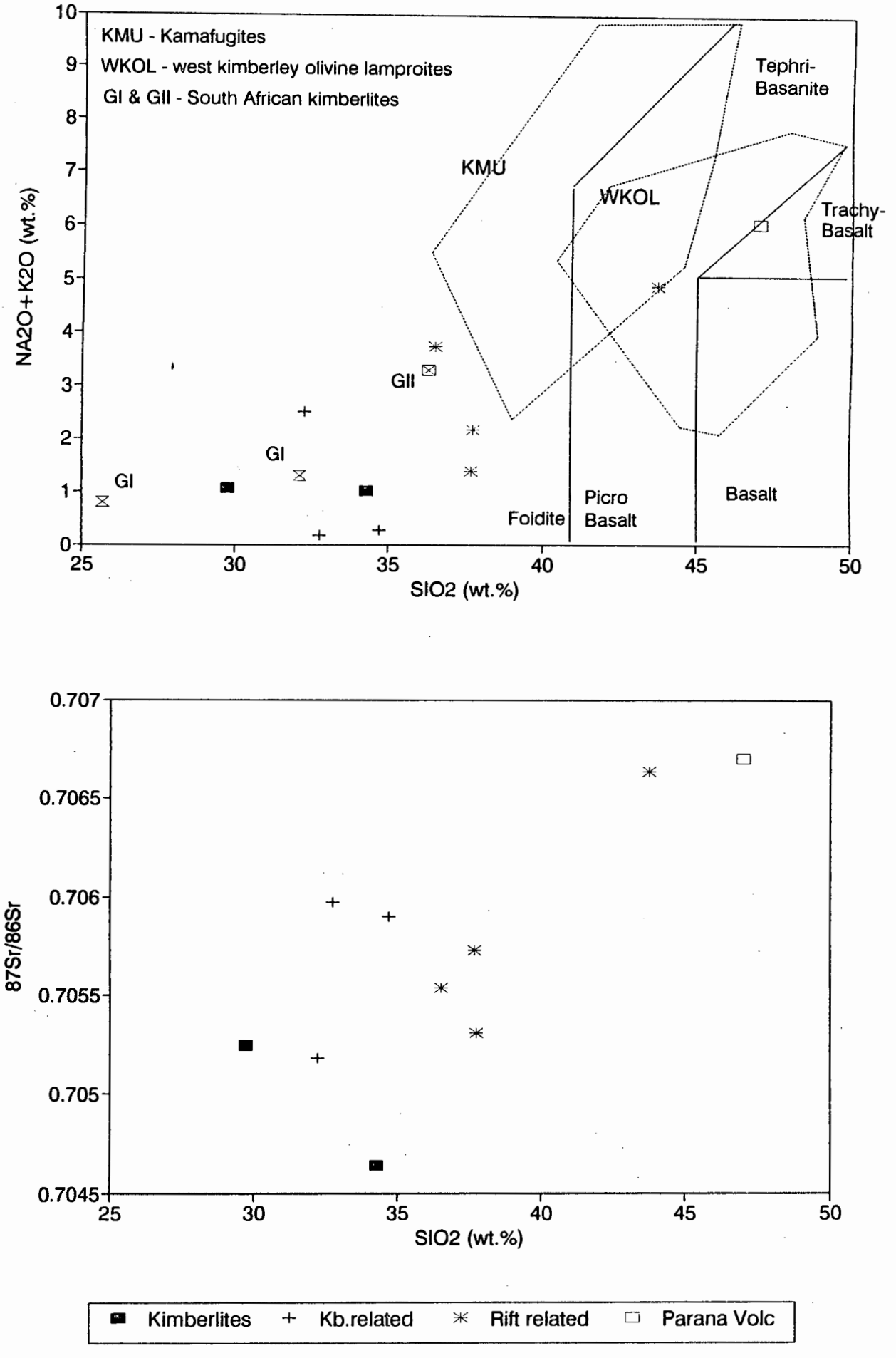

Figure II.10 - Silica contents related to isotopic signatures and total alkalis content.

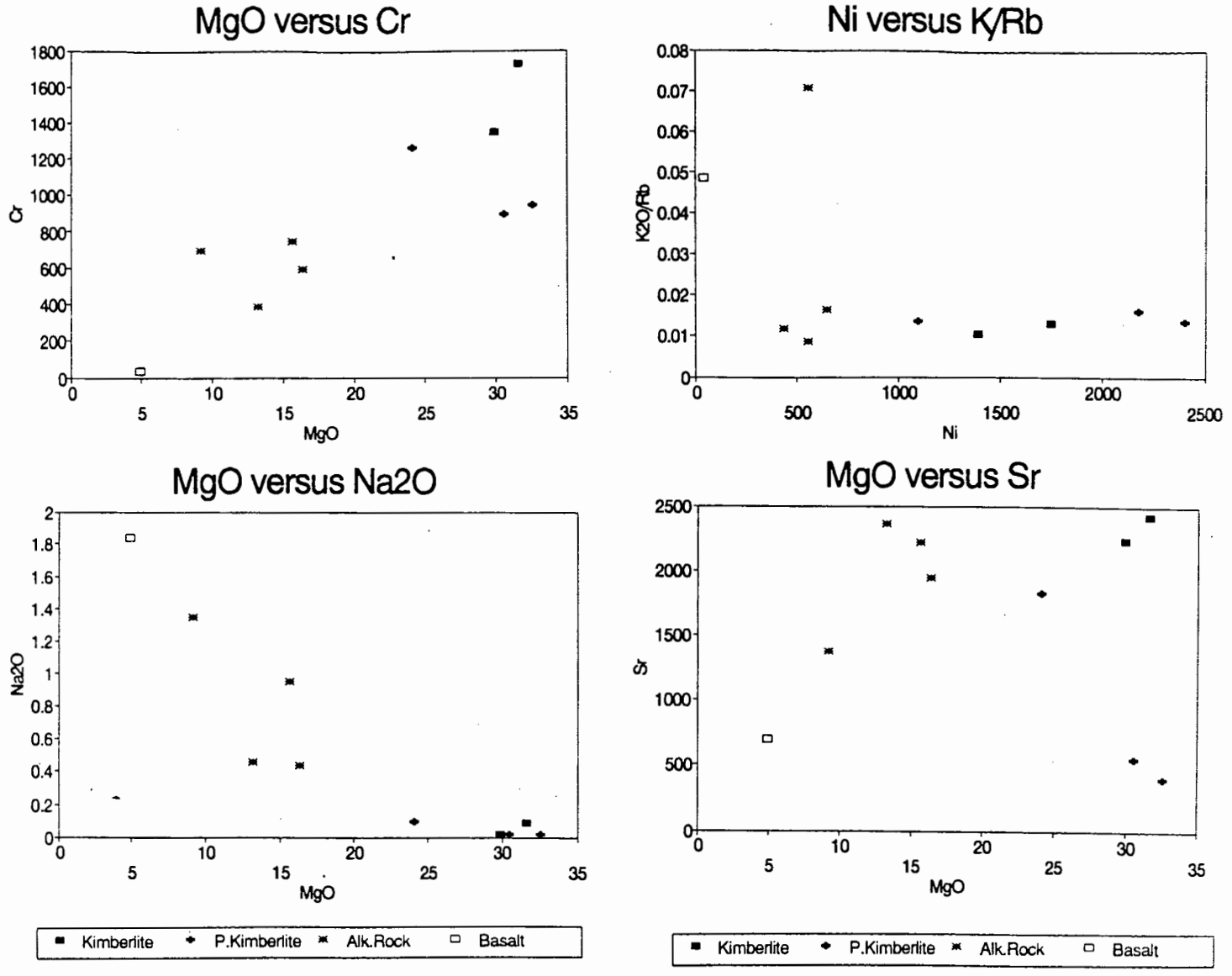

Figure II.11 - Selected major element variation diagrams.

The kimberlites and rocks of kimberlitic affinity have MgO contents ranging from 24 to 33 wt. % and Mg# ranging from 63 to 76. The overall composition of these rocks (Table II.2) are similar to those representing primary liquids derived from melting of upper mantle peridotite. Relative to the studied kimberlites, and to kimberlites in general, the "rift-related" alkalic rocks have more evolved bulk compositions (MgO contents ranging from 10 to 17 wt. % and Mg# from 49 to 53), also reflected by their lower Ni and Cr contents and are all indicative of olivine (and possibly chromite) fractionation from the magmas.

The usual occurrence, particularly in the kimberlites, of phlogopite as a groundmass mineral suggests that late-crystallizing liquids had high potassium contents. Relative to kimberlites and related rocks, the rift-related rocks are also distinguished by their higher Al_2O_3 and K_2O contents. Overall, as illustrated in Figure II.10, the studied samples exhibit trends of increasing Al_2O_3, Fe_2O_3, CaO and Na_2O with increasing SiO_2.

Variation diagrams show a tendency of the studied rocks to display a continuum of major and trace element compositions (Figure II.11). This apparent affinity of the different rock-types could be misleading because different proportions (and compositions) of macrocrystic olivines, perovskites and phlogopites may, to a large extent, control the major element geochemistry of these rocks. If much of the macrocrystic material is xenocrystic in nature, than the whole-rock compositions shown in Tables II.2 and II.3 may not be truly representative of the initial magmas. Conversely, because of the common source character of the different rock types (see following discussion on isotopes), and because of petrographic evidence for shallow-level differentiation, the linear relationships between various oxides and MgO (and other fractionation indices) in the more evolved rock-types could be tentatively ascribed to melt extraction trends and fractional crystallization dominated by Mg-rich olivine, pyroxene and chromite. Modal abundances, as well as increasing SiO_2 and CaO with decreasing MgO contents, point to a major role for clinopyroxene in controlling the whole-rock composition of the more evolved rock-types.

The kimberlitic rocks from Tres Ranchos and Limeira contain large (up to 15 cm in maximum

dimensions), relatively dense, peridotite xenoliths of mantle rock. The xenoliths are presumed to have ascended rapidly from the region where they were incorporated, otherwise they would have been completely resorbed. The required rapid ascent of the xenoliths leaves little opportunity for efficient fractionation processes to operate on the kimberlitic liquids. In contrast, the kimberlite-related (i.e. Japecanga and Pantano) and the rift-related rocks (i.e. Presidente Olegário, Sucesso and Carmo do Paranaíba) normally do not contain any xenolithic nodules. The few nodules recovered from the Presidente Olegário body are different from those recovered from the kimberlites. Especially significant are a number of cognate nodules comprising cumulus perovskites and olivines, which probably relate to previous stage(s) of equilibration in deep reservoirs. It is conceivable that partial melts generated at depth in the mantle might have risen to shallower level and then reequilibrated with the local lithospheric mantle peridotite. Wall-rock melting and assimilation may have occurred during the storage in the lower pressure reservoirs, and fractionation processes would then have altered the overall bulk chemical composition of the magma. Fractionation processes could also have been active during magma ascent.

Samples derived from different parts of the same occurrence may have slightly different compositions. For example, the composition of samples JAP.60 and JAP.65 (two pieces of the same drill-core, 60 and 65 meters deep, respectively), SUC.R and SUC.G (samples from the same outcrop, slightly Reddish and Greenish in hand specimen), given in Tables II.2 to II.5, illustrate small-scale heterogeneities which are not related to source heterogeneities. The most likely uncertainties regarding the interpretation of these heterogeneities are variable oxidation states and mineral phases acting as buffers during melting. Unlike the radiogenic isotopes, however, the amount of information available from the major and trace element composition of these rocks is rather restricted, and not enough for a sound petrological modelling of the variations observed.

II.3.3 - Incompatible trace elements

Trace element compositions are listed in Tables II.2 to II.4. Although abundances of incompatible trace elements in the studied rocks may have been reduced by the dilution effects of olivine macrocrysts and groundmass spinels, or enhanced by perovskite and titanosilicates,

the interelement relationships should have remained virtually unaffected. Because incompatible trace elements are not effectively removed from the liquid until the late stages of groundmass crystallization, whole-rock analyses are expected to provide useful information regarding the source regions of magma. In the following discussion special attention is given to the behavior of Rare-Earth-Elements (REE), U, Th, Nb and Ba in the studied rock samples.

Chondrite normalized REE compositions shown in Figure II.12 indicate that the studied occurrences are highly LREE (Light-Rare-Earth-Elements) enriched (La = 70 to 430 ppm) and exhibit steep profiles (Ce/Yb = 130.4 to 424.7) which tend to flatten out in the HREE (Heavy Rare-Earth-Elements). Europium anomalies are absent. Because of the high bulk partition coefficients for HREE into garnet, the high LREE/HREE ratios observed in the studied rocks are thought to imply that melting occurred in the presence of residual garnet (an argument which is supported by the presence of garnets in the mineral concentrates as reported in table II.1). All rock-types have similar parallel to sub-parallel REE trends and, with the exception of Japecanga, there are no significant variations in REE contents between the intrusions. Such similarity in REE normalized patterns (Figure II.12) suggests that all the studied rocks have undergone similar processes. The lower LREE/HREE ratios of the rift-related alkalic rocks compared to those of the kimberlites indicate that higher degrees of partial melting were probably associated with their formation. The samples from the Catalão carbonatite have significant internal REE variability. This is presumably due to metasomatic processes involved in their generation.

Both LREE and HREE contents of the studied rocks are comparable to those reported for kimberlites elsewhere (Tainton and McKenzie, 1994 and references therein). The arguments presented by those authors to constrain the composition of the source rocks from which kimberlitic melts originate should, therefore, apply to the SW margin of the São Francisco craton as well. As is found in the South African kimberlites, the enrichment of LREE in the Brazilian kimberlites is greater by more than a factor of 1/D (where D is the bulk partition coefficient) with respect to both the primitive and the MORB sources. The implication is that their source must have been enriched before magmas were generated from it (Tainton and McKenzie, 1994; see also following section on isotope geology).

The high HREE concentrations observed (Yb contents in the studied rocks average 6.28 times chondrite) cannot be ascribed to the same enrichment event which enhanced the LREE values because the concentrations of Tm, Yb and Lu in melts generated from enriched sources decrease as the amount of metasomatic melt that has been added increases (Tainton and McKenzie,op.cit.). In addition, because of their compatibility, Tm, Yb and Lu will tend to remain behind as LREE is removed by the melt, the implication being that the concentration of such elements in the liquid may be less than that in the source. Because of such constraints, Tainton and McKenzie (op.cit.) argued that the high concentration of HREE in kimberlitic melts migh have been produced by depletion, instead of enrichment, of the source, and that the concentrations of Tm, Yb and Lu in particular are strongly affected by the depth at which depletion accurred in the first place.

Even when such constraints are taken into account and the REE partition coeficients corrected for changes in temperature and melt compositions (Watson and Green, 1981), calculations to evaluate the nature of the source rocks on the basis of REE compositions (e.g. Tainton and McKenzie, op.cit.) become progressively less reliable as the number of depletion and enrichment events increases (see arguments for multiple enrichment events below) because the errors are cumulative.

The near constant HREE contents observed indicate that changes in depth of final melt segregation were unlikely to have been accompanied by significant changes in source minerals. The usefulness of comparing obtained REE compositions to those models simulating the influence of changing source depth (e.g. McKenzie and O'Nions, 1991), however, is limited by both the differential effects of fractional crystallization in the variably evolved rocks, and by entrainment of lithospheric material (either mantle or crust) which tend to obliterate the primary REE that carries the information of depth of formation.

Mantle normalized trace element concentrations (listed in Tables II.2 and II.3, respectively) are plotted in Figure II.13. Average values for South African kimberlites from Smith et al. (1985) are also plotted for comparison. Of all of the rocks studied, the Tres Ranchos kimberlite

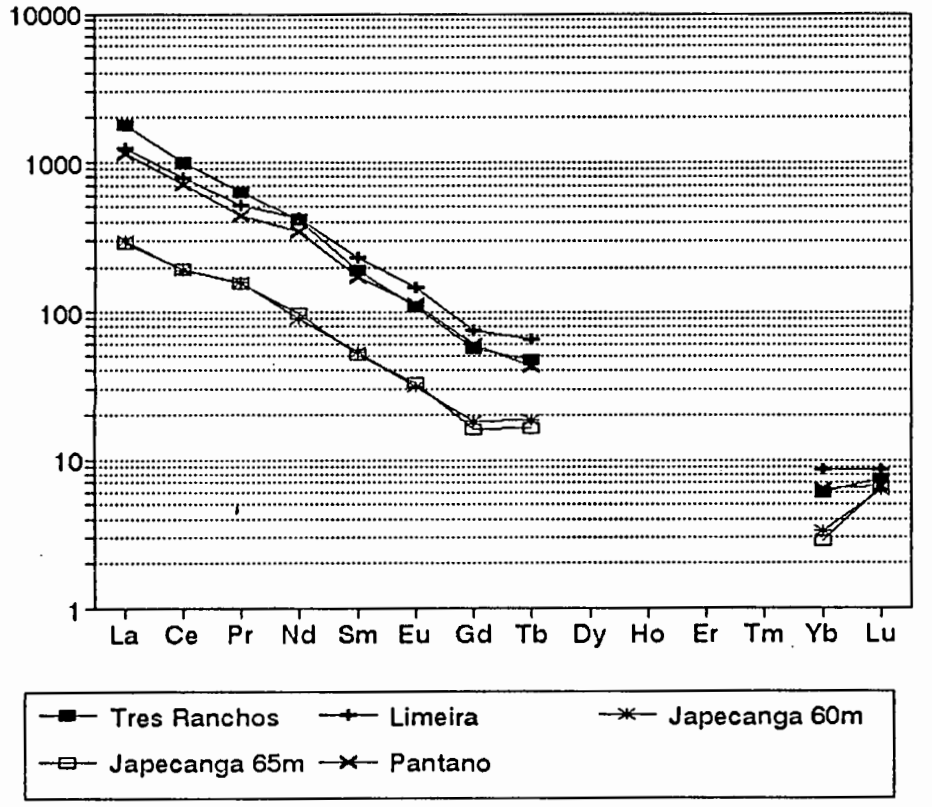

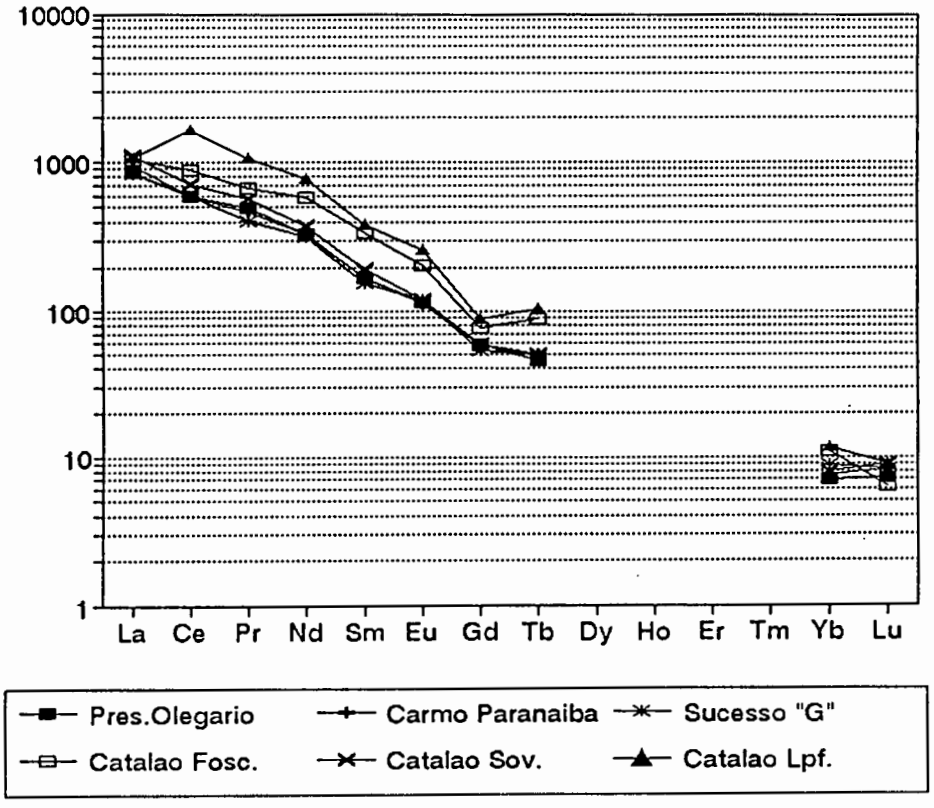

Figure II.12 - Chondrite-normalized REE.

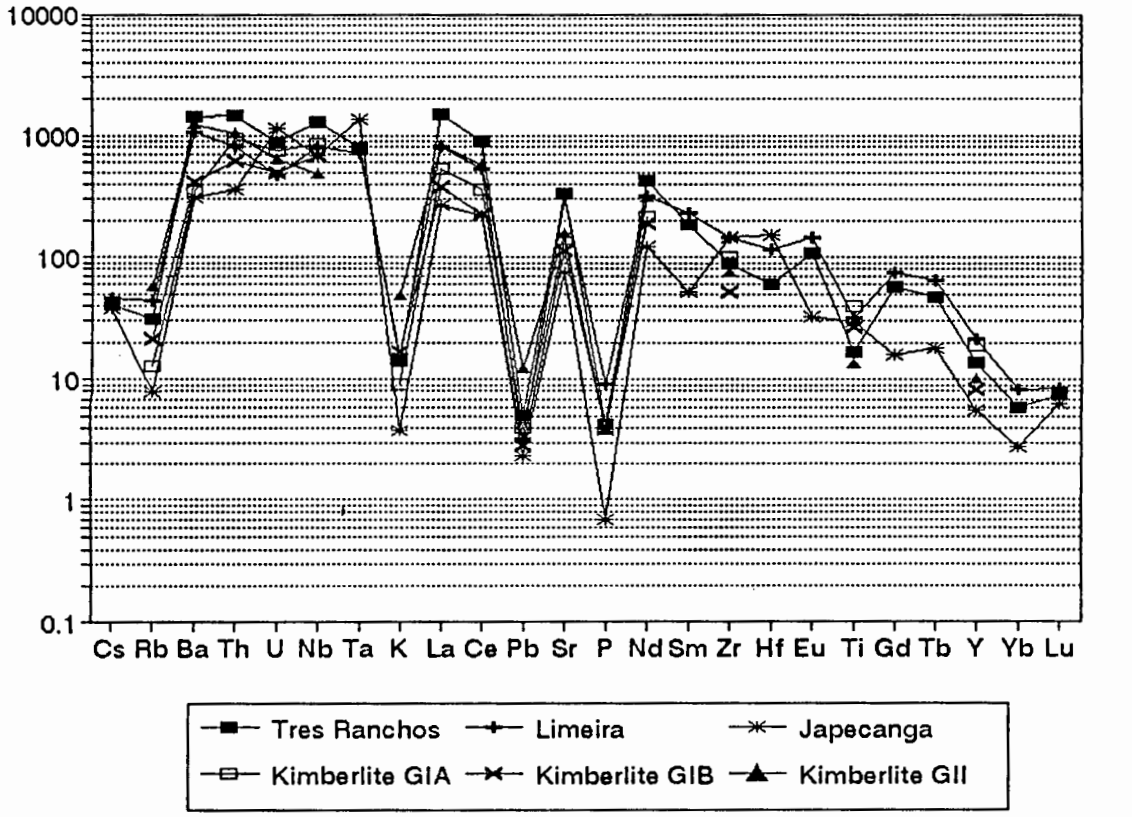

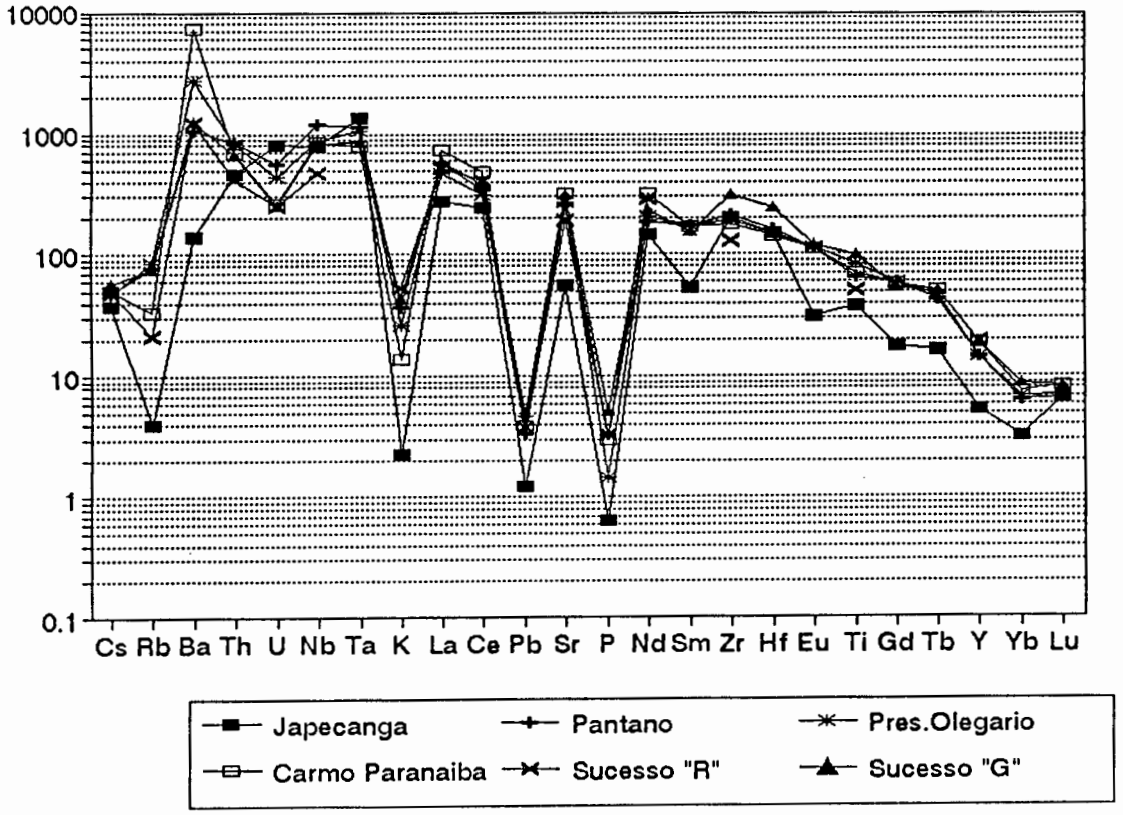

Figure II.13 - Mantle normalized trace element compositions.

intrusion displays the greatest degree of enrichment in incompatible trace elements such as La, Ce, Th, Nb and Nd. This kimberlite is more enriched in these elements than South African Group II kimberlites. The concentrations observed in the Limeira kimberlite, however, are comparable to those of the South African kimberlites. Apart from the high Ba contents, the range of normalized trace element composition of the rift-related rocks is not dissimilar to that of the kimberlites and kimberlite-related rocks.

Like the REE, Uranium, Thorium and Niobium are also incompatible in kimberlite-related melts (e.g. Mitchell, 1986). Notwithstanding the rather restricted amount of trace element data available, Uranium and Thorium appear to behave coherently in the studied rocks and present positive correlations with LREE/HREE ratios (Figure II.14). The affinity among the very incompatible U, Th and the moderately incompatible REE is normally assumed to have originated during the melting event rather than inherited from source compositions (e.g. Chauvel et al., 1992). This is because of the strong fractionation of U and Pb during small degrees of partial melting, as a result of the higher compatibility of Pb relative to U (e.g. Halliday et al., 1990; McKenzie and O'Nions, 1991). Another interpretation for the coherent behavior of these elements, however, is that they were all compatible with some accessory residual phase like phlogopite, apatite or amphibole in the magma source. Assessing the relation of these trace elements (i.e. U, Th and REE) to either source characteristics or to melt production and/or fractionation in the studied rocks is a difficult task, in part because these rocks are not simply melts but hybrid volcanic breccias with a major lithospheric input. A further limitation of such an exercise is the fact that the interelement relationships observed in basaltic melts, which are believed to have been generated by much greater degrees of partial melting, does not necessarily apply to the complex elemental geochemistry of kimberlites and other exotic rock types dealt with in this project, in which the chemical effects of much smaller degrees of partial melt are superimposed on trace-element enriched source characteristics.

One way of investigating the possible relation of REE, U and Th to the source composition and fractionating phases, is by examining the correlation between K/U, Ce/Pb and U/Pb ratios. The

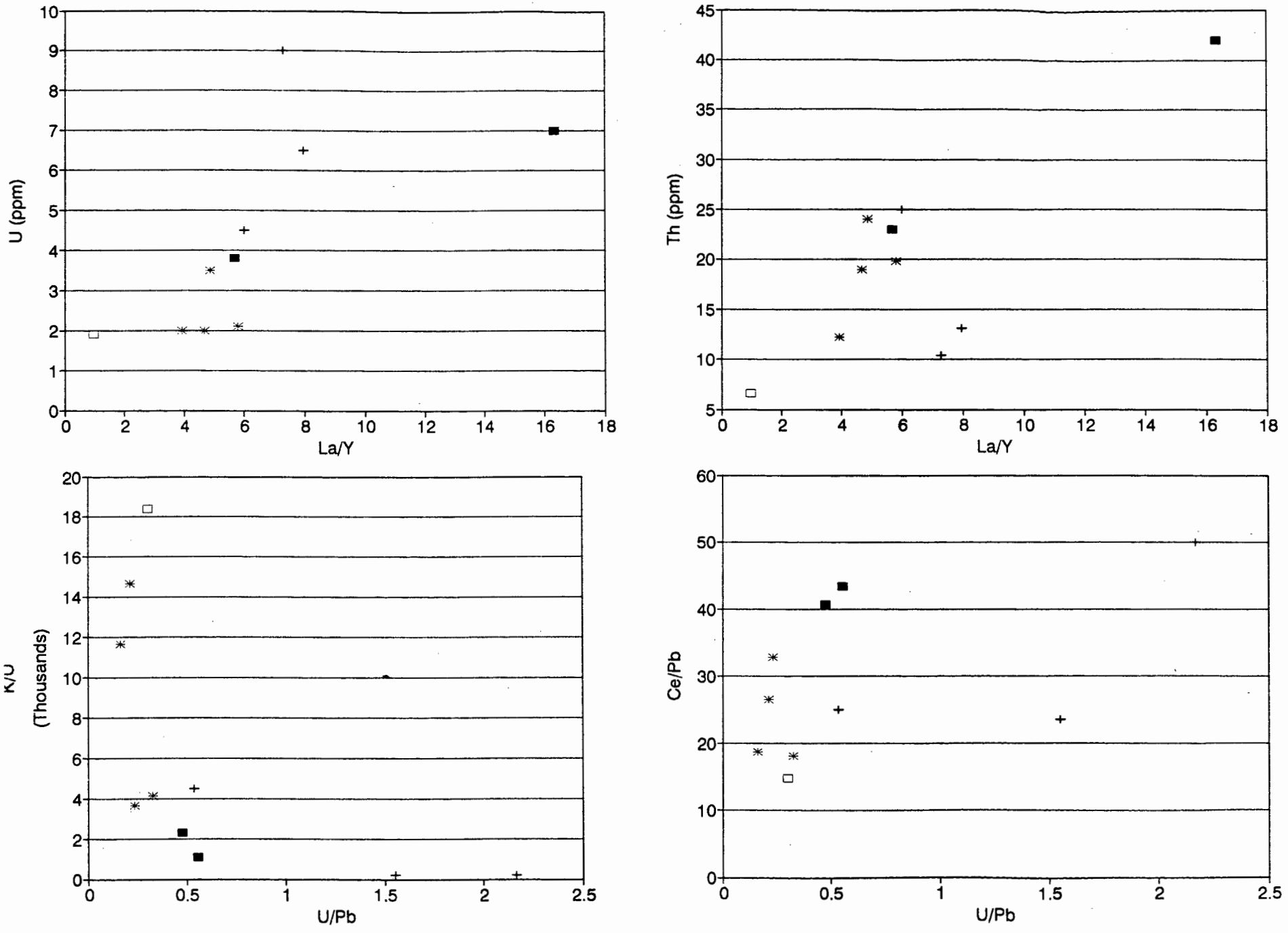

Figure II.14 - U and Pb relationship to other trace elements.

negative correlation between U/Pb and K/U ratios illustrated in Figure II.14 indicates a process that fractionated both K and Pb relative to U, and suggests that the U/Pb fractionation was influenced by a potassic phase, probably phlogopite. That is consistent with the relatively low K abundances in the mantle normalized diagrams. The Ce/Pb and U/Pb ratios of the studied rocks have a positive relationship, as also illustrated in Figure II.14. The Ce/Pb ratios are normally interpreted as being representative of source characteristics because, under "normal" circumstances, the two elements are not expected to fractionate relative to each other at the time of melting (c.f. Hoffman et al., 1986). Small-degree partial melting of only the main "normal" upper-mantle mineral phases (without plagioclase), however, cannot produce such a positive correlation between U/Pb and Ce/Pb because of the very different distribution coefficients of U and Ce (Halliday et al., 1992; McKenzie and O'Nions, 1991). The positive correlation between U/Pb and Ce/Pb is, therefore, probably related to the presence of "exotic" metasomatic minerals as residuals in the continental mantle source.

The arguments that both K/U and Ce/Pb ratios could be reproducing enriched source characteristics lead to the assumption that the variable U/Pb ratios observed in the studied rocks (U/Pb ratios in the kimberlite-related rocks are significantly higher than in the rift-related volcanics), which correlate with both K/U and Ce/Pb ratios (Figure II.14), could also reflect variable source compositions. The correlation of such variability to source composition is supported by the observation that the kimberlites have higher time integrated U/Pb ratios (represented by higher $^{206}Pb/^{204}Pb$ initial ratios) than the rift-related volcanics (see next section). Nevertheless, an important implication of the large range in parent/daughter ratios observed is that they would generate a mantle that is extremely heterogeneous isotopically if allowed to evolve over long periods of time. Such heterogeneity is not represented in the Pb signatures of the studied rocks. Also, a consequence of the observed negative relationship between U/Pb and Sm/Nd ratios is that, with time, increased U/Pb should be accompanied by relatively less radiogenic Nd. The $^{143}Nd/^{144}Nd$ initial-ratios, however, display a positive relationship with $^{206}Pb/^{204}Pb$ (next Section). Presumably this is because the variable inter-element ratios inherited as source characteristics (see following discussion on isotopes) have been overprinted by variable inter-element ratios acquired during the partial melting event due to the higher incompatibility

of U compared to the other three elements.

In conclusion, it seems that the unusually high U/Pb ratios of some of the studied rocks cannot be readily ascribed to source characteristics, nor to very small degrees of melting. It envisaged that these anomalous U/Pb ratios, and their relationship to elements like Ce and K, can only be explained if time-integrated fractionated trace element compositions of heterogeneous enriched source materials had been enhanced/modified during the process of partial melting.

The various magma types recognized in this study all have positive Nb anomalies on mantle normalized trace element diagrams. Niobium tends to correlate positively with LREE, and the high Nb/La ratios in these rocks are similar to those of OIB (Figure II.15). Nb also correlates positively with Th and U; and negatively with Y and HREE. K/Nb seems to increase with increasing Nb. U/Nb, Th/Nb and Rb/Nb ratios are consistently lower than the ratios of the primitive mantle (after Hoffman, 1988), probably indicating that the source of the studied rocks was enriched in Nb relative to these very incompatible elements. The lack of significant correlation between Zr and Nb indicates a rather erratic behavior of Nb. Perovskite is possibly the best candidate to host Nb in kimberlite-related magmas (c.f. Mitchell, 1986). Microprobe data on perovskite grains from Limeira and Pântano, indicate Nb_2O_3 values between 0.28 and 0.56 wt% (Meyer et al., 1993). Because widespread perovskite accumulation/fractionation should result in negative Nb and Ti anomalies, it is envisaged that the effects of any possible accumulation of perovskite are negligible. Alternatively, Nb could have behaved as a compatible element with respect to some mineral phase incorporated as a xenocryst into the magmas. If, for example, Nb-rich perovskites from cognate nodules, similar to those identified in the Presidente Olegario area (Figure II.18, bottom), had been assimilated by the rising magma batches. Perovskite modal distribution, however, does not seem to support the hypothesis that Nb contents in these rocks are hosted by perovskite, which is a common groundmass phase in the Nb-rich kimberlites but which also occurs as a much more abundant mineral in the Nb-poor Presidente Olegário and Carmo do Paranaíba lavas. Another candidate which could host Nb is ilmenite. This is not, however, supported by the observation that the Três Ranchos kimberlite, the most Nb-rich among the studied rocks (except for the carbonatites), is ilmenite-free.

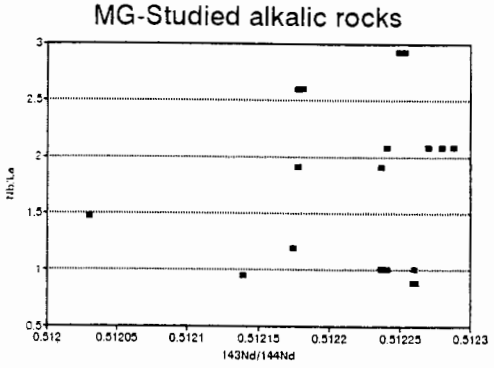

Figure II.15 - Nb/La histograms in mantle and crustal rocks (after Arndt and Christensen, 1992) compared the characteristics of the studied occurrences and those of volcanics in the Paraná fields, in Rio de Janeiro and in Tristan da Cunha (references in the text).

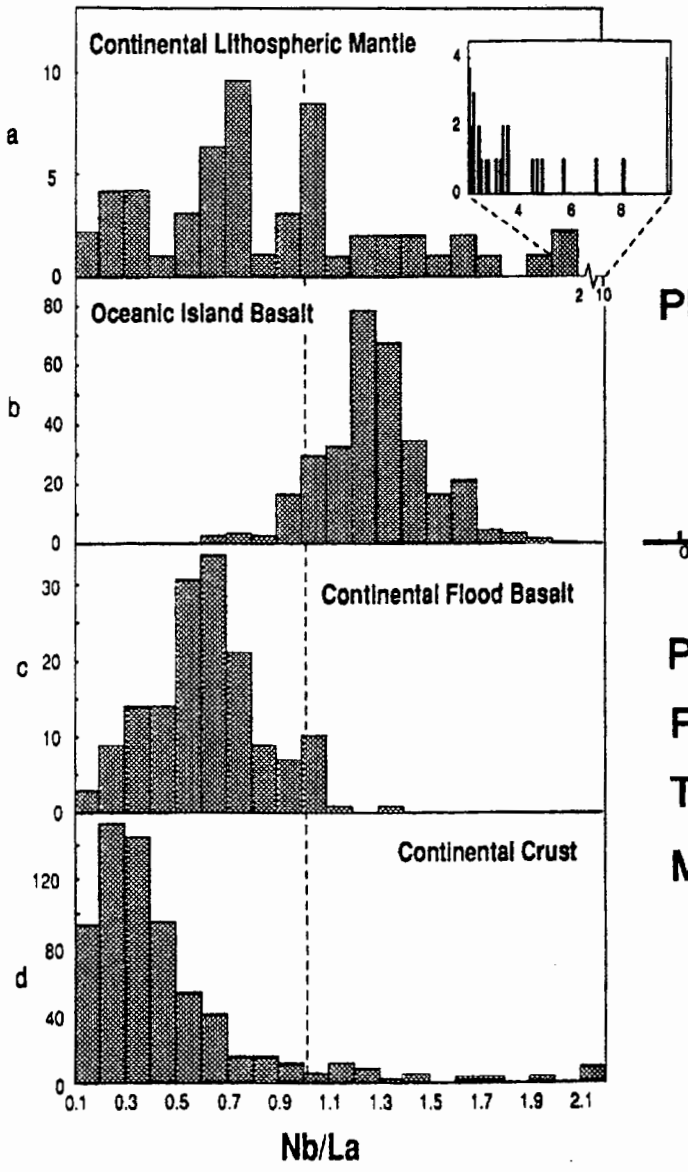

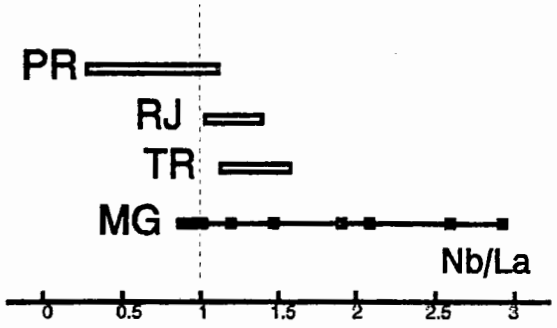

PR=Parana Volcanics

RJ=Rio de Janeiro dykes

TR=Tristan da Cunha

MG=Studied alkalic rocks

(References in the text)

Unlike the northern Paraná CFB, ratios of Nb to elements like La or U are higher than for most rocks in the continental crust and for most peridotite xenoliths from the lithospheric mantle (Figure II.15). Note that the samples from the Tres Ranchos kimberlite plot very close to primitive mantle ratios, and that there is some overlap between the chemistry of the rocks from this study with those of Dupal basalts from the southern Indian ocean, which also have Nb/La distinct from the majority of CFB (see Figure II.15 and references in Arndt & Christensen, 1992).

Ba/Nb ratios in the studied rocks, with the exception of Japecanga, are higher than primitive mantle ratios (after Hoffman, 1988). Barium contents of the rock samples from the Mata da Corda Formation are exceptionally high (6500 to 17500 ppm) compared to the other rock-types. Leonardos et al. (1991) have reported abundant Ba-zeolites, Ba-orthoclase, apatite and Ba-rich K-feldspar in these rocks, and indicated that their mineralogy is compatible with such extremely Ba-enriched bulk compositions. The negative correlation of Ba/Nb and $^{143}Nd/^{144}Nd_i$, however, suggests that this trace element characteristic of the studied rocks was probably not the product of recent enrichment but of some older event.

In spite of the many arguments against modelling the geochemistry of kimberlites and related rocks on the basis of their trace elements (e.g. Mitchell, 1986), and the fact that the suite of rock samples being discussed originated from different localities and represent different rock types, trace element ratios and major element compositions obtained were combined and tentatively used to test for a fractional crystallization hypothesis. No reasonable fit emerged from the exercise. In most cases, compatible elements such as Cr and Ni show only limited correlation with the incompatible elements. Incompatible element contents (Figure II.13) and ratios cannot be simulated using theoretical limits for enrichment either by differential degrees of partial melting of a homogeneous source (note the similar isotopic signatures discussed in section II.4) or by crystal fractionation processes. This poor correlation mimics the trace-element composition of the groundmass Ni-rich olivines and Cr-rich spinels (see section II.2 and references therein), which also suggests that the enhancement of incompatible elements is unlikely to be the result of fractionation of a material initially poor in incompatible elements.

The lower trace element concentration of Japecanga (with the exception of U) correlates with a predominance of phenocrystic phases over xenocrystic materials in this rock. In contrast, the exceptionally high incompatible trace element concentration observed in the Tres Ranchos kimberlite reveals no relation to modal proportions. The distinct incompatible element contents and ratios (e.g. Rb/Sr) of the Tres Ranchos and Limeira kimberlites shown in Figure II.13 do not fit theoretical limits for enrichment by differential degrees of partial melting of a homogeneous source (again, note the similar isotopic signatures) or by crystal fractionation processes. The possibility that the pattern shown by the Três Ranchos kimberlite could be reproduced by addition of a "Catalão carbonatite" component to a component similar to the less enriched Limeira kimberlite was also simulated, but no reasonable fit was obtained.

The extreme enrichment in incompatible trace elements observed in some of the intrusives, therefore, is thought to reflect significant variations in the source prior to melting rather than being due to changes during melt extraction or subsequent differentiation. In some situations the extremely high alkalinity of some of the kimberlites in the study area is likely to be inherited from portions of the lithosphere which were heterogeneously enriched during earlier metasomatism. That is probably the case for the 95 Ma old Tres Ranchos kimberlite which intruded within 20 km distance from the 119 Ma old Catalao carbonatite (see section II.4 and chapter III).

The possibility that multiple enrichment events might have affected the source region of the studied rocks precludes a clear distinction between source variations and variations due to partial melting on the basis of parent-daughter element relationship. Any tentative reconciliation of the long-term heterogeneities in the source rocks with the present-day inter-element ratios would have to rely on the assumption that one single homogeneous source was involved in the generation of all the different rock types, a conjecture that does not tally with a more detailed analysis of their trace element and isotope characteristics (see Chapter III).

II.3.4 - Platinum-group-elements and gold

Table II.4 shows the noble metal concentrations determined from the studied samples using the

combined nickel sulphide fire-assay and NAA procedure described by McDonald et al. (1992). The studied rocks are typically characterized by PGE and Au concentrations of less than 20 ppb. Such concentrations are compatible with the range of values in South African kimberlites reported by McDonald et al. (1992), but are lower than calculated PGE abundances in average spinel and garnet lherzolites (e.g. Mitchell and Keays, 1981). Some of the inter-PGE ratios are shown in Figure II.17 and the chondrite normalized PGE patterns shown in Figure II.16.

Different samples have distinct PGE patterns and there are well-defined trends amongst the various rock types. The samples from Sucesso (SUC.R and SUC.G) display the strongest fractionation from Os and Ir to Pd. In contrast, the sample from Japecanga (JAP.65) shows the lowest Pd/Ir ratio and the least fractionated pattern, with only a slight depletion in Os and Ir and almost chondritic proportions of Ru, Rh, Pt and Pd. Both the overall PGE pattern and the inter PGE ratios of Japecanga overlap with those measured in the on-craton and craton-margin Group I and Transitional kimberlites from Southern Africa (McDonald et al., 1995). The other localities show a very consistent series of Pd/Ir ratios and pattern shapes intermediate between the fractionated and the unfractionated extremes.

The Tres Ranchos and Limeira kimberlites have higher absolute concentrations of PGE than any of the other rocks and display moderately fractionated PGE patterns with Pt/Ir and Pd/Ir ratios of $\sim$6 and 4.5 respectively. A small negative Ir anomaly is shown by the Limeira sample while Tres Ranchos display a slightly positive Ir anomaly. The PGE pattern for the kimberlite-related peridotite at Pantano is similar to that shown by Limeira, with a more pronounced negative Ir anomaly. The kimberlites and kimberlite-related peridotites generally have similar or slightly higher abundances of Pt and Pd than the basalts and carbonatites, but have much higher (5 to 7 times) concentrations of Os, Ir and Ru. This has the effect of flattening the slope of the PGE pattern and suggests that the kimberlites have an Os, Ir and Ru rich component which is absent from the basalts and carbonatites. This is discussed in greater detail in Chapter III.

The PGE contents and PGE fractionation patterns have a positive correlation with LREE/HREE ratios (note the near constant HREE contents). The correlation between lower PGE contents with

Figure II.16

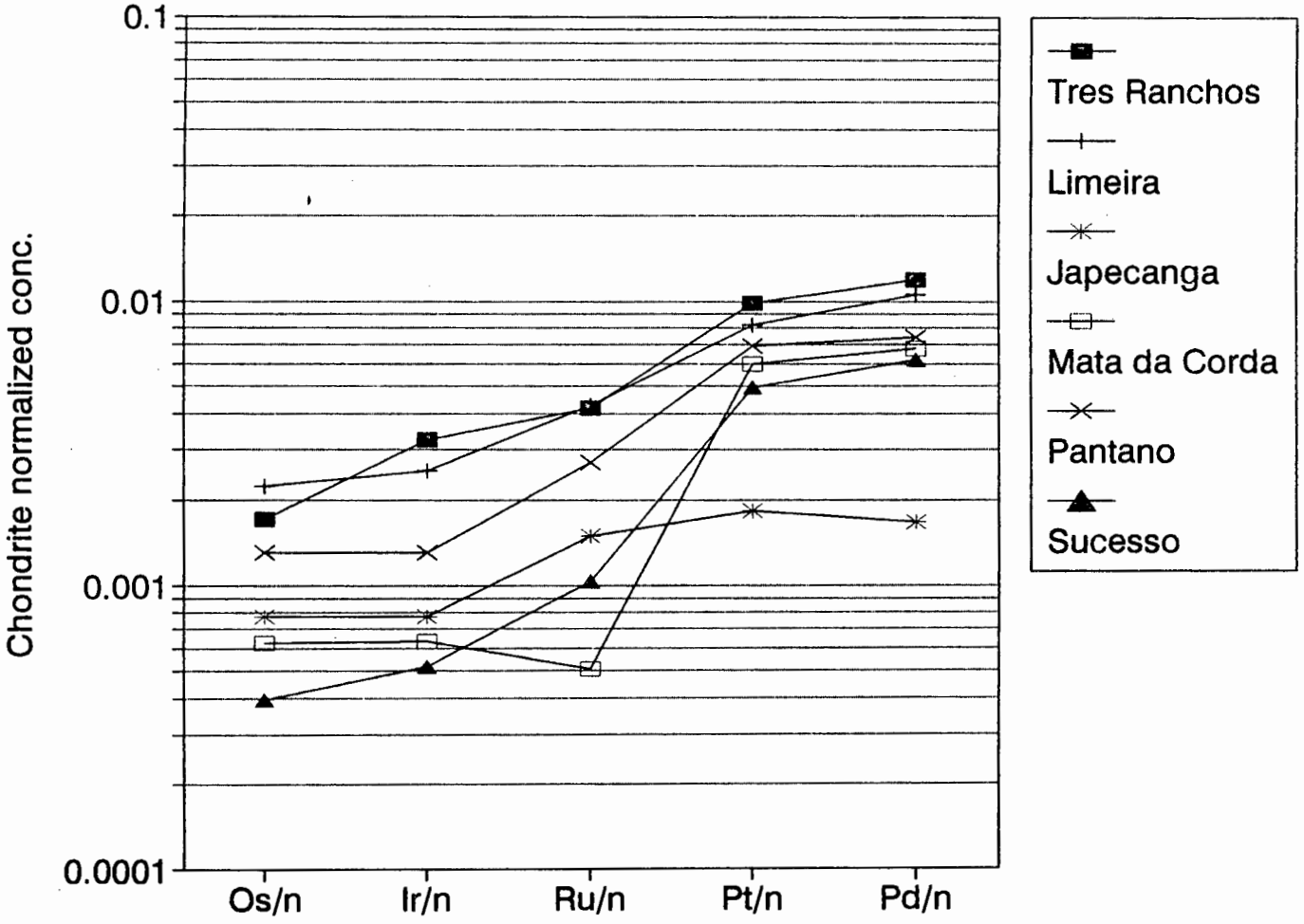

Figure II.16 - Chondrite-normalized PGE patterns. Key as in Table II.1.

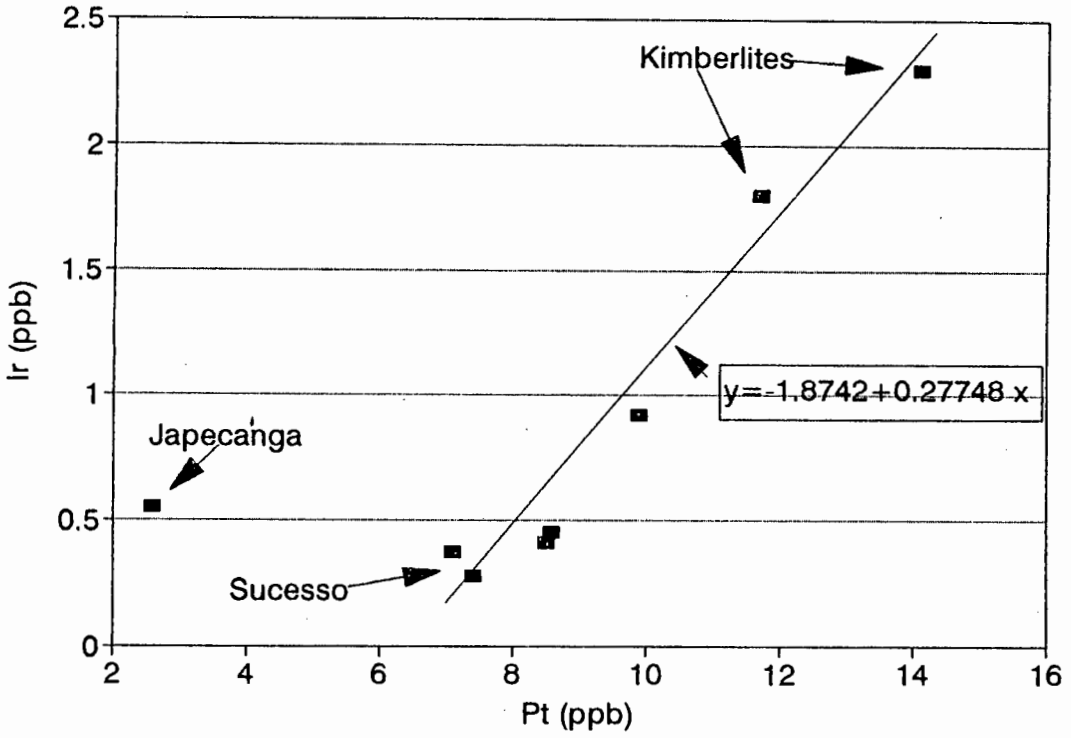

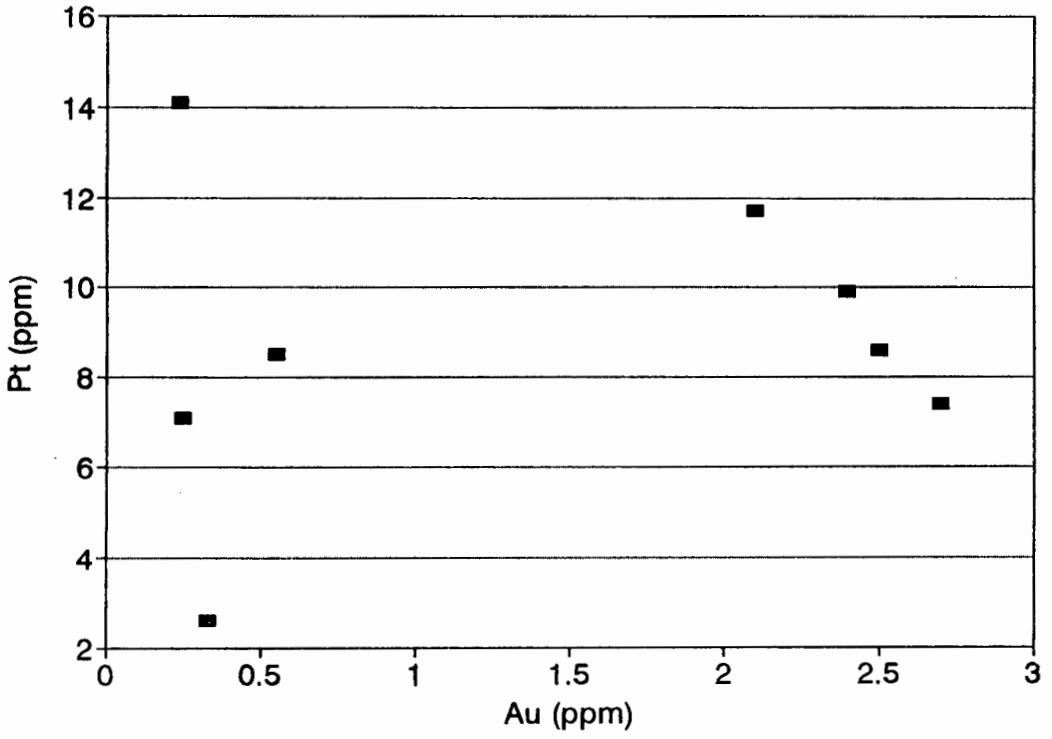

Figure II.17 - Inter PGE ratios and Pt versus Au contents.

lower LREE/HREE ratios and lower concentration of incompatible elements, however, does not apply to the sample from Japecanga, which has the lowest REE concentration of all the samples. The linear relationship between PGE and REE in the studied rocks is at odds with the observations by Morgan et al. (1981) in the Kilbourne Hole spinel lherzolite.

From the plots of Pd/Ir, Ir and Pt *versus* Au for the studied rocks (see Figure II.17) it appears that changes in PGE contents and PGE fractionation patterns are independent of Au concentration. The implied decoupling between gold and the PGE during magmatic processes does not support chemical theory that PGE and Au should behave coherently (e.g. Bowles, 1986). Similar conclusions with respect to the lack of PGE-Au coherence were reached by Mitchell and Keays (1981), Tredoux et al. (1989) and Tredoux (1990). In the samples included in this study, the PGE-Au variation is considered more likely to mirror the greater mobility of gold relative to PGE.

II.4 - ISOTOPE GEOCHEMISTRY

II.4.1 - Emplacement ages

The majority of the occurrences that were studied contain phlogopite, which may be present as both macrocrysts and phenocrysts. Emplacement-ages obtained by Rb-Sr analysis of leached phlogopite-separates from seven of the occurrences have been included in Table II.1, and plots of individual isochrons/errorchrons are shown in Figure II.18. Data are given in Table II.6.

Sr concentrations are unusually high, ranging from approximately 100 to 1500 ppm, in micas from all the studied occurrences, with the exception of Japecanga. Replicate analysis have proven that the unusually high Sr contents are characteristic of these micas, and are not an artifact of laboratory contamination or a consequence of "dirty" mica separates. Therefore, most of the alkaline rocks in the Minas Gerais District, including the ones classified as kimberlites on the basis of petrography, have a carbonatite "flavor" reflected in the chemistry of their micas. In this respect the studied kimberlitic rocks differ from what are normally regarded as "true"

kimberlites. The high Sr contents of the micas results in higher uncertainty in the age determinations because lower Rb/Sr ratios and non-radiogenic Sr contents limit the precision of the Rb-Sr dating technique.

The $^{87}Sr/^{86}Sr$ and $^{87}Rb/^{86}Sr$ data obtained for the Tres Ranchos kimberlite (representing four mica populations and one whole-rock sample) is suggestive of an age of about 95 Ma (an errorchron of 95.09 $\pm$ 9.7 Ma obtained in this work compares well with 97 Ma zircon ages obtained previously; J. Bristow pers. comm., 1989) with a low initial $^{87}Sr/^{86}Sr$ ratio of 0.704383. Although Sr is a little more radiogenic in these samples than in the others discussed below, there is still a great deal of scatter with the most and the least radiogenic samples giving rather different numbers.

The twelve data points obtained for the Limeira kimberlite define an isochron of 94.78 $\pm$ 8.48 Ma (initial $^{87}Sr/^{86}Sr$ ratio of 0.704901 and MSWD = 1.99). Though mathematically defined as an isochron, there is a great deal of scatter shown by the data and some runs were very poor for Rb, Sr or both. Because of the parallels with the Tres Ranchos samples, this age is suspected to have geological significance.

The eleven data points obtained for the Carmo do Paranaíba extrusives defined an errorchron of 86.07 $\pm$ 14.01 Ma with a high initial $^{87}Sr/^{86}Sr$ ratio of 0.705745. Whether this is a time emplacement age is arguable, because the data show extreme scatter and because of the very limited variation in Sr isotopic compositions due to extraordinarily high Sr. The age is, however, compatible with the age range assumed for the Mata da Corda volcanics (U. Cordani, pers. comm., 1990).

Despite the very limited compositional range of the five data points obtained for the samples from Sucesso, this is the best age determination of the group. An isochron of 118.15 $\pm$ 10.72 Ma (initial $^{87}Sr/^{86}Sr$ ratio of 0.705546; MSWD = 2.3) was obtained. This age determination indicates that the emplacement of these rocks was probably more closely related to the Serra Geral volcanism of the Paraná basin than to the Mata da Corda Formation.

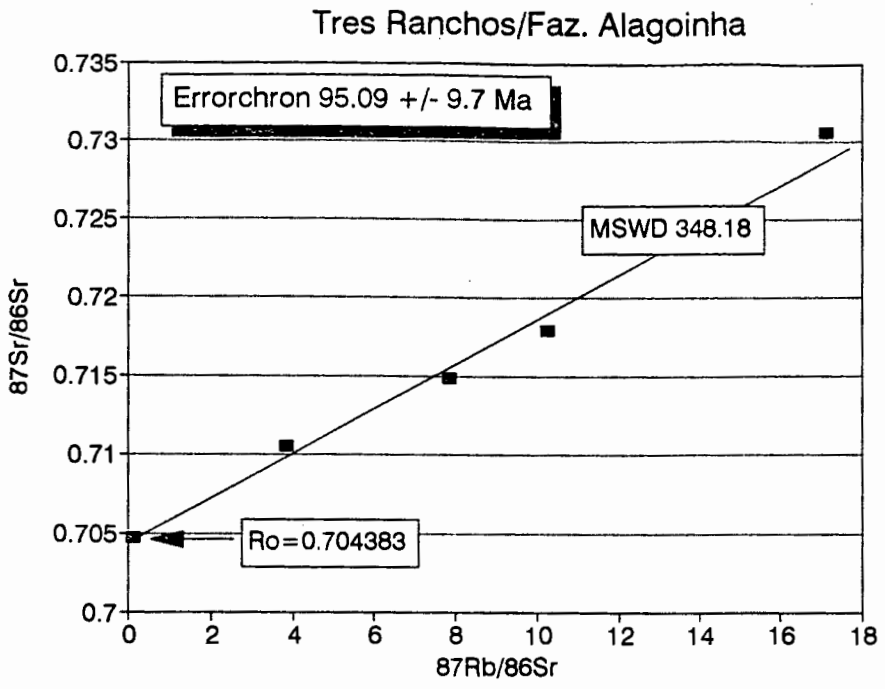

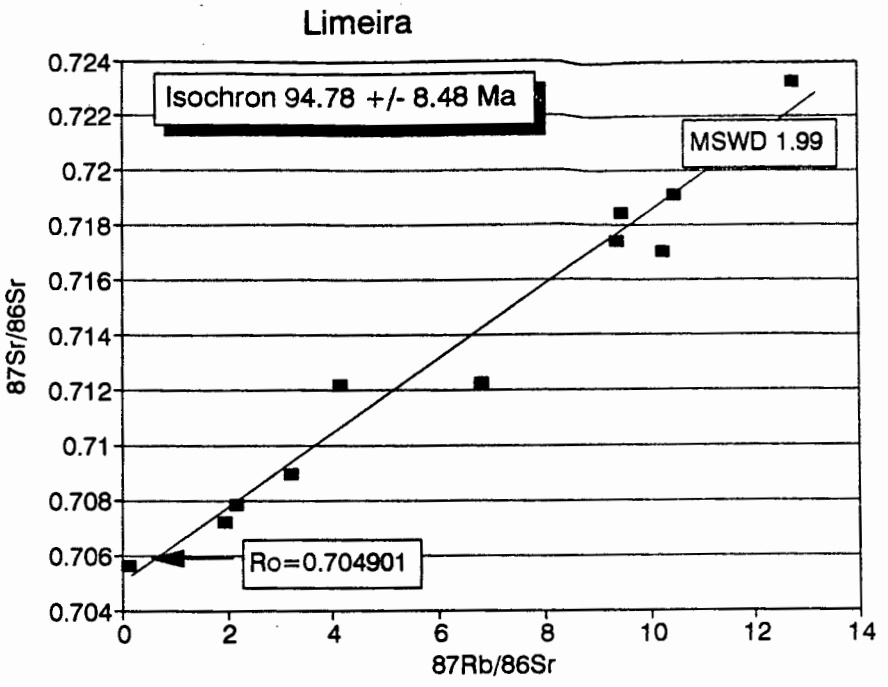

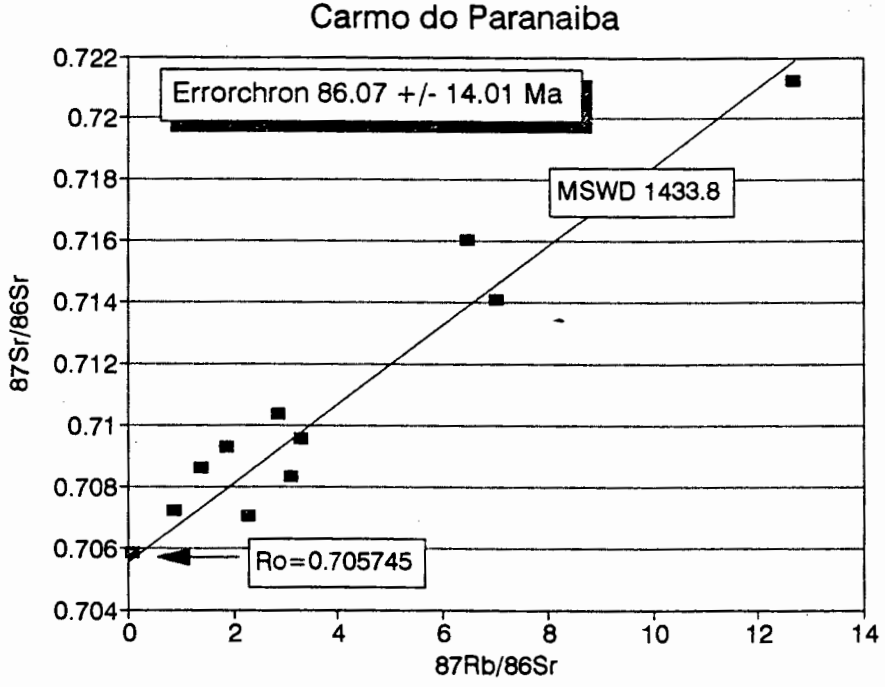

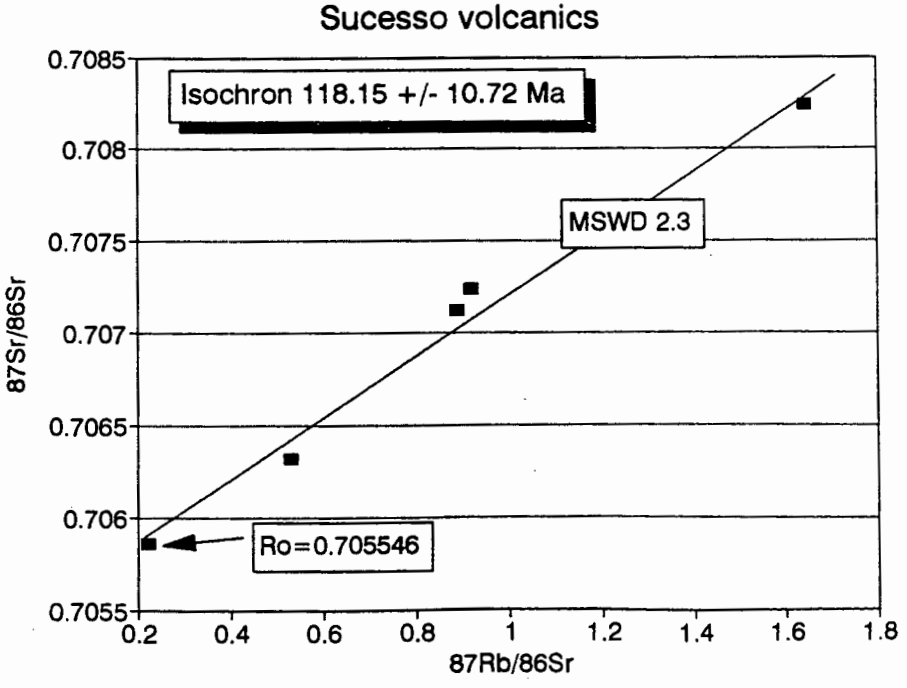

Figure II.18 - Emplacement ages for kimberlites and kimberlite related rocks obtained by Rb-Sr analysis of phlogopite separates. Decay constant used 1.42000E-11. Sample uncertainty 1 sigma. Confidence limits 95%. Determination was made using Geodate V.2.1.

Three out of the four mica samples run for the Catalão carbonatite yield an isochron of 119.30 ± 28.77 Ma (initial $^{87}Sr/^{86}Sr$ ratio of 0.705462; MSWD = 0.241). Because of the large error, the limited number of points with reliable runs, and because the mica samples represent a multi-stage intrusion, additional samples were selected and submitted for Ar-Ar dating (to Sam Bowring, MIT). No results are available to date. A similar 119 Ma age has been obtained by fission track on apatites from Catalão (A. Mariano, pers. comm., 1991).

Mica samples were hand-picked and distinct populations separated from the Presidente Olegário rock samples but they failed to run on the mass spectrometer.

II.4.2 - Whole rock isotope geochemistry

Sr, Nd and Pb isotope ratios (both present-day and initial ratios) and Rb, Sr, Sm, Nd, U and Pb concentrations obtained from whole-rock samples of the occurrences selected for the project are listed in Table II.5. As illustrated in Figures II.19 to II.22, compositions are surprisingly uniform and Nd, Sr and Pb isotope ratios are coherently correlated, despite the variable bulk chemistry and petrographic character of the intrusions.

The studied rocks have present-day $^{143}Nd/^{144}Nd$ ratios ranging from 0.51216 to 0.51234 (initial ratios @ 100 Ma ranging from 0.51210 to 0.51228), and $^{87}Sr/^{86}Sr$ ratios ranging from 0.7047 to 0.7068 (initial ratios @ 100 Ma ranging from 0.7046 to 0.7066). T_{CHUR} model ages average 478 Ma. Individually, the kimberlites and carbonatites have slightly more radiogenic Nd (average present-day $^{143}Nd/^{144}Nd$ = 0.51230; which corresponds to an ϵ_{Nd} value of -5.0) and less radiogenic Sr (average $^{87}Sr/^{86}Sr$ = 0.705) than the rift-related alkalic rocks. A crude positive correlation exists between initial $^{87}Sr/^{86}Sr$ and $^{87}Rb/^{86}Sr$ ratios (Figure II.20) but no geochronological significance can be inferred from it. The restricted range in $^{143}Nd/^{144}Nd$ ratios precludes the determination of crystallization ages using 147Sm/144Nd *versus* $^{143}Nd/^{144}Nd$ isochrons.

Present day Pb isotope signatures range as follows: $^{206}Pb/^{204}Pb$ = 17.07 to 20.96; $^{207}Pb/^{204}Pb$ = 15.31 to 15.68 and $^{208}Pb/^{204}Pb$ = 30.16 to 40.15. $^{238}U/^{204}Pb$ ratios range from 10.18 to 144.73.

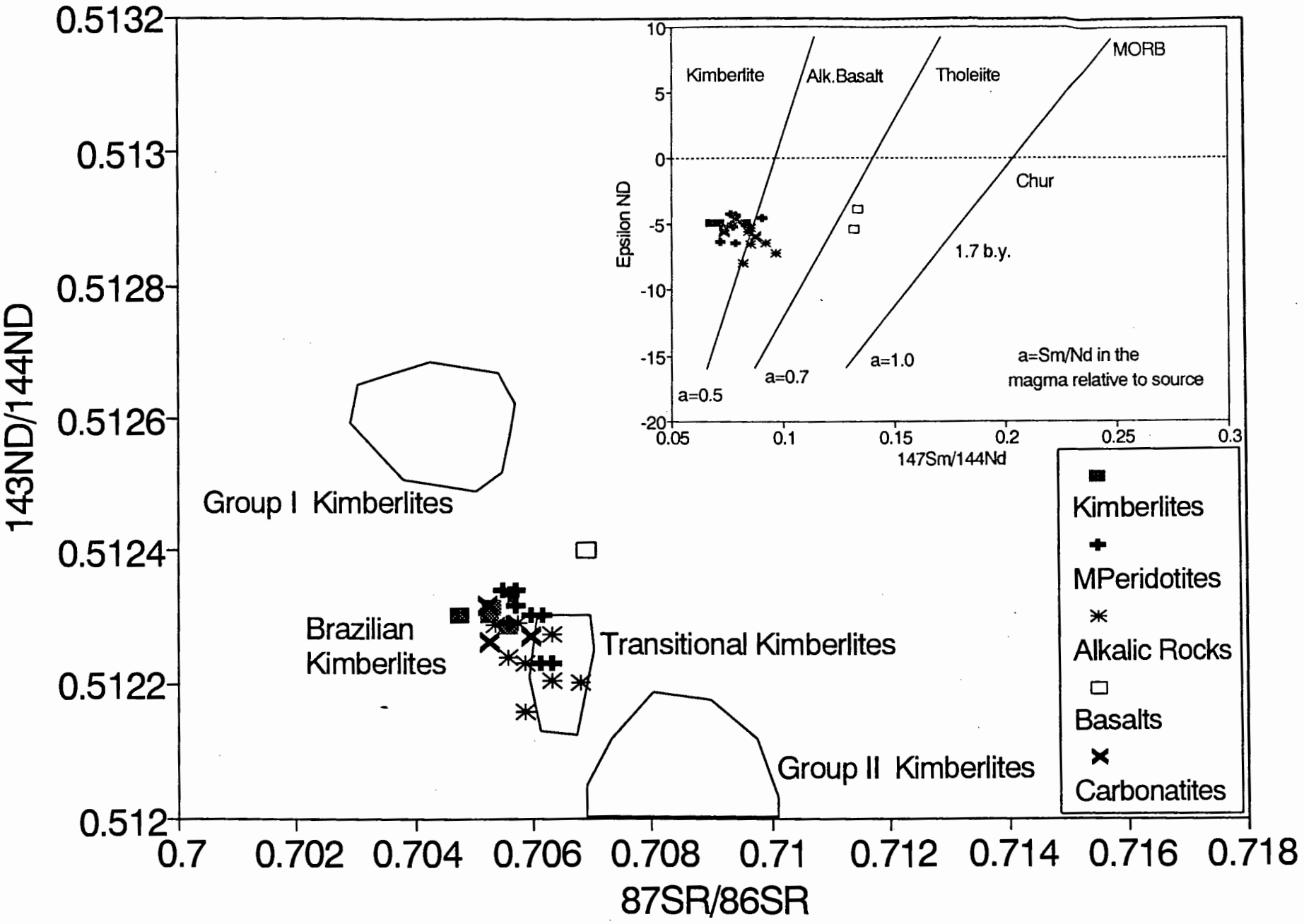

Figure II.19 - Sr and Nd isotopic signatures of studied alkaline rocks compared to Group I, Group II and Transitional kimberlites (after Smith, 1983; and Clark et al., 1991). Fields in the inset after DePaolo (1988).

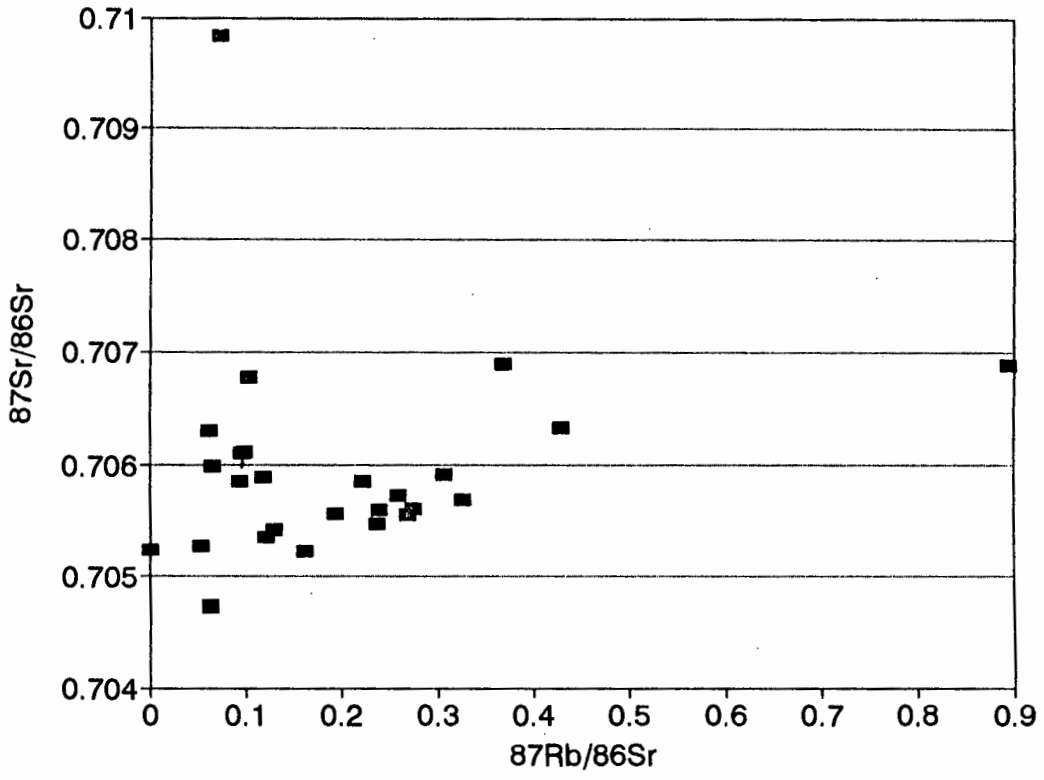

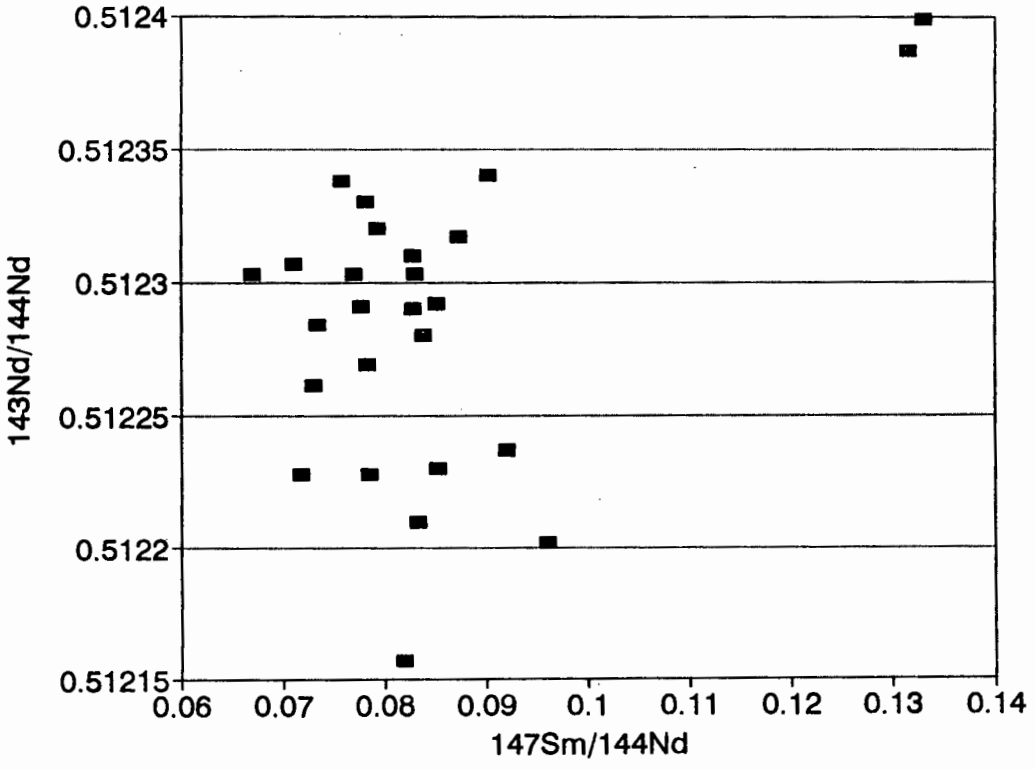

Figure II.20 - $^{87}Sr/^{86}Sr$ *versus* Rb/Sr and $^{143}Nd/^{144}Nd$ *versus* Sm/Nd

SW SAO FRANCISCO CRATON – PRESENT–DAY VALUES

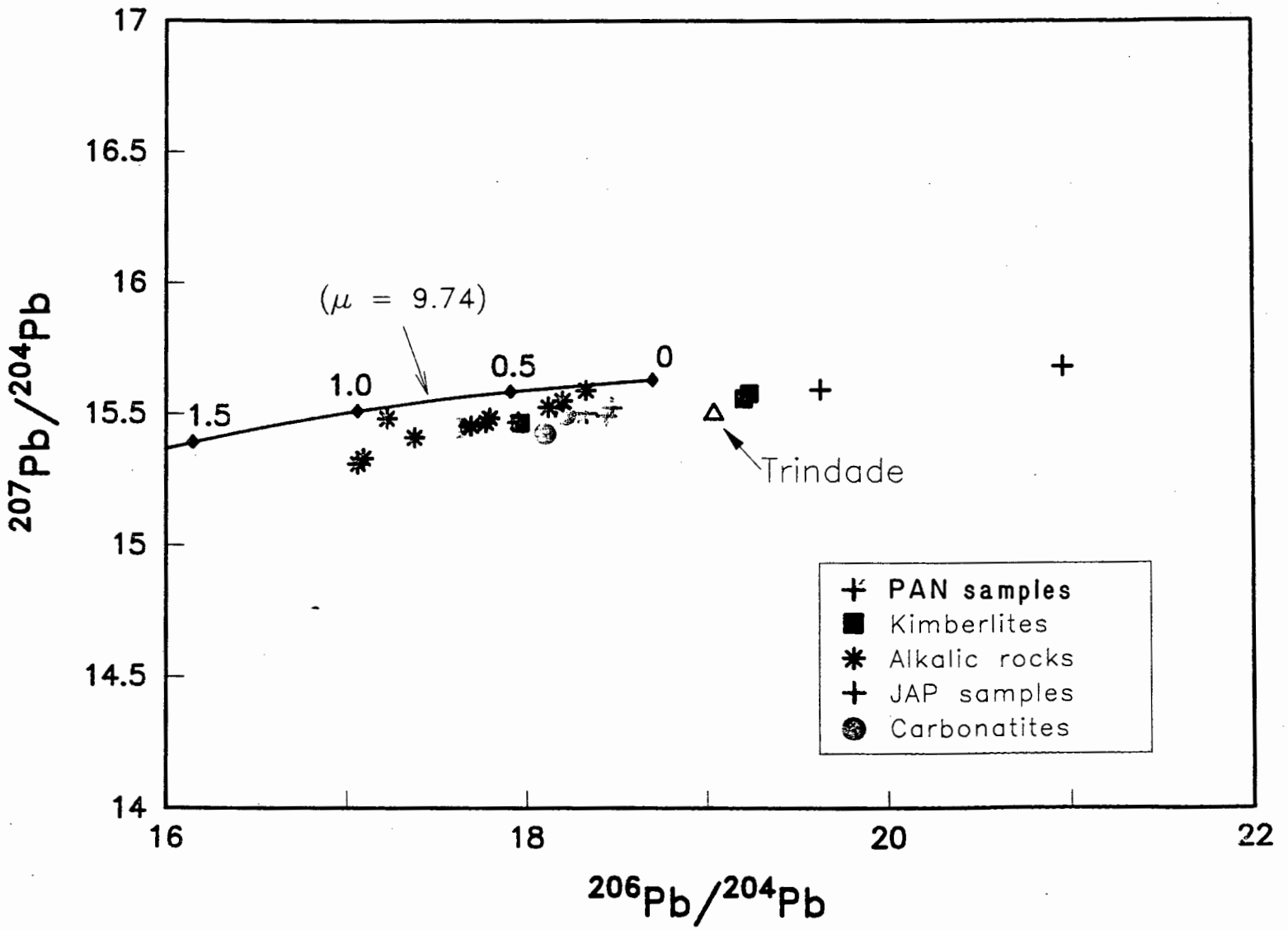

SW SAO FRANCISCO CRATON – PRESENT–DAY VALUES

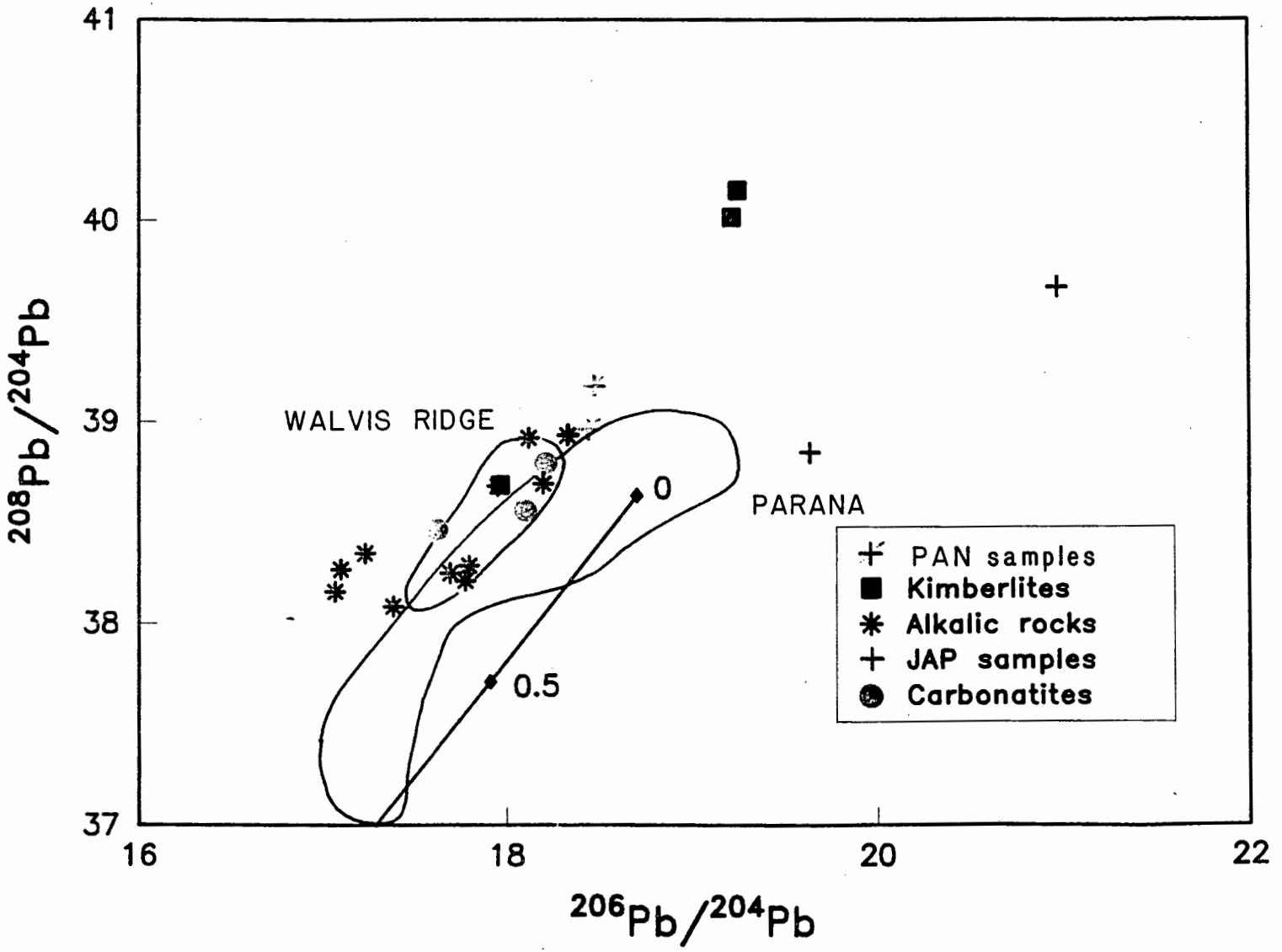

SW SAO FRANCISCO CRATON – 110 Ma

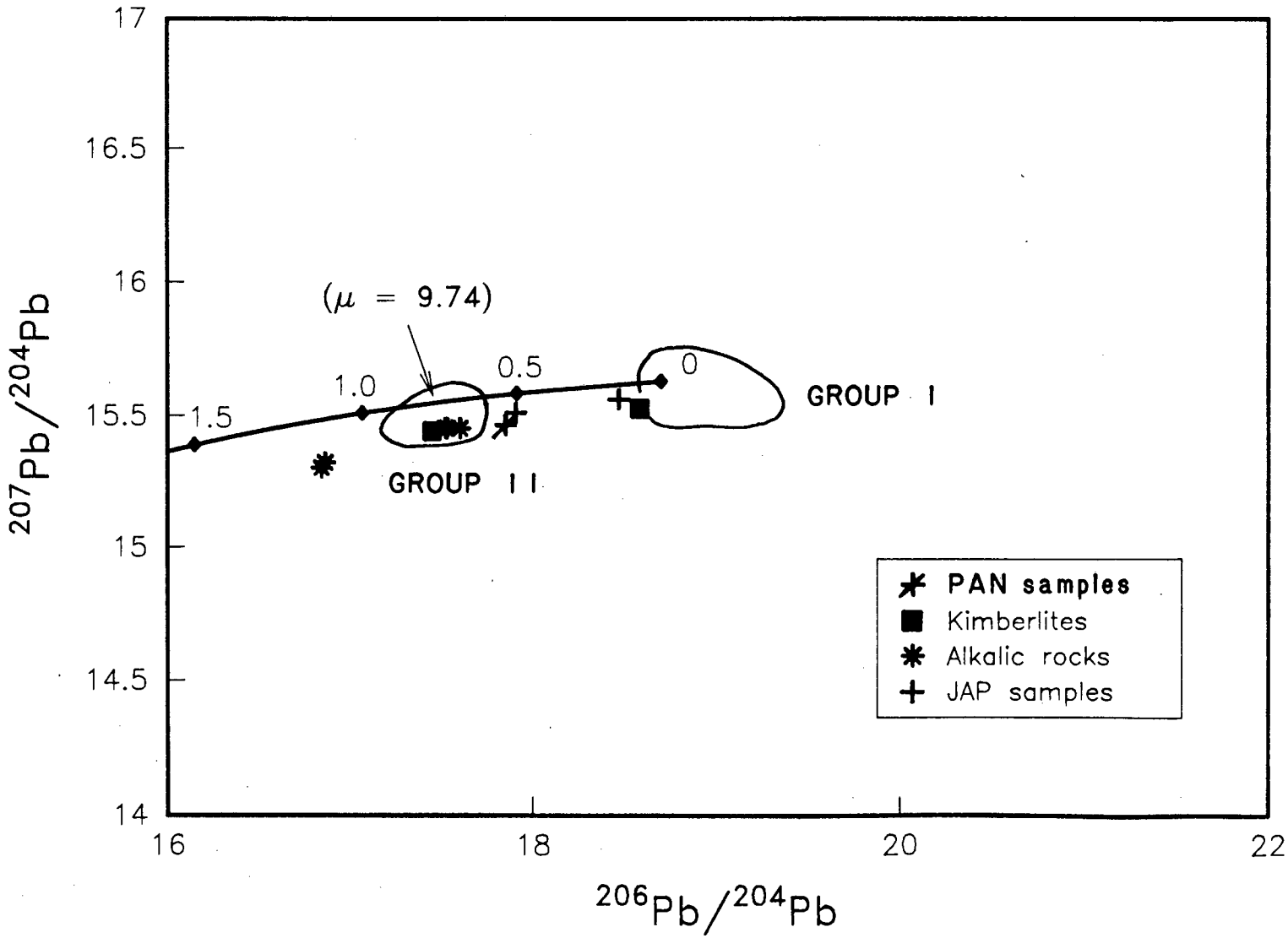

brazil.ini

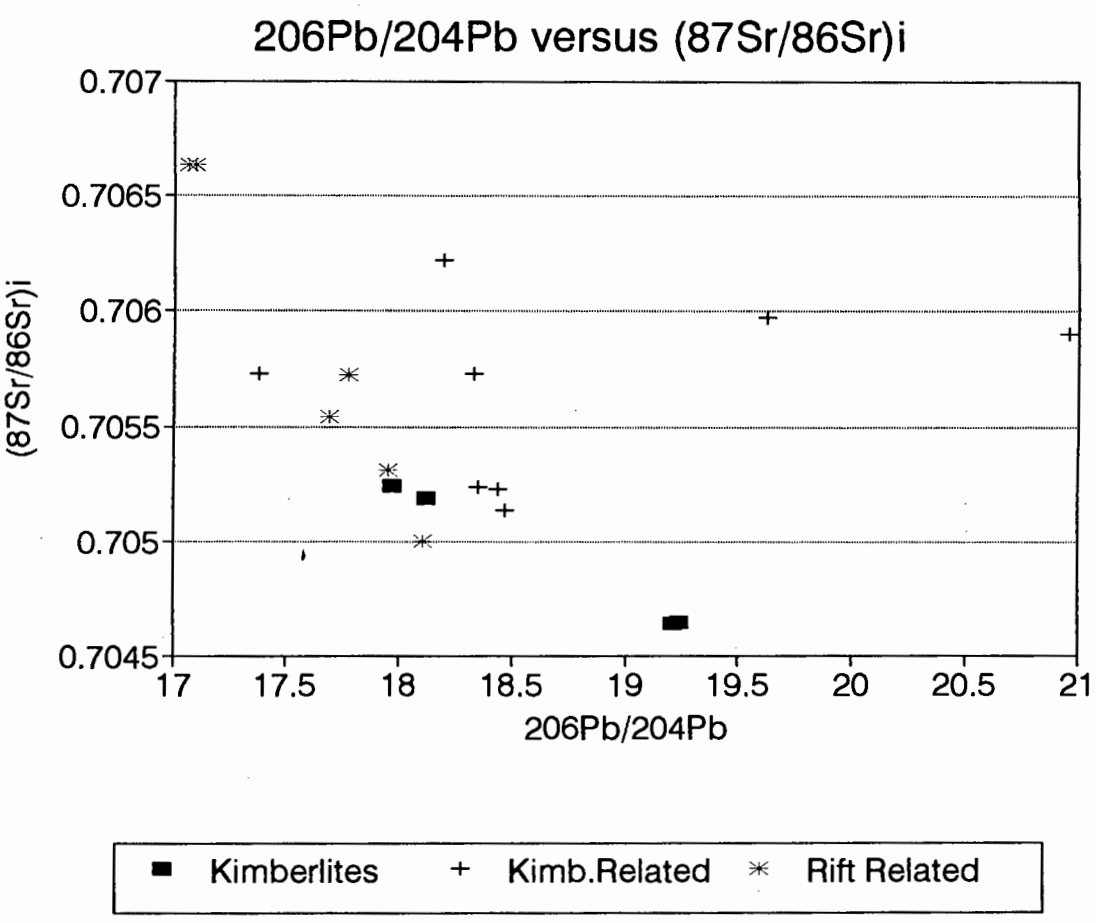
206Pb/204Pb versus (87Sr/86Sr)i
0.707
0.7065
0.706
0.7055
0.705
0.7045
(87Sr/86Sr)i
17
17.5
18
18.5
19
19.5
20
20.5
21
206Pb/204Pb
Kimberlites
Kimb.Related
Rift Related

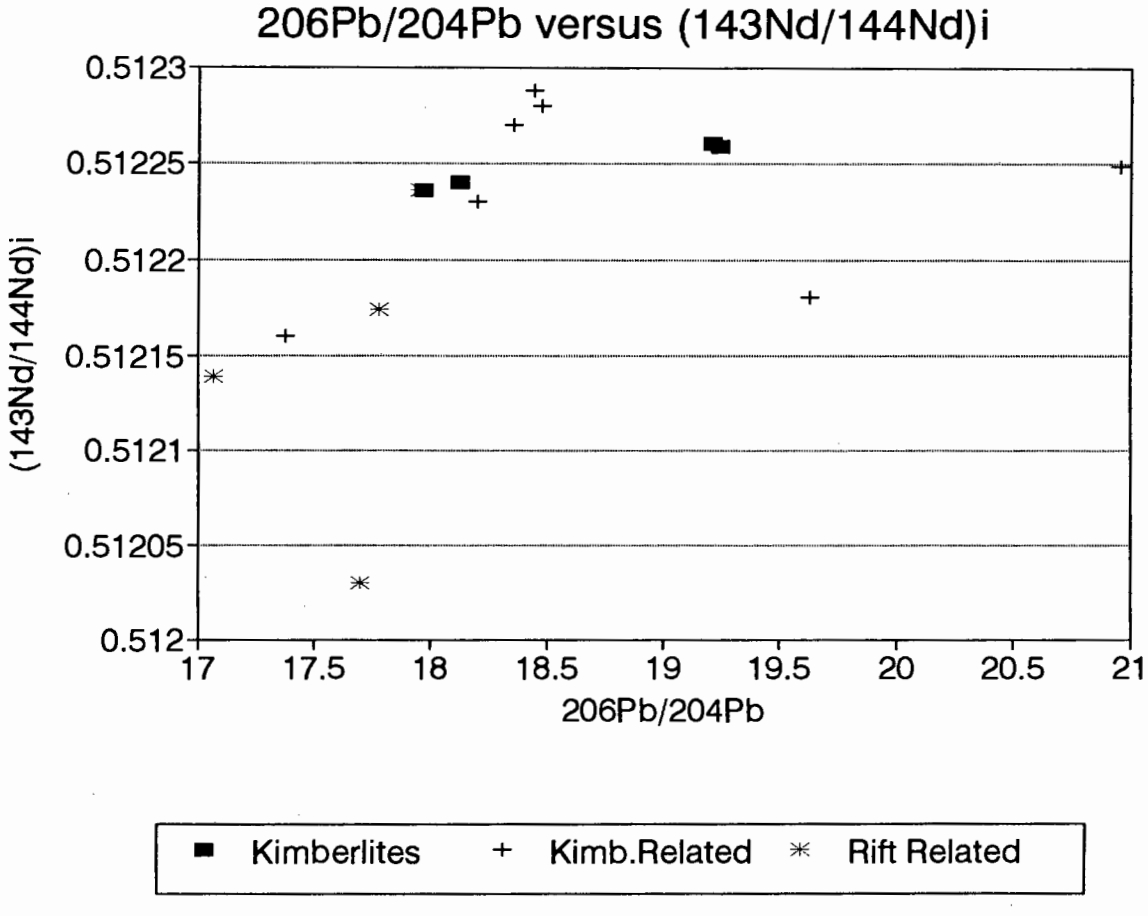
206Pb/204Pb versus (143Nd/144Nd)i
0.5123
0.51225
0.5122
0.51215
0.5121
0.51205
0.512
(143Nd/144Nd)i
17
17.5
18
18.5
19
19.5
20
20.5
21
206Pb/204Pb
Kimberlites
Kimb.Related
Rift Related

Initial ratios @ 100 Ma range from 17.44 to 19.41; and from 15.44 to 15.61 for $^{206}Pb/^{204}Pb$ and $^{207}Pb/^{204}Pb$, respectively. The kimberlites *(sensu latu)* have initial $^{206}Pb/^{204}Pb$ ratios higher than 18; whereas the other alkalic rocks have initial $^{206}Pb/^{204}Pb$ ratios between 17 and 18. Pb isotope compositions of the carbonatites are intermediate between these of the kimberlites and the rift-related rocks.

As shown in Figure II.21, notwithstanding analytical error and possible differential radiogenic Pb growth, the $^{206}Pb/^{204}Pb$ *versus* $^{207}Pb/^{204}Pb$ data define a linear array with a small degree of scatter about a reference secondary isochron of 925 Ma. Such Pb isotopic array could have age significance (*i.e.* the age of enrichment of the source) if a single component is represented. As will be discussed in Chapter III, however, there is evidence for mantle mixing in the data set. The 925 Ma reference isochron is thus best interpreted as a mixing line without age significance.

Despite their similarities in bulk composition, mineralogy and petrographic character, the isotopic composition of the kimberlites among these intrusives is very distinctive when compared to kimberlite provinces worldwide (see Figure II.19). These are the first documented examples of kimberlites with such isotopic compositions. Compared to Group I kimberlites (Smith, 1983), the Brazilian kimberlites originated from mantle source rocks with higher time-averaged Rb/Sr, Nd/Sm and Pb/U ratios (indicative of ancient LILE enrichment in the source of the Brazilian kimberlites). Compared to the source of micaceous Group II kimberlites (Smith, 1983) and isotopically transitional kimberlites (Clark et al., 1990 and 1991; Skinner et al., 1993) from southern Africa, however, the Brazilian rocks originated from sources with lower time-averaged Rb/Sr, Nd/Sm and Pb/U. The ancient enrichment of their source, therefore, was either not as intense or not as old (or possibly both) as that of the source of their South African counterparts.

II.5 - DISCUSSION

The remarkably tight clustering of the isotopic signatures suggests that a common source component may have been involved in the generation of the studied kimberlites, kimberlite-

related mica-peridotites, carbonatites and other local Mesozoic alkalic rocks. The nature of the observed Sr-Nd isotopic signatures implies that this source component involved in the petrogenesis of the studied occurrences was relatively homogeneous and enriched in Rb ($fRb > 0$) and depleted in Sm ($fSm < 0$) relative to bulk Earth, and thereafter remained isolated for a sufficient interval of time to acquire these distinctive Sr and Nd isotope compositions. Moreover, the isotope similarity of the studied rocks to those of the northern high-Ti CFB's of the Paraná Basin (in Cordani et al. 1988) and to basalts dredged from the Walvis Ridge in the south Atlantic (Richardson et al. 1984), strongly suggests their sources are closely related.

The variation in incompatible element ratios and in isotopic character suggests derivation from a heterogeneous source. The lack of correlation between $^{87}Sr/^{86}Sr$ and 1/Sr argues against large-scale contamination processes. Also, Sr and Nd contents of the studied rocks (537-13346 ppm and 19-439 ppm, respectively) are significantly higher than average upper-crust (260-500 ppm Sr and 16-23 ppm Nd; Weaver and Tarney, 1984). The enriched isotopic signatures obtained are thus unlikely to have been derived simply by interaction between OIB-like melts and continental crust. Alternative models which might account for the isotopic and incompatible trace-element compositions include *(i)* melting of a mantle with small-scale heterogeneities and *(ii)* mixing of melts from distinctive isotope reservoirs (at least one of which being the enriched mantle lithosphere), which will be discussed in Chapter III.

The derivation of the Minas Gerais magmas is suggested to follow models which favor the production of progressively more alkali-rich mafic to ultramafic magmas, ranging from alkali-olivine basalts to olivine melilitites and kimberlites, at progressively greater depths with decreasing degrees of melting and increasing amounts of CO_2 and H_2O in the melt (e.g. Eggler, 1989). In addition, the "rift-related" extrusives of the Mata da Corda Formation appear to have experienced melting, assimilation, storage and homogenization processes at relatively shallow levels. Evidence for such shallow-level processes can be summarized as follows:

(a) the volumetric dominance of "evolved" rock types associated with distinctly shallower

mantle nodules in Presidente Olegário and Carmo do Paranaíba;

(b) higher Ba/Nb, Ba/La and Sr/Nd ratios (possibly indicating assimilation of continental crust); overabundances of alkalies relative to idealized fractional-crystallization models; and large ranges in ratios of incompatible elements over limited ranges of MgO; and

(c) the identification of spinel peridotite xenoliths and cognate nodules of cumulus olivine and perovskite in the Mata da Corda volcanics, suggesting that temperature-zoned reservoirs near the density discontinuity at the base of the crust (30-40 km deep) might have existed in the area.

The volcanic rocks with these characteristics are not necessarily related in time (e.g. compare SUC to POL and CPB samples), but all have a limited areal distribution. A common geologic setting and, possibly, a major discontinuity in the local sub-continental lithospheric mantle are suspected. Such a discontinuity could possibly be interpreted as a manifestation of the western limits of the São Francisco Craton, delineated at the surface by the rocks of the Mata da Corda Formation (which were deposited within a NNE-SSW system of grabens now preserved as Cenozoic plateaux). The marginally cratonic setting could have favored the formation of alkaline ultramafic magmas by volatile influx along a steeper mantle geotherm.

II.6 - CONCLUDING REMARKS

The isotope and geochemical work thus far completed have provided two important insights. First, because of the nature and restricted variation in isotopic ratios, the kimberlites, carbonatites and other alkalic rocks in the SW São Francisco Craton were either derived from, or were intensely involved with, a common enriched lithospheric source. This source is possibly also the source for the northern Paraná basalts and is likely a component of some of the ocean island basalts (OIB's) with Dupal signatures in the south Atlantic (viz. the Walvis Ridge-type). This lithospheric source, however, is definitely dissimilar to the sources involved in the generation of Southern African kimberlites. Secondly, bulk chemistry and petrography indicate

that the magmas have probably been modified in one or more stages of diversification processes by differentiation/dilution; but the derivation of the different rock types cannot be modeled by partial melting of a relatively homogeneous mantle source region nor by crustal contamination processes. The close isotopic similarities between these Brazilian kimberlites, continental flood basalts and carbonatites (which are generally believed to be of shallow derivation), and the chemical evidence of major involvement of enriched subcontinental lithosphere in their origin, could indicate that derivation at depth was followed by further melting, assimilation, storage and homogenization processes on the way up.

A shallow (< 100 km) lithospheric source is indicated for the xenoliths in the Limeira kimberlite on the basis of geothermobarometric calculations (H.O.A. Meyer, pers. comm., 1989). This observation is consistent with the general lack of high-pressure xenolith populations (i.e. garnet peridotites and diamonds) in the studied rocks compared to kimberlites elsewhere, and could possibly explain the general lack of diamonds in Cretaceous kimberlites found to date in the Minas Gerais area.

Table II.1 - Summary of alkaline rocks

Occ. Name: Tres Ranchos/Alagoinha (TRX). Group: kimberlites.
Petrography:Hypabbysal calcite-monticellite Kimberlite.
Heavy Minerals: +8# 19 gnt + 1 ilm(*)
+16# 83 gnt + 23 ilm(*) + 5 sp
+35# 343 gnt + 31 ilm(*) + 25 cpx + 330 sp
+50# 358 gnt + 9 ilm(*) + 23 cpx + 407 sp
(*)ilmenites recovered only from concentrate collected downstream.
Emplacement age: 95 Ma.

Occ. Name: Limeira (LIM). Group: kimberlites.
Petrography: Hypabbysal calcite-monticellite Kimberlite.
Heavy Minerals: +8# 307 ilm + 2 cpx
+16# 2 gnt + 578 ilm + 147 cpx
+35# 8 gnt + 581 ilm + 497 cpx
+50# 8 gnt + 517 ilm + 550 cpx
Emplacement age: 95 Ma.

Occ. Name: Japecanga (JAP). Group: kimberlite-related.
Petrography: Phlogopite-monticellite peridotitic dykes cross-cutting volcaniclastic material.
Heavy Minerals: Not sampled.
Emplacement age: 109 Ma.

Occ. Name: Pantano (PAN). Group: kimberlite-related.
Petrography: Hypabbysal phlogopite-monticellite peridotite.
Heavy Minerals: Samples not hand-picked.
Emplacement age: 87 Ma.

Occ. Name: Sucesso (SUC). Group: rift-related.
Petrography: Alkaline basalt breccia.
Heavy Minerals: +16# 2 gnt + 4 cpx
+35# 26 gnt + 77 cpx
+50# 62 gnt + 213 cpx.
Emplacement age: 118 Ma.

Occ. Name: Presidente Olegário (POL). Group: rift-related.
Petrography: Alkaline ultramafic composite flow, breccia and surge deposits.
Heavy Minerals: +8# 5 ilm + 1 cpx
+16# 2 ilm
+35# 7 ilm
+50# 1 gnt + 3 ilm + 2 sp.
Emplacement age: Unknown.

Occ. Name: Carmo do Paranaíba (CPB). Group: rift-related.
Petrography: Alkaline ultramafic composite flow, breccia and surge deposits.
Heavy Minerals: +16# 11 ilm
+35# 56 ilm
+50# 1 gnt + 68 ilm + 8 cpx.
Emplacement age: 85 Ma.

Table II.2 - XRF analyses of samples used for isotope work.

Ref	TRX	LIM	JAP65	JAP60	PAN	POL	CPB	SUC.G	SUC.R
SiO2	34.47	29.74	34.70	32.76	32.27	37.74	37.69	36.52	43.74
TiO2	1.25	2.41	2.22	2.88	4.78	6.14	5.19	7.24	3.78
Al2O3	2.57	1.85	0.9	0.59	2.49	5.02	5.51	4.66	7.41
FeO*	9.82	10.98	12.74	13.94	14.06	14.41	14.05	14.73	11.67
MnO	0.24	0.22	0.19	0.18	0.24	0.21	0.34	0.21	0.17
MgO	31.62	29.88	30.51	32.58	24.09	16.35	13.20	15.66	9.19
CaO	4.63	10.84	2.63	2.61	10.95	10.29	11.84	9.03	11.11
Na2O	0.09	0.02	0.02	0.02	0.10	0.44	0.46	0.95	1.35
K_2O	0.93	1.05	0.25	0.15	2.42	1.74	0.92	2.81	3.53
P2O5	1.21	2.57	0.19	0.18	0.93	0.41	0.84	1.44	0.93
H2O	1.07	0.69	2.56	1.23	1.54	1.84	1.98	1.69	2.67
LOI	11.64	9.04	12.82	12.87	5.09	3.73	4.45	4.34	3.86
Total	99.33	99.25	99.70	99.97	98.96	98.32	96.46	99.27	99.41
S	554	701	982	591	3331	579	315	310	21
F	3375	2141	1491	1382	1754	2565	2829	1470	1804
Rb	72	102	18.5	9.4	179	200	78	173	50
Cs	7.7	8.6	7	7	9.1	9	9.6	10.8	9.3
Ba	3406	2551	760	335	2540	6597	17541	3070	2979
Sr	2420	2237	547	400	1825	1946	2356	2214	1377
Zr	342	573	561	770	798	744	686	1181	496
Nb	317	195	166	193	288	214	208	206	116
Y	22	34	8.8	8.3	23	23	30	30	31
La	359	193	64	66	138	112	174	140	122
Ce	547	325	136	150	210	194	295	230	249
Nd	199	151	58	68	88	95	150	109	134
U	7	3.8	9	6.5	4.5	3.5	2.1	2	2
Th	42	23	10.4	13.1	25	24	19.8	19	12.2
Mo	0.7	0.7	0.6	0.6	0.7	0.7	0.7	0.7	0.7
Ni	1747	1389	2403	2172	1094	557	437	647	559
Co	99	95	126	118	106	83	70	92	64
Mn	1798	1659	1247	1150	1784	1463	2396	1549	1261
Cr	1725	1347	893	942	1257	591	389	746	697
V	17.8	141	136	269	53	250	261	247	152
Sc	19.7	23	11.6	12.5	30	27	27	24	19.7
Pb	12.6	8	5.8	3	8.4	10.7	9	12.3	9.4
Zn	75	79	68	65	88	103	106	128	103
Cu	37	53	11.2	9.9	124	122	129	92	55

Key: TRX=Tres Ranchos kimberlite, LIM=Limeira kimberlite, JAP=Japecanga mica-peridotite, PAN=Pântano mica-peridotite, POL=Presidente Olegario alkalics, CPB=Carmo do Paranaíba alkalics, and SUC=Sucesso alkalic volcanics.
Note: total iron expressed as FeO* and LOI not adjusted for oxidation. Location as shown in Figure II.1.

Table II.3 - INAA of samples used for isotope work.

Ref	TRX	LIM	JAP60	JAP65	PAN	POL	CPB	SUC.G	CAT.F	CAT.L	CAT.S
La	429	291	71.2	68.1	274	202	224	197	247	264	251
Ce	614	480	116	117	435	364	366	366	542	438	1010
Pr	59.5	49.0	14.6	14.9	42	46.8	44.1	38.6	63.2	54.0	101
Nd	191	194	42.3	45.2	160	156	156	150	274	176	360
Sm	28.7	35.6	8.1	7.9	26.9	26	25.7	23.8	51.5	29.3	58.2
Eu	6.3	8.5	1.8	1.9	6.5	6.6	6.5	6.9	12	6.9	15
Gd	11.8	15.4	3.7	3.3	12.3	12.2	11.9	10.9	15.5	12.2	17.9
Tb	1.8	2.4	0.69	0.62	1.6	1.7	1.9	1.9	3.3	1.9	3.9
Tm	0.26	0.53	nd	nd	nd	nd	nd	nd	nd	0.36	0.60
Yb	1.01	1.44	0.55	0.47	1.09	1.18	1.29	1.51	1.86	1.35	1.98
Lu	0.19	0.22	0.16	0.17	0.17	0.18	0.21	0.21	0.16	0.23	0.23
Ba	2730	2150	548	634	2580	6540	17660	3120	419	5400	2750
Au(*)	19	34	10	9.6	30	39	32	102	49	36	66
U	7.7	5.4	7.6	7.2	6.0	5.6	5.7	3.4	2.0	5.2	nd
Co	90	82	117	113	89	75	70	76	57	61	1.2
Ta	11	10	19	19	16	15	11	12	41	10	0.84
Rb	71.7	99.6	22.2	17.3	162	203	91.4	176	111	240	nd
Sc	15	20	12	12	24	25	28	23	8.8	27	0.60
Ni	1546	1204	1999	1974	902	528	484	563	149	410	218
Sr	1490	2160	156	231	1830	1870	1960	1850	1730	1950	10100
Hf	6.5	12.3	16.1	16.4	17.2	16.2	15.2	25.8	59.5	16.4	0.13
Cr	1640	1230	1280	1270	1080	582	332	624	355	512	5.8
Th	41	23	9.0	9.1	26	25	20	19	10	18	0.99
Zn	9.9	8.2	20	24	12	15	nd	17	nd	nd	nd

Key:
TRX - Tres Ranchos kimberlite
LIM - Limeira kimberlite
JAP - Japecanga mica-peridotite
PAN - Pântano mica-peridotite
POL - Presidente Olegario alkalics
CPB - Carmo do Paranaíba alkalics
SUC - Sucesso alkalic volcanics
CAT - Catalão carbonatite (F=foscorite, L=Lamprofire, S=Sovite.

All data expressed in ppm with the exception of Au(*) which is expressed in ppb. Location as shown in Figure II.1.

Table II.4 - INAA (PGE) of samples used for isotope work.

Ref	TRX	LIM	JAP65	PAN	POL	CPB	SUC.G
Os	1.3	1.7	0.59	0.99	0.48	0.50	0.35
Ir	1.7	1.8	0.55	0.92	0.45	0.40	0.26
Ru	4.5	4.6	1.6	2.9	0.54	0.60	0.74
Pt	14	11.7	2.6	9.9	8.6	8.5	7.4
Pd	9.9	8.8	0.8	6.2	5.5	7.0	3.1

Key:
TRX - Tres Ranchos kimberlite
LIM - Limeira kimberlite
JAP - Japecanga mica-peridotite
PAN - Pântano mica-peridotite
POL - Presidente Olegario alkalics
CPB - Carmo do Paranaíba alkalics
SUC - Sucesso alkalic volcanics

Material preconcentrated by nickel sulphide fire-assay and PGE determination by neutron activation analysis. Location of samples as shown in Figure II.1.

Table II.5 - Whole-rock isotope compositions of studied alkalics.

Ref	TRX(k)	TRX(k)	TRX(d)	TRX(d)	LIM(k)	LIM(k)	LIM(k)	JAP60(p)	JAP60(p)	JAP65(p)	JAP65(p)
$^{87}Sr/^{86}Sr$	0.70473	0.70562	0.70689	0.70690	0.70543	0.70528	0.70536	0.70599	0.70598	0.70611	0.70612
$^{87}Rb/^{86}Sr$	0.0636	0.0637	0.89450	0.36824	0.12923	0.0530	0.121	0.06637	0.07278	0.0969	0.0988
Sr	1215	2412	417	668	2278	2687	2401	400	142	537	294
Rb	54.28	52.94	211.79	84.90	101.62	48.9	100.1	9.2	9.5	17.9	18.4
Ro	0.70464	0.70465	0.70561	0.70638	0.70525	0.70521	0.70523	0.70590	0.70598	0.70597	0.70598
$^{147}Sm/^{144}Nd$	0.0711	0.0678	0.13151	0.13292	0.0828	0.0839	nd	0.08310	0.07706	0.07181	0.07857
$^{143}Nd/^{144}Nd$	0.51231	0.51230	nd	0.51240	0.51228	0.51231	0.51228	0.51230	0.51230	0.51223	0.51223
Sm	46	25.4	9.7	9.63	27.9	29.5	32.4	6.5	7.0	6.1	6.5
Nd	391.5	229.2	46.7	43.8	229.8	212.6	236.7	47.3	55.1	51.3	50.1
Ro	0.51226	0.51226	nd	0.51231	0.51224	0.51226	nd	0.51225	0.51225	0.51218	0.51218
$^{206}Pb/^{204}Pb$	19.21	19.24	nd	nd	17.97	nd	18.12	20.96	nd	19.62	nd
$^{207}Pb/^{204}Pb$	15.56	15.57	nd	nd	15.46	nd	15.53	15.68	nd	15.59	nd
$^{208}Pb/^{204}Pb$	40.01	40.15	nd	nd	38.68	nd	38.92	39.67	nd	38.34	nd
$^{238}U/^{204}Pb$	36.38	nd	nd	nd	30.02	nd	nd	144.73	nd	99.98	nd

Ref	PAN(p)	PAN(p)	PAN(p)	POL(a)	POL(a)	CPB(a)	SUC.G(a)	SUC.R(a)	CAT.F(c)	CAT.S(c)	CAT.L(c)
$^{87}Sr/^{86}Sr$	0.70556	0.70562	0.70548	0.70568	0.70557	0.70586	0.70586	0.70678	0.70523	0.70525	0.70592
$^{87}Rb/^{86}Sr$	0.2686	0.2744	0.2370	0.2593	0.19308	0.0944	0.2225	0.10386	0.1616	0.0005	0.3066
Sr	1899	1874	1766	2278	991	2355	2248	1374	2218	13346	2523
Rb	176	177	145	201	66	76.7	172.6	49.25	123.7	2.2	267
Ro	0.70518	0.70523	0.70514	0.70531	0.70530	0.70573	0.70554	0.70663	0.70500	0.70524	0.70548
$^{147}Sm/^{144}Nd$	0.0777	0.0758	0.0903	0.0851	0.0919	0.0852	0.0819	0.09611	0.0873	0.0731	0.0783
$^{143}Nd/^{144}Nd$	0.51229	0.51234	0.51234	0.51229	0.51224	0.51223	0.51216	0.51220	0.51232	0.51226	0.51227
Sm	24.6	23.2	26.7	23.9	6.2	24.4	20.4	17.0	46.7	53.1	28.2
Nd	19.2	185.0	178.7	170.2	40.7	173.4	150.6	107.1	323.2	439.5	217.9
Ro	0.51224	0.51229	0.51228	0.51224	0.51218	0.51217	0.51210	0.51214	0.51226	0.51221	0.51222
$^{206}Pb/^{204}Pb$	18.44	18.33	18.47	17.95	17.8	17.78	17.70	17.07	18.11	17.63	18.22
$^{207}Pb/^{204}Pb$	15.49	15.50	15.53	15.47	15.48	15.47	15.45	15.31	15.43	15.45	15.50
$^{208}Pb/^{204}Pb$	38.96	38.94	39.18	38.68	38.28	38.21	38.25	38.16	38.56	38.47	38.80
$^{238}U/^{204}Pb$	34.22	nd	nd	20.67	nd	14.61	10.18	13.16	nd	nd	nd

Key: TRX=Tres Ranchos kimberlite, LIM=Limeira kimberlite, JAP=Japecanga mica-peridotite, PAN=Pântano mica-peridotite, POL=Presidente Olegario alkalics, CPB=Carmo do Paranaíba alkalics, SUC=Sucesso alkalic volcanics and CAT=Catalão carbonatite (L=lamprofire, S=sovite and F=foscorite). (k)=kimberlites, (d)=dolerite dikes, (p)=kimberlite-related "peridotites", (a)=rift-related alkalic rocks and (c)=carbonatite complexes. $^{143}Nd/^{144}Nd$ reported relative to 0.51264 in BCR/1 and $^{87}Sr/^{86}Sr$ reported relative to 0.7080 in EnA Sr standard. Initial ratios calculated for 100 Ma. Decay Constants 1.42000E-11 and 6.54000E-12 for Sr and Nd, respectively.

Table II.6 - Isotope compositions of Phlogopites.

Ref	LIM(1)	LIM(1)	LIM(2)	LIM(2)	LIM(3)	LIM(3)	LIM(4)	LIM(4)	LIM(5)	LIM(5)	LIM(6)	LIM(6)	LIM(7)	LIM(8)
$^{87}Sr/^{86}Sr$	0.71847	0.71740	0.72329	0.71911	0.71219	0.71216	0.70896	0.72121	0.71225	0.71434	0.70721	0.70721	0.71706	0.70783
$^{87}Rb/^{86}Sr$	9.291	9.345	12.74	12.87	4.141	4.151	3.215	3.223	6.801	6.773	1.945	1.950	10.231	2.151
Sr	134.8	134	102.8	101.7	287	286.3	340.4	340	163.2	163.9	598.5	597	145.1	513.9
Rb	439.9	433	452	nd	410.7	nd	378.3	nd	383.5	nd	402.9	402.5	nd	nd

Ref	CPB(1)	CPB(2)	CPB(3)	CPB(4)	CPB(4)	CPB(5)	CPB(6)	CPB(7)	CPB(8)	CPB(9)	CPB(10)	CPB(11)	TRX(1)	TRX(2)
$^{87}Sr/^{86}Sr$	0.71604	0.71037	0.70862	0.70929	0.70911	0.70831	0.70723	0.70626	0.70706	0.71411	0.72125	0.70955	0.71796	0.71057
$^{87}Rb/^{86}Sr$	6.393	2.842	1.378	1.852	1.856	3.981	0.874	0.387	2.267	7.019	12.670	3.281	10.25	3.831
Sr	170	347	662	497	496.3	198.6	859	1939	337.4	118.2	105.1	248.0	157.1	284.0
Rb	379.5	341	315.5	318	nd	273.3	259.6	nd	nd	nd	nd	nd	556.1	376.0

Ref	TRX(3)	TRX(4)	SUC(1)	SUC(2)	SUC(3)	SUC(4)	CAT(1)	CAT(2)	CAT(3)	CAT(4)	POL(1)	POL(2)
$^{87}Sr/^{86}Sr$	0.71488	0.73060	0.70824	0.70724	0.70632	0.70712	0.70641	0.70706	0.71474	0.70741	0.71874	0.71865
$^{87}Rb/^{86}Sr$	7.851	17.13	1.642	0.919	0.530	0.888	0.568	0.922	18.42	1.159	9.899	nd
Sr	191.8	122.1	355.1	648.3	1437	583.7	1546	1510	73.66	1133	135.8	135.1
Rb	520.2	721.3	201.6	205.9	263.4	179.2	303.8	481.5	468.6	454.1	464.2	nd

Key: TRX=Tres Ranchos kimberlite, LIM=Limeira kimberlite, POL=Presidente Olegario alkalics, CPB=Carmo do Paranaíba alkalics, SUC=Sucesso alkalic volcanics and CAT=Catalão carbonatite. $^{87}Sr/^{86}Sr$ reported relative to 0.7080 in EnA Sr standard.
Decay Constant used 1.42000E-11.

Chapter III

Evidence for interaction of discrete mantle reservoirs beneath the craton margin.

III.1 - INTRODUCTION

The nature, evolution and distribution of isotopically discrete mantle domains are first-order constraints on models of mantle dynamics. Isotopic heterogeneities in the mantle occur on both small and large scales, and the case for a chemically heterogeneous mantle has now been firmly established for both sub-oceanic and sub-continental mantle (Allégre, 1982; Zindler and Hart, 1986; Hart, 1988; and Hart and Zindler, 1989). Isotopic and trace-element variations in mantle-derived potassic and ultrapotassic alkaline volcanics (e.g. references in Fitton and Upton, 1987; and Menzies and Hawkesworth, 1987) and many mantle derived xenoliths (references in Nixon, 1987) testify to the operation of mantle-enrichment processes in continental settings. Evidence for enrichment processes has also been recognized in the source regions of both Ocean Island Basalts (OIB) and Mid-Ocean Ridge Basalts (MORB) (references in Menzies and Hawkesworth, 1987). At least three distinct enriched mantle end-member components (HIMU, EMI and EMII) are necessary to accurately fingerprint the enriched sub-oceanic mantle signatures recognized to date (e.g. Hart, 1988). The mantle locations of these reservoirs, however, are uncertain; both deep seated asthenospheric plumes and continental lithosphere have been suggested (e.g. Hart, 1988; and Allégre, 1982).

In this chapter the isotopic characteristics of the Mesozoic alkalic magma-types discussed in chapter II are used to characterize an isotopically discrete and physically continuous mantle domain underlying the craton margin. Radiogenic isotopes and Platinum-Group-Elements (PGE) are used, along with mineralogical and geochemical data, to constrain a systematic variation of

source characteristics and possible mixing of mantle reservoirs. Modelling of isotope and petrological data are used to unravel the nature of the source components and the mixing processes, whilst PGE variations are used to constrain entrainment or remobilization of PGE into kimberlite-related magmas. At the end of this chapter, the time-integrated Nd isotope evolution of on- and off-craton supracrustal rocks discussed in Chapter I is compared with that of the section of enriched sub-continental mantle lithosphere involved in the generation of the alkalic magmas discussed in Chapter II.

III.2 - EVIDENCE FOR MANTLE HETEROGENEITIES

III.2.1 - Source characteristics

The isotopic signatures of the Mesozoic alkalic magmas which intrude the southwestern São Francisco craton margin reveal a relatively high degree of isotopic uniformity of the upper-mantle sources beneath the 200 km E-W traverse represented at the surface by the studied occurrences. The tight clustering of Sr-Nd signatures obtained is such that a common source component can be postulated to have been involved in the generation of all the studied alkalic rocks. This source component was enriched in Rb and depleted in Sm relative to bulk Earth for a significant period of time, and had overall chemical compositions which are typical of enriched mantle lithosphere. In addition, this common source is also isotopically similar to the source of the high-Ti-flood basalts of the northern Paraná basin up to 250 km south of the study area (data for the Paraná basalts are compiled from Cordani et al., 1988). Because both the flood-basalts and the studied alkalic rocks have similar emplacement ages, it is difficult to escape the implication that they shared a common mantle source, and that the portion of the mantle which is under discussion might be physically contiguous and relatively uniform on a regional scale.

Such general regional uniformity, however, conceals two significant observations at a finer scale. First, the isotopic variation within each group of rocks (*i.e.* kimberlites, carbonatites, etc), in any isotopic space considered, is less than that between the different groups (see Figure III.1). Secondly, from the data available to date, it appears that kimberlite type magmas tend to

concentrate in the west of the study area and the Mata da Corda volcanics in the east. Should this observation apply widely, then it would imply a small but distinctive lateral variation of source characteristics observable on a regional scale.

Because such systematic changes in isotopic signatures are accompanied by changes in rock types, and because the different rock types are believed to have been derived from different depths, it is suggested that the different isotopic compositions in the area may be representative of different source depths. Relative source depth profiles indicated in Figure III.2 have been constructed on the basis of xenolith composition and geothermobarometry, presence or absence of diamonds, and petrographic and compositional characteristics of the studied rocks in the light of experimental and theoretical studies. Systematic lateral variations of the source are evident on a regional scale: a higher proportion of primitive magmas with higher ϵ_{Nd} values and lower $^{87}Sr/^{86}Sr$ values occur in the west of the study area; whilst a higher proportion of evolved magmas with lower ϵ_{Nd} and higher $^{87}Sr/^{86}Sr$ values occurs in the east (see Figure III.2). It is speculated that such lateral variations result from a progressive vertical shift in the zone of melting from west to east, in which case vertical geochemical heterogeneities may have been translated into lateral geochemical heterogeneities, at surface, by control of the source depth.

Another important source characteristic of the studied alkalic rocks is that they all have typical Dupal anomaly characteristics (both in terms of $^{207}Pb/^{204}Pb_i$ and $^{208}Pb/^{204}Pb_i$ deviation from a northern hemisphere reference line - NHRL; and in terms of absolute value of $^{87}Sr/^{86}Sr_i$; *c.f.* Hart, 1984). The relevance of this observation is emphasized by the isotopic similarities between these rocks and some OIB with Dupal signatures in the South Atlantic (viz. the Walvis Ridge Basalts).

It is indicated, therefore, that both large scale and small scale heterogeneities are represented in the data set under consideration: at the largest regional scale the Brazilian rocks were derived from a relatively homogeneous mantle reservoir, which resembles EMI and as such is distinctive from the average subcontinental mantle lithosphere; at the smallest local scale heterogeneities are apparent and some input from a mantle reservoir with distinctive characteristics is suspected.

Isotopic Signatures

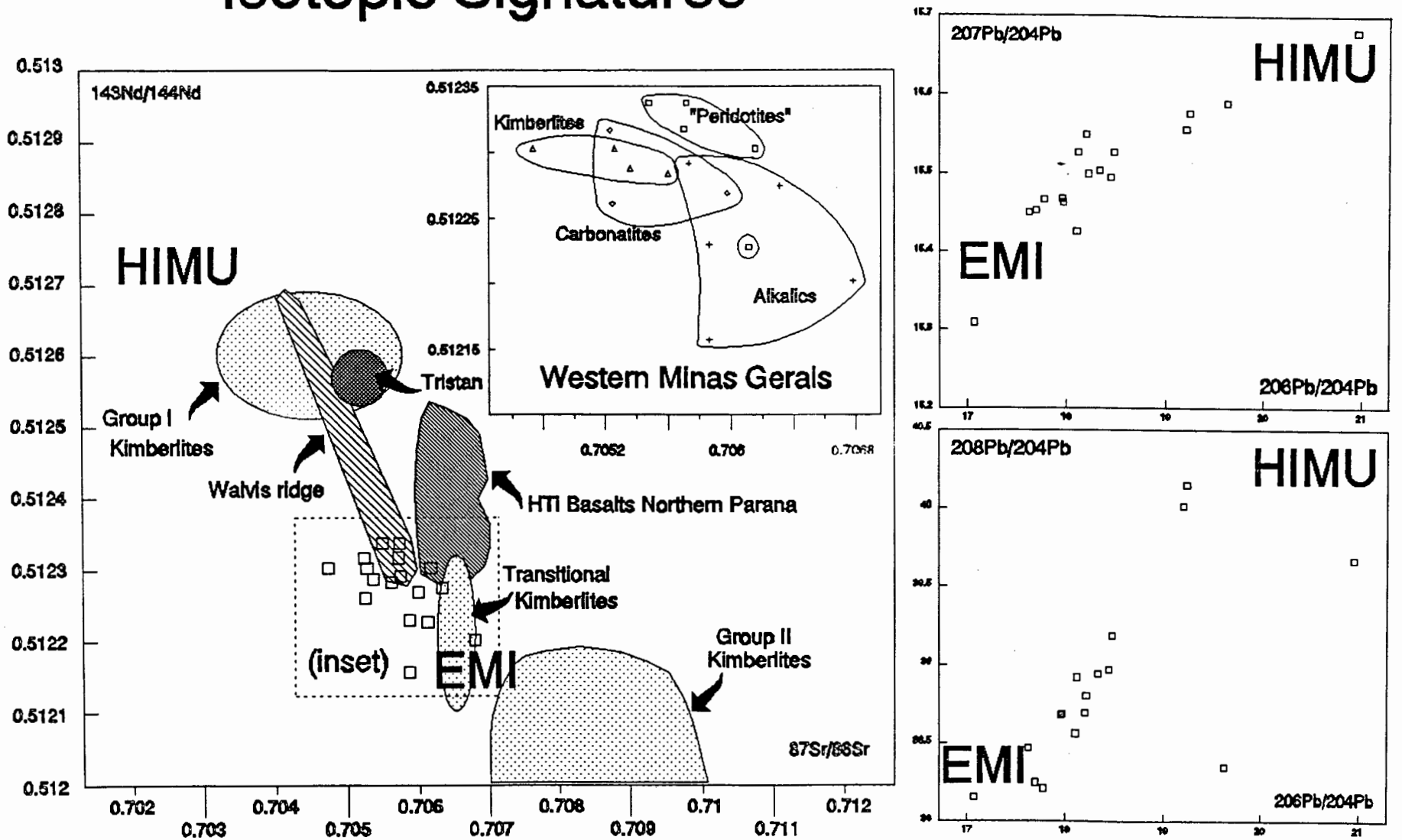

Figure III.1 - Sr, Nd and Pb isotopic signatures and their possible relationship to EMI and HIMU theoretical components. Note (inset) that despite the significant overlap between Sr and Nd isotopic compositions of the different rock types, the internal variation within the different petrographic types is less than that between the different Groups (i.e. kimberlites, "peridotites" or rocks with kimberlitic affinity, carbonatites, and rift-related "alkalics"

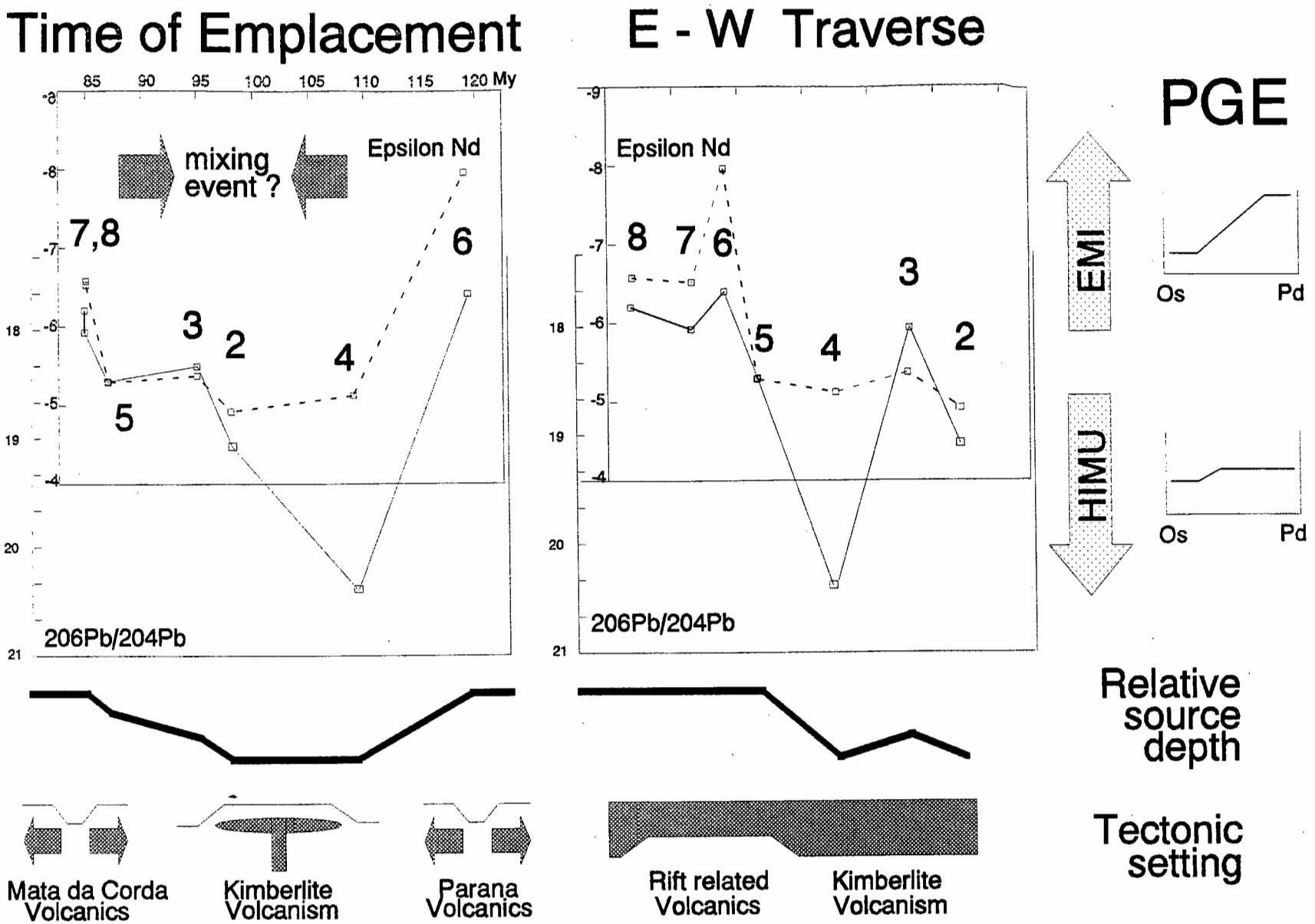

Figure III.2 - Summary of source depth profiles related to isotopes and PGE characteristics. Neodymium isotopic signatures and U/Pb ratios are plotted against time of emplacement and according to the E-W distribution of the intrusives, and compared to relative source depth profiles constructed on the basis of xenolith composition, geothermobarometry, presence of diamonds, petrographic and compositional characteristics. The systematic change in isotopes and PGE with the nature of the rock-types may be depth related and represent differences in the tectonic setting of the intrusives. Possible implications for the nature and evolution of the local mantle lithosphere and for the ultimate origin of EMI- and HIMU-like signatures are discussed in the text.

III.2.2 - Further evidence from PGE geochemistry for source heterogeneity

This study shows that the PGE concentrations of the Brazilian samples are compatible with the range of values reported by McDonald et al. (1992) for South African kimberlites. The relationship between PGE and some trace-elements in the Brazilian rocks, however, differs from what has been identified in South African kimberlites derived from enriched sources (Figure III.5, after McDonald, 1994). The link of such distinct PGE signatures to time-integrated source character is supported by the intrinsic relationship between isotopes and PGE characteristics identified in the Brazilian data set and illustrated in Figure III.6. In addition, the reconciliation of the PGE concentrations and fractionation patterns observed for the studied rocks with those typically found in subcontinental lithospheric mantle peridotites (2 to 6 ppb; see Morgan et al., 1981; Mitchell and Keays, 1981; and Morgan, 1983) provide useful constraints for the processes of mobilization of PGE in the sub-continental mantle lithosphere and shed new light on the nature of mantle heterogeneities beneath the SW São Francisco craton.

It is envisaged that three factors could have influenced the fractionation of PGE in the studied rock samples:

(i) Degree of partial melting: the tendency of Pd/Ir ratios of mantle melts to decrease as the degree of partial melting increases has long been recognized (e.g. Pd/Ir decreases in the sequence continental flood basalts > mid-ocean ridge basalts > high MgO basalts > komatiites; Barnes et al., 1985; Tredoux et al., 1986). The less fractionated PGE patterns of the kimberlites compared to the rift-related rocks (Figure II.16), however, would appear to contradict the evidence from REE that the kimberlites were derived by smaller degrees of partial melting than the other rock types.

(ii) Temperature: it has been suggested that temperature, rather than degree of partial melting, may be a most important and determining factor in influencing the behavior of two groups of PGE which fractionate relative to each other during upper mantle magmatic processes (Tredoux et al., 1986). The two groups of PGE have been referred to as the high temperature group (HTPGE, with melting point of the pure element >2000°C and

comprising of Os, Ir and Ru); and the low temperature group (LTPGE, with melting point $<2000^{o}C$ and comprising of Pt, Pd and Rh). Because most mantle melts tend to be enriched in LTPGE and mantle residues tend to be relatively enriched with HTPGE, the crust should be relatively more enriched with LTPGE, whereas the lithospheric mantle should be relatively more enriched with HTPGE (Tredoux et al., 1986 and 1989; Tredoux, 1990). Considering the intrinsic relationship between source characteristics and PGE characteristics illustrated in Figures III.5 and III.6, this hypothesis could possibly apply to the data set obtained in this study. The possibility that such variations could be related to temperature variations of the order suggested by Tredoux et al.(op. cit), however, would imply that extreme temperature gradients exist between the two mixing reservoirs.

(iii) Source depth: Hamlyn et al. (1985) first suggested that the enhanced concentrations of Ir in kimberlites compared to boninitites and MORB might be related to source depth and the prevailing mineralogy. Such a suggestion seem to apply well to the southwestern São Francisco craton. The PGE characteristics of the studied rocks follow the relative source depth profiles indicated in Figure III.2 in such a way that the rift-related rocks, presumed to have been derived from shallower depths than the kimberlites, lack the very characteristic HTPGE enrichment and signature (with the pronounced Ir anomaly) observed in the latter rocks. Moreover, the clear correlation between PGE ratios and isotope compositions illustrated in Figure III.6 suggests that both PGE contents and interelement characteristics of the studied rocks might be related to time-integrated source characteristics rather than to fractionation processes. Such observations apply widely in the studied rocks and seem to indicate that, as for the radiogenic isotopes, the observed systematic variations in PGE may accompany a vertical shift in the zone of melting.

The observed variations of PGE cannot be readily related to fractionation during melting processes and are unlikely related to unrealistic within-lithosphere temperature gradients. A preferred alternative is that the systematic variations in radiogenic isotopes and PGE observed in the studied rocks represent a concomitant vertical shift in the zone of melting. Similar depth-dependent variations have been documented by McDonald et al. (in the press) who contrasted

on-craton and off-craton South African kimberlites and lamproites. Following the reasoning presented by McDonald et al., it is suggested that such vertical variations in the Brazilian rocks could be the result of physical assimilation and dilution of PGE-fractionated (i.e. HTPGE-rich) material from the upper mantle lithosphere by unfractionated PGE-poor melts.

III.2.3 - Use of PGE and isotope data in mixing and addition models

The possibility that the PGE patterns shown by Japecanga and Sucesso might represent two end members which could be combined to produce the PGE patterns found in the other associated occurrences was tested with mixing and addition models. Deficiencies in Pt and Pd were found in mixing combinations involving the unfractionated Japecanga-like component with a fractionated Sucesso-like component. However, addition of variable concentrations of a PGE material with Japecanga-like PGE-unfractionated characteristics to a PGE-fractionated reservoir is able to reproduce the full range of PGE patterns observed. The PGE compositions of the samples SUC (from Sucesso), CPB (from Carmo do Paranaíba) and POL (from Presidente Olegário) can be satisfactorily duplicated by the addition of a small amount of Japecanga-like component to a SUC.G composition. The addition model results in negligible dilution of the fractionated reservoir because of the relatively small volume of contaminant. The patterns for Tres Ranchos, Limeira and Pântano can also be closely modelled by the addition of à Japecanga-like component to SUC.G, but only if large amounts of this component (up to two times the PGE content of Japecanga) are used.

Plots of Pt and Pd *versus* Ir (see Figure II.17) show a close correlation between the noble metal contents of the various rock types. The slopes of the curves are very similar to the observed Pt/Ir and Pd/Ir ratios in Japecanga. The behavior of these metals can be represented by a linear type of relationship " **y = mx + c** " where the constant " **c** " is the fractionated component SUC.G and " **m** " is the proportion of JAP component. The mixing proportions calculated using this equation compare favorably to the concentrations calculated using the above mentioned addition models and to those calculated using isotope data (see Figure III.3 and Table III.1).

It is conceivable that other unfractionated rock types might also produce the observed range in patterns when combined with a fractionated Sucesso-type pattern. Similar mixing and addition relationships were thus attempted using PGE concentrations of garnet lherzolite (taken from Morgan et al., 1981) and residual dunites and chromitites (taken from Page & Talkington, 1984). None of these other components are able to simulate the observed patterns, suggesting that the composition of Japecanga most accurately reflects the possible component which attributed Os and Ir to the other melts.

Taken together, the systematic change in the nature of correlated rock-types and isotopic compositions, the range of PGE signatures which complements the isotopic data, and the small degree of overlap between the different groups of rocks, all suggest that there may be a progressive regional change in end-member proportions and that systematic change of end-member contributions exist among rock types. There is, therefore, evidence that more than one component was probably involved in the generation of the observed compositions.

With that in mind, I propose that the trends observed for the Minas Gerais rocks in Figures III.I and III.3 depict mixing lines between two end-members: viz. (i) deep-derived melts represented by the kimberlites and related rocks; and (ii) a volumetrically dominant lithospheric mantle peridotite which is represented to a larger extent in the shallower rift-related alkalic rocks. The first end member has lower time averaged Rb/Sr, Nd/Sm and Pb/U ratios and is, therefore, isotopically more similar to OIB's and Group I kimberlites (Smith, 1983) than the second end member. Such distinctive isotope characteristics are prevalent in the rock samples in which higher Pt contents and less fractionated PGE signature were documented (Figure III.6). The second component is present in all the studied rocks, but clearly dominates in the alkalic rocks of the Mata da Corda Formation (represented in Tables II.1 to II.4 by the POL and CPB samples) and in those related to the Paraná volcanics (SUC samples). Compared to the first end member, this second end member records higher time-averaged source enrichment in Nd, higher time-averaged enrichment in Rb and less radiogenic $^{206}Pb/^{204}Pb$ values (presumably reflecting lower time-averaged U/Pb ratios). The rocks in which a higher proportion of the second end member is inferred are the ones in which lower Pt contents and more fractionated PGE

signatures have been recorded (Figure III.6).

The overall isotope compositions obtained are typical of enriched lithosphere (Hawkesworth et al., 1990) and, together with the geochemical and petrographic characteristics of the rift-related rock types and their xenoliths (see chapter II), indicate that these melts either interacted extensively with the local enriched lithosphere or were derived from it. The negative covariation of $^{87}Sr/^{86}Sr$ *versus* both $^{206}Pb/^{204}Pb$ and $^{143}Nd/^{144}Nd$ provides further evidence for the involvement of continental mantle lithosphere as a major component in the generation of these rocks. It also demonstrates that the higher Rb/Sr ratios representative of the second component correlate with lower time averaged U/Pb and Sm/Nd ratios.

Implicit in the discussion of end member characterization is the contention that isotopic signatures reflect mixing between two end-members. The accuracy of the mixing hypothesis is reflected by the fact that the relative positions of individual localities, with respect to the two end members, remain relatively constant from one isotopic space to the next (see Figures II.19, II.21, III.I and III.3). Because of the restricted isotopic variation among the studied rocks, the definition of mixing lines is necessarily imprecise on this scale and dependent on chosen end-members and respective concentrations. Both analytical uncertainties and small-scale source heterogeneities are significant sources of scatter in the modelling, and preclude the possibility of delineating unique component contribution to the compositional varieties at the individual localities. Approximate Pb isotopic compositional limits for the most light-REE enriched end member composition (indicated as "EMI") are estimated from those samples with the lowest mu values. Corresponding $^{143}Nd/^{144}Nd$ and $^{86}Sr/^{87}Sr$ were then extrapolated from Figure II.22. HIMU (high $^{238}U/^{204}Pb$ OIB), PREMA (Prevalent Mantle), DMM (Depleted Mantle Material), and BSE (Bulk Silicate Earth) end-members have been used as hypothetical limits for the more depleted end-member composition. Isotopic compositions and elemental concentrations used for these end-members in the calculations were extracted from Hart and Zindler (1989). Mixing lines obtained are illustrated in Figure III.3. The methodology used in the calculations is the one described in Faure (1986).

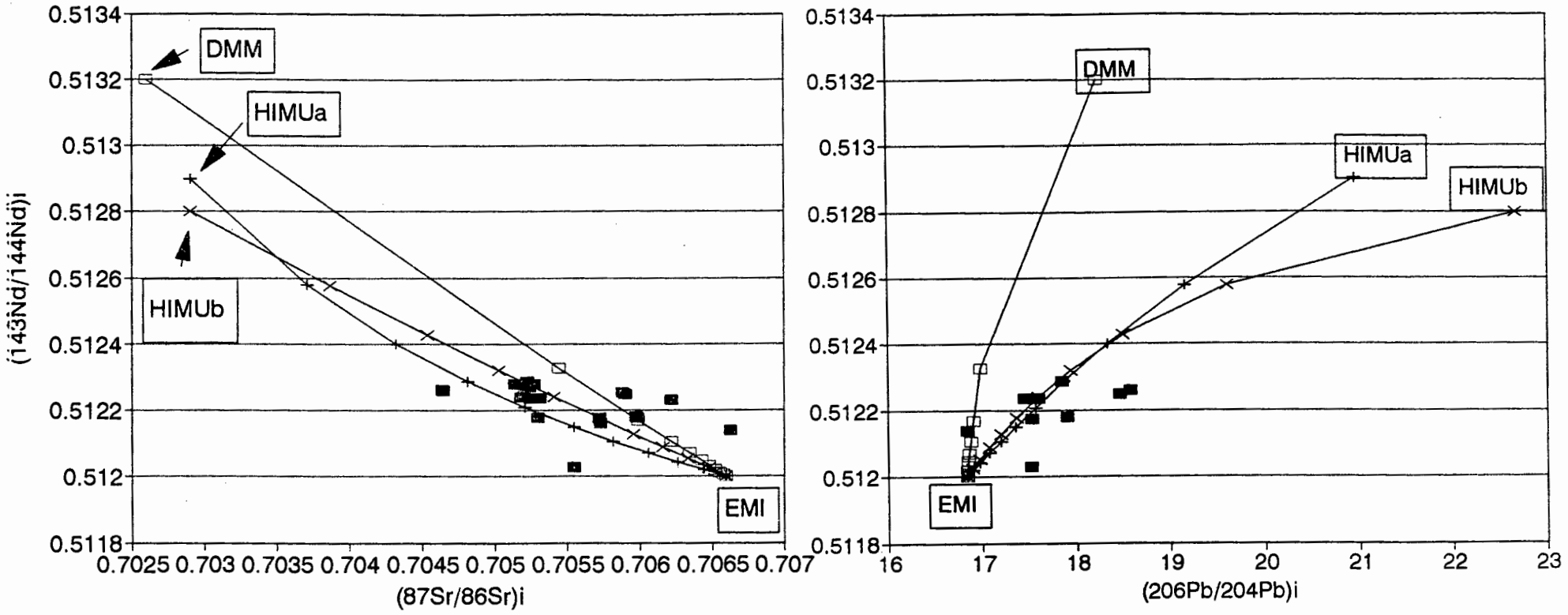

Figure III.3 - Mixing lines calculated according to the methodology described in Faure (1986). HIMU (high $^{238}U/^{204}Pb$ OIB) and DMM (Depleted Mantle Material) end-members (isotopic compositions and elemental concentrations used in the calculations from Hart and Zindler, 1989; and Chauvel et al., 1991) have been used as hypothetical end-members in lines of mixture with an EMI (Enriched Mantle I) composition defined from the rift-related volcanics. Though imprecise, the accuracy of the mixing hypothesis is reflected by the fact that the relative positions of individual localities, with respect to the components, remain relatively constant from one isotopic space to the next.

Table III.1 - Illustration of parameters used in the calculation of mixing lines shown in Figure III.3. See discussion in the text.

Occ	U	Pb	Nd	Sr	Nd/Nd	Sr/Sr	%EMI-Sr	%EMI-Nd
EMI	0.7	11	32.5	300	0.512	0.706	1	1
HIMU	0.1	0.4	6.5	120	0.5129	0.7029	0	0
TRX	7	12.6	39.1	1215	0.51226	0.70464	0.338521	0.329897
LIM	3.8	8	272	2687	0.51224	0.70525	0.556213	0.354839
JAP	9	5	47	400	0.51225	0.7059	0.923077	0.342105
PAN	4.5	8.4	20	1899	0.51224	0.70518	0.526559	0.354839
POL	3.5	11	41	991	0.51218	0.70531	0.58283	0.444444
CPB	2.1	9	173	2355	0.51217	0.70573	0.807418	0.462025
SUC.G	2	12	150	2248	0.5121	0.70554	0.69657	0.615385
CAT.F			323	2218	0.51226	0.705	0.456522	0.329897

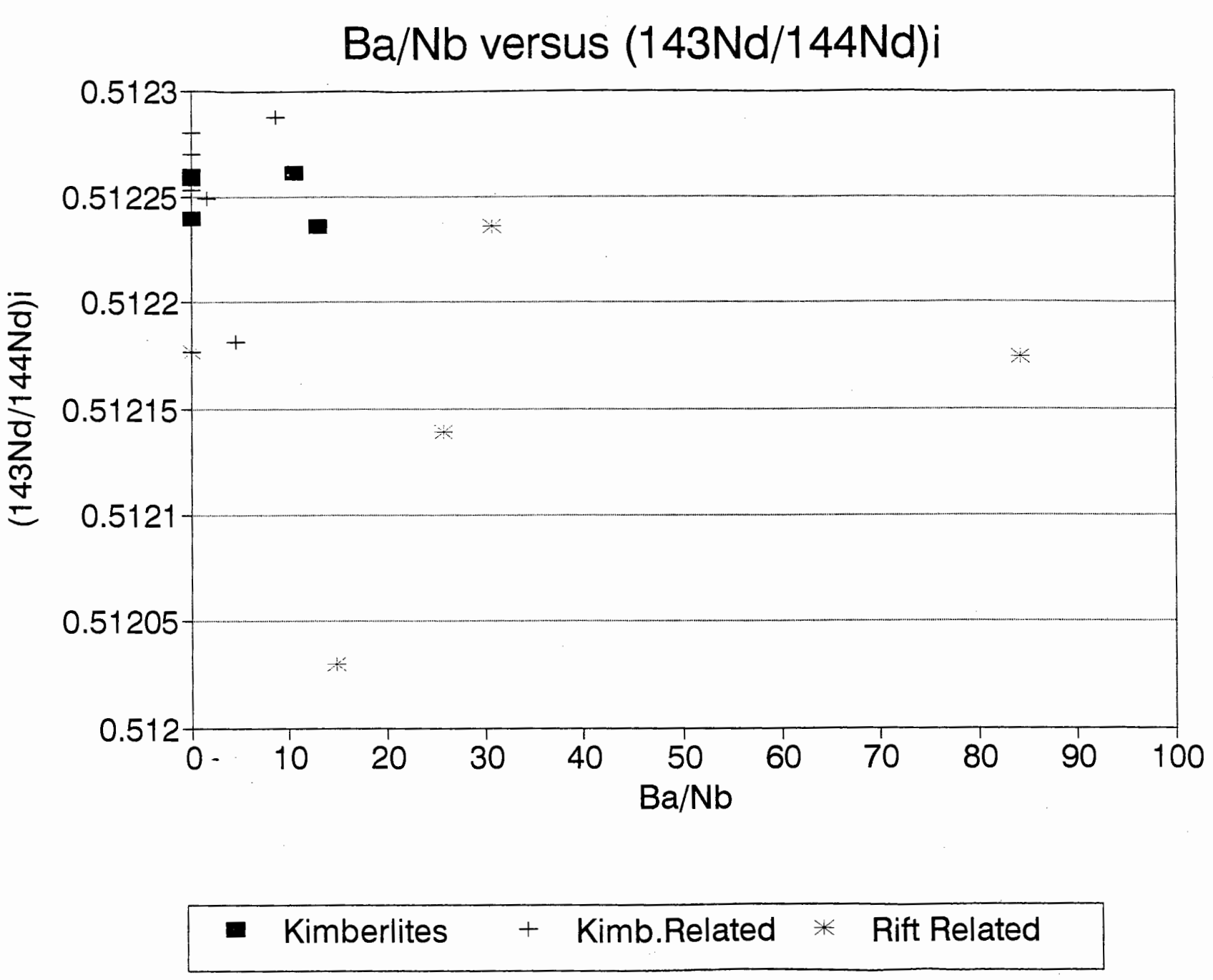
Ba/Nb versus (143Nd/144Nd)i
0.5123
0.51225
0.5122
0.51215
0.5121
0.51205
0.512
(143Nd/144Nd)i
0 -
10
20
30
40
50
60
70
80
90
100
Ba/Nb
Kimberlites
Kimb.Related
Rift Related

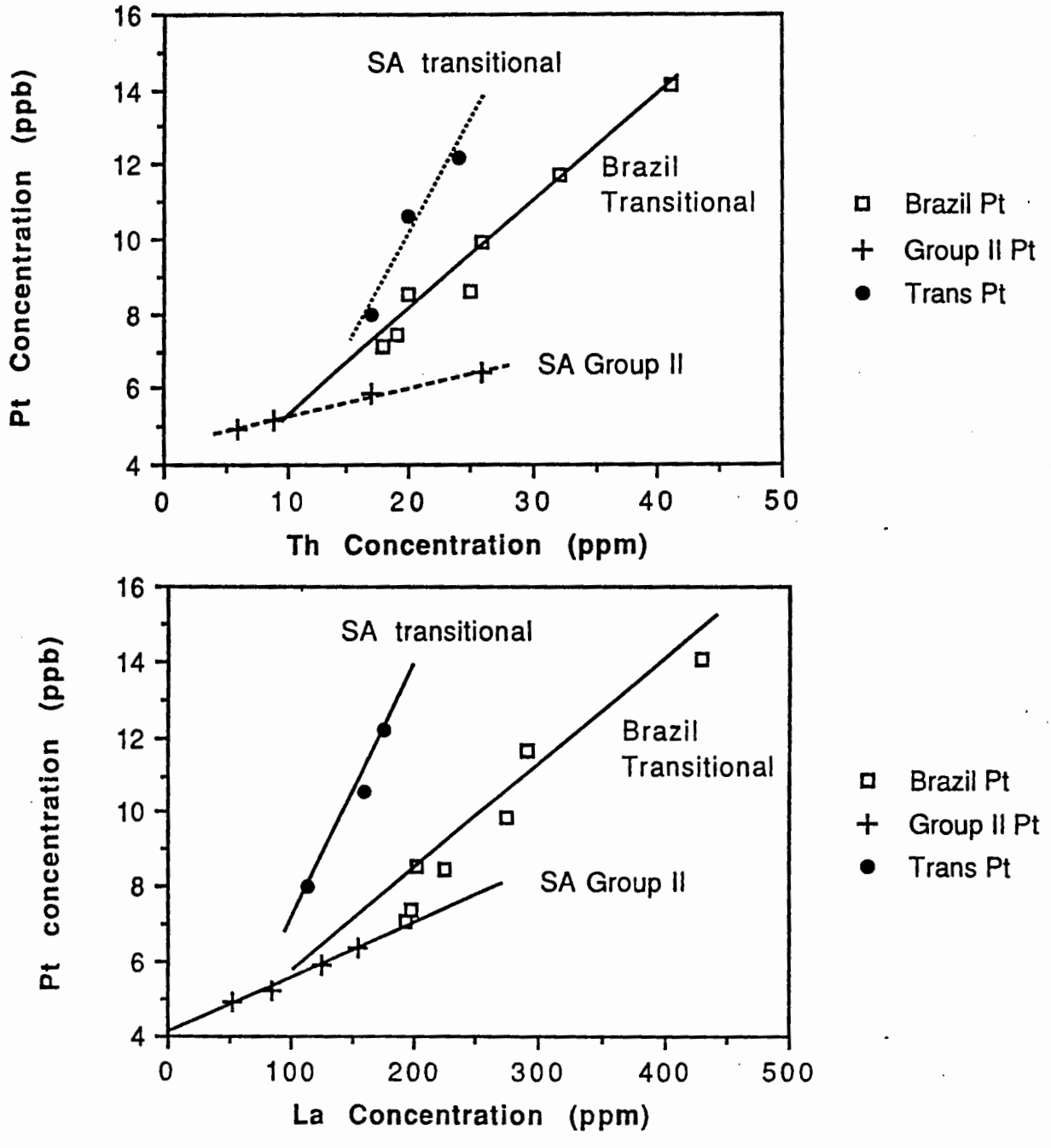

Figure III.5 - Plots of Pt versus La and Pt versus Th comparing the studied rocks ("Brazil Transitional") to inedit data for transitional kimberlites from Prieska ("SA Transitional") and Group II kimberlites ("SA Group II") provided by Iain Mcdonald. The linear relationship is not observed in Group I kimberlites (Mcdonald, pers. comm., 1992) and may be related either to (i) enriched source characteristics or (ii) petrological processes (see also Figure III.6).

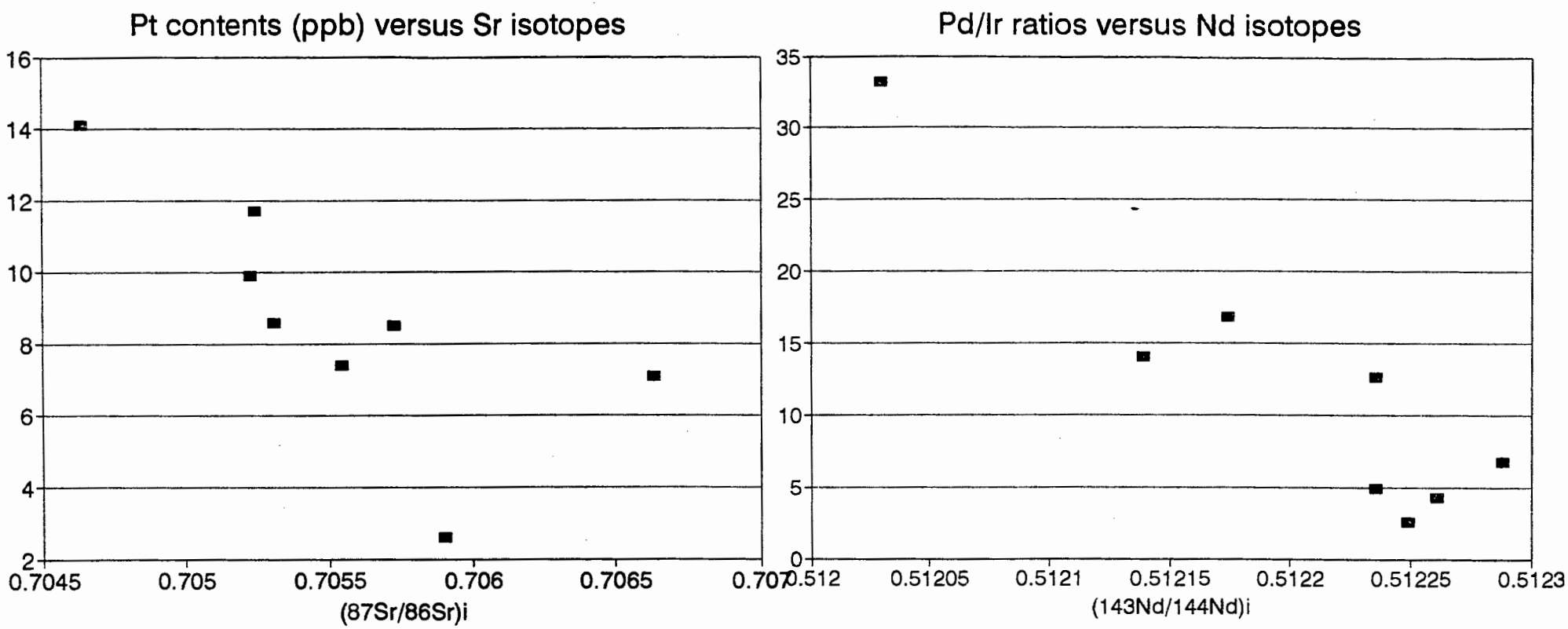

Figure III.6 - PGE relationship with Sr and Nd isotopes for the Brazilian rocks suggest that PGE contents and interelement characteristics might be related to time-integrated source characteristics rather than to fractionation processes.

III.3 - COMPONENT CHARACTERIZATION AND THE MIXING PROCESS

III.3.1 - The "shallow-derived" enriched mantle component, EMI and LTPGE

The negative correlation between Ba/Nb and $^{143}Nd/^{144}Nd$ observed in the alkalic rocks and illustrated in Figure III.4 indicates that the high Ba/Nb ratios were not a product of enrichment during melting, but rather reflect lithospheric source composition related to some older enrichment event. This observation is particularly relevant because the unique Sr, Nd and Pb isotopic compositions and the high Ba/Nb contents of the shallow-derived rift-related alkalic rocks correlate extremely well with the EMI component (Zindler and Hart, 1986; Hart, 1988; Hart and Zindler, 1989). In fact the average of the rift-related volcanics (see Tables II.1 to II.5) could be taken as currently the best approximation of the EMI end-member, which was previously only manifested as an extreme composition of the Walvis ridge basalts (Richardson et al., 1982 and 1984). The Walvis ridge basalts may themselves, therefore, be mixtures of EMI and more typical, "normal" oceanic compositions lying within the mantle array (see Figures II.19 and III.1).

The shallow origin and the discrete geochemical and the petrographic characteristics of the rocks in which the EMI component is best represented suggest that, locally at least, the distinctive EMI signature is restricted to the upper parts of the subcontinental lithospheric mantle. The samples with EMI-like isotopic characteristics tend to show fractionation of PGE from Os and Ir to Pd (see Figure III.6). Among them, the samples from Sucesso show the highest Pd/Ir ratio and portray a strongly fractionated PGE pattern. It is speculated that brecciation and entrainment by gas-rich volcanism could cause fractionated PGE-bearing materials, such as the metal-rich intergranular components described by Mitchell & Keays (1981), to be incorporated. The PGE-fractionated pattern represented by the rocks generated at shallower levels by the highest degrees of melting (i.e. Sucesso) and the non-fractionated pattern represented in the tuffisitic kimberlitic breccias (where xenocrysts probably had little time to reequilibrate) could have been produced by PGE fractionation processes incurred during melting or by entrainment of PGE at the time of emplacement, or a combination of both.

III.3.2 - The "deep-derived" mantle component, LoNd, HIMU and HTPGE

Kimberlites, among all the studied rocks, are the rocks believed to have been generated at greatest depths (Figure III.2) and by smaller degrees of partial melting (Figure II.12). They are also the rocks in which the EMI-component is represented to the least extent. The array linking these compositions to EMI sub-parallels the mantle-array with lower $^{143}Nd/^{144}Nd$ and lower $^{87}Sr/^{86}Sr$ and is, therefore, distinctive from the trend observed in Walvis ridge basalts. Hart et al. (1986) described similar mixing for several oceanic localities, and suggested that such an array (termed LoNd) existed as a continuum between HIMU and EMI. This trend is presumed to be linked to some Dupal compositions in oceanic basalts (Zindler and Hart, 1986; Hart, 1988).

The higher U/Pb and lower Rb/Sr time-integrated compositions of the source of the kimberlites and kimberlite-related rocks parallel the time-integrated source characteristics of the HIMU-OIB's. It is possible, therefore, that these rocks have a small HIMU-component in them. Mixing calculations of the EMI component (defined on the basis of the rift-related rocks) with HIMU, PREMA, BSE and DMM (Depleted Mantle Material) were attempted and the most reasonable fit emerged when the mixing of EMI and HIMU was simulated (see Figure III.3). After correcting for the lower concentrations of U, Pb, Sr and Nd in HIMU as compared to EMI, it is estimated that a mixture of about 63% HIMU and 37% EMI would produce the isotopic signature of the Tres Ranchos kimberlite in all three isotopic spaces. Smaller amounts of the HIMU component would be necessary to reproduce the isotopic signature of the other occurrences.

The range of magma compositions observed could represent a mixture of HIMU and EMI if either i) a homogeneous HIMU-like mantle component was mixed with (or contaminated by)

variable proportions of shallower EMI-like components; or ii) the vertical mantle heterogeneities observed represent layering in the local lithosphere, and the depth of melt generation (and, most probably, the local lithospheric thickness; see Figure III.2) restricted sampling of the shallower rocks to EMI, while the kimberlites sampled the transition zone between HIMU and EMI. In either case, it can be inferred that the HIMU-like mantle component resides at greater depths (at least 150 Km, within the diamond stability field) compared to the EMI component. Using major element compositions to calculate depth and temperature of melting, Chauvel et al. (1992) have also concluded that HIMU rocks melted at higher pressure and temperature (49 kbar and 1640°C) compared to EMI (35 kbar and 1455°C).

It is envisaged that the HIMU-like component could originally have been resident in the metasomatised subcratonic lithosphere, as a result, for example, of enrichment in LIL elements and higher Th/U values with sufficient time to acquire high $^{208}Pb/^{204}Pb$ values. Alternatively, the input of the HIMU-like component could be related to relatively young asthenospheric upwelling in the area (*c.f.* Halliday et al., 1990). Such asthenospheric input could be related either to lithospheric stretching (linked to the formation of the proto-South Atlantic) or to the influence of a mantle plume. Because of the positioning of the study area relative to the tracks of both the Tristan da Cunha and Trindade hot-spots, one could speculate that such component might have been through quite a complex history. It is possible, for example, that such enriched materials formed by low degrees of melting under the influence of the Tristan da Cunha hot-spot (circa 130 Ma), which had been trapped and left to evolve until further melting occurred under the influence of the Trindade hot spot (circa 90 Ma).

III.3.3 - The Mixing Process

A sequence of events is proposed with the assumption that rifting and continental extension had influence over the magmagenesis. It is possible that extension of the crust during the outpouring of the Paraná Basalts was accompanied by upwelling of hotter mantle material, and that the elevated geotherms induced large degrees of melting at low pressures. As extension waned, the geotherm reversed to normal, the depth of melting increased, the degree of partial melting decreased and magmas became more alkalic. At the onset of the second extensional phase, which

was accompanied by the Mata da Corda volcanism, the elevated geotherm once-again changed the chemical character of the magmas produced. Conversely, the peculiar inter-element ratios (e.g. high Nb/La and Nb/Ba) observed in the studied rocks could be considered direct evidence for the involvement of typical plume-related OIBs in their generation. Hawkesworth et al. have identified similar compositions in coast parallel Paraná dykes in Rio de Janeiro (Hawkesworth et al., 1992; see also Chapter IV). Nevertheless, because the more volumetrically significant magmas in the study area are predominantly associated with lower ϵ_{Nd} and higher $^{87}Sr/^{86}Sr$ values, it seems unlikely that the proposed mass mixing (and, implied, HIMU-like asthenospheric input) was directly associated to the peak of the magma generation processes.

The development of PGE fractionated patterns is a common feature among the studied rocks and, apparently, the melts became progressively more contaminated by the un-fractionated PGE component as the focus of melting moved downwards. There is evidence that Os-Ir are not affected by the temperature regime ($<1300°C$) in the upper-mantle (Davies and Tredoux, 1985; Bacuta et al., 1988). It is unlikely, therefore, that the higher HTPGE contents observed at lower source-depths could relate to temperature variation in the lithosphere. Brecciation or mechanical assimilation/entrainment of HTPGE enriched heterogeneities could perhaps have occurred. If that was the case, the Japecanga component is an accurate reflection of the relative proportions of PGE in the unfractionated reservoir and provides indications of what other rock types might have provided this signature. Some komatiites show broadly similar unfractionated patterns, but if they were the source of the contamination, huge volumes of these rocks would have had to be involved.

Tredoux et al. (1989) suggested that PGE enriched heterogeneities (Fe-Ni alloy pods) left over from incomplete core formation may exist at depth in the lower mantle. Those authors believe that such alloy pods may have been brought up in mantle plumes during the Archean and that they were incorporated first into the oceanic and then subsequently in the continental lithosphere underneath old cratons. Old (Archean) continental lithosphere is thus thought to contain PGE enriched keels which might interact with or be sampled by later magmatism. Data from the Bon Accord Group A samples analyzed by Tredoux et al. (1989) are extremely enriched in all of the

PGE, but have PGE patterns and inter-PGE ratios which are similar to Japecanga and some kimberlites from South Africa analyzed by McDonald et al. (1992). The very characteristic Pt anomaly seen in the Bon Accord samples is also present in all of the South African kimberlites but are only slightly developed at Japecanga. A notable negative Ir anomaly is evident in the South African kimberlites and in all of the Brazilian samples with the exception of SUC.G (McDonald et al., 1995). Such arguments suggest it is possible that the primitive component seen in the Brazilian kimberlites incorporated a small amount of Bon Accord-like material into a PGE fractionated melt as it rose through the continental lithosphere.

III.4 - TIME-INTEGRATED Nd ISOTOPE EVOLUTION

The combination of the information available on the source characteristics of the kimberlites and alkalic rocks and the information from the crustal sequences can potentially provide for a three-dimensional integrated model for the evolution of the crust and the mantle lithosphere. The isotopic characteristics of the alkaline rocks and those of the crustal sequences (see chapter I) are given in Figure III.7. Two first order observations emerge from this plot. First, when plotted against crystallization age, the initial ϵ_{Nd} values of the EMI-like enriched mantle component fit the evolution paths defined by the lower limits of post-orogenic granites in the Tocantins Province. The data show that this mantle component is likely to be related to the tectonic processes which led to the formation and evolution of the southwestern margin of the craton. Note that there are no initial ϵ_{Nd} values clearly displaced from the limits defined by the above mentioned "Proterozoic Nd evolution curves", which should be the case if large volumes of pristine Archean enriched material (with very low ϵ_{Nd} values in the Mesozoic) were involved in their generation. Secondly, the wide range of ϵ_{Nd} values in the Proterozoic crustal rocks are not observed in the isotopic characteristics of the underlying sub-continental lithosphere, as inferred from the Mata da Corda and the Paraná rift-related volcanics. This may indicate that either *(i)* the upper mantle materials involved in the generation of the alkaline rocks had been rehomogenized to a greater degree then the overlying upper crust after the cessation of the accretionary process; or *(ii)* the local mantle lithosphere was detached from the overlying continental crust.

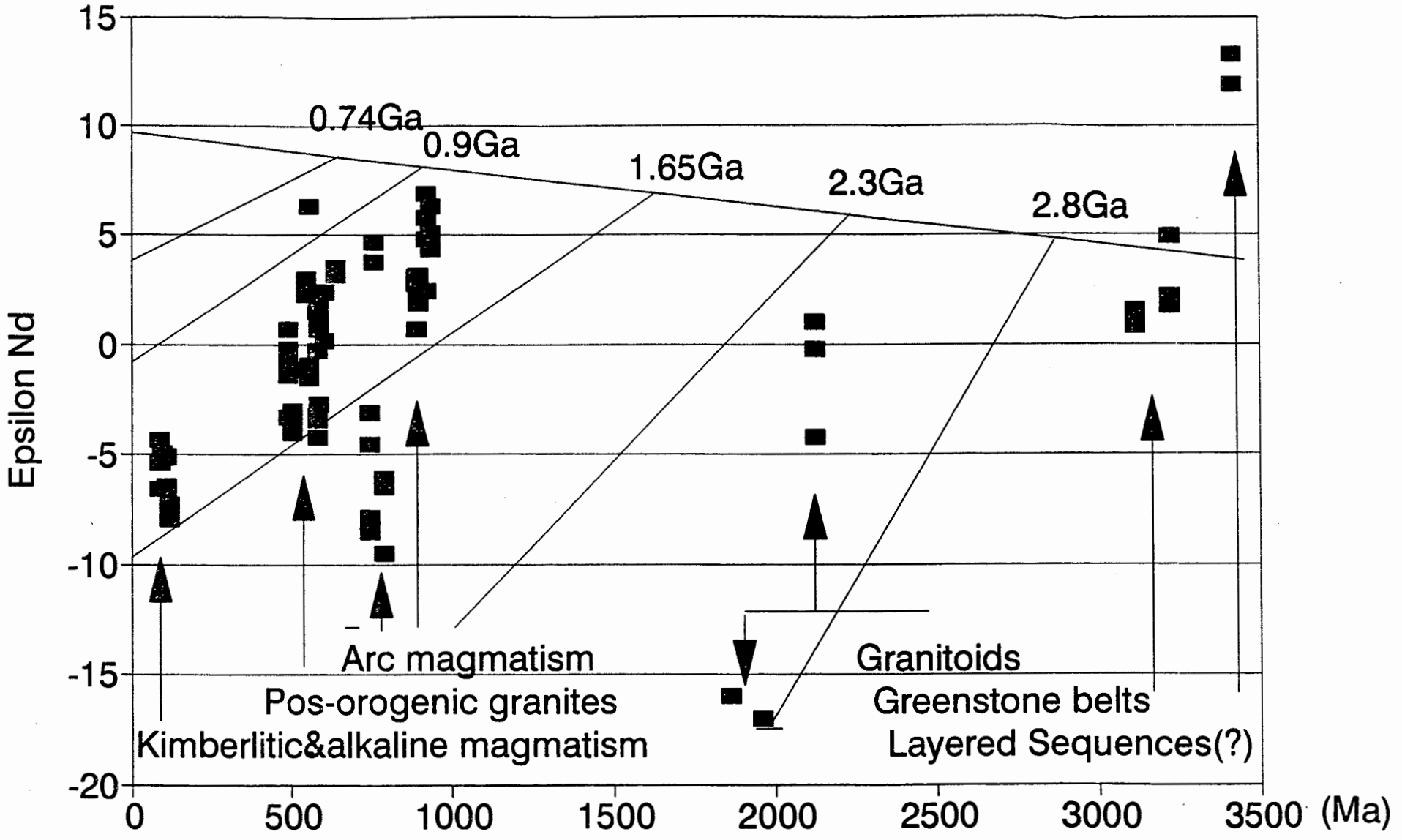

Figure III.7 - Epsilon Nd versus time of emplacement. Initial Nd signatures are used to examine possible relationship of the enriched mantle component to evolutionary paths defined for the crust in the area (see Figure I.9). It is suggested that mantle enrichment event is likely to be related to tectonic events and melting of arc-related magmas which led to the formation and evolution of the Tocantins Province.

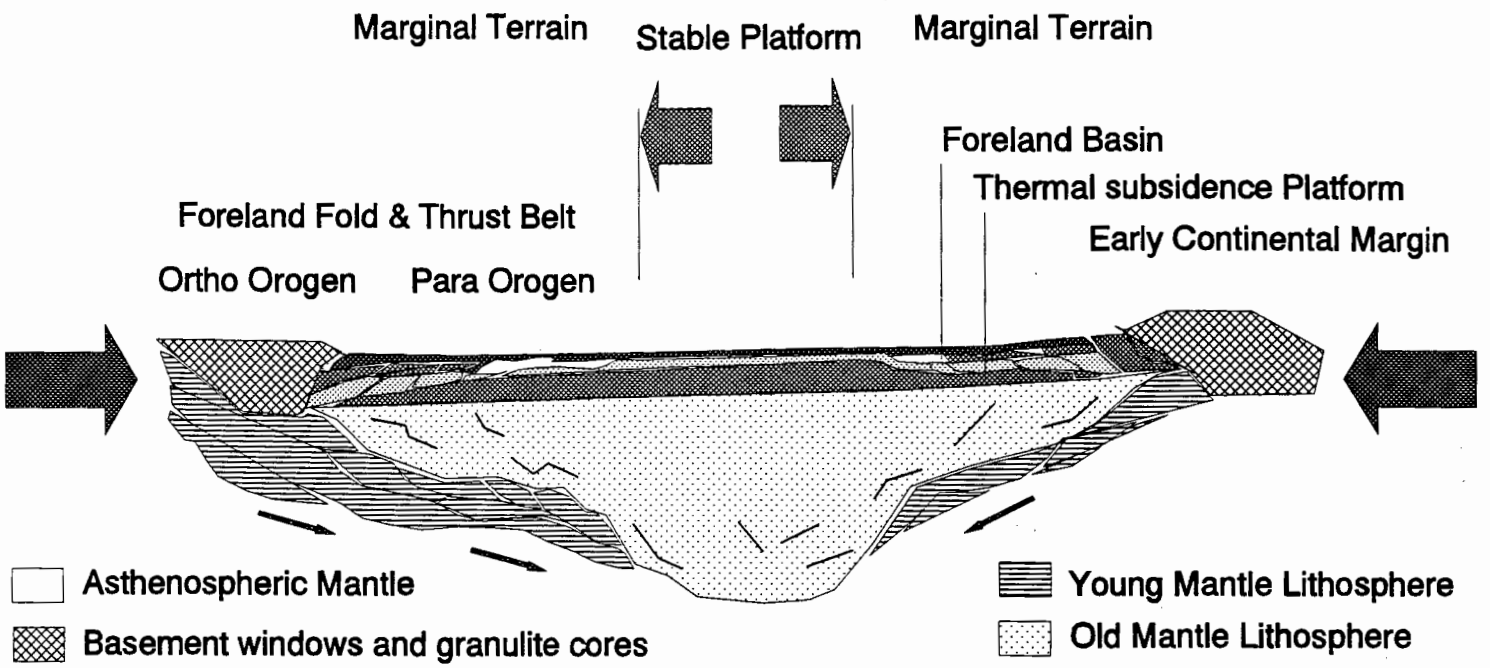

Figure III.8 - Tectonic zones and a model for craton evolution (modified from de Wit, Bizzi and Baars, 1991). Schematic section through an old cratonic nucleus, flanked in both sides by later orogenic zones and foreland zones. The marginal foreland zones (para-orogenic zones comprised of allochtonous to para-allochtonous fold and thrust belts) rest on variably disturbed old cratonic lithosphere. Remobilization of this lithosphere is a complex function of early extensional and subsequent shortening processes. The external orogenic zone (the ortho orogen) is comprised of metasediments, metavolcanic and metaplutonic assemblages of various ages which might include granulite cores and orthogneisses. A possible scenario for the mid- to upper-Proterozoic evolution of the southwestern margin of the São Francisco craton with underthrusting of both young subducted slabs and older lower crust. Lenses of deformed and eclogitized oceanic crust within slivers of ultramafic rocks would induce continued growth of the sub arc lower crust during the accretionary process.

It is possible to construct tectonic models in which a crustal section can be of very different average age and composition at different depths but still have considerable lateral homogeneity. Beneath magmatic arcs, for example, the deepest crust is likely to contain, on average, the youngest material as the result of the persistent growth of the lower crust by intrusion of basaltic magma and deep underthrusting. This would appear to be the case for the southwestern São Francisco craton. The situation is illustrated schematically in Figure III.8. It is envisaged that the Brasiliano-age thin-skinned tectonism along the western margin of the São Francisco craton could have been accompanied at depth by underthrusting and down buckling of both younger subducted slabs and older lower crust. Associated arc-forming igneous processes involving pre-existing crustal materials might also have induced continued growth of the sub-arc lower crust via intrusion of mantle derived basalt. The latter would have diluted the effects of local heterogeneities and perturbations in the accretionary process.

The following processes, or a combination of them, could possibly have operated during the development of the lithospheric mantle source for the alkalic volcanics intruded along the south-western margin of the São Francisco craton.

III.4.1 - Remobilization or recycling of continental and oceanic lithosphere

If the evolution of the EMI-like source material recognized in the study area is related to that of the Neo Proterozoic (ca. 900 to 600 Ma) orthogneisses and metavolcanic arc suites described further to the west (Pimentel and Fuck 1987, 1992; and Pimentel et al., 1991), then the mantle lithosphere which hosts the source component(s) was probably affected by juvenile island-arc crust of Neo-Proterozoic age which was accreted against the São Francisco craton margin during the Brasiliano event. In such case, it is envisaged that tectonic accretion of materials against the craton margin would have affected the lower section of the lithosphere and been an efficient mechanism for enrichment and generation of small- and large-scale heterogeneities. During the process the mantle sources would have been permeated by fluids, and would have undergone melting (either direct melting or subduction induced). Metasomatic fluids and small-volume enriched melts would have crystallized as veins which were not in isotopic equilibrium with the mantle wall rock.

If terrigenous and pelagic sediments were involved, they would predominate relative to other mantle-derived materials because the isotopic evolution of the crust + sediment mixture have higher Rb, Sr, Sm, Nd, U, Th and Pb contents (e.g. Othman et al., 1989). The deeper the waters, the higher the pelagic/terrigenous sediment ratio and, by consequence, the lower the resulting $^{87}Sr/^{86}Sr$ ratios resulting from the input of sediments. It is conceivable that the EMI-like component could have been produced "*in situ*" due to remobilization/enrichment of upper-mantle materials during the Neo-Proterozoic and have resided within the sub-continental lithospheric mantle until the Mesozoic, when it was remobilized during the generation of the alkaline-rich volcanics. Because sediments subducted in the Proterozoic would tend to have high Sr isotope ratios by the time of the Cretaceous magmatism, and because all subduction related processes result in relatively low Nb and Ta abundances (and since the studied mantle derived rocks don't have those characteristics), it is suggested that either (i) Neo-Proterozoic shallow level subduction processes did not have much of a role in determining the source characteristics of those rocks; or (ii) the subducted sediments were dominantly pelagic (as opposed to terrigenous); or (iii) the whole source region was geochemically modified after the enrichment event.

Recycled oceanic crust, with or without sediments, could have generated HIMU-like isotopic signatures observed in OIB following hydrothermal alteration, subduction, and storage of the slab and of the overlying sedimentary layer within the mantle (e.g. Hoffman & White, 1982; McKenzie and O'Nions, 1983; Ringwood & Irifune 1988; Chauvel et al., 1992). In this model, the recycled components remain isolated from the surrounding mantle and only mix during ascent of a subsequent plume event. The composition of 2 Ga old recycled crust should have Pb and Sr isotopes slightly more radiogenic than those of present-day MORB (*e.g.* Chauvel et al., 1992). The Nd isotopic composition should be slightly less radiogenic than that of MORB and the Ce/Pb ratio of such altered crust should be much higher than that of MORB. According to Chauvel et al. (1992), the HIMU composition can be simulated by a mixture of 25-30% old oceanic crust and a minimum of 70% residual mantle peridotite. The composition of HIMU suggested by these authors and a theoretical mixing line between this component (denominated $HIMU_b$) and the enriched EMI-like component calculated for the studied rocks are presented in Figure III.3. Again, because altered oceanic crust is characterized by high Rb/Sr ($\sim$0.1), and

because even small amounts of sediment will dominate (over MORB) the composition in case of mixture, it is speculated that subduction and ageing of this material should lead to higher $^{87}Sr/^{86}Sr$ ratios and lower Nb and Ta abundances than found in the Mesozoic volcanics intruded along the São Francisco craton margin.

As material is subducted, temperatures increase and the hydrous silicate phases breakdown; and compositions are variably affected by dissolution in the dehydration fluids. Factors like temperature and composition of the fluid strongly influence the mobility of U, Pb and alkalis in general (e.g. Michard et al., 1983), and incompatible trace elements (including Th) would be relatively depleted. These processes could produce low U/Pb and low Th/U materials which in turn, with time, would induce to low $^{206}Pb/^{204}Pb$ and $^{208}Pb/^{204}Pb$ signatures (e.g. Othman et al., 1989; and references therein) similar to the ones obtained in the Mesozoic rift-related volcanics. The deepest crust is likely to contain, on average, the youngest material as a result of growth of the lower crust by underplating (both magmatic and tectonic). Old heterogeneities would thus not be represented in the lower levels of a section of sub-continental lithosphere built that way. Internal rehomogenization of heterogeneities would possibly also have been induced during tectonic overthickening processes.

III.4.2 - Entrainment by lower mantle materials

Xenoliths in the alkalic volcanics in the area provide mineralogical and chemical evidence for infiltration metasomatism (H.O.A. Meyer, pers.comm., 1989). Richardson et al. (1984) favored derivation of the Walvis Ridge basalts from a mantle which had been enriched by small volume melts and metasomatic fluids. The enrichment (which led to the formation of the EMI-type compositions) was suggested to have a minimum age of ~800 Ma, and to be associated with intracontinental tectonics which affected the sub-continental African lithosphere. Such a process might also be applicable for the generation of EMI-like compositions in the SW São Francisco craton. Should the arguments for mixed sources be discarded and age significance be attached to the isotopic signatures obtained in this study on the most enriched source characteristics, then the radiogenic isotopes reported herewith would be consistent with a derivation of such small volume melts from a mantle lithosphere that was enriched in incompatible elements circa 900

Ma ago.

In this model, the mantle enrichment would not relate necessarily to remobilization processes. Rather, it might have been related to entrainment by primitive lower mantle and infiltration metasomatism during the Neo Proterozoic extensional and subsequent cooling events which affected the SW margin of the craton and led to the deposition of the Bambuí Group. The Walvis Ridge basalts may also have inherited their chemical signature from equivalent events in Southern Africa. The extent of the relatively homogenous (or rehomogenizing?) enrichment and the limited capability of infiltration metasomatism to chemically modify a large volume of mantle material, however, argue against the possibility that this process alone could account for the development of the EMI-like isotope signatures in the local sub-continental mantle lithosphere.

Entrainment by primitive upper mantle and long-term entrapment of blobs and weak plumes could lead to the formation of a "layer" of HIMU-type material at the base of the lithosphere (Hart, 1988). Such process would produce HIMU-like characteristics at a deeper lithospheric level by trapping volatiles generated by semi-continuous degassing of the deeper mantle or released during phase transformations both at the Core-Mantle Boundary (CMB) and at the Transition Zone (TZ) (e.g. Vollmer, 1983; Allégre et al., 1980 and 1987).

Another mechanism which must be considered as plausible means by which to produce the observed signatures is the mobilization of Pb and Rb in a metasomatic fluid and subsequent removal from some mantle segment. Taking into consideration the behavior of Pb and Rb in the continental crust suggest their affinity for volatile-rich fluids, it is possible that mantle metasomatism might result in the production of residual degassed HIMU-like components and complementary gas-rich EMI-like components elsewhere in the mantle.

III.4.3 - Contamination by granulites, CO2 metasomatism and delamination

The range of isotope signatures observed in the studied rocks tend to deviate away from more typical enriched mantle values towards lower $^{87}Sr/^{86}Sr$ and $^{143}Nd/^{144}Nd$ values. The trend is similar to that expected if mixing of mantle-derived magma with small amounts of granulite

rocks had occurred. The presence of widespread granulite metamorphism along the outer margins of the São Francisco craton, as well as a continuous zone of thick crust with high density materials (as defined by gravity data along the outermost southwestern craton limits; e.g. Haralyi and Hasui, 1982; see Figure II.2) suggest that granulite facies metamorphic rocks are likely to be present at the lower part of the lithosphere in these marginal regions.

The relatively low SiO_2 contents of even the most evolved lavas in the study area do not favor the possibility that the signatures of the Mesozoic volcanics might have resulted from large-scale contamination of the primitive magmas by basement granulites. Moreover, the incompatible elements compositions of the alkalic rocks do not compare to those of lavas from type-localities documenting significant granulite contamination (e.g. the Tertiary lavas from Skye, Northwest Scotland; Carter et al., 1978; Thompson et al., 1982; and Thirwall and Jones, 1983). Moreover, the application of models of assimilation accompanied by fractional crystallization in undersaturated trace-element enriched mantle-derived magmas is dependent on the assumptions made about the properties of the mantle-derived magma that initiated the process and the nature and composition of the contaminants.

As an alternative for contamination by granulitic materials at sub-crustal levels, it is envisaged that such interaction could have occurred at deeper levels where Rb depletion could have followed phase transformations under CO_2-rich conditions. It has been argued that increased mantle metasomatism and metasome fractionation should occur at craton margins as a result of processes like lithospheric thinning, increased heat flow, magma production, stagnation and reservoir accumulation of fluids and volatiles (e.g. Haggerty, 1991). Some authors even believe that granulitization processes might be linked to increased CO_2 activity (Newton, 1992). Whatever the case, it is widely accepted that mantle metasomatised by CO_2-rich fluids will generate, with time, isotopic ratios that lie to the left of the mantle array (Menzies & Wass, 1983).

It has been proposed that ancient delaminated continental lithosphere would likely manifest isotopic signatures similar to those obtained in this study (McKenzie and O'Nions, 1983;

Hawkesworth et al., 1986), and that delamination processes could probably be induced by crustal overthickening (Kay and Mahlburg Kay; 1991). I propose that the nature of the shallow-derived EMI-type materials could possibly be reconciled with these models if phase transformations had occurred but sufficient density inversion had not been attained to induce total delamination. In other words, a situation in which lithospheric materials had been reequilibrated and extensively affected by garnet forming phase transitions but did not separate from the lithosphere and rather remained there as a "density liability" for delamination (e.g. Molnar & Gray, 1979).

During the Brasiliano orogenensis, convergence along the SW margin of the São Francisco craton was accommodated in a thin-skinned tectonic regime at the surface. It is thus conceivable that the tectonic overthickening of the crust led to gabbro-granulite-eclogite phase transformations at lower crust and upper mantle levels. A series of complex phase transformations could have occurred as the tectonic loading provoked increasing depth conditions. Pressure and temperature increases most probably caused dehydration processes, but apparently the overthickening did not procede far enough to induce phase transformations and density inversion to the extent suggested by Kay and Mahlburg Kay (1991).

The lower 87Sr/86Sr of the studied Mesozoic volcanics relative to Group II kimberlites and other enriched mantle derived rocks could thus have been an artifact of the dehydration processes which induced Rb depletion in the lower portions of the local lithosphere which were reequilibrated. Left to evolve with time, such a Rb depleted zone would have resulted in low $^{87}Sr/^{86}Sr$ ratios, similar to those observed on the studied rocks. Continued tectonic overthickening would eventually have lead to total density inversion and lithospheric delamination with removal of the EMI-like lower crust into the convecting asthenosphere (Kay and Mahlburg Kay, 1991). Such a delamination process, however, either did not occur beneath the marginal São Francisco craton or did not entirely remove the EMI-like lower crust.

III.5 - CONCLUDING REMARKS

The nature and restricted range of Sr and Nd isotope compositions indicate that the Mesozoic

alkalic magmas of the study area either interacted extensively with or were derived from a LREE enriched homogeneous lithospheric mantle source. Whatever the case, the incompatible element budget was dominated by such source. If the isotope and trace element signatures were generated by mixing between a volumetrically dominant lithospheric component with negative ϵ_{Nd} and a minor asthenospheric component with positive or close to chondritic ϵ_{Nd} values, then the latter had trace element enriched characteristics which are similar to those plume-related magmas of the Trindade Island (see discussion in Chapter IV).

The isotopic and incompatible element relationships of the studied alkalic rocks probably arose from a common set of petrogenetic processes. The overlap of isotopic signatures and the envelope of REE distribution, however, are opposed by the differences in major element geochemistry (particularly Al_2O_3, MgO, Mg# and Na_2O contents) which exist between kimberlites and the other alkaline rocks in this study. The conflicting behavior of major and trace elements may be explicable in terms of varying depths of partial melting and magma segregation. The small-scale isotopic variations and the range of PGE signatures were successfully modeled as a process of contamination by a PGE-rich component resident in the upper mantle lithosphere. Such systematic variations in rock types and geochemistry are evident on a regional scale and are believed to be indicative of vertical geochemical heterogeneities which are translated into lateral heterogeneities at surface as a consequence of different depths of melting.

Upper-Mesozoic binary mixing between up-welling HIMU-like melts and volumetrically dominant old EMI-like mantle materials from the Mechanic Boundary Layer (MBL) lithospheric mantle is capable of satisfying the constraints of the data obtained in this study. HIMU, and EMI in particular, may occur in laterally extensive but vertically distinctive portions of the continental lithosphere beneath the SW São Francisco craton. EMI signatures seem to be restricted to more shallow derived volcanism (e.g. carbonatites and rift-related volcanics in Brazil and East Africa) compared to HIMU rocks (e.g. high-temperature megacrysts and diamond bearing southern African kimberlites).

HIMU-type signatures seem to come from a source that was hotter and which started melting deeper in the mantle. This source could be the asthenosphere, brought up either by a potent mantle plume active at the time of the emplacement, or by long-term entrapment of blobs and weak plumes accumulated in the lower subcontinental lithosphere. Alternatively, the mobilization of Pb and Rb in a (CO_2-charged?) metasomatic fluid and subsequent removal from the mantle segment could be considered as a plausible means by which to produce a residual, degassed, HIMU-like component and a complementary gas-rich EMI-like component elsewhere in the mantle.

Plotted against crystallization age, the initial ϵ_{Nd} values of the alkalic volcanics fit the evolution path defined from the Neo Proterozoic crustal sequences of the Tocantins Province. Starting on the mantle evolution curve and progressing linearly to lower values with time, the data clearly show that the EMI-type ϵ_{Nd} values are connected to the tectonic processes which led to the formation and evolution of the crustal sequences within the Neo Proterozoic Tocantins Province. The absence of initial ϵ_{Nd} displaced from the evolution curves followed by the Proterozoic rocks indicates that those portions of the upper-mantle lithosphere beneath the craton margin which equilibrated with the Mesozoic volcanics did not contain significant amounts of pristine Archean materials. Much lower ϵ_{Nd} values should otherwise have been observed.

CHAPTER IV

The kimberlitic and rift related magmatism in a regional perspective.

IV.1 - INTRODUCTION

In the preceding chapters, isotopic signatures and elemental characteristics of the Mesozoic volcanics of the southwestern São Francisco craton were used to model their time-integrated source evolution and the interaction of distinct mantle reservoirs. The discussion focused *inter-alia* on large-scale mantle processes, hot-spot activity and heat flux of large-scale significance during the late Mesozoic. Here, an overview is attempted to evaluate the significance of the Brazilian data at an even larger scale during the evolution of the South Atlantic. The isotopic characteristics of the Mesozoic alkalic magma-types discussed in Chapter II are compared to the characteristics of the Paraná Basalts, the Walvis Ridge Basalts, and of other OIB-type enriched mantle components. The discussion is extended to the continental and oceanic sectors of West Gondwana (c.f. McWilliams, 1981) with respect to processes operating during its break-up and the northwards propagation of the proto-South Atlantic rift.

The alkaline igneous activity along the southwestern margin of the São Francisco craton and the Paraná volcanic province are part of a larger assemblage of Mesozoic mantle-derived magmas associated with the breakup of southwestern Gondwana. A review of the tectonic framework of southwestern Gondwana and of its Paleozoic to Cenozoic geological history provides a background against which the sequence of events leading to the rifting of the South Atlantic, and the kimberlitic and rift-related magmatism in particular, can be analyzed. In this chapter, emphasis is placed on source characteristics of continental flood basalt (CFB) provinces in this sector of the supercontinent in an attempt to constrain the nature of the magmatism, the extent to which the underlying sub-continental lithospheric mantle was implicated, and to provide insights in the origin of regional-scale mantle discontinuities.

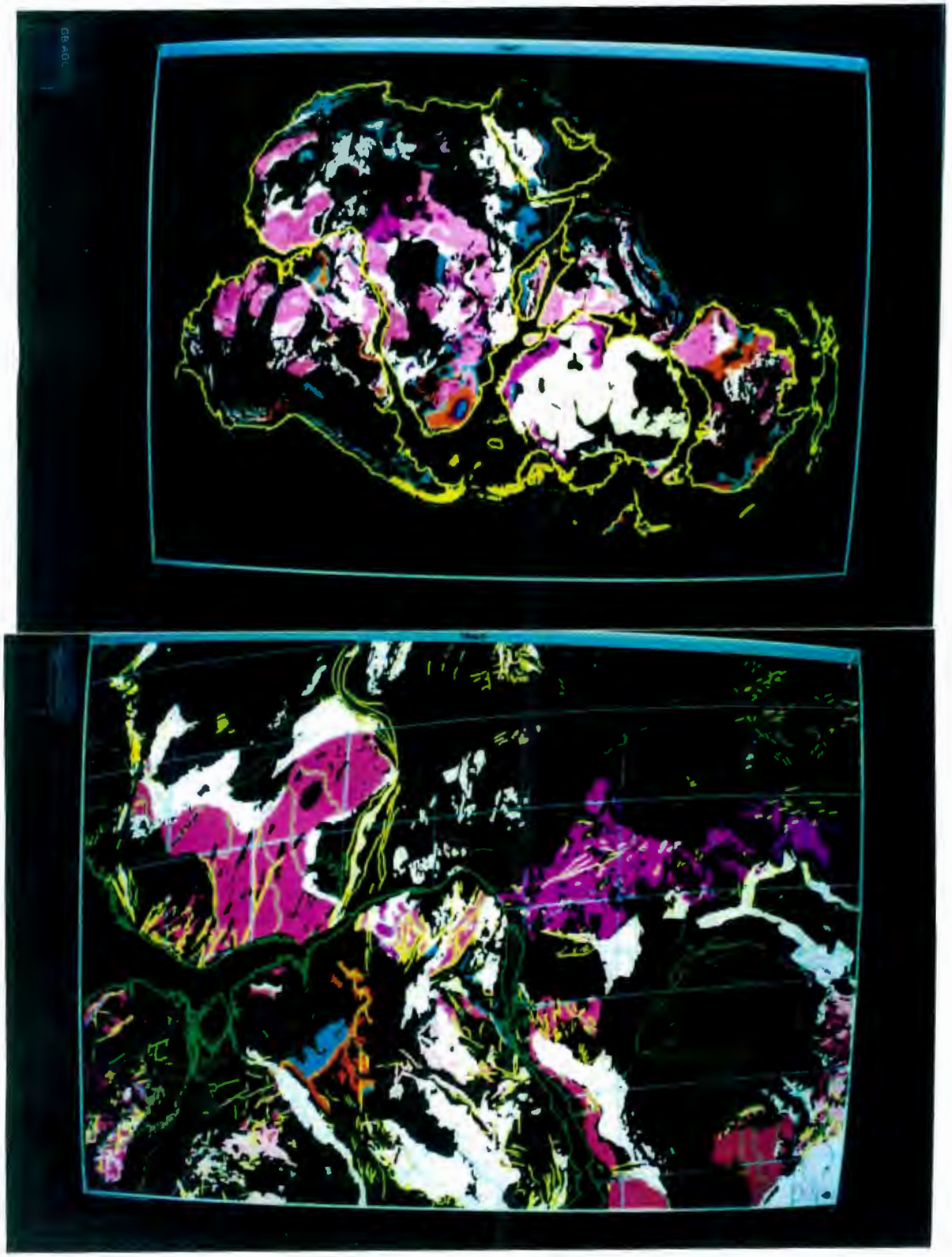

Figure IV.1 - Photographs illustrating the manipulation of the GO-GEOID relational database using GIS technology in an Intergraph workstation. Photo 01 shows the graphic response to enquiries on the distribution of Proterozoic rocks and Mesozoic vulcanism. Different color represent rocks from different time-slices which are distributed throughout Gondwana. Photo 02 zooms in the relation of the West African and Central African Shields to the São Francisco and western Amazonian Shields. Major thrusts, faults and planar tectonic fabrics (in yellow), rivers (in green) and grid (in blue) have been added for reference. Photo 03 (next page, at the top) is the graphical representation of the data base and illustrates the process of enquiring about specific areas on-screen using the graphic environment. Photo 04 illustrates the outpouring of volcanic units during supercontinental break-up and separation.

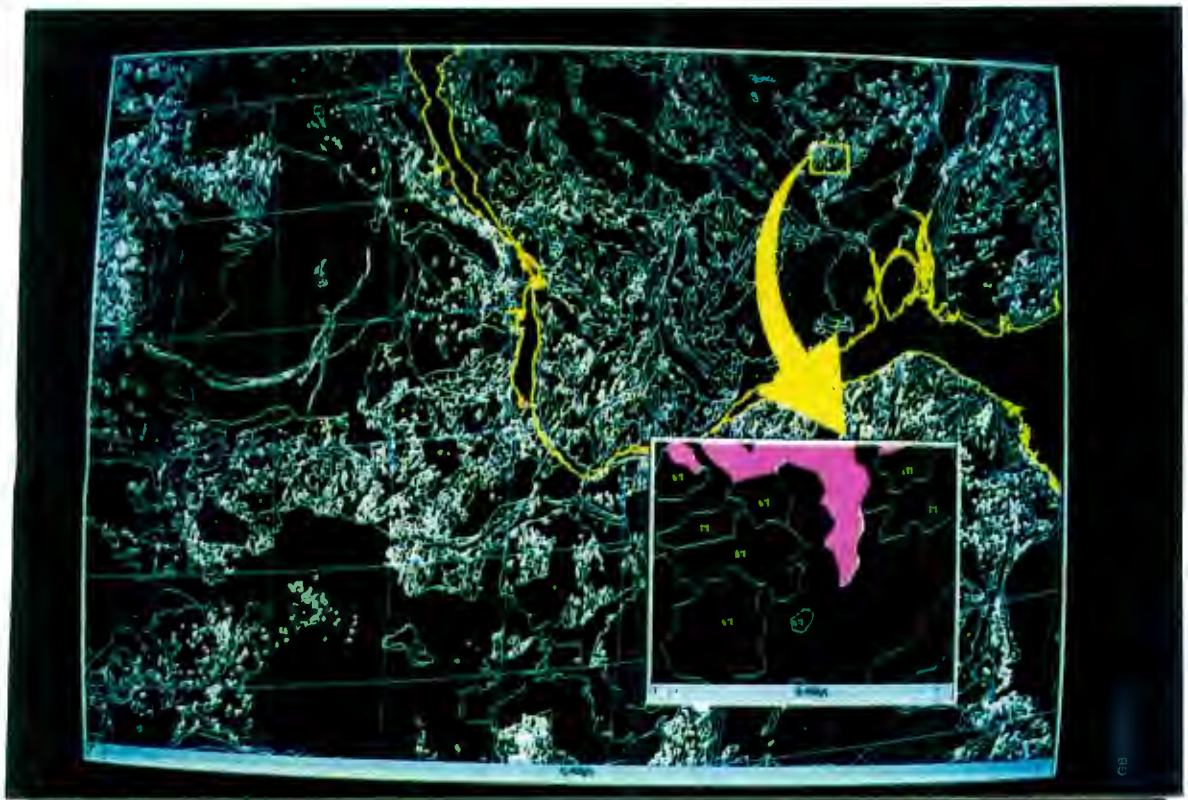

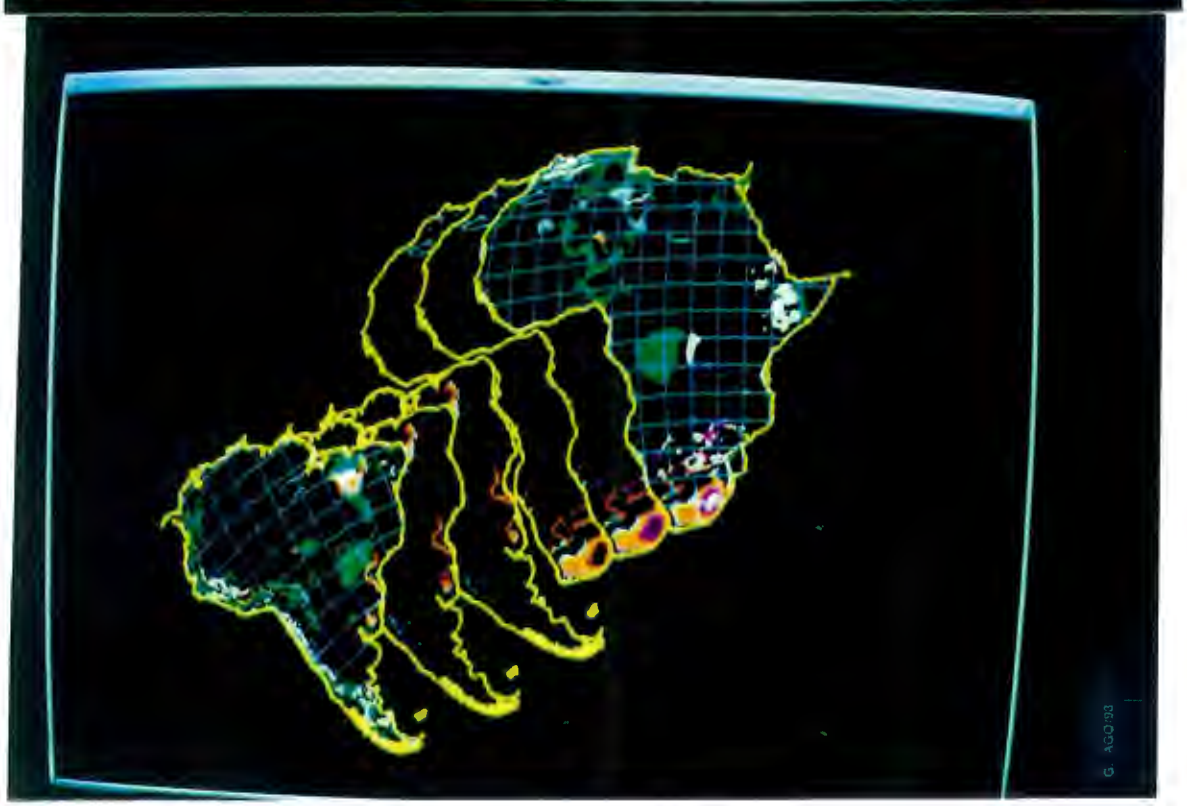

The interactive nature of geologic processes involved in the generation of continental-scale magmatism during mid to late Mesozoic extension in southwestern Gondwana are still very poorly understood. First-order assessments of the relation between lithospheric stretching, thermal and mechanical subsidence, and mantle processes which led to emplacement of the Karoo and the Parana-Etendeka flood basalt provinces have been attempted by many (e.g. Cox, 1978; White & McKenzie, 1989; de Wit & Ransome, 1992; Hawkesworth et al., 1992). One of the major limitations for a better constrained multivariate model is the lack of sufficient quality data sets that can be interactively used. The GO-GEOID (**Go**ndwana **Geo**scientific **I**ndexing **D**atabase) relational database of the digital geological map of Gondwana (Wilsher et al., 1989) incorporates otherwise fragmented geographical, geological, tectonic and geochronologic data in a form that can easily be manipulated using **g**eographic **i**nformation system (GIS) technology (Figure IV.1). Enquiries were made in an interactive time-frame from the graphic environment using GIS technology and a set of semi-quantitative geological maps were produced in an attempt to better evaluate the chronology of the tectonothermal events which culminated in the kimberlitic magmatism discussed in the previous Chapters.

IV.2 - THE TECTONIC FRAMEWORK OF WEST GONDWANA

The amalgamation of lithospheric plates and cratonic blocks of west Gondwana culminated during *two* major episodes: *(i)* at approximately 650 Ma during the assembly of the greater proto-Gondwana (which probably included North America; Hoffman, 1991); and *(ii)* 250 Ma ago with the formation of Pangea during the amalgamation between Gondwana and Laurentia, South China and Chimmeria (Veevers, 1988 and 1989; Hoffman, 1991; and de Wit & Ransome, 1992). The distribution of major cratons and other chrono-tectonic provinces in the Gondwana framework (Figure IV.2) is the subject of active research and has been discussed by many in recent publications (e.g. Fisher, 1984; Worslay et al., 1984 and 1986; de Wit, 1990 and in prep.; de Wit & Ransome, 1992; de Wit et al., 1988; Nance et al., 1988; Hoffman, 1989 and 1991). As illustrated in Figures IV.2 and IV.3, some northwestern (the Amazonian and West

African cratons), central (the São Francisco and Congo cratons) and southern (the Kalahari craton) portions of the Gondwana supercontinent comprise large domains which lack Brasiliano/Pan-African-age deformation and thermal remobilization. These domains behaved most probably as large lithospheric plates which colided along the Brasiliano-Pan African (Pan-Gondwanean) mobile belts to form the proto-continent (e.g. Brito Neves & Cordani, 1991; Cahen et al., 1984; Hoffman, 1991). The other portions of West Gondwana comprise a series of smaller cratons and fragments of continental plates and microplates, magmatic arcs and allochthonous terrains that were most likely assembled during the convergence of Gondwana in Meso-Proterozoic to early-Paleozoic.

The "heartland" of Gondwana was largely shielded from the effects of the second period of convergence related to the assembly of Pangea in the late-Paleozoic (*circa* 250 Ma). Allochthonous terrains were accreted to western South America and along the southern margin of Gondwana in the Paleozoic and early Mesozoic, in the form of "docking" of microcontinents and sea mounts or offscrapped pelagic sediments and slivers of oceanic lithosphere along a subduction zone of the proto-Andean mobile belt (e.g. Dalziel & Forsythe, 1985; Ramos, 1988; Daly et al., 1991).

One first order observation from the mosaic of crustal fragments and high strain zones is that the areas affected to a greater extent during Mesozoic and Cenozoic intracontinental rifting episodes were also areas which had experienced extensive deformation and/or remobilization during the Neo-Proterozoic Pan-Gondwanean orogenesis (Figures IV.2 and IV.3). For example, the zone along which the South Atlantic rifted coincides closely to Pan-Gondwanean suture zones (Figures IV.2 and IV.3). In the northern South Atlantic, between northeastern Brazil and Equatorial Africa for example, right-lateral transform motion parallels the grain of the Pan-African/Brasiliano Rockelides belt. East of the Togo-Transbrasiliano discontinuity, the South Atlantic rifting event was superimposed on intensely reworked rocks, and the propagation of the proto-Atlantic rift led to the formation of a NE trending wrench displacement with left lateral shear movement along a Pan-African right lateral shear zone (south of the Benue through; Benkhelil et al., 1988). From this point, however, the central Atlantic rift cuts across the shear

zones in Nigeria and NE Brazil. This is the only place in the South Atlantic where the structural grain of the Pan Gondwanean mobile belt is cut at a high angle. The reason for this is unknown. It could possibly be linked to activity along the transform zone west of the Cameroon (the Equatorial Fracture Zone) under the influence of the St Helena plume, concomitant with the rapid propagation of rifting north of the Tristan and Trindade plume heads. Southwards, the opening of the northern South Atlantic also occurred sub-parallel to tectonic anisotropies inherited from the Neo-Proterozoic tectonism.

The kinematics of accretion and the continuity of the individual NeoProterozoic belts marginal to the São Francisco craton are currently not well constrained or understood. Archean granulites of the northwestern Congo craton and the Congolian fold belt seem to correlate with Archean granulites of the eastern São Francisco craton and the Araçuai-Ribeira Atlantic belt, respectively. One difference between the provinces on either sides of this section of the Atlantic, however, is that NeoProterozoic strike-slip tectonics characterizes the Brazilian side, whilst fold and thrust tectonics dominates the east-Congolian belt. Paleomagnetic and geochronologic constraints suggest that the São Francisco and Congo cratons were separated continental blocks which collided in Brasiliano/Pan-African times (Renne et al., 1990). De Wit (pers. comm. 1988) suggested that the eastern São Francisco craton was accreted to the Congo craton during the early Pan-Gondwanean times along a North-South cryptic suture zone west of the West Congolian fold belt. As discussed in Chapter I, there is evidence for accretion of magmatic arcs and allochtonous terrains, and maybe even smaller cratons, to the western margin of the São Francisco craton during the early formation of Gondwana. Because of the paucity of reliable age information, however, there is disgreement as to where the terrane boundaries should be placed.

Further south, the Pan-Gondwanean Don Feliciano and Ribeira belts in Brazil and Uruguay correlate with the Damara and Gariep belts in Namibia and South Africa. On the Brazilian side strike slip structures predominate (in Schobbenhaus, 1984), whilst on the African side complex fold and thrust structures are more prevalent (Figure IV.3).

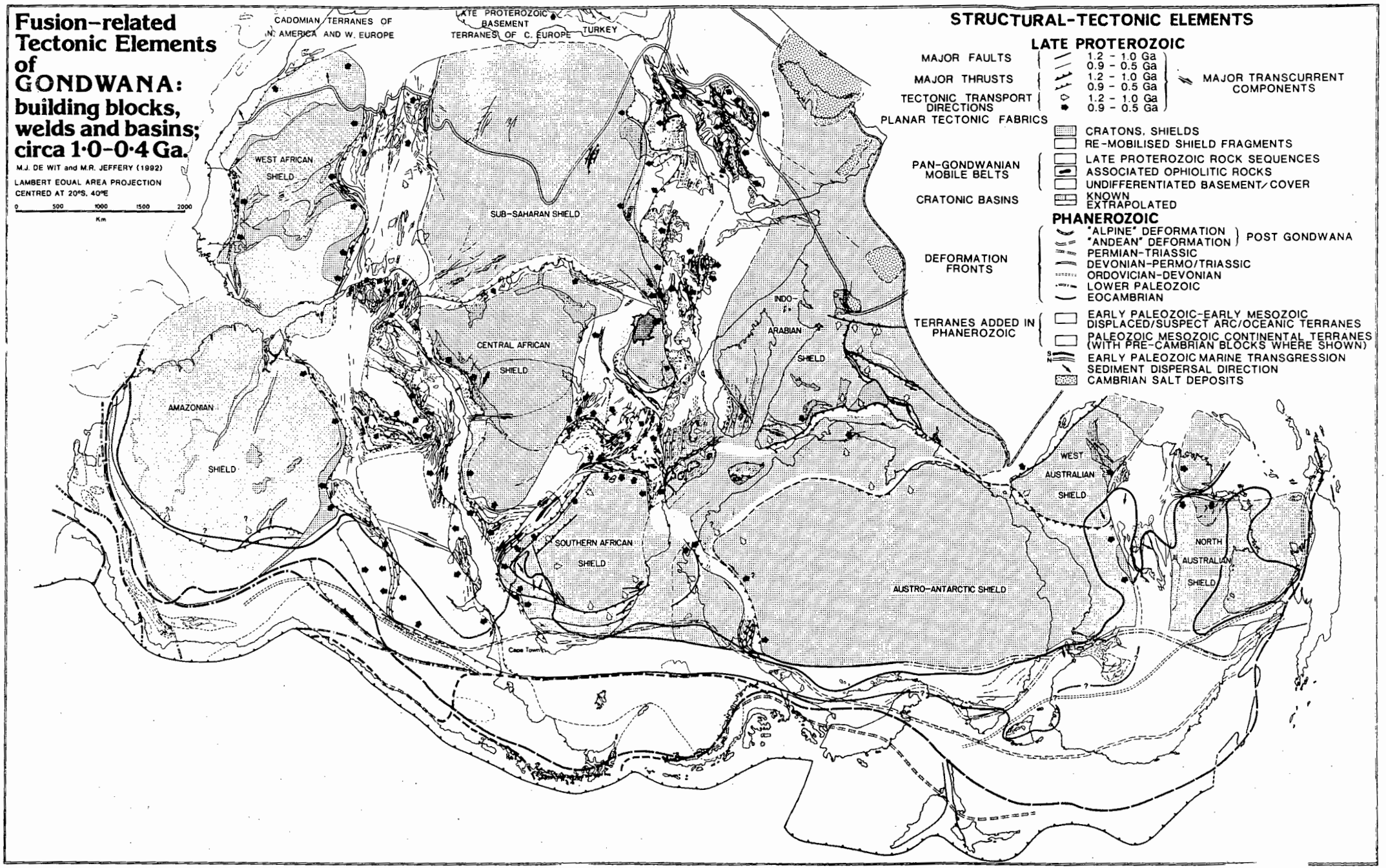

Figure IV.2 - Cratons and major chrono-tectonic provinces of Gondwana (from Maarten de Wit, in PREP.)

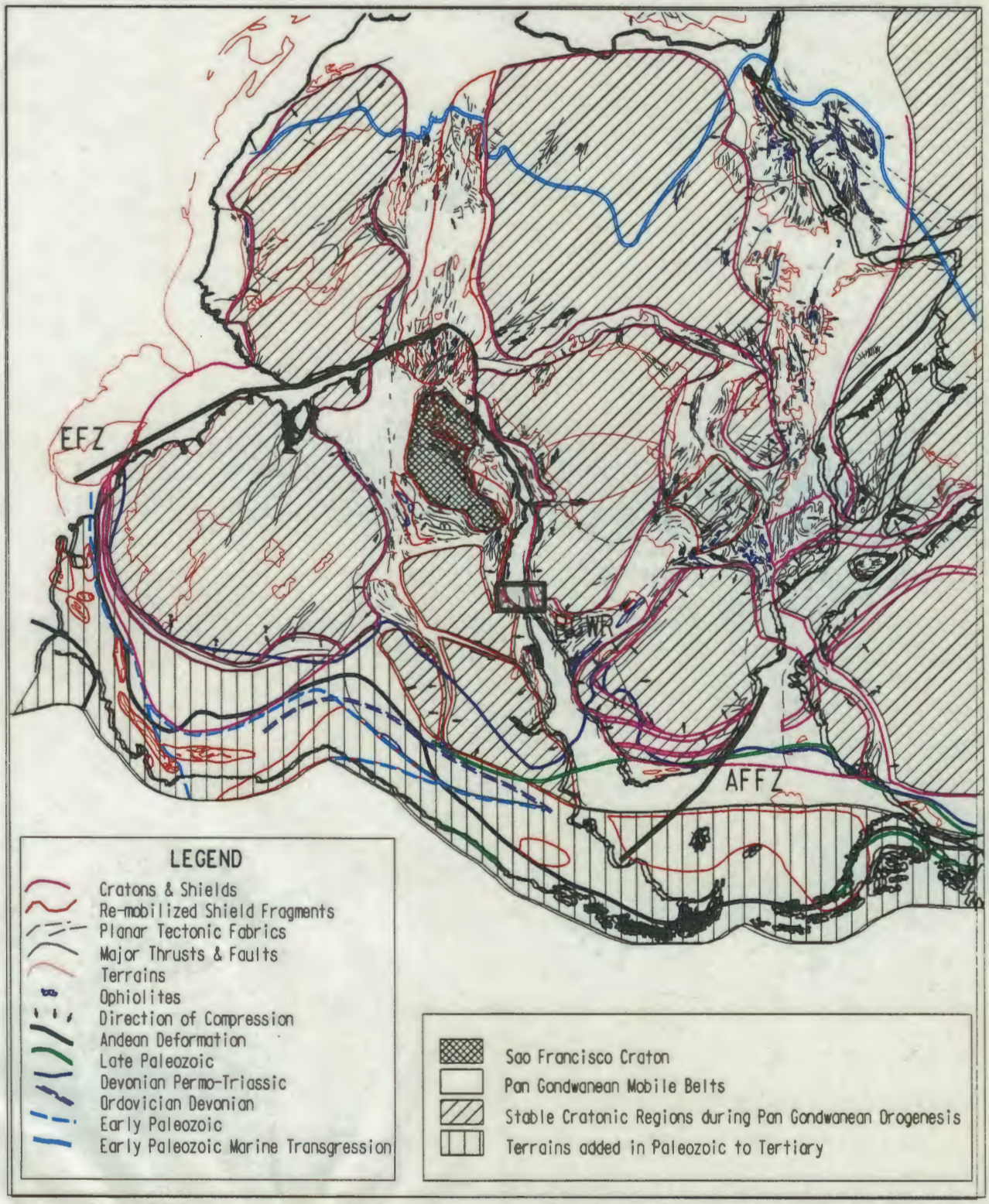

Figure IV.3 - GIS generated tectonic map for western Gondwana (adapted from Maarten de Wit, in prep.).

IV.3 - BREAK-UP OF SOUTHWESTERN GONDWANA

The late Proterozoic Gondwana supercontinent was extended and fragmented during the Paleozoic and early Mesozoic, and was finally dispersed in the late Mesozoic. The first-order large-scale inversions from NeoProterozoic compression to Paleozoic extension seems to correlate with global events of plate reorganization (Veevers, 1989). In southwestern Gondwana, this NeoProterozoic to Phanerozoic tectonic inversion is recorded in a succession of sediments and lava flows distributed over a considerable area (Figures IV.4 and IV.7; after de Wit & Ransome, 1992). Because of subsequent tectonic shortening and erosion, however, the present configuration of sedimentary basins does not truly reflect what once may have been a much more extensive basin which covered large parts of Gondwana and which was directly connected to the proto (Paleozoic) Pacific Ocean.

IV.3.1 - Prolonged South Atlantic sedimentation and rifting precursors to the igneous activity in Brazil

Paleozoic to Mesozoic depositional sequences indicate that peaks of sedimentation in southwestern Gondwana occurred during three major subsidence phases (viz. Cambro-Ordovician to Silurian-Devonian, Permian-Carboniferous, and late Jurassic-early Cretaceous). Zalan et. al (1990) indicated five depositional sequences (or synthems, as defined by Chang, 1975) bounded by unconformities of regional scale, each consisting of one or more lithostratigraphic units that can be correlated and extended across the whole of southwestern Gondwana (e.g. Milani, 1992; Visser, 1992; Figure IV.5).

Paleozoic sedimentary accumulation in southwestern Gondwana started as marine transgressions from the west, becoming continental in the Mesozoic and essentially marine again during the opening of present oceans (Figure IV.5). Early Paleozoic tectonism resulted in the development of an extensive Atlantic-type passive rift continental shelf along the southern margins of Gondwana (see Figure IV.4). This margin subsequently evolved into a convergent margin by the

Figure IV.4 - Tectonic evolution of Gondwana (from de Wit and Ransome, 1992). Cratonic blocks of Gondwana were welded along late Precambrian Pan Gondwanan mobile belts. At that time (i.e. 650 +/- 100 Ma) Gondwana was surrounded along its northern and southern margins by subduction zones. Extensive rift continental shelf margins developed along the northern and southern margins of Gondwana during the early Paleozoic. The late Paleozoic accretion tectonics along the southern margin led to the formation of extensive foreland basins. The orientation of the various fault systems are compatible with stress induced failure due to terrane accretion along the southern margin of Gondwana.

Mid-Paleozoic. The following transition to a continental environment, in the late Permian to early Triassic, was abrupt, as testified by a marked regional unconformity accross most of southwestern Gondwana. This is believed to be due to collisional events and probably reflects the transition of a passive rift margin basin along the entire southwestern Gondwana margin into an intercontinental foreland basin during the "Hercynian" orogeny. In the Gondwana "heartland" the formation and evolution of this foreland basin was accompanied by generalized uplifting, block tilting and rifting prior to and overlapping with the onset of Mesozoic magmatism. For example, the late Permian and early Triassic collision along the southern margin of Gondwana resulted in intracontinental compressional tectonic activity and deformation as far north in Africa as Zaire (Daly et al., 1991). Large scale normal, strike-slip and even thrust faulting resulted from the N-S contraction and led to the formation of extensive rift structures and extensional tectonic activity in south and central Africa in which "Karoo-type" sequences were deposited. The subsequent transition (inversion) to continental extension (leading to the opening of the South Atlantic Ocean) was diachronous in the different segments of western Gondwana and in many places overlapped with voluminous **C**ontinental **F**lood **B**asalts (CFB's).

Intensive early Mesozoic lithospheric extension and associated faulting occurred both along the present South Atlantic margin and inland. Intraplate stresses were accommodated in several zones of oblique slip coincident with east-west striking tension faults, concentrated along three relatively continuous zones of failure; viz. *(i)* the Agulhas-Falklands/Malvinas Fault Zone - AFFZ; *(ii)* the Rio Grande-Walvis Ridge Rise - RGWR; and (iii) the Equatorial Fracture Zone - EFZ (Rabinowitz & LeBreque, 1979; Ploskiewicz et al., 1984; Uliana et al., 1989; Fouche et al., 1992; see Figure IV.3). These features extended as much as 1500 km inland of the present passive margin along interior rift systems like the San Jorge basin (the extension of the AFFZ into Argentina) and along the southern coast of South Africa (de Wit and Ransome, 1992).

During the Mesozoic to Cenozoic opening of the South Atlantic ocean, the South Atlantic margin was characterized by three distinct tectonic zones, as illustrated in Figure IV.3. Along the dextral transform zone west of Cameroon (the Equatorial Fracture Zone - EFZ), E-W translation movements generated semi-isolated basins accommodated within extensional structures at a low

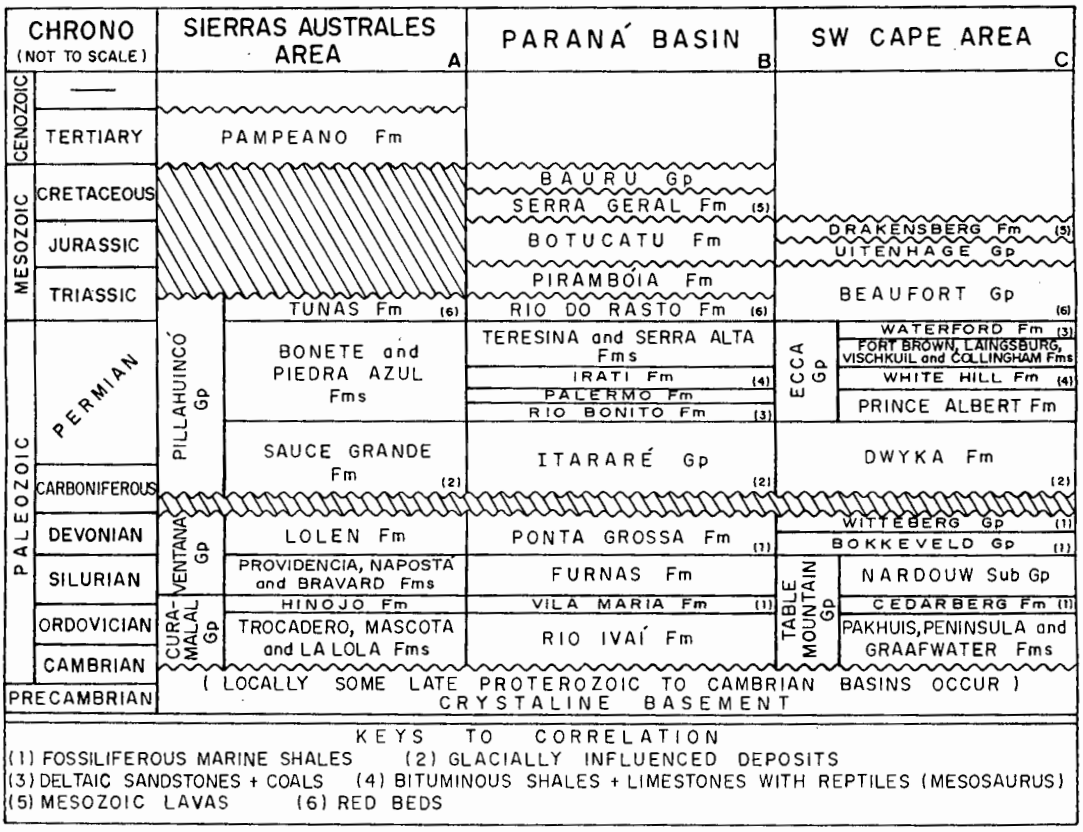

Figure IV.5 - Lithostratigraphy of the southern sector of Gondwana (from Milani, 1992).

angle to the present continental edge. Sheared boundary zones along the EFZ were the principal sites for dissipating stresses of the differential opening between Central and South Atlantic Oceans (Uchupi, 1989). South of the EFZ, and as far as the Agulhas-Falklands/Malvinas Fault zone - AFFZ, rift propagation was predominantly N-S. Here a different tectonic style is evident from that observed in the bounding EFZ and AFFZ: rifted margins display extensional structures oriented at right angles to the E-W fracture zones and parallel to the present coast. Contrasting features occur north and south of the Rio Grande Walvis Ridge Rise - RGWR. Neocomian

continental lithosphere stretching and rift basin formation in the northern sector led to rapid subsidence and deposition of extensive salt deposits, but without significant oceanic growth by plate accretion (e.g. Stark et al., 1991). In contrast, south of the RGWR production of oceanic floor began as early as Valangian times. A third tectonic regime occurs further south. The dextral transform zone defined by the AFFZ generated semi-isolated basins accommodated within extensional structures at an angle to the present continental edge (Fouché et al., 1992). The South African extensional features are a series of dominantly asymmetrical rifts and rotated blocks with master faults that follow the Paleozoic Cape Fold Belt structures (Dingle et al., 1983).

The two master boundary zones of the South Atlantic (EFZ and AFFZ) were the principal sites for dissipating stresses of the differential motion between southern South America and Southern Africa. During the pre-drift stage, volcanic ridges parallel to graben-bounding faults, thin basaltic flows, and sedimentary hinterland sequences accompanied the appearance of large crustal domes and major igneous activity between 200-170 Ma (Asmus, 1981; Asmus & Baish, 1983; Bristow & Saggerson, 1983; and Dingle et al., 1983). By the mid-Jurassic voluminous continental bimodal volcanic activity occurred in Patagonia (the Tobifera event, 160-170 Ma; Gust et al., 1985 and references therein) and central Karoo (180 Ma; Bristow & Saggerson, 1983; and various authors in Erlank, 1984); accompanied by minor alkaline and tholeiitic activity within the Paraná basin domain (Piccirillo et al., 1990; and references therein) as well as along coastal Namibia and Angola (Dingle et al., 1983; Erlank et al., 1990; Milner et al., 1992).

By late-Jurassic the volcanic activity in Patagonia and the central Karoo began to abate (Dingle et al., 1983; Uliana et al., 1989, Piccirillo et al., 1990), and a broad peneplanation followed to form the Gondwana surface. At this time, still well before the onset of seafloor spreading between South America and Africa, the area in the extreme south continued to evolve through crustal attenuation and development of extensional basins both within and behind the island-arc system between 150 and 138 Ma (de Wit & Stern, 1980 and references therein; Grunow, 1993). To the north, along subsidiary aborted rifts in southern Brazil, Argentina and Uruguay,

Figure IV.6 - Early Aptian (~120 Ma) reconstruction of the Angolan and Brazilian rifted margins (after Stark et al., 1991). Sea-floor spreading by plate accretion is about to break northwards through a structural discontinuity zone under the influence of the Walvis hotspot (in red), then splitting and separating the extended continental lithosphere. Dots refer the Cretaceous alkaline intrusives. Note the alignment defined by the intrusives discussed in Chapters II and III and those emplaced along the Southern Angola Arch, which parallels the Lineament 125 AZ.

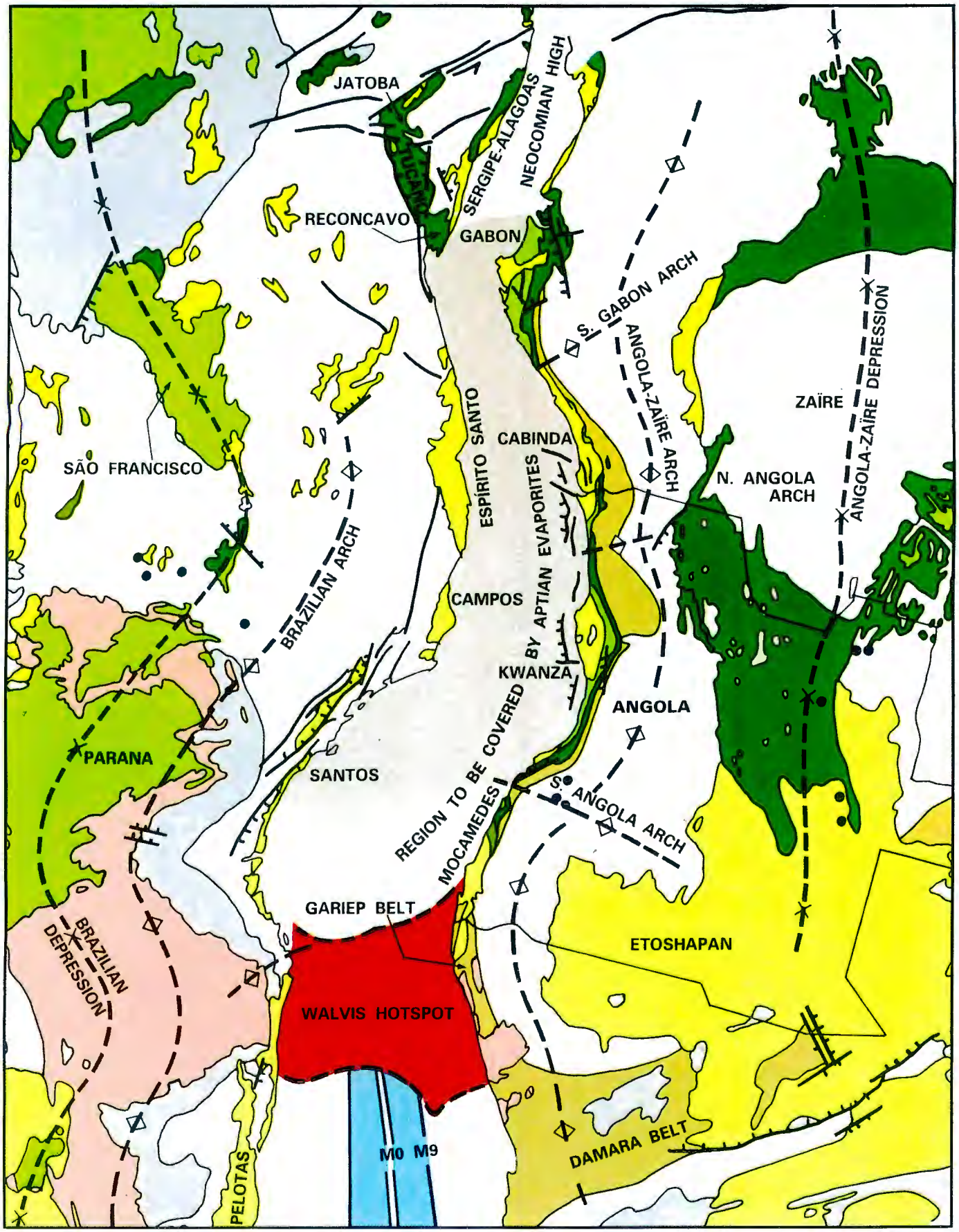

Cenozoic
Cenozóico

Neocomian
Neocomiano

Middle and Upper Cretaceous
Cretácico Médio e Superior

Palaeozoic to earliest Jurassic Karoo cycle sediments and volcanics
Sedimentos e rochas vulcânicas do Paleozóico ao início do Karoo Jurássico

Early Cretaceous basalts
Basaltos do Cretácico Inferior

Magmatic hotspot
Ponto quente magmático

Area to be covered by Aptian evaporites
Área a recobrir pelas evaporites do Apciano

Late Precambrian Pan-African deformation zones
Zonas de deformação do final do Precâmbrico Pan-Africano

volcanism and dike emplacement increased along areas close to the future South Atlantic margins (Uliana et al., 1989; Piccirillo et al., 1990 and references therein). Radiometric dates from continental flood basalts interbedded with syn-rift clastics suggest that, as far north as latitudes 20-25° south, attenuation of Gondwana lithosphere along the proto-South Atlantic margin started roughly at the same time as the Paraná Serra Geral basaltic event (130 Ma; Austin & Uchupi, 1982; Fodor et al., 1983; Peate et al., 1990).

A wide range of ages has been published for the initiation of sea floor spreading between Africa, South America and Antarctica (for a review see Rabinowitz & Le Brecque, 1979; Austin & Uchupi, 1982; Dingle et al., 1983; Uchupi, 1989; Fouche et al., 1992; and references therein). There is still, however, no complete agreement about the precise chronology of all these events, and there is as yet no real convergence towards a consensus with respect to the kinematics of the early dispersal of the three continents (Grunow, 1993). The lack of agreement largely is the result of uncertainty regarding spreading rates, magnetic-reversal time scale used, and the precise position of the continent-ocean boundary. It is likely that the separation of the Falklands/Malvinas plateau from the Agulhas bank occurred between 145 and 122 Ma (Martin & Hartnady, 1986). Recent detailed studies of the off-shore South African basins, however, indicate a much more complex history for the area than hitherto realized, including at least five phases of structural inversion since the onset of rifting (Van der Merve & Fouche, 1992). There is reasonable consensus that the breakthrough of the Agulhas Falklands/Malvinas Fracture Zone (AFFZ) was controlled by the early opening of the proto-Indian Ocean (Grunow, 1993; Ben-Avraham et al., 1993).

Plate torsional rigidity associated to the movements along the AFFZ promoted crustal extension within the Falklands/Malvinas plateau and further to the west. Extensional faulting occurred along the South Atlantic margin, south of the RGVR, during the early Cretaceous (Berriasian), initially as non-marine rift basins (Uliana et al., 1989) rapidly followed by marine sediments. The rifting extended northwards for more than 1500 Km along a continuous zone of faulting between the AAFZ and the Rio Grande/Walvis Rise (RGWR; Rabinowitz & Le Brecque, 1979; Uchupi, 1989). Oceanic growth by sea floor spreading in this sector of the South Atlantic begun

by Valanginian times (circa 130 Ma; Stark et al., 1991). Until the end of Neocomian (circa 120 Ma), this activity along the proto-South Atlantic was accompanied by voluminous continental tholeiitic flood basalts and later followed by rhyolites and intermediate rock types emplaced along fissure vents of the Parana-Etendeka CFB Province (in Piccirillo et al., 1990). Within the inner parts of the basin such fissures are commonly covered by their own eruptive products. Along the borders, and in areas which experienced extensive lithospheric doming (e.g. at the Ponta Grossa arch), massive dykes,sills and intrusive sheets and a widespread suite of mainly intermediate alkaline intrusions are exposed (e.g. Piccirillo et al., 1990). With time, the focus of magmatism migrated northwards at a rate of about 30 cm/yr both along the proto-South Atlantic fissure zone (Austin & Uchupi, 1982) and within the domain of the Parana-Etendeka Province (Peate et al., 1990).

To the north of the RGWR, Neocomian continental stretching resulted in deep (>1 Km) non-marine rift-basins with extensive salt deposits and minor basaltic volcanics (the Campos, Tucano and Jatobá basins in NE Brazil; Mohriak et al., 1989; Santos et al., 1990; and the Namibe, Kwanza, Congo and Gabon basins of western Africa; Stark et al., 1991). In this central sector of the South Atlantic sea floor spreading started only in late-Aptian times (circa 105 Ma). Continental separation was influenced by north-south Pre-Cambrian basement structures; by the right-lateral transform motion between Brazil and equatorial Africa; and by the change in position of the South America/Africa rotation pole; and by decrease in the angular separation rate northwards (Rabinowitz & Le Brecque, 1979; O'Connor & Duncan, 1990). The rupture accross the RGWR rift by northward rift propagation in the early-Aptian caused an almost "instantaneous" marine transgression up to northern Gabon and deposition of evaporite sequences (see Figure IV.6). Thereafter, carbonate platform deposition on both sides of the Atlantic marks the beginning of the post-rift thermal subsidence.

IV.3.2 - Continental flood basalts, dike swarms and alkaline volcanism

Large volumes of continental flood basalts (CFB) erupted in southern Gondwana during two major episodes (see Figure IV.7). First, in early to mid Jurassic, the earlier break-up of western

Gondwana and separation between [Africa-South America] and [India-Antarctica] (i.e. early opening of the Indian Ocean) was accompanied by extensive volcanism within the Karoo CFB Province. This peak of volcanic activity occurred at about 180-190 Ma and presently outcrops *ca.* 140.000 km^2 throughout southern Africa (see review in Erlank, 1984). Second, in the early Cretaceous (at about 130 Ma), the separation between Africa and South America was accompanied by extensive volcanism within the limits of the Paraná-Etendeka CFB Province. The majority of lavas related to this later event yield ages of 135-115 Ma,and cover an area of about 1,3 million km^2 in Brazil and Namibia (see reviews in Erlank, 1984; and Piccirillo et al., 1988). Though different in age, both the Paraná and the Karoo flood magmatism events consisted of diabase dykes, sills and extensive plateaux of tholeiitic basalt, and terminated with intermediate and acid volcanism. The low diversity in composition of these magmatic provinces compared to the great varieties in composition of arc and back-arc volcanics is characteristic of magmatic activity along the edges of more stable cratonic areas (Bristow & Saggerson, 1983).

Post-CFB intrusions of alkali granites, gabbros and syenite complexes, carbonatites and K-rich volcanics in the form of central ring structures and dike swarms occur throughout the former southern Gondwana continent, and especially within rift zones and thermal uplifts of late-Mesozoic to Eocene age along both sides of the South Atlantic. Structurally controlled alkaline intrusives and dike swarms with NE and NW trending zones have been studied in some detail. Kimberlites and other deeply-derived low-volume volcanics are more unusual aspects of the alkalic outpourings, and are not so obviously linked to tectonic events or structures at surface.

Off-craton alkaline ultrabasic magmatism in Southern Africa was concentrated in western Angola, Namibia, Namaqualand and in the Central Cape Province of South Africa. Gabbroic and granitic-syenitic high-level plutons in these areas are spatially connected with intrusive and extrusive ultrabasic rocks of diverse character which contain variable amounts of silica-deficient minerals such as melilite, monticellite, nepheline, leucite and perovskite (Moore & Verwoerd, 1985; Colgan et al., 1989; Rogers et al., in press). Closer to the margin of the Kaapvaal craton, the magmas change gradually from olivine nephelinites and carbonatites to olivine melilitites, lamprophyres and non-mineralized kimberlites (e.g. Shee et al., 1989). On-craton alkaline

ultramafic magmatism within the Kalahari craton is dominantly represented by deeply-derived kimberlites and lamproites. Approximately 840 kimberlites (Skinner, 1989) and a few lamproite dykes have been reported, and comprehensive reviews of their distribution, petrology and xenolith contents have been produced (e.g. Dawson, 1980 and 1989; Mitchell, 1989; Gurney et al., 1991). Group I kimberlites (which are younger - 75 to 114 My - and have primitive Nd, Sr and Pb isotopic compositions similar to OIB; Smith, 1983) are widely distributed accross the Kalahari craton with no obvious age progression, whereas Group II kimberlites (which are older - 114 to 204 My - and have isotopic and trace element characteristics similar to Dupal-type OIB; Le Roex, 1986)' are roughly linearly distributed with NE-SW trends and with apparent decreasing ages towards the southwest (Skinner, 1989). This deep-derived alkaline activity during the Mesozoic has been attributed to uplift and faulting of the Kalahari craton during lithospheric stretching (Dawson, 1980; Ferguson & Jaques, 1984) and to hot-spot activity (Crough et al., 1980; Smith, 1983; Le Roex, 1986; and Skinner, 1989).

In South America, the margins of the Paraná basin were also affected by extensive alkaline igneous activity throughout the late-Mesozoic and early Tertiary (Ulbrich & Gomes, 1981; Almeida, 1983 and 1986). Alkaline activity tends to concentrate along major tectonic boundaries in the Precambrian basement and appears to be related to basaltic activity. Most of the known kimberlite-related magmatism is confined to the lineament 125AZ (Bardet, 1977) which crosscuts the southern portions of the São Francisco and Guaporé cratons of Brazil (e.g. Tompkins & Gonzaga, 1989 and 1991; Almeida & Svisero, 1991). Though variable in the detail, there is a progressive increase in the age of the kimberlites towards NW along the 125AZ lineament. Minor deeply-derived occurrences have also been reported around the La Plata craton in Argentina (Meyer & Villar, 1984) and Paraguay (Comin-Chiaramonti et al., 1991).

Emplacement ages presently available indicate that alkaline igneous activity (including kimberlites) in South America and Southern Africa overlap in age, unlike their respective CFB Provinces. This appears to indicate that the alkaline igneous activity relates to advanced stages of the South Atlantic opening and not to the opening phase of the southern Indian Ocean.

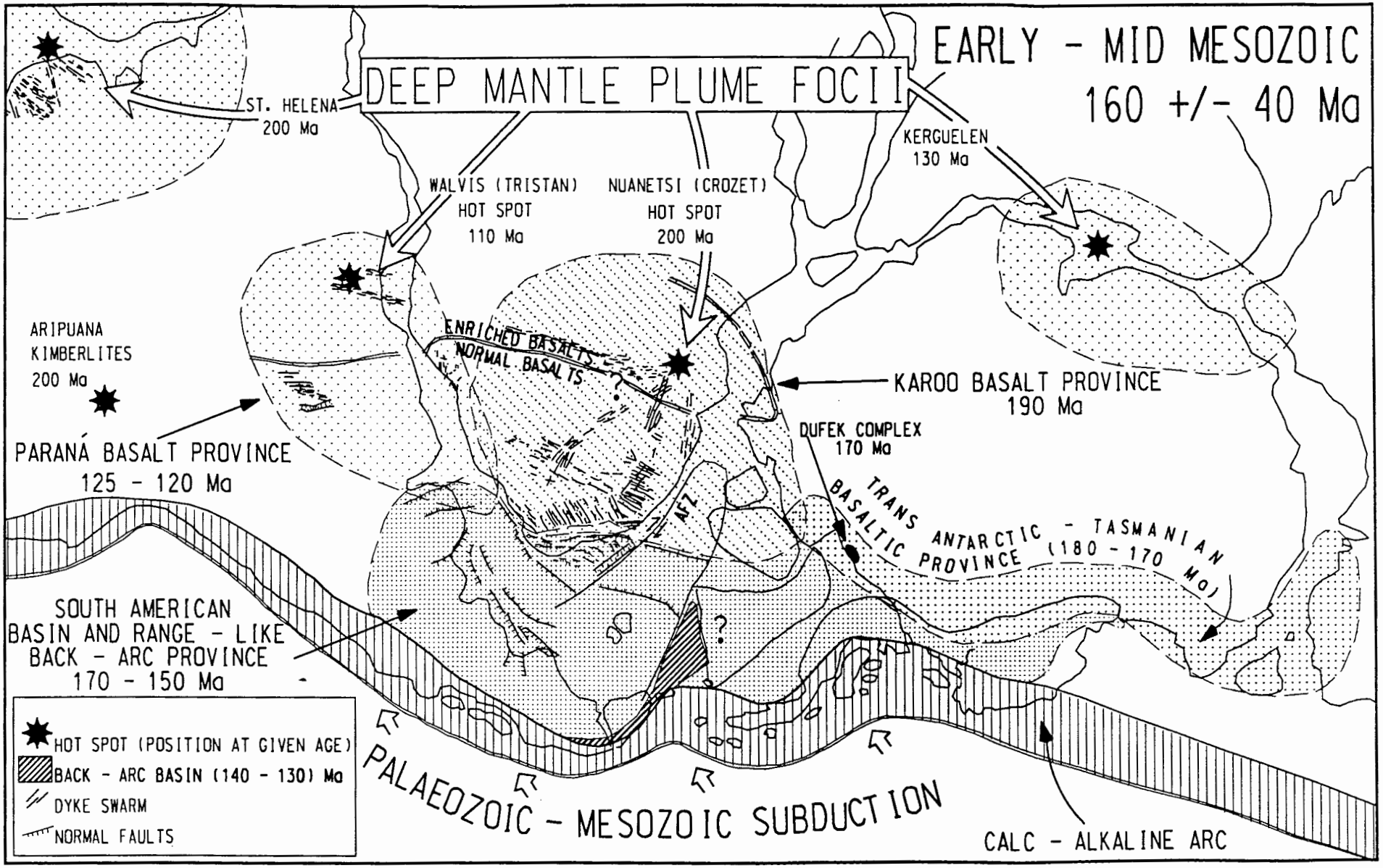

Figure IV.7 - Provinciality of voluminous continental magmatism during Gondwana breakup (after de Wit and Ransome, 1992).

IV.4 - LARGE-SCALE MANTLE HETEROGENEITIES OF SW GONDWANA

Geochemical and isotopic tracer data from the Karoo and Parana flood basalt provinces and their associated dike swarms provide evidence for a complex history of mantle source heterogeneities on a regional scale which involves the source of the alkaline volcanics emplaced along the SW São Francisco craton margin. For example, a fundamental geochemical boundary, separating areas of dominantly "enriched" (with respect to incompatible trace element concentrations) basalts in the north from "normal" basalts in the south, has been suggested to exist across both the volcanic CFB province of southern Africa and Brazil, despite their differences in age (Cox et al., 1967; Rhodes & Bornhorst, 1976; Erlank, 1984; Bellieni et al., 1984; Mantovani et al., 1985; Hawkesworth et al., 1986; Piccirillo et al., 1988; Erlank et al., 1980, 1984, 1988, 1989 and 1990). In pre-drift reconstructions (see Figure IV.8) this 60 km to 100 km wide geochemical boundary zone is apparently continuous for thousands of kilometers (e.g. Erlank et al., 1990). Another important aspect with regard to large-scale mantle heterogeneities is the recognition that both the studied alkalic rocks along the SW São Francisco craton margin and some OIB in the South Atlantic have typical Dupal anomaly (Hart, 1984) characteristics.

The immobile elements Ti and Zr have been suggested to be reliable discriminants between the "enriched" and "normal" basalts (Erlank, 1984; Bellieni et al., 1984), referred to here as HTZ (high Ti and Zr) and LTZ (low Ti and Zr) basalts, respectively (following the notation of Erlank et al., 1988, 1989 and 1990). Significantly, isotopic and trace-element data have led to the recognition of a number of sub-provinces within the HTZ and LTZ domains, some of them with intermediate compositions. For example, Peate (1989) has recognized six different magma types within the Paraná extrusive basalts and basaltic andesites. Hawkesworth et al (1992) demonstrated the existence of an overlapping series of units dipping northwards, and argued that the dominant magma type evolved from low Ti, to high Ti and then to intermediate Ti, as the source of the Paraná magmas migrated northwards. In Northwestern Namibia, the Etendeka volcanics display similar geochemical characteristics and variable compositions (Erlank et al., 1984; Bellieni et al., 1984; Duncan et al., 1990; S. Milner, pers.comm., 1992). Duncan & Erlank et al., (1980) recognized four major chemical provinces or magma types in the Karoo

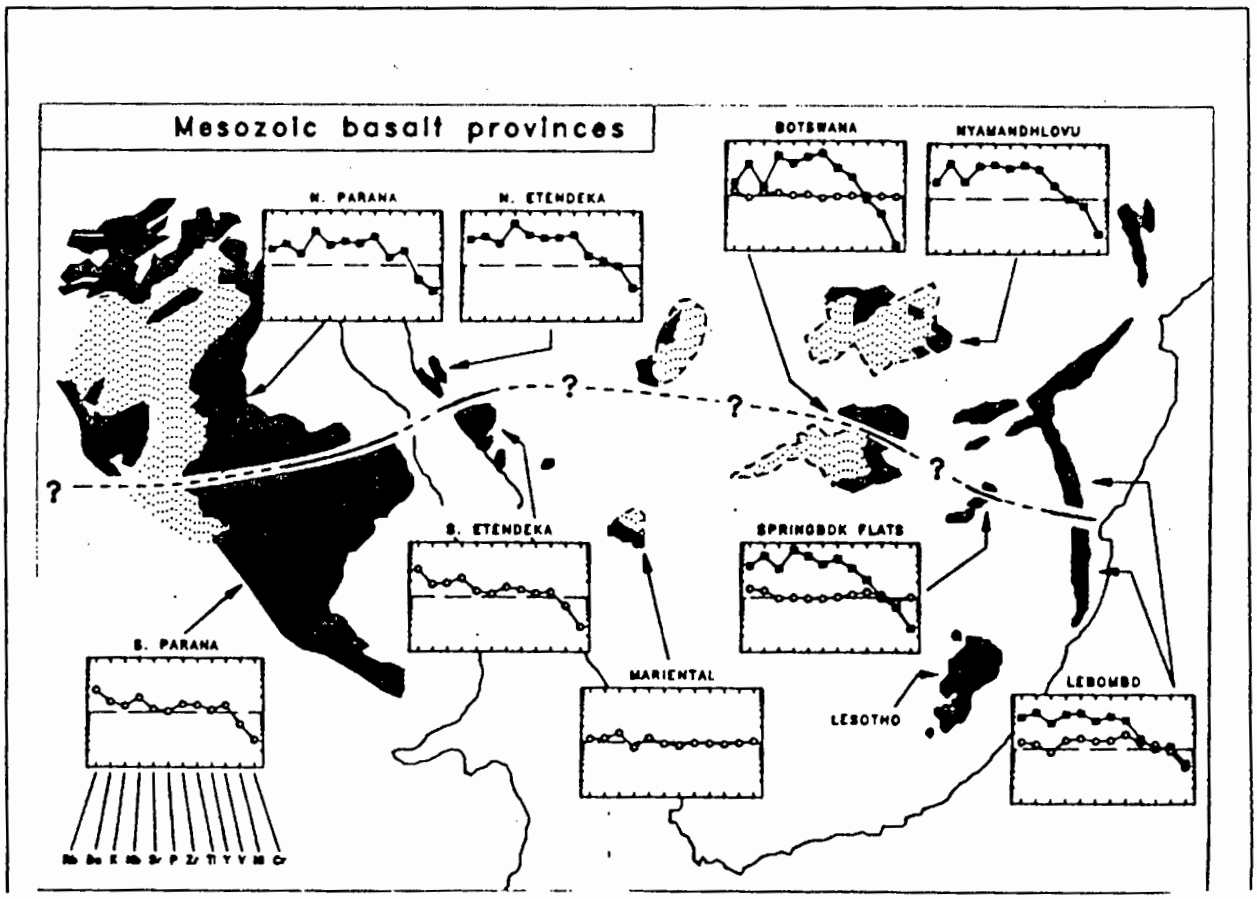

Figure IV.8 - HTZ and LTZ zonation from Erlank et al. (1990). Spidergrams normalized to average Lesotho Formation basalt.

basaltic volcanics. Subsequent studies by these and other authors (e.g. various authors in Erlank, 1984; Cox, 1983 and 1988; Erlank et al., 1990) have led to the recognition of additional sub-provinces in the Karoo Province as well.

Fundamental differences between the HTZ and LTZ magma types in terms of incompatible element abundances (at similar MgO contents), incompatible element ratios and isotopic signatures argue against the hypothesis of their derivation from the same source by different

degrees of partial melting or the derivation of either group from the other by fractional crystallization. The HTZ basalts, sometimes also referred to as HPT (high phosphorous and titanium) basalts (Mantovani et al, 1985), typically contain $>2.5\%$ TiO_2, >250 ppm Zr and $>0.3\%$ P_2O_5. These basalts are also characterized by Ti/Y ratios >410, Zr/Y ratios >6, and high LREE contents (La $>$ 80 x chondrite) without any appreciable Eu anomaly. Conversely, the LTZ (low titanium and zirconium) basalts, also referred to as LPT (low phosphorous and titanium; Mantovani et al., *op.cit.*) basalts, contain $<2.0\%$ TiO_2, <250 ppm Zr, $<0.3\%$ P_2O_5, Ti/Y ratios <400 and Zr/Y ratios <6. The LTZ tholeiites are characterized by a slightly fractionated LREE pattern and a nearly flat HREE pattern. Though not uncommon, negative Eu anomalies are often absent. Sr and Nd isotope characteristics are variable but distinctions exist between the HTZ and LTZ magmas. The HTZ basalts tend to have low initial $^{87}Sr/^{86}Sr$ (0.7048-0.7058) and low ϵ_{Nd} values (from -2.5 to -4.6) relative to the mantle array, whereas the LTZ basalts tend to have higher and more variable $^{87}Sr/^{86}Sr$ values (in many areas linked with variations in minor and trace-elements) and slightly lower ϵ_{Nd} (from -3.7 to -7.9). MORB- and OIB-type isotopic signatures have been observed in LTZ- and HTZ-type dolerites in NW Namibia (Duncan et al., 1990; Milner et al., in prep.), in the Ponta Grossa arch (Piccirillo et al., 1990) and in the Rio de Janeiro coastal area of Brazil (Hawkesworth et al., 1992); and in HTZ-type picrites in the Nuanetsi-northern Lebombo area of southern Africa (Ellam & Cox, 1991; and Ellan et al., 1992).

The overall composition of the HTZ magmas is typical of mantle-derived melts, segregated from a mantle similar to or more refractory than OIB or MORB compositions. The involvement of a deep garnet-bearing source has been suggested on the grounds of their REE fractionated pattern (e.g. Mantovani et al., 1985), and by comparing major element compositions of the HTZ picrites with experimentally deduced *liquidus* phase relationships of mantle peridotites (Sweeney et al., 1991). HTZ basalts show reasonably well defined inter-element variation trends which can be modelled by fractional crystallization of olivine and orthopyroxene and which, at shallow levels, might also involve plagioclase (e.g. Bristow, 1984; Bellieni et al., 1984). Incompatible element compositions, however, are not consistent with fractional crystallization processes, even if assimilation or variable degrees of partial melting are involved (Cox, 1983; Erlank et al.,

1984; Mantovani et al., 1985; Duncan et al., 1990). Crustal contamination has been investigated by many (e.g. Bristow, 1984; Cox, 1983; various authors in Erlank, 1984, and Piccirillo et al., 1990; Peate, 1989) and evidence for significant contamination has been reported absent. Sweeney et al. (1991) demonstrated that greater concentrations of K_2O, TiO_2 and Zr contents which occur specifically in alkali enriched HTZ picrites and which they named the "high-*NaK#*" group (*NaK#* = $[Na_2O+K_2O]/ [Na_2O+K_2O+CaO]$) are correlated with greater depths of magma segregation. This group, also characterized by greater Mg#, lower Fe_2O3 and lower Al_2O3 and CaO contents, is thought to have segregated at higher pressures (ca. 18-32 kb) relative to the low-*NaK#* HTZ picrite group. The "low-*NaK#*" HTZ Karoo picrites segregated at pressures of 10-22 kb from a lithospheric mantle source more refractory than MORB or OIB. Arndt & Christensen (1992) indicate that the high concentrations of Ti and other more incompatible elements in high-Ti basalts and picrites derive mainly from elevated abundances of these elements in the parent magma, which in turn result from low degrees of melting or elevated abundances in the source peridotite.

Both the major and trace element compositions of the LTZ CFB are different from those in oceanic basalts. This has been attributed to segregation from a relatively refractory mantle (Hergt et al., 1991; Sweeney et al., 1991). Flat HREE pattern, low Ti/Zr ratios and major element compositions have been suggested by these and other authors, to indicate that residual garnet was not present in the source of the LTZ magmas. The major element compositional variations of the LTZ rocks can be explained in terms of fractional crystallization of olivine, pyroxene, plagioclase and subordinate iron-oxides from tholeiitic parental magmas within the continental crust (Mantovani et al., 1985). Though major and trace elements appear to be linked, distinct degrees of enrichment are observed in rocks of similar major element composition, indicating that geochemically distinct source regions were involved in the generation of the parental LTZ magmas. Positive correlation between ϵ_{Sr} and SiO_2, Rb, Zr and Sr contents, coupled with negative correlation with CaO and MgO, have been rationalized as evidence for crustal-level contamination and AFC processes operative during stagnation and fractionation of the LTZ magmas within the crust (Mantovani et al., 1985; Cox, 1988). Hergt et al. (1989 and 1991), however, considered more probable that the tholeiites had inherited their apparently

"crustal " features from an upper mantle source which had incorporated subducted sediment.

The position of the fundamental HTZ/LTZ geochemical boundary at surface has been suggested to represent both compositional variations at relatively shallow levels in the sub-continental mantle (e.g. Sweeney & Watkeys, 1990; Hawkesworth et al., 1986) and the interaction of lithosphere with mantle plume structures (e.g. Erlank et al., 1989; Ellam & Cox, 1991). One first order observation regarding such provinciality, however, is that the geochemical boundary cuts across major cratonic and Pan Gondwanean orogenic domains with different lithospheric thickness, composition and ages. This demonstrates that the observed geochemical features are not simply inherited from an old continental lithosphere because the continuous geochemical boundary was not present prior to the formation of Gondwana. The arguments that the HTZ/LTZ boundary represents ancient lithospheric chemical domains cannot easily explain its position in the tectonic framework of southwestern Gondwana. The spacial relationship of the "enriched" basalts to mantle plumes (e.g. Erlank et al., 1990) and their geochemical similarities to plume-related volcanics (e.g. Ellam & Cox, 1991; Hawkesworth et al., 1992; this work) are also important observations which, together with the position of the LTZ magmas relative to the active paleo-continental margin of Gondwana (Hergt et al., 1991), suggest there may have been a geodynamic interrelationship between subduction processes and mantle plumes during the breakup of Gondwana (e.g. de Wit & Ransome, 1992; and references therein). In this sense it is likely that asthenospheric (or deeper?) mantle upwellings may have supplied significant chemical flux in order to "buffer" the geochemical characteristics of the subcontinental lithosphere. The application of this model to southwestern Gondwana follows Erlank et al. (1989 and 1990), who suggested that the distribution of HTZ basalts in southwestern Gondwana could be a consequence of the influence of two separate and perhaps chemically different mantle plumes (i.e. Tristan da Cunha and Crozet/Marion; see Figure IV.7).

IV.5 GEOCHEMICAL HETEROGENEITIES AND THE VOLCANISM ALONG THE SOUTHWESTERN SÃO FRANCISCO CRATON MARGIN

The distinct source character of the studied alkalic occurrences in the Coromandel region and the relative homogeneity of the isotopic signatures of these rocks (which were collected along a 200 km E-W traverse away from the craton margin) both suggest that a unique sub-continental mantle lithosphere underlies the SW São Francisco craton. In addition, the isotopic similarity of the studied kimberlites and rift-related rocks to the CFB's of the northern Paraná basin suggests their source(s) might be not only closely related (Figure II.19) but physically continuous as well. The magmatism which displays this isotopic similarity occurred over a region of approximately 200km x 250km for a period of approximately 45 My. In spite of being located within the area of influence of both the Tristan and the Trindade hot spot tracks, on the scale of the study area the magmatism displays no obvious age progression. Apparently, the loci of the magmatism was mainly controlled by intraplate stresses focused along pre-existing Brasiliano/Pan-African structural discontinuities. This implies prolonged tapping of a single mantle source between 130 to 85 Ma, a period during which the Coromandel area was displaced westward over an estimated distance of at least 90 km during continuous Gondwana dispersion. The relatively homogeneous mantle source required for the basic-alkalic magmatism, therefore, either moved with the South American Plate or was available to be tapped over great distances.

The data now available for the Minas Gerais region, along with the above mentioned geochemical and isotopic tracer-data from the Karoo- and Paraná/Etendeka-flood basalt provinces, argue for mantle sources which may be heterogeneous on a 20 to 100 km scale or less, but which are relatively homogeneous on a larger (>1000 km) scale. Moreover, the arguments presented which suggest that the mantle anomaly underlying the southwestern margin of the São Francisco craton has been in existence for a long time, are in agreement with the ancient nature of some of the source heterogeneities (e.g. Hawkesworth et al., 1983 and 1986). These observations constrain local mantle convection models and provide clues to the evolution and distribution of discrete mantle domains, both prior to and contemporaneous with the opening of the South Atlantic.

The voluminous outpouring of tholeiitic magma of the Paraná basalts is thought to be related to flexural lithospheric decompression or extension linked to the rise of the Tristan plume during the early opening of the South Atlantic (e.g. White and McKenzie, 1989; Peate et al., 1990), but there remains considerable uncertainty about the causes of the CFB volcanism in southwestern Gondwana, on the extent to which the local continental mantle lithosphere was remobilised, and on the role of mantle plumes during their emplacement (e.g. White & McKenzie, 1989; Hawkesworth et al., 1992; Gallagher & Hawkesworth, 1992). Ellam and Cox (1991) presented a model in which the Karoo picrite basalts in the Nuanetsi area of southern Africa result from interaction between asthenospheric magmas and an enriched lithospheric mantle (with trace element characteristics similar to lamproitic magmas). The mechanism proposed by these authors could conceivably have produced the range of chemical compositions observed in the SW Minas Gerais area, but their model requires the asthenospheric end-member to be greatly depleted in incompatible elements. Unlike the Karoo picrites, however, the Minas Gerais rocks have high incompatible trace element contents and isotope characteristics which are more similar to OIB than MORB.

A variation of the Ellam and Cox (1991) model has been proposed by Hawkesworth et al. (1992) to explain compositional variations in the Paraná volcanics as well as in the coastal basic dikes in Brazil. Hawkesworth et al., (1992) have shown that a number of dike samples from the Rio de Janeiro-Santos section display Nb/Ti and Zr/Ti variations comparable to those observed in Tristan da Cunha basalts. These variations are also comparable to the OIB-like compositions of the alkalic rocks reported in this work. Variations of Nb/La shown in Figure II.15 illustrate the relation of the studied rocks to OIB and to Parana CFB, and specifically to the high Nb/Zr coastal dikes in the Rio de Janeiro area and the Paraná basalts which have been interpreted as evidence for involvement of typical plume-related OIB in the Paraná Province (c.f. Hawkesworth et al., 1992).

More recently, Gibson et al. (in press) suggested that the location of the Alto Paranaiba igneous province coincided with the postulated position of the present-day Trindade (or Martin Vaz) plume at circa 85 Ma, and that the widespread late Cretaceous alkaline magmatism in SE Brazil

may have been caused by impingement of the Trindade mantle plume on the base of the subcontinental lithosphere.

Assuming that the hypothetical mushroom-shaped heads of the Tristan and Trindade mantle plumes occupied the areas indicated by O'Connor & Duncan (1990), parts of the southwestern São Francisco craton would have been affected by both these plumes (Toyoda et al., 1994). The rather limited data available to date does not allow a clear distinction between effects of rift-induced active melting processes and those of passive melting processes imposed upon continental lithosphere affected by mantle plumes. It does appear, however, that the location of the intrusives was conditioned by the long-lived Pan African anisotropies in the upper-crust, and that the isotopic and trace-element signatures of these rocks were dominated by the upper-mantle lithosphere and were not plume-derived sensu-strictu.

The Sr-Nd and Pb-Pb isotopic signatures obtained in both the studied alkalic rocks and the high-Ti basalts of the northern Paraná basin are presumed to have been generated through direct melting of, or extensive contamination by, an upper mantle lithosphere which had been chemically modified previously. The high abundances of REE reported earlier on in this thesis cannot possibly be explained by crystal fractionation or different degrees of partial melting. They are more easily explained as being due to enrichment prior to their emplacement. The lack of characteristic geochemical features of subduction-related magmas, such as relative depletions in high-field-strength elements (e.g. Nb, Ta), suggests that the mantle enrichment was unlikely to have been associated with fluids or melts derived from a downgoing slab to the west. Alternatively, if the enrichment was due to either veining or infiltration metasomatism caused by migration of relatively low-temperature small fraction melts from the asthenosphere, then the lower solidus of the enriched portions would represent preferential foci for melting. The extraction of incompatible elements during such melting should be very effective under such circumstances, and the incompatible element budget of the rocks discussed in previous chapters would have been dominated by the composition of the enriched lithospheric mantle source.

Gibson et al. (in press) have indicated that features such as the temporal and spatial association

of carbonatite bearing complexes, the isotopic similarity between carbonatitic and silicate melts in the southwestern São Francisco craton, the high Ca/Al ratios of the Mata da Corda and other volcanics in the area, and mineralogical evidence of high Co2/H2O conditions, would be compatible with carbonatite metasomatism. Compositional variations such as those reported in Chapter II, however, cannot readily be explained solely by carbonatite metasomatism. Rather, silicate melts involving the addition of major elements such as Si, Fe, Al, Ca and Ti and trace elements are also required. Gibson et al. (in press) also suggested that both carbonatite and silicate melts might have taken part in a multi-stage metasomatic process.

The evidence that isotope and trace element features of both the alkalic volcanics and the flood basalts were largely derived from the continental lithosphere might be reconciled with plume models if most of the plume-derived asthenospheric source material accumulated near the base of the lithosphere where the plume may have been horizontally deflected. This is comparable to fluid mechanical models which suggest that in continental settings most of the plume material may never reach the surface because of very low efficiency of magma extraction (e.g. Olson, 1990). The large ($\sim$2000 km) surface expression postulated for mantle plumes flattened against the lower lithosphere (Campbell & Griffiths, 1990) implies that magmatism and active rifting credited to these thermal anomalies are not necessarily confined to narrow linear belts. In fact, the surface expression of the plume might be "accommodated" by inhomogeneities of the overlying lithosphere and could be displaced from its rising system (Thompson & Gibson, 1991). In such a complex dynamic system, lithospheric rifting and deflection of the plume are initially two processes operating independent of each other. These two processes feed on and reinforce each other differently at different evolutionary stages and must include complex penetrative convection and magmatism (e.g. Dixon et al., 1989). It is advocated that zones of structural anisotropy developed during the Pan-Gondwana event might have acted as the controlling features during the early stages of magmatism, despite the influence of thermal plume anomalies. The distinctive distribution of rift structures and CFB provinces, therefore, are likely to have been controlled by crustal and upper mantle weaknesses.

The hypothesis that most of the magmatic activity in SE Brazil during the late Cretaceous (the

Mata da Corda and other volcanics included in this study) was induced by the impingement of the Trindade mantle plume (Gibson et al., in press) faces two main problems: first, the evidence for important volcanic activity at about 100 to 110 Ma, such as represented by the kimberlites examined in this study; secondly, the assumption that a non-Dupal hotspot is able to produce magmas with Dupal-type characteristics. Gibson's et al reliance onto emplacement ages to constrain plume tracks in southeastern Brazil might be considered misleading because, as discussed previously, the peaks of volcanic activity in SE Brazil coincided with the general large-scale plate reorganization during the advanced stages of opening of the South Atlantic, which included the rupture of the RGWR zone. The lack of isotopic correlation between the non-Dupal hotspot volcanics and the Dupal-type rocks documented earlier on in this study could possibly be rationalized in two ways: (i) the source of the Mata da Corda and other upper Cretaceous alkali volcanics in the southwestern São Francisco craton is the Dupal-type Tristan plume carbonate-rich material which had once been trapped under the crust and which was reactivated by the Trindade plume activity (Toyoda et al., 1994); and (ii) the EMI-like materials involved in the generation of the volcanics in this study, the northern high-Ti basalts of the Paraná basin and the Tristan da Cunha OIB were generated from a locally-derived enriched subcontinental lithospheric mantle source that was not available along the entire Trindade hotspot track.

Hawkesworth et al. (1986 and 1990) suggested that the Dupal signature in the South Atlantic may be of a shallow origin and that its evolution in the continental lithosphere involved thermal reactivation and detachment of metasomatized lithosphere from Southern Africa and South America. Should the suggestion (this work) that the characteristic $^{87}Sr/^{86}Sr$ of the EMI-like signatures of the alkalic volcanics represent time-integrated modifications of the local enriched lithosphere following tectonic overthickening at the end of the Brasiliano orogeny apply widely, then one would expect similar isotopic signatures at other craton margins subjected to similar tectonic processes. Indeed, Figure IV.9 shows that the Prieska kimberlites, which in terms of isotopic composition are the closest kimberlitic equivalents to the Brazilian kimberlites (Bizzi et al., in press; Clark et al., 1991; Skinner et al., 1993), also intrude an old cratonic margin (of the Kaapvaal craton) which was affected later by Proto to Meso-Proterozoic thin-skinned

tectonism. The east-African Carbonatites (Bell and Blenkinsop, 1987), that intrude the eastern margin of the Tanzanian craton which has similarly been affected by thin skinned tectonism during the Pan-African orogeny, have isotopic signatures also very similar to the LoNd line. The high $^{143}Nd/^{144}Nd$ & low $^{87}Sr/^{86}Sr$ North American lamproites also intrude overthickened craton margins which were tectonically extended and compressed in the Meso-Proterozoic (Mitchell and Bergmann, 1991). In addition, steep geotherms in marginal cratonic settings should favor CO_2-rich volatile influx and accumulation (Bailey, 1987; McKenzie, 1989; Sweeney et al., 1991). It is possible, therefore, that the similar $^{87}Sr/^{86}Sr$ ratios in kimberlitic and carbonatitic rocks in all these above mentioned marginally cratonic areas might reflect first order modifications to ancient upper mantle lithosphere imposed by Proterozoic convergent tectonic processes in peri-cratonic domains. These processes are manifested at surface by thin skinned tectonism. Tectonic remobilization with overthickening and CO_2 influx might thus be overriding factors in the development of $^{87}Sr/^{86}Sr$ signatures in primary melts intruded along craton margins. Densifying gabbro-eclogite-granulite phase transformations could eventually lead to density inversion and delamination, with consequent removal of EMI-like material into the surrounding convecting asthenosphere (e.g. Kay & Mahlburg Kay, 1991).

The possibility that portions of ancient Brazilian lithosphere were delaminated and subsequently entrained into a zone of South Atlantic asthenosphere with enriched material, has been suggested by several authors in the past (e.g. Mackenzie and O'Nions, 1983; Hawkesworth et al., 1986). Such a model is supported by the occurrence of enriched basalts and peridotites in the South Atlantic. Here it is suggested that delamination of continental lithosphere and its entrainment in the upper mantle circulation might also account for EMI-like occurrences in some localities as previously proposed by McKenzie and O'Nions (1983), and that the ultimate origin of the EMI-like signatures can be traced back to Proterozoic overthickened lithosphere along the margins of craton regions.

According to the above overthickening-delamination-contamination model, both Trindade and Tristan OIB signatures in the South Atlantic Ocean are viewed as mixtures between similar plume components and different proportions of delaminated EMI-like continental lithosphere.

Figure IV.9 - Tectonic elements of the São Francisco and Kaapvaal cratons at the same scale (from de Wit, Bizzi and Baars, 1991). Note that the Brazilian kimberlites and the transitional kimberlites have similar isotope characteristics and both intrude thin skinned terrains in marginally cratonic settings. It might not be a coincidence that the East African carbonatites (Bell and Blenkinsop, 1987), which intrude the eastern margin of the Tanzanian craton which has been affected by neo-Proterozoic thin skinned tectonism during the Pan-African orogeny, also have isotopic signatures very similar. The high $^{143}Nd/^{144}Nd$ low $^{87}Sr/^{86}Sr$ ratios observed in all those areas might reflect first-order modifications to ancient upper lithosphere imposed by thin skinned Proterozoic tectonic processes in peri-cratonic domains. The craton limits presented in this diagram are those published elsewhere (e.g. de Wit et al., 1992; Almeida, 1977; Almeida et. al, 1981). The location of terrain boundaries derives from the work by Franciscus Baars (PhD thesis in preparation) and the characterization of each tectonic zone, as well as the principles/concepts used will be discussed in his thesis.

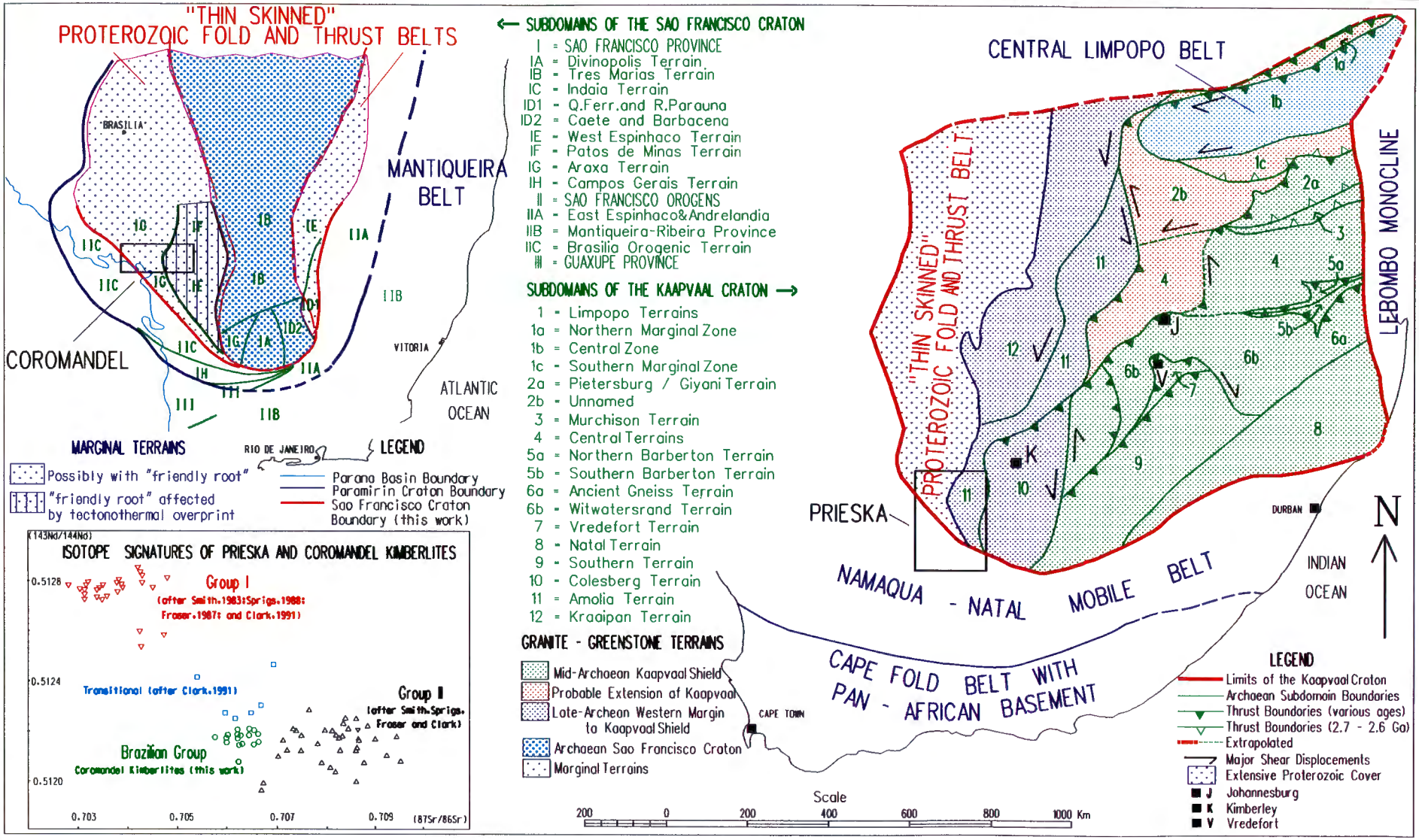

Tectonic Terrains of the Kaapvaal and Sao Francisco Cratons Compared at the Same Scale

/usr5/luiz/luiz7.dgn Feb. 15, 1993 12:31:52

The Trindade Island would represent near pristine plume-related components exposed to very little contamination, whereas some of the basalts collected along the Walvis Ridge would represent extensive contamination by a EMI component, the location of which is uncertain. It is unlikely, however, that the delamination process alone can explain the Dupal anomaly of the southern Atlantic and Indian oceans since such anomaly does not occur in other regions with similar tectonic histories (e.g. the North Atlantic and the West Indian oceans).

Because both the studied rocks and the CFB's from northern Paraná Basin preserve isotope and trace element ratios similar to those in oceanic basalts with the Dupal signature in the South Atlantic, it may be that in some areas the Dupal anomaly marks a mixing of old enriched continental lithosphere and comparatively deep-level melts.

IV.6 - CONCLUDING REMARKS

The Paleozoic and Mesozoic depositional sequences of southwestern Gondwana record two first-order tectonic inversions related to the "fusion and fission" history of Gondawana: (i) the Pan-Gondwanean convergence circa 750-650 Ma, followed by (ii) the late Proterozoic to early Paleozoic extension circa 600-500 Ma, and (iii) the late Paleozoic convergence circa 300-250 Ma, followed by (iv) the mid to late Mesozoic extension circa 200-150 Ma (various references mentioned in the text). Long-lived structural discontinuities formed and acted as both transtensional and transpressional fault systems during these inversions. These structures controlled not only the formation and evolution of sedimentary basins, but also linear trends of magmatic intrusions.

The studied rocks, together with the northern Paraná basalts, provide further evidence that discrete large-scale geochemical domains existed in a southern Gondwana framework. The scale length over which isotopic heterogeneities exist range from mineralogical (centimeter) scale, to mantle dimensions (200 km). From this work it appears that those domains were not necessarily solely related to ancient lithospheric chemical domains or delineated by ancient structural

features, but rather that they reflex mixing processes that can be ascribed to specific geodynamic mechanisms. Conception of such mechanisms, however, is dependent on three-dimensional modeling; and inferring three-dimensional domain sizes of mantle heterogeneities based on proven two dimensional heterogeneities is a very complex task. One major ambiguity is related to the fact that there is very poor control on the depth of origin of "basaltic" magmas. Based on phase equilibria and trace element patterns, MORB and CFB melts are believed to segregate at pressures of 10-25 kb, whereas alkali basalts and kimberlites segregate at pressures greater than 25 kb. In most cases, however, the uncertainty in segregation depth estimates is at least 12 kb (e.g. Sweeney et al., 1991). Moreover, basalt melting presumably occurs in response to adiabatic decompression within rising diapirs of mantle material. Even if the depth of magma segregation could be precisely determined, this does not equate the depth of the diapir origin. In addition, if the uprising plumes or blobs undergo any solid-state mixing during their ascent, the final basaltic melt product will merely represent an average of vertical sections of mantle.

Alkaline magmatism along the southwestern Sao Francisco craton was contemporaneous with changes in the direction of plate movements. Such plate vector changes induced reactivation of lithospheric shear zones and rifting within plates. Because of reactivation along the N-S megashear zones in the Brasiliano and Pan-African domains, the associated oblique sets of transcurrent faults during the Neo Proterozoic and Late Paleozoic, originally under compression, opened and propagated as tensional faults during the Mesozoic, allowing for fracturing through the continental lithosphere. Presumably, in places where the pressure release, the channeling of volatiles and the partial melting at lithospheric levels were coincident with zones of hot asthenospheric upwelling, larger volumes of magma were generated.

Seen in the regional framework of Gondwana break-up, the alkaline volcanism activity along the southwestern São Francisco craton margin is part of the evidence that deep-derived, possibly long-lived, mantle plumes were active and that regional-scale crustal failure occurred in the heart-land of South America at the onset of Gondwana disintegration. The inferred interaction between asthenospheric mantle plumes and enriched lithospheric materials during the generation of the Minas Gerais kimberlites, and the geochemical similarities of those rocks to the northern

HTZ Paraná basalts, support the close relationship of "enriched" basalts to mantle plumes proposed elsewhere (Erlank et al., 1990; Ellam and Cox, 1991; Hawkesworth et al., 1992).

Mantle plumes and subduction processes have interacted in close association to drive the above mentioned first-order tectonic inversions. The location of the Atlantic-Africa Geoid high and long wavelength bathimetric anomalies, and the distribution of hot spots, all seem to be related to the pre-Mesozoic continent configuration and to subduction zones that formerly encircled southwestern Gondwana and which since evolved to the present circum-Pacific subduction system (Richards & Engebretson, 1992; and references therein). These features have been proposed to represent either thermal coupling of subducted slabs (Chase & Sprowl, 1983) or long term insulating effects of a stationary supercontinent (Anderson, 1982); both of which could have induced convective upper mantle upwelling and horizontal temperature gradients, the ultimate driving mechanisms for continental drift. The postulated increased outer-core convective activity in the mid-Cretaceous (Larson, 1991) would only add to the dynamic feedback between the motions of continental plates and mantle convection predicted in these models.

Today's position of the continents relative to the large scale pattern of mantle convection indicates that South America moved away from the regions of hotter mantle upwelling towards regions of cooler mantle downwelling (Figure 1 in Richards & Engebretson, 1992). The present distribution of buoyancy forces associated with lateral heterogeneity of mantle density revealed through seismic tomography is in good agreement with locations of surface ridges and trenches (Peltier et al., 1989). Significantly, the latitudinal redistribution of continents and excess masses associated with the geoid highs are also influenced by their tendency to stabilize in the equatorial plane to conserve angular momentum. That may foster a situation in which the Dupal and several geophysical anomalies dominated by low-degree harmonics with equatorial placement (Hart, 1988; Peltier et al., 1989; and references therein) formed in response to long-term low-degree general mantle upwelling being induced into the equatorial plane in order to attain global thermal and rotational stability.

Chapter V

Summary and conclusions

- The São Francisco craton (Almeida, 1977) is a mid- to late-Archean granite-gneiss and granite-greenstone terrain. Its southern boundary is marked by a steep, seismically active, strike-slip fault system, whilst its western margin is overprinted by Brasiliano-age (0.5 to 0.8 Ga) tectonism and is peripherally overlain by a "thin skinned" fold and thrust belt of allochtonous and para-allochtonous units. The thin skinned fold and thrust belt (the Brasília Belt) is coupled to an external Neo-Proterozoic orogenic zone (the Uruaçú belt) of metasediments, orthogneisses, metavolcanic and metaplutonic assemblages of various ages.

- New Sm-Nd and Rb-Sr data from a collection of crustal samples from the Congonhas do Campo area in the southern São Francisco craton yield 3194 Ma and 3224 Ma ages, respectively. These ages, supported by widespread 3.2 Ga old zircons in the area, probably indicate a significant episode of crustal generation, and extraction of rocks of the Rio das Velhas Supergroup from a light-REE depleted source at this time. Basement and juvenile granitoids yield a 2128 Ma Rb-Sr age, which is supported by 2124 Ma old zircons recovered from the same sample locality. These younger ages are representative of the emplacement of large syntectonic tonalitic batholiths.

- Brasiliano-age granitoids and metabasalts of the Araxá Group, which occur in the far western orogenic portion of the Brasília belt, define a 711 Ma Rb-Sr age which is interpreted as a Sr-isotope re-homogenization event during the development of the Brasiliano orogenic zone and its foreland fold and thrust belts. A 823 Ma Sm-Nd age indicates that these rocks may be coeval to the Araxá felsic volcanism which has been dated using U/Pb at 794 Ma by Pimentel et al. (1991). The isotopic characteristics of this group of rocks indicate their derivation was dominated by remelting of pre-existing Proterozoic crustal

material. The overall isotope characteristics are consistent with a model which requires that large volumes of crust, derived in the Neo-Proterozoic from mantle reservoirs similar to the sources for modern oceanic basalts, were accreted onto the pre-existing Archean nucleus during the Brasiliano orogenic event.

- The Niquelândia complex represents basement windows of deep crustal layered mafic-ultramafic sequences which protrude through the tectonic cover of the Paranoá Group in the Goiás Massif domain. Samples from this complex yield a 1262 Ma Rb-Sr isochron. This age is similar to the 1266 Ma age attributed to the high-grade metamorphism of the complex (Fuck et al., 1988). The $^{87}Sr/^{86}Sr$ initial ratio indicates that the protolith might have been incorporated into the crust long before the rehomogeneization event.

- Eight of the freshest occurrences of alkaline magmatic activity along the southwestern margins of the São Francisco craton have been described in terms of their age and mode of emplacement, petrography and whole-rock geochemistry. The petrography and mineralogy of the kimberlites in this area are similar to those of Group I kimberlites elsewhere in the world. Both ilmenite-rich and ilmenite-poor varieties occur. Their bulk chemical compositions are typical of primary liquids derived from garnet peridotites. It is suggested that the overall chemical characteristics of the kimberlites and kimberlite-related magmas resulted from entrainment of enriched lithosphere in plume-derived small-volume melts.

- The kinship between the kimberlites and the shallower alkalic rocks in the western Minas Gerais area has been characterized using whole rock isotope geochemistry. Rocks with "transitional" petrographic characteristics have also been identified. Major and trace elements of the alkalic rocks change systematically with petrographic character towards more evolved compositions, approximating liquid evolution paths produced by shallow-level, olivine-dominated crystal fractionation. A restricted range of isotopic signatures, and the absence of any correlation between $^{87}Sr/^{86}Sr$ and 1/Sr, suggest that the shallower alkalic rocks were probably derived by melting of a light-REE enriched lithospheric mantle source rather than through crustal contamination of asthenospheric melts.

- The studied rocks display Dupal characteristics and have a relatively restricted range of isotopic compositions with an average of $^{143}Nd/^{144}Nd_i = 0.5122$ and $^{87}Sr/^{86}Sr_i = 0.7046$. Pb isotope signatures range for $^{206}Pb/^{204}Pb_i$ from 17.44 to 18.41; for $^{207}Pb/^{204}Pb_i$ from 15.44 to 15.61; and for $^{238}U/^{204}Pb$ from 10.18 to 144.73. The kimberlites in this study are the first documented examples with such Sr-Nd isotopic signatures. This new group of kimberlites, here designated the "Brazilian Group", has a source character which is similar to that of carbonatites and other evolved alkalic volcanics in the area but is dissimilar to that of kimberlites elsewhere in the world. Considering their similar isotopic compositions, it is suggested that the source of the studied occurrences, the source of the high-Ti basalts of the northern Paraná Basin, and the source of some OIB (Ocean Island Basalts) with Dupal signatures in the South Atlantic (viz. the Walvis Ridge basalts) are closely related. The derivation of these rocks involved partial melting of a relatively homogeneous enriched mantle lithosphere.

- Available emplacement ages indicate that alkaline magmatic activity along the southwestern margins of the São Francisco craton range from ~120 Ma (related to the Paraná volcanism) to ~80 Ma (related to the Mata da Corda volcanism). The emplacement ages available for kimberlites and kimberlite-related intrusives in the area seem to concentrate in the time bracket 110 Ma to 95 Ma.

- Systematic isotopic variations accompany progressive vertical shift in the zone of melting, and isotopic characteristics are controlled by source depth. Isotope characteristics of alkalic magma types which equilibrated within the upper portions (<100 Km) of the local lithospheric mantle, represent the best candidates to date for the Enriched Mantle I (EMI) component. Kimberlites and kimberlite-related magmas equilibrated within the lower portions of the local mantle lithosphere (120-250 Km), resulted in entrainment of the EMI-like lithosphere by plume-derived small-volume melts. The source of kimberlites and kimberlite-related magmas had lower time-averaged Rb/Sr, Nd/Sm and Pb/U ratios which might be related to input of small but significant quantities of a HIMU-like component. The range of Platinum Group Element (PGE) characteristics of the kimberlites and shallower

alkalic rocks was successfully modelled as a process of contamination with a PGE-rich component and mirrors the range of isotopic signatures which is believed to represent mixing of two mantle reservoirs (i.e. the sources for the EMI-like and the HIMU-like components).

- The Nd isotopes characteristics of the EMI-like component in the source of the Mesozoic volcanics are compatible with an origin closely related to the evolution of the Neo-Proterozoic rocks of the Tocantins Province. Lower ϵ_{Nd} values, which would be expected if large amounts of pristine Archean enriched mantle lithosphere were available at the source region, have not been found. Also, the homogeneous character of the source for the alkalic magmas indicate a pervasive enrichment event might have affected the entire cratonic margin area. The lower $^{87}Sr/^{86}Sr$ of the Mesozoic volcanics compared to other enriched mantle derived rocks could be related either to (i) subduction of pelitic sediments in a juvenile Neo-Proterozoic arc environment or to (ii) time-integrated Rb depletion at lower crust/upper mantle levels attained during densifying gabbro-eclogite-granulite phase transformations (which could have been accompanied by CO_2 metasomatism) following tectonic overthickening at the end of the Neo-Proterozoic Brasiliano orogeny.

- The Paleozoic and Mesozoic depositional sequences in southwestern Gondwana record two first-order tectonic inversions related to the formation and breakup of Gondawana. Two successive compressional and extensional episodes have been documented viz. (i) Pan-Gondwanean convergence circa 750-650 Ma, followed by (ii) late Proterozoic to early Paleozoic extension circa 600-500 Ma, and (iii) late Paleozoic convergence circa 300-250 Ma, followed by (iv) mid to late Mesozoic extension circa 200-150 Ma.

- Mantle plumes have played an important role in the initial opening of the South Atlantic, but the broad regional tectonic evolution was highly influenced by the geometry of the Proterozoic and Paleozoic orogenic zones. Dextral movement along the Agulhas-Falklands/Malvinas transform zone accompanied the Crozet/ Marion plume-induced magmatism of the Karoo Province. Subsequently, rapid northward propagation of rifting into

the region above the heads of the Tristan, Trindade and St Helena plumes induced magmatism in the Paraná-Etendeka province. Opening in the Central Atlantic region was linked to movement along the transform zone west of the Cameroon (the Equatorial Fracture Zone) and the Fernando de Noronha plume.

- Late-Mesozoic Gondwana break-up related magmatism involved melts derived from both the crust (rhyolite ash-flows and related potassic granites) and the upper-mantle (kimberlites, alkaline complexes, flood basalts and related dike swarms). The compositional and isotopic characteristics of basaltic volcanism that occurred shortly before the opening of the new ocean basins are explained by plume models, but how the lithospheric and asthenospheric materials were remobilized during the melting process remains controversial.

- In the southwestern Sao Francisco craton hotspot activity was probably a catalyst to kimberlitic and kimberlite-related activity, providing the triggering mechanism for diapiric processes of magma generation in the asthenosphere. Structural geology analysis and the overall plate-tectonic setting, however, suggests that within-plate stress fields and fault reactivation ultimately control the sites of alkaline magmatism in the continental lithosphere. Alkaline magmatism along the southwestern Sao Francisco craton margin was contemporaneous with changes in plate vectors which possibly induced reactivation of lithospheric shear zones and rifting within plates. Because of reactivation along N-S megashear zones in the Brasiliano and Pan-African domains, associated oblique sets of transcurrent faults opened and propagated as tensional faults, allowing for fracturing through the continental lithosphere, pressure release, channeling of volatiles and partial melting such as along the Mata da Corda rift in western Minas Gerais.

- The alkaline volcanics emplaced along the southwestern margin of the São Francisco craton and the northern Paraná basalts provide further evidence that discrete large-scale geochemical domains existed in southern Gondwana. It is suggested that these domains were not necessarily related to ancient lithospheric chemical heterogeneities or bound by ancient structural features, but rather to mixing processes that can be ascribed to specific

geodynamic mechanisms in the upper mantle.

- It is argued that the composition of the Walvis Ridge basalts are mixtures of delaminated enriched lithosphere and typical "normal" oceanic compositional sources lying within the oceanic mantle array. The isotopic similarity between such OIB and the Brazilian alkaline volcanics in this study may indicate that the sub-continental mantle lithosphere underlying the SW margin of the São Francisco craton provided materials which were incorporated into the OIB-type oceanic magmas possibly through delamination processes. Thus, similarly to Hawkesworth et al. (1986), I propose that large portions of ancient Brazilian lithosphere which had been overthickened at the end of the Brasiliano tectonothermal event delaminated and contaminated a belt of South Atlantic asthenosphere which is still erupting at hot spot islands in the central South Atlantic (e.g. Tristan da Cunha).

- During the Gondwana breakup, magmatism was more prevalent at the junction between cratonic blocks and mobile-belts or in zones of major crustal weakness within cratonic blocks (e.g. in the Nuanetsi-northern Lebombo area of South Africa), indicating that both heat and deep-derived fluids were diverted from old cratonic areas towards anisotropic thinner lithospheric domains. The present distribution of buoyancy forces associated with lateral heterogeneity of mantle density revealed through seismic tomography is in good agreement with locations of surface ridges and trenches, suggesting a dynamic feedback between convective upper mantle upwelling, horizontal temperature gradients and continental drift.

References

Allegre C.J. (1982). Chemical geodynamics. Tectonophysics 81, 109-132.

Allegre C.J., Dupré B., Sobolev A.V. and Kogarko L.N. (1987). The Asian province in OIB cartography. EOS 68, 1445.

Almeida F.F.M. de (1977). O craton do São Francisco. Rev. Bras. Geociências, 7, 394-364.

Almeida F.F.M. de (1983). Relações tectônicas das rochas alcalinas Mesozoicas da região meridional da Plataforma Sul Americana. Rev. Bras. Geociências 13(3) 139-158.

Almeida F.F.M. de (1986) Distribuição regional e relações tectônicas do magmatismo pós-Paleozoico no Brasil. Rev. Bras. Geociencias, 16, 325-349.

Almeida F.F.M. de, Hasui Y., Neves B.B.B. and Fuck R.A. (1981). Brazilian structural provinces: an introduction. Earth Sci. Rev. 17, 1-29.

Almeida F.F.M. de and Svisero D.P. (1991). Structural setting and tectonic control of kimberlite and associated rocks of Brazil. In: Fifth International Kimberlite Conference. CPRM Spec. Publ. 2/91. Ext. Abstr. 3-5.

Anderson D.L. (1982). Hotspots, polar wander, Mesozoic convection and the geoid. Nature 297, 391-393.

Araújo S.M. and Nilson A.A. (1987). Caracterização petroquímica e petrotectônica dos anfibolitos da sequência vulcano sedimentar de Palmeirópolis, GO. I Congr. Bras. Geoquim. Porto Alegre, 1, 335-348.

Arndt N.T. and Christensen U. (1992). The role of lithospheric mantle in continental flood volcanism: thermal and geochemical constraints. Jour. Geophys. Res. 97, 10967-10981.

Asmus H.E. (1981). Geologia das bacias marginais Atlânticas Meso-sedimentarias del Jurasico y Cretácico de America del Sur. Comite SudAmericano del Jurasico y Cretacico 1, 127-155.

Asmus H.E. and Baisch P.R. (1983). Geological evolution of the Brazilian continental margin. Episodes 4, 3-9.

Austin J.A. and Uchupi E. (1982). Continental-oceanic crustal transition off southwest Africa. American Association of Petroleum Geologists. Bulletin 66, 1328-1347.

Babinski M., Chemale Jr. F. and Van Schmus W.R. (1991). Geocronologia Pb/Pb em rochas carbonáticas do Supergrupo Minas, Quadrilátero Ferrífero, Minas Gerais, Brasil. ÍÍÍ Congr. Bras. Geoquim. São Paulo, Brazil. Resumos 628-631.

Bacuta G., Kay R.W. and Gibbs A.K. (1988). Platinum-group element (PGE) geochemistry in chromite deposits of the Acoje Ophiolite block, Zambales Ophiolite Complex. Philippines. V.M.Goldsmith Conference, Baltimore, USA.

Baeker M.L. (1983). A mineralização de Nióbio no solo residual laterítico e a petrografia das rochas ultramáficas-alcalinas do domo de Catalão I, Goiás. Unpublished MSc thesis, Universidade de Brasília.

Bailey D.K. (1987). Mantle metasomatism, perspective and prospect. In: Fitton J.G & Upton B.G.J. (Eds). Alkaline igneous Rocks, 15-27.

Barbosa O., Svisero D.P., and Hasui Y. (1976). Kimberlitos na região do Alto Paranaíba, Minas Gerais. (Abstr.). 29 Congr. Bras. Geologia, Ouro Preto, Brazil, 323.

Bardet M.G. (1977). Geologie du Diamant. Troisieme parte: Gisements de diamants d'Asia, D'Amerique, d'Europe et d'Australasie. Bureau des Recherches Geologiques et Miniéres. Memoir 83, 169.

Bell K. and Blenkinsop J. (1987). Archean depleted mantle - evidence from Nd and Sr initial isotopic ratios of carbonatites. Geochimica and Cosmochimica Acta 51, 291-298.

Bellieni G., Comin-Chiaramonti P., Marques L.S., Melfi A.J., Nardy A.J.R., Piccirillo E.M. and Roisenberg A. (1984). High- and low-TiO_2 flood basalts from the Paraná Plateau (Brazil): petrology and geochemical aspects bearing on their mantle origin. Neues Jahr. Miner. Abh. 150, 273.

Ben-Avraham Z., Hartnady C.J.H. and Malan J.A. (1993) Early tectonic extension between the Agulhas Bank and the Falkland Plateau due to the rotation of the Lafonia microplate. Earth Planet. Sci. Letters 117, pp.43-58.

Benkhelil et al (1988). Benue through and Benue chain. Geol. Mag. 119, 155-168.

Bennet V.C. and DePaolo D.J. (1987). Proterozoic crustal history of the western United States as determined by neodymium isotope mapping. Bull. Geol. Soc. Am. 99, 674-685.

Bianucci H.A. and Homovc J.F. (1982). Tectogénesis de un sector de la cuenca del subgrupo Pirgua, Noroeste Argentino. 5 Congr. Lat. Americ. Geologia, Actas 1, 539-546.

Bizzi L.A. (1989). The geological setting of the asthenospheric diamonds in Aripuana, southwestern Guaporé Shield, Brazil. Ext. Abstr. Senior Geologists Conference in Maccauvlei by De Beers.

Bizzi L.A., Smith C.B., Meyer H.O.A. and de Wit M.J. (1990). Geology and source character of Mesozoic kimberlites and alkalic rocks in western Minas Gerais, Brazil (abstr.). International

volcanological congress - IAVCEI, Mainz.

Bizzi L.A.; Smith C.B.; de Wit M.J.; Armstrong R.A. and Meyer H.O.A. (1991). Mesozoic kimberlites and related alkalic rocks in south western Sao Francisco craton: a case for local mantle reservoirs and their interaction (Ext. Abstract). In: Abstract Volume of the 5th International Kimberlite Conference.

Bizzi L.A.; Smith C.B.; de Wit M.J.; Armstrong R.A. and Meyer H.O.A. (1993). Mesozoic kimberlites and related alkalic rocks in south western Sao Francisco craton: a case for local mantle reservoirs and their interaction. In: Proceedings of the 5th International Kimberlite Conference.

Bizzi L.A.; de Wit M.J. and Smith C.B. (in press). Isotope composition of the subcontinental lithosphere underlying the SW São Francisco craton margin, Brazil: clues to the origin of EMI-type enriched mantle reservoirs. In: Proceedings of the 6th International Kimberlite Conference (submitted).

Black, R. (1984). The Pan African event in the geological framework of Africa. Pangea, 2, 6-16.

Bond G.C., Nickeson P.A. and Kominz M.A. (1984). Break-up of a supercontinent between 625 and 555 Ma: new evidence and implications for continental histories. Earth Planet. Sci. Lett. 70, 325-345.

Bowles J.F.W. (1986). The development of platinum-group minerals in laterites. Econ. Geol. 81, 1278-1285.

Bristow J.W. (1984). Picritic rocks of the north Lebombo and south-east Zimbabwe. In: Erlank A.J. (Ed) Petrogenesis of the volcanic rocks of the Karoo Province. Spec. Publ. Geol. Soc. South Africa. 13, 105-123.

Bristow J.W. and Saggerson E.P. (1983). A general account of Karoo volcanicity in Southern Africa. Geol. Rundsch. 72, 1015-1060.

Brito Neves B.B., Fuck R.A., Cordani U.G. and Tomaz Filhº (1984). Influence of basement structures on the evolution of the major sedimentary basins of Brazil: a case of tectonic heritage. Journal of Geodynamics, 1, 495-510.

Brito Neves B.B. and Cordani U.G. (1991). Tectonic evolution of South America during the late Proterozoic. Precambrian Research, 53, 23-40.

Cahen L., Snelling N.J., Delhal J., Vail V.R., Bonhomme M., and Ledent D. (1984). The geochronology and evolution of Africa. Book volume. Claredon Press, Oxford, UK.

Campbell I.H. and Griffiths R.W. (1990). Implications of mantle plume structure for the evolution of flood basalts. Earth Planet. Sci. Lett. 99, 79-93.

Campos L.F.G (1891). Jazidas diamantíferas de Água Suja (Bagagem), estado de Minas Gerais. Editora Fluminense, Rio de Janeiro, 52. Not seen; extracted from Leonardos et al. (1991) The Mata da Corda volcanic rocks. Field guide book for the 5th Int. Kimb. Confer., 65-73.

Carter S.R., Evensen N.M., Hamilton P.J. and Onions R.K. (1978). Neodymium and strontium isotope evidence for crustal contamination of continental volcanics. Science 202, 743-747.

Chang K.H. (1975). Concepts and terms of uniformity-bounded units as formal stratigraphic units of distinct category. Geol. Soc. of America. Bull. 86, 1544-1552.

Chase C.G. and Sprowl D.R. (1983). The modern Geoid and ancient plate boundaries. Earth Planet. Sci. Lett. 62, 314-320.

Chauvel C., Hoffman A.W. and Vidal P. (1992). HIMU-EM: the French Polynesian connection.

Earth Planet. Sci. Lett. 110, 99-119.

Clark T.C., Smith C.B., Bristow J.W., Skinner E.M.W. and Viljoen K.S. (1991). Isotopic and geochemical variations in kimberlites from the south western craton margin, Prieska area, South Africa. Fifth International Kimberlite Conference, Ext. Abstr. Volume, 46-48.

Clement R. (1982). A comparative geological study of some major kimberlite pipes in the northern Cape and Orange Free State. PhD thesis (unpublished), Univ. of Cape Town.

Colgan E.A., Clark T.C., Bristow J..W. and Allsopp H.L. (1989). Geological setting, petrography and petrogenesis of olivine melilitites of the Natal coast, South Africa. In: Kimberlites and related rocks: their composition, occurrence and emplacement. Geol. Soc. of Australia Spec. Publ. 14. Book volume 1, 417-435.

Comin-Chiaramonti P., Civeta L., Petrini R., Piccirillo E.M., Bellieni G. Censi P., Bitschene P., Demarchi G., de Min A., Gomes C.B., Castillo A.M. and Velazquez J.C. (1991). Tertiary nephelinitic magmatism in eastern Paraguay: petrology, Sr-Nd isotopes and genetic relationships with associated spinel-peridotite xenoliths. Eur. J. Mineral. 3, 507-525.

Cordani U.G., Civetta L., Mantovani M.S., Petrini R., Kawashita K., Hawkesworth C.J., Taylor P., Longinneli A., Cavazzini G. and Piccirillo E.M. (1988). Isotope geochemistry of flood volcanics from the Paraná Basin, Brazil. In: Piccirillo E.M. and Melfi A.J. (Eds), The Mesozoic flood volcanism of the Paraná Basin: petrogenesis and geophysical aspects. Book volume, Instituto Astronômico e Geofísico USP publishers, 157-178.

Cordani U.G., Teixeira W., Tassinary C.C.G., Kawashita K. and Sato K. (1988). The growth of the Brazilian Shield. Episodes 11, 163-167.

Cordani U.G., de Brito Neves B.B., Fuck R.A., Porto R., Thomaz Filho A. and Cunha F.M.B. (1984). Estudo preliminar de integracao do Precambriano com os eventos tectonicos das bacias

Daly M.C., Lawrence S.R., Kimuna D. and Binga M. (1991). Late Paleozoic deformation in Central Africa: a result of distant collision? Nature 350, 109-117.

Dalziel I.W.D and Forsythe R.D. (1985). Andean evolution and the terrane concept. In: D.G.Dowel (Ed) Tectonostratigraphic terranes of the Circun Pacific Region. Book volume, Circun Pacific Council Energy and Mineral Resources, Houston. Earth Sciences Series 1, 565-581.

Danni J.C.M., Fuck R.A. and Leonardos Jr. O.H. (1982). Archean and lower Proterozoic units in central Brazil. Geol. Rundsch., 71, 291-317.

Danni J.C.M., Gaspar J.C., and Gonzaga G.M. (1991). The Fazenda Alagoinha intrusion, Três Ranchos, Goiás. Fifth International Kimberlite Conference, field guide book, 31-35.

Danni J.C.M. and Kuijmjian R.M. (1984). A origem dos anfibolitos basais na sequência vulcano-sedimentar de Juscelândia, Goiás. 33 Congr. Bras. Geol. SBG, 9, 4126-4136.

Davies G. and Tredoux M. (1985). The platinum-group element and gold contents of the marginal rocks and sills of the Bushveld complex. Econ Geol. 80, 838-848.

Dawson J.B. (1980). Kimberlites an their xenoliths. Book volume, Springer, New York.

Dawson J.B. (1989). Geographic an time distribution of Kimberlites and Lamproites: relationships to tectonic processes. In: Ross J. et al. (Eds) Kimberlites and Related Rocks, Vol. I: Their composition, occurrence, origin an emplacement. Book volume, Geol. Soc. Australia & Blackwell Scientific Publ. GSA Spec. Publ. 14, 324-342.

Delhal J. and Demaiffe D. (1985). U-Pb Archean geochronology of the São Francisco craton (eastern Brazil). Rev. Bras. Geoc. 15 (1) 55-60.

DePaolo D.J. (1981). A neodymium and strontium isotopic study of the Mesozoic calc-alkaline granitic batholiths of the Sierra Nevada and Peninsular Range, California. J. Geophys. Res. 86, 10470-10488.

DePaolo D.J. (1981). Neodymium isotopes in the Colorado front range and crust-mantle evolution in the Proterozoic. Nature 291, 493-196.

DePaolo D.J. (1988). Neodymium isotope geochemistry, an introduction. Book volume, Springer Verlag.

de Wit M.J. (1990). Gondwana research: new break-through old supercontinent. South African Jour. Sci. 86, 479-483.

de Wit, M.J., Jeffery, M., Bergh, H., and Nicolaysen, L. (1988). Geological map of sectors of Gondwana reconstructed to their disposition 150 Ma. Publ. American Association of Petroleum Geologists.

de Wit M.J., Stern C.R. (1981). Variations in the degree of crustal extension during formation of a back-arc basin: Tectonophysics 72,229-260.

de Wit M.J., Ransome I.G.D. (1992). Regional inversion tectonics along the southern margin of Gondwana. In: de Wit M.J. and Ransome I.G.D. (Eds) Inversion Tectonics of the Cape Fold Belt, Karoo and Cretaceous basins of Southern Africa, 15-22.

de Wit M.J., Ransome I.G.D. (1992). Inversion Tectonics of the Cape Fold Belt, Karoo and cretaceous basins of Southern Africa. Book Volume. Balkema, Rotterdam.

de Wit M.J., Roering C., Hart R.J., Armstrong R.A., de Ronde C.E.J., Green R.W.E., Tredoux M., Peterby E. and Hart R.A. (1992). The formation of an Archean Continent. Nature 357, 553-562.

Dingle R.V., Siesser W.G. and Newton A.R. (1983). Mesozoic and Tertiary geology of Southern Africa. Book volume, Balkena, Rotterdam.

Dixon T.H., Ivins, E.R. and Franklin, B.J. (1989). Topographic and volcanic asymmetry around the red sea: constraints on rift models. Tectonics. 8, 1193-1216.

Dossin I.A., Chaves M.L.S.C. Uhlein A. and Alvarenga C.J. de S. (1985). Geologia e depositos diamantíferos da região de Sopa-Diamantina, MG. Geologia de Minas Gerais, Symposium, 3rd, 276-289.

Duane M.J. and de Wit M.J. (1988). Pb-Zn ore deposits of the northern Caledonides: products of continental-scale fluid mixing and tectonic expulsion during continental collision. Geology, 16, 999-1002.

Duncan A.R., Erlank A.J., Marsh J.S. and Armstrong R.A. (1990). MORB-related dolerites associated with the Etendeka volcanics, Northwestern Namibia. 23rd Earth Sci. Congr. Geol. Soc. South Africa, Cape Town, 143-146.

Duncan A.R., Marsh J.S., Erlank A.J. and Milner S.C. (1990). Geochemistry and petrogenesis of the basaltic rocks of the Etendeka Formation, NW Namibia. 23rd Earth Sci. Congr. Geol. Soc. South Africa, Cape Town, 139-142.

Duncan R.A. and Richards M.A. (1991). Hot spots, mantle plumes, flood basalts and true polar wander. Rev. Geophys. 29, 31-50.

du Toit, A. (1937). Our Wondering continents. Oliver and Boyd, Edinburgh. Not seen; extracted from de Wit, M.J. et al. (1988). Geological map of sectors of Gondwana reconstructed to their disposition 150 Ma. Publ. American Association of Petroleum Geologists.

Eggler D.H. (1989). Kimberlites, how do they form? In: Kimberlites and related rocks: their

composition, occurrence, origin and emplacement. Ross J.(Ed) Spec. Publ. Geol. Soc. Australia number 14, Blakwell, vol. 1, 489-504.

Ellam R.M., Carlson R.W. and Shirey S.B. (1992). Evidence from Re-Os isotopes for plume-lithosphere mixing in Karoo flood basalt genesis. Nature 359, 718-721.

Ellam R.M. and Cox K.G. (1991). An interpretation of Karoo picrite basalts in terms of interaction between asthenospheric magmas and the mantle lithosphere. Earth Planet. Sci. Lett. 105, 330-342.

Emeri K.O. and Uchupi E. (1984). The geology of the Atlantic Ocean. Book volume, Springer Verlag, Munich.

Erlank A.J. (1984). Petrogenesis of the volcanic rocks of the Karoo Province. Book volume, Spec. Publ. Geol. Soc. South Africa.

Erlank A.J., Allsop H.L. Duncan A.R. and Bristow J.W. (1980). Mantle heterogeneity beneath Southern Africa: evidence from the volcanic record. Philos. Trans. Royal Soc. London, 295-307.

Erlank A.J., Marsh J.S., Duncan A.R., Miller R.McG., Hawkesworth C.J., Betton P.J. and Rex D.C. (1984). In: Erlank A.J. (Ed) Petrogenesis of the volcanic rocks of the Karoo Province. Spec. Publ. Geol. Soc. South Africa. 13, 195-245.

Erlank A.J., Duncan A.R., Marsh J.S., Sweeney R.J.,Hawkesworth C.J., Milner S.C., Miller R.M. and Rogers N.W. (1988). A laterally extensive geochemical discontinuity in the sub-continental Gondwana lithosphere. Ext. Abstr. Int. Conf. Geochem. Evol. Continental crust. Poços e Caldas, Brazil, 1-10.

Erlank A.J., Duncan A.R., Sweeney R.J. Milner S.C., Marsh J.S., Hawkesworth C.J., Rogers

N.W. and Miller R.M. (1989). Is there a laterally extensive geochemical boundary in the Mesozoic basalts of Southern Gondwanaland? 28th Int. Geol. Congress, Washington DC. (Abstr.), 1, 458-459.

Erlank A.J., Duncan A.R., Marsh J.S., Sweeney R.J. Milner S.C., Hawkesworth C.J., Miller R.M. and Rogers N.W. (1990). Distribution of Mesozoic Karoo basalts from Southern Africa. 23rd Earth Sci. Congr. Geol. Soc. South Africa (Abstr.), 754-757.

Farmer G.I and DePaolo D.J. (1983). Origin of Mesozoic and Tertiary granites in the western U.S. and implications for pre-Mesozoic crustal structure. 1. Nd and Sr isotopic studies in the geocline of the northern Great Basin. Journal Geophys. Research, 88, 3379-3401.

Farmer G.I. and DePaolo D.J. (1984). Origin of Mesozoic and Tertiary granites in the western US and implications for pre-Mesozoic crustal structure. 2. Nd and Sr isotopic studies of unmineralized and Cu- and Mo-mineralized granites in the Precambrian craton. Journal Geophys. Research, 89, 10141-10160.

Faure G. (1986) Principles of Isotope Geology. Book Volume. John Wiley & Sons Inc.

Ferguson A.K. and Jacques A.L. (1984). Structural controls of kimberlite (Abstr). In: Glover J.E. and Harris P.G. (Eds) Kimberlite occurrence and Origin: a basis for conceptual models in exploration. Univ. Western Australia, publ. 8, 291-292.

Ferreira Filho G.F., Nilson A.A. and Naldrett A.J. (1993). The Niquelandia Mafic-ultramafic complex, Goiás, Brazil: a contribution to the ophiolite *versus* stratiform controversy based on new geological and structural data. Precambrian Research, 57 (in press).

Fisher A.G. (1984). The two Phanerozoic supercycles. In: Berggren W.A. and Van Couvering J. (Eds) Catastrophes and Earth history. Princeton University Press, 129-150.

Fitton J.G. and Upton B.G.J. (1987). Alkaline igneous rocks. Blackwell Sci. Publ.

Fodor R.V., McKee E.H. and Asmus H.E. (1983). K-Ar ages and the opening of the South Atlantic ocean: basaltic rock from the Brazilian margin. Marine Geology 54, 111-118.

Foley S.F., Venturel G., Green D.H. and Toscani L. (1987). The ultrapotassic rocks: classification and constraints for petrogenetic models. Earth Sci. Rev. 24, 81-134.

Fouché J., Bate,K.J. and Van der Merwe R. (1992). Plate tectonic setting of the Mesozoic basins, southern offshore, South Africa. In: de Wit M.J. and Ransome I.G.D. (Eds) Inversion tectonics of the Cape Fold Belt, Karoo an Cretaceous basins of Southern Africa, 33-48.

Froidevaux C. and Nataf H.C. (1981). Continental drift: what driving mechanism? Geol. Rundsh. 70, 166-176.

Fuck R.A., Brito Neves B.B., Cordani U.G. and Kawashita K. (1988). Rb-Sr measurements on metamorphic rocks from the Barro Alto complex, Goiás, Brazil. Ext. Abstract. Int. Conf. on Geoch. Evol. Cont. crust. Poços e Caldas, 131-138.

Fuck R.A., Pimentel M.M. and Botelho N.F. (1987). Granitoid rocks in west central Brazil: a review. In: International Symposium on Granites and Associated Mineralization. Extended abstracts. Salvador, Brazil. Secretaria de Recursos Minerais, 53-59.

Gallagher K. and Hawkesworth C.J. (1992). Dehydration melting and the generation of continental flood Basalts. Nature 358, 57-59.

Gibson S.A., Thompson R.N., Leonardos O.H., Dickin A.P. and Mitchell J.G. (in press). The late Cretaceous impact of the Trindade mantle plume: evidence from large-volume, mafic, potassic magmatism in SE Brazil. Journal of Petrology Vol. 36, 189-229.

Girardi V.A.V., Rivalenti, G. and Sinigoi S. (1986). The petrogenesis of the Niquelândia layered basic-ultrabasic complex, central Goiás, Brazil. J.Petrol., 27, 715-744.

Gonzaga G.M. and Tompkins L.A. (1991). Geologia do diamante. In: Principais Depósitos Minerais do Brasil. DNPM/CPRM. 4a. Brasília, DF.

Griffiths R.W. and Campbell I.H. (1990). Stirring and structure in mantle starting plumes. Earth Planet. Sci. Lett. 99, 66-78.

Grunov, A.M. (1993) Creation and destruction of Weddell Sea floor in the Jurassic. Geology Vol. 21, pp.647-650.

Grunov, A.M. (1993) New Paleomagnetic data from the Antartic Peninsula and their tectonic implications. Journ. Geophys. Res. Vol. 98, pp.13815-13833.

Guimarães D. (1932). Sobre a rocha matriz do diamante de Minas Gerais, Brazil. Academia Brasileira de Ciências. Anais, 4, 173-176. Not seen; extracted from Meyer H.O.A. and Svisero D.P. (1980) Kimberlites and diamonds in Brazil: windows to the upper-mantle. Academia Brasileira de Ciencias, 52, 819-825.

Gurney J.J., Moore R.O., Otter M.L., Kirkley M.B., Hops J.J. and McCandless T.E. (1991). Southern African kimberlites and their xenoliths. In: Kampunsu A.B. and Lubala R.T. (Eds) Magmatism in extensional structural settings: the Phanerozoic African plate. Springer-Verlag, Berlin Heidelberg, 495-536.

Gust D.A., Biddle K.T., Phelps D.W. and Uliana M.A. (1985).. Associated middle to late Jurassic volcanism and extension in southern South America. Tectonophysics 116, 223-253.

Haggerty S.E. (1991). Emplacement and implications of ultra-deep xenoliths and diamonds from the Transition Zone (ext. Abstr.). Fifth Int. Kimb. Conf. Abstr. volume, 157-159.

Halbich I.W. (1992) The Cape Fold Belt orogeny: state of the art 1970's-1980's. In: Inversion tectonics of the Cape Fold Belt, Karoo and Cretaceous Basins of Southern Africa. de Wit and Ransome (Eds), 141-158.

Halbich I.W., Fitch F.J. and Miller J.A. (1983). Dating the Cape Orogeny. In: Sohnge A.P.G. and Halbich I.W. (Eds) Geodynamics of the Cape Fold Belt. Spec. Publ. Geol. Soc. South *Africa, 12:* 149-164.

Halliday A.N., Davidson J.P., Holden P., de Wolf C., Lee D.C. and Fitton J.G. (1990). Trace-element fractionation in plumes and the origin of HIMU mantle beneath the Cameroon line. Nature 347, 523-528.

Halliday A.N., Davies G.R., Lee D.C., Tommasini S., Paslick C.R., Fitton J.G. and James D.E. (1992). Lead isotope evidence for young trace element enrichment in the oceanic upper mantle. Nature 359, 623-627.

Haralyi N.L.E. and Hasui Y. (1982). Compartimentação tectônica do Brasil oriental com base na informação geofísica. 31 Congr. Bras. Geologia, 374-385.

Hart S.R. (1984). A large-scale isotope anomaly in the southern hemisphere mantle. Nature 309, 753-757.

Hart S.R. (1988). Heterogeneous mantle domains: signatures, genesis and mixing chronologies. Earth and Planet. Sci. Letters 90, 273-296.

Hart S.R., Gerlach O.C. and White W.M. (1986). A possible new SR-Nd-Pb mantle array and consequences for mantle mixing. Geoch. Cosmoch. Acta 50, 1551-1557.

Hart S.R. and Zindler A. (1989). Constraints on the nature and development of chemical heterogeneities in the mantle. In: Peltier W.R. (Ed) Mantle Convection, 261-388. Gordon and

Breach Sci. Publ. 261-388.

Hartnady C.H.J and Le Roex A.P. (1985). Southern ocean hot spot tracks and the Cenozoic absolute motion of the African, Antarctic and South American plates. Earth Planet. Sci. Lett. 75, 254-257.

Hasui Y. and Cordani U.G. (1968). Idades de potássio argônio de rochas eruptivas Mesozóicas do oeste mineiro e sul de Goiás. Anais 22nd Congr. Bras. Geol. SBG, Belo Horizonte.

Hasui Y., Sadowski G.R., and dal Re Carneiro C. (1977). A zona marginal sul do craton do São Francisco. Reunião preparatória do simpósio do craton do São Francisco e suas faixas marginais. Anais, 205-224.

Hawkesworth C.J., Gallagher K., Kelley S., Mantovani M., Peate D.W., Regelous M. and Rogers N.W. (1992). Paraná magmatism and the opening of the South Atlantic. Geol. Soc. London. Special Publication. 221-240.

Hawkesworth C.J., Kempton P.D. Rogers N.W., Ellam R.M. and van Calsteren P.W. (1990). Continental mantle lithosphere and shallow level enrichment processes in Earth's mantle. Earth Planet. Sci. Letters 96, 256-268.

Hawkesworth C.J., Erlank A.J., Marsh J.S., Menzies M.A. and Van Calsteren P. (1983). Evolution of the continental lithosphere: evidence from volcanics and xenoliths in southern Africa. In: Hawkesworth C.J. and Norry M.J. (Eds) Continental basalts and mantle xenoliths. Shiva, UK. 111-138.

Hawkesworth C.J., Hergt J.M., Ellam R.M. and Dermott F.M. (1991). Element fluxes associated with subduction related magmatism. Phil. Trans. R. Soc. Lond. 335, 393-405.

Hawkesworth C.J., Mantovani M.S.M. and Peate D.W. (1986).Lithosphere remobilization

during Paraná CFB magmatism. In: Cox K.G. and Menzies M.A. (Eds) Oceanic and Continental lithosphere: similarities and differences. Journal of petrology, special volume, 205-223.

Hawkesworth C.J., Mantovani M.S.M, Taylor P.N. and Palacz Z. (1986). Evidence from the Parana of south Brazil for a continental contribution to Dupal basalts. Nature 322, 356-359.

Hergt J.M., Peate D.W. and Hawkesworth C.J. (1991). The petrogenesis of Mesozoic Gondwana low-Ti flood basalts. Earth Planet. Sci. Lett. 105, 134-148.

Hergt J.M., Chappell B.W., McCulloch M.T. McDougall I and Chivas A.R. (1989). Geochemical and isotopic constraints on the origin of the Jurassic dolerites of Tasmania. Jour. Petrology 30, 841-883.

Hoffman A.W., Jochum K.P., Seufert M. and White W.M. (1986). Nb and Pb in oceanic basalts: new constraints on mantle evolution. Earth Planet. Sci. Lett. 79, 33-45.

Hoffman A.W. (1988). Chemical differentiation of the Earth: the relationship between mantle, continental crust, and oceanic crust. Earth Planet. Sci. Lett. 90, 297-314.

Hoffmann P.F. (1989). Speculations on Laurentia's first Gigayear (2.0 to 1.0 Ga). Geology 17, 135-138.

Hoffman P.F. (1991). Did the breakout of Laurentia turn Gondwanaland inside out? Science 252, 1409-1412.

Hussak E. (1894). Sobre o depósito diamantífero de Água Suja, perto de Bagagem, Minas Gerais. Comissão de Exploração do Planalto Central do Brazil. Anexo 5, H.Lambert & Cia, Rio de Janeiro, 281-319. Not seen; extracted from Leonardos et al. (1991). in Field guide book for the 5th Int. Kimb. Confer. 65-73.

Jordan T.H., Lerner-Lam A.L. and Creager K.C. (1989). Seismic imaging of boundary layers and deep mantle convection. In: Peltier W.R. (Ed) Mantle convection, plate tectonics and global dynamics. 97-201.

Kay R.W.and Mahlburg-Kay S. (1991). Creation and destruction of lower continental crust. Geol. Rundsch. 8012, 259-278.

Kiang C.H., Miranda F.P., Magalhães L. and Alkmin F.F. (1988). Considerações sobre a evolução tectônica da bacia do São Francisco. Congr. Bras. Geol. Belém. 5, 2076-2090.

Kuehner S.M., Edgar A.D. and Arima M. Petrogenesis of the ultrapotassic rocks from the Leucite Hills. Am. Mineralogist 66, 663-677. 1981.

Larson R.L. (1991). Latest pulse of Earth: evidence for a mid-Cretaceous superplume. Geology 19, 547-550.

Larson R.L. and Olson P. (1991). Mantle plumes control magnetic reversal frequency. Earth Planet. Sci. Lett. 107, 437-447.

Lay T. (1988). The deep roots of continents. Nature 333, 209-10.

Le Roex A.P. (1986). Geochemical correlation between South African kimberlites and South Atlantic hotspots. Nature 324, 243-245.

Le Roex A.P., Cliff R.A. and Adair B.J.I. (1990). Tristan da Cunha, South Atlantic: Geochemistry and Petrogenesis of a basanite-phonolite lava series. Jour. Petrol. 31, 779-812.

Leonardos O.H. and Ülbrich M.N.C. (1987). Lamproitos de Presidente Olegário, Minas Gerais. (abstr.). Soc. Bras. Progr. Ciência, 39 Congr., Brasília. Anais, 343.

Leonardos O.H., Ulbrich M.N. and Gaspar J.C. (1991). The Mata da Corda volcanic Rocks. In: Field guide book for the Fifth International Kimberlite Conference (Leonardos O.H., Meyer H.O.A. and Gaspar J.C. Eds.) 65-74. CPRM.

Machado N., Noce C.M., Oliveira O.A.B. de, and Ladeira E.A. (1989). Evolução geológica do Quadrilátero ferrífero no Arqueano e Proterozóico inferior com base em geocronologia U-Pb. Anais 5 Symp. Geol. Núcleo MG/1st Symp. Geol. Núcleo Brasília, SBG, 01-05.

Machado N, and Schrank A.(1989). Geochronologia U/Pb no maçiço de Piumhi: resultados preliminares. V Symp. Geol. Núcleo MG/I Symp. Geol Núcleo Brasília. SBG, 45-49.

Mantovani M.S.M., Marques L.S., de Sousa M.A., Civetta L., Atalla L. and Innocenti F. (1985). Trace element and strontium isotope constraints on the origin and evolution of Paraná continental flood basalts of Santa Catarina state (Southern Brazil). Journal of Petrology, 26, 187-209.

Mariano A.N. and Marchetto M. (1991). Serra-Negra and Salitre-carbonatite alkaline igneous complex. Field guide book 5th Int. Kimb. Conf. 75-79.

Marini, O.J. and Botelho, N.F. (1986). A província de granitos estaníferos de Goiás. Rev. Bras. Geociências 16, 119-131.

Marini O.J., Fuck R.A., Dardenne M.A. and Danni J.C.M. (1984). Província Tocantins. Setores central e sudeste. In: Almeida F.F.M de and Hasui Y. (Eds). O pré-Cambriano no Brasil. São Paulo, Edgar Blucher, 205-264.

Martin A.K. and Hartnady C. J.H.(1986). Plate tectonic development of the South West Indian Ocean: A revised reconstruction of East Antarctica and Africa. Jour. Geophys. Res. 91, 4767-4786.

Martin H. (1993) The mechanisms of petrogenesis of the Archean continental crust: a comparisson with modern processes. Lithos, 30, pp.373-388.

Marshak S. and Alkmin F.F. (1989). Proterozoic contraction/extension tectonics of the southern São Francisco region, Minas Gerais, Brazil. Tectonics, 8, 555-571.

McDonald I., Hart R.J. and Tredoux M. (1992). The analysis of the Platinum-group-elements in South African kimberlites by Nickel sulphide fire-assay and neutron activation analysis. Anal. Chim. Acta.

McDonald I., Bizzi L.A., Smith C.B. de Wit M.J. and Viljoen K.S. (in press). The geochemistry of the platinum group elements in Brazilian and southern African kimberlites. Geochim. Cosmochim. Acta.

McKenzie D. (1989). Some remarks on the movement of small melt fractions in the mantle. Earth Planet. Sci. Lett. 95, 53-72.

McKenzie D. and O'Nions R.K. (1991). Partial melt distributions from inversion of rare-earth-element concentrations. Jour. Petrology, 32, 1021-1091.

McWilliams M.O. (1981). Paleomagnetism and Precambrian tectonic evolution of Gondwana. In: Kroner A. (Ed), Precambrian plate tectonics, Elsevier, Amsterdam, 649-687.

Menzies M.A. and Hawkesworth C.J. (1987). Mantle Metasomatism. Book volume 472p. Academic Press, London.

Menzies M.A. and Wass S.Y.(1983). Co_2- and LREE-rich mantle below eastern Australia, a REE and isotopic study of alkaline magmas and apatite-rich mantle xenoliths from Southern Highlands Province, Australia. Earth Planet. Sci. Lett. 65, 2287-302.

Meyer H.O.A. and Svisero D.P. (1980). Kimberlites and diamonds in Brazil: windows to the upper-mantle. Academia Brasileira de Ciencias, 52, 819-825.

Meyer H.O.A. and Svisero D.P. (1991). Limeira and Indaia intrusions, Minas Gerais. Fifth International Kimberlite Conference, field guide book, 49-56.

Meyer H.O.A., Garwood B.L. and Svisero D.P. (1991). The Pântano intrusion. Fifth International Kimberlite Conference, field guide book, 59-64.

Meyer H.O.A., Garwood B.L., Svisero D.P. and Smith C.B. (1993). Alkaline ultrabasic intrusions in western Minas Gerais, Brazil. In: Proceedings of the 5th International Kimberlite Conference. 140-155.

Meyer H.O.A. and Villar L.M. (1984). An alnoite in the Sierra Subandinas, northern Argentina. J. Geol. 92, 741-751.

Milani E.J. (1992). Intraplate tectonics and the evolution of the Paraná Basin, SE Brazil. In: de Wit M.J. and Ransome I.G.D. (Eds) Inversion tectonics of the Cape Fold Belt, Karoo and Cretaceous basins of Southern Africa, 101-108.

Milner S.C., Le Roex A.P. and Watkins R.T. (1992). Rb-Sr age determinations of rocks from the Okenyenya igneous complex, NW Namibia. Geol. Magazine (in press).

Mitchell R.H. (1985). A review of the mineralogy of lamproites. Trans. Geol. Soc. South Afr, 88, 411-437.

Mitchell R.H. (1986). Kimberlites: mineralogy, geochemistry and petrology. Book volume. Plenum, New York.

Mitchell R.H. (1989). Aspects of the Petrology of kimberlites and lamproites: some definitions

and distinctions. In: Kimberlites and related rocks: their composition, occurrence, origin and emplacement. Ross J. (Ed) Vol. 1, 7-45.

Mitchell R.H. and Bergman S.C. (1991). The petrology of lamproites. Book volume. Plenum Press, N.Y.

Mitchell R.H. and Keays R.R. (1981). Abundance and distribution of gold, palladium and iridium in some spinel and garnet lherzolites: implications for the nature and origin of precious metal-rich intergranular components in the upper mantle. Geochim. Cosmochim. Acta, 45, 2425-2442.

Mohriak W.V., Mello M.R., Karner G.D., Dewey J.F. and Maxwell J.R. (1989). Structural and stratigraphic evolution of the Campos Basin, offshore Brazil. In: extensional tectonics and stratigraphy of the North Atlantic margins, by Tankard A.J. and Balkwill (Eds). AAPG memoir 46, 577-598.

Molnar P. and Gray D. (1979). Subduction of continental Lithosphere: some constraints and uncertainties, Geology 7, 58-62.

Moore A.E. and Verwoerd W.J. (1985). The olivine melilitite-kimberlite-carbonatite suite of Namaqualand and Bushmanland, South Africa. Trans. Geol. Soc. South Africa. 88, 281-294.

Moraes L.C., Seer H.J., Fogaça A.C.C., Scarbi P.B.A., and Scarbi G.N.L. (1986). Geologia das unidades Cretáceas da área compreendida entre Lagoa Formosa and Carmo do Paranaíba, MG. In: 34 Congr. Bras. Geol. Goiânia. 1, 337-345.

Moraes L.C., Seer H.J. and Kattah S.G. (1987). Aspectos petroquímicos das rochas vulcânicas alcalinas cretáceas da porção meridional da bacia Sanfranciscana, MG. I Congr. Bras. Geoquim. Porto Alegre. Anais. 81-84.

Morgan W.J. (1981). Hot-spot tracks and the opening of the Atlantic and Indian Oceans. In: The Sea 7, 443-488. Wiley Interscience, New York, 1981.

Morgan W.J. (1983). Hot-spot tracks and the early rifting of the Atlantic. Tectonophysics 94, 123-139.

Morgan J.W. Wandless G.A., Petrie R.K. and Irving A.J. (1981). Composition of the Earth's upper mantle. 1. Siderophile trace elements in ultramafic nodules. Tectonophysics 76, 47-67.

Nance R.D., Worsley T.R. and Moody J.B. (1988). The supercontinent cycle. Scientific American July 1988, 44-51.

Nelson B.K. and DePaolo D.J. (1984). Origin of 1700 Myr greenstone successions in southwestern North America and the isotopic evolution of Proterozoic Mantle. Nature, 311, 143-146.

Nelson B.K. and DePaolo D.J. (1985). Rapid production of continental crust 1.7 - 1.9 by ago: Nd and Sr isotopic evidence from the basement of North American mid continent. Geol. Soc. Am. Bull. 96, 746-754.

Nixon P.H. (Ed) Mantle xenoliths. Wiley, 1987.

O'Connor J.M. and Duncan R.A. (1990). Evolution of the Walvis Ridge-Rio Grande Rise hot-spot system: implications for African and South American plate motions over plumes. Jour. Geophys. Research 95, 17475-17502.

Oliveira L.O.A. (1989). Aspectos da evolucao termomecanica da bacia do Paraná no Brasil. Rev. Bras. Geociências, 19(3), 330-342.

Oliveira O.A.B. and Teixeira W. (1990). Evidencias de uma tectônica tangencial Proterozóica

no Quadrilátero Ferrífero. 36 Congr. Bras. Geol. Natal, Brazil. 6., 2589-2604.

Olson P. (1990). Hot spots, swells and mantle plumes. In: magma transport and storage. Ryan M.P. (Ed). John Wiley & Sons, 33-51.

Othman D.B., White W.M. and Patchett J. (1989). The geochemistry of marine sediments, island-arc magma genesis and crust-mantle recycling. Earth Planet. Sci. Lett. 94, 1-21.

Page N.J. and Tankington R.W. (1984). Palladium, Platinum, Rhodium, Ruthenium and Iridium in peridotites and chromitites from ophiolite complexes in Newfoundland. Can. Mineral. 22, 137-149.

Parenti Couto J. G., Cordani U.G., Kawashita K., Lyer S.S. and Moraes N.M.P. (1981). Considerações sobre a idade do Grupo Bambuí com base em análises isotópicas de Sr e Pb. Rev. Bras. Geoc. 11, 5-16.

Paul D., Crocket J.H. and Nixon P.H. (1979). Abundances of Palladium, Iridium and Gold in kimberlites and associated nodules. In: Proc. 2nd Int. Kimb. Conf., 1, 272-279.

Peate D.W. (1989). Stratigraphy an petrogenesis of the Paraná continental flood basalts, southern Brazil. PhD Thesis (unpublished). The Open University.

Peate D.W., Hawkesworth C.J., Mantovani M.S.M. and Shukowsky W. (1990). Mantle plumes and flood-basalt stratigraphy in the Paraná, South America. Geology. 18, 1223-1226.

Peate D.W., Hawkesworth C.J. and Mantovani M.S. (1992). Chemical stratigraphy of the Paraná lavas (South America): classification of magma types and their sptaial distribution. Bull. Volcanology 55, 119-139.

Peltier W.R., Jarvis G.T., Forte A.M. and Solheim L.P. (1989). The radial structure of the

mantle general circulation. In: Mantle Convection, Plate Tectonics and Global dynamics. Peltier W.R. (Ed), 765-815.

Pflug R. and Renger F. (1973). Estratigrafia e evolução geológica da margem sudoeste do craton Sanfranciscano. 27 Congr. Bras. Geol., Aracajú, SBG. 2, 5-19.

Pflug R. and Scholl (1975). Proterozoic glaciation in eastern Brazil: a review. Geol. Rundschau, Sttutgard, 64, 287-299.

Piccirillo E.M., Bellieni G., Cavazzini, G., Comin-Chiaramonti P., Petrini R., Melfi A.J., Pinese J.P.P., Zantadeschi P. and de Min A. (1990). Lower Cretaceous tholeiitic dyke swarms from the Ponta Grossa Arch (southeast Brazil): petrology, Sr-Nd isotopes and genetic relationships with the Paraná flood volcanics. Chemical Geology 89, 19-48.

Pimentel M.M. and Charnley N. (1991). Intracrustal REE fractionation and implications for Sm-Nd model age calculation in late-stage granitic rocks: an example from central Brazil. Chemical Geology (Isot. Geosc. Section). 86, 123-138.

Pimentel M.M. and Fuck R.A. (1987). Origem e evolução das rochas metavulcânicas e metaplutônicas da região de Arenópolis (GO). Rev. Bras. Geociências, 17, 2-14.

Pimentel M.M. and Fuck R.A. (1987). Late Proterozoic granitic magmatism in southwestern Goiás, Brazil. Rev. Bras. Geociências, 17, 415-425.

Pimentel M.M. and Fuck R.A. (1992). Neoproterozoic crustal accretion in central Brazil. Geology, 20, 375-379.

Pimentel M.M., Heaman L. and Fuck R.A. (1991). U-Pb zircon and sphene geochronology of late Proterozoic volcanic arc rock units from southwestern Goiás, central Brazil. Journal of South American Earth Science.

Pimentel M.M., Heaman L. and Fuck R.A. (1991). Idade do meta-riolito da sequência Maratá, Grupo Araxá, Goiás, central Brazil. Academia Brasileira de Ciências, anais.

Pimentel M.M., Heaman L., Fuck R.A. and Marini, O.J. (1991). U-Pb zircon geochronology of Precambrian tin-bearing continental-type acid magmatism in central Brazil. Precambrian Research 52, 321-335.

Pires F.R.M. (1986). The southern limits of the São Francisco craton. Academia Brasileira de Ciências. Anais, 58, 139-145.

Ploszkiewicz J.V., Orchuela I.A., Vaillard and Vines R.F. (1984). Compresión des plazamientos laterales em la zona de falla Huincul, estruturas associadas, Provincia de Neuduen. 9 Congresso Geol. Argent., Actas 2, 163-169.

Porada H. (1989). Pan African rifting and orogenesis in southern to equatorial Africa and eastern Brazil. Precambrian Research, 44, 103-136.

Queménéur J.J. (1987). Esboço estratigráfico, estrutural e metamórfico da Serra do Bom Sucesso, M.G. IV Simp. Geol. Minas Gerais, Belo Horizonte. Bol. 7, 135-148.

Rabinowitz P.D. and La Brecque J. (1979). The Mesozoic South Atlantic Ocean and evolution of its continental margin. Jour. Geophys. Res. 84, 5973-6002.

Ramos V.A. (1988). Late Proterozoic-Early Palaeozoic of South America - A collisional story. Episodes 11, 168-173.

Reis Neto J.M. and Cordani U.G. (1984). Influência do evento geodinâmico Brasiliano nos resultados radiométricos do centro-oeste brasileiro. 33 Congr. Bras, Geol., Rio de Janeiro, Anais, SBG, 2276-2288.

Renne P.R., Onstott T.C., D'Agrella Filho M.S., Pacca I.G. and Teixeira W. (1990). $^{40}Ar/^{39}Ar$ dating of 1.0-1.1 Ga magnetization from the São Francisco and Kalahari cratons: tectonic implications for Pan-African and Brasiliano mobile
belts. Earth Planet. Sci. Lett. 101, 349-366.

Rhodes R.C. and Bornhorst R.J. (1976). Petrologic Provinces in Jurassic tholeiites of Gondwanaland. Geol. Rundsch. 65, 930.

Richards M.A. and Engebretson D.C. (1992). Large-scale mantle convection and the history of subduction. Nature 355, 437-440.

Richards M.A., Duncan R.A. and Courtillot V.E. (1989). Flood basalts and hot-spot tracks: plume heads and tails. Science. 246, 103-107.

Richardson S., Erlank A.J., Reid D.L. and Duncan A.R. (1984). Major and trace elements and Nd and Sr isotope geochemistry of basalts from the deep sea drilling project leg 74, Walvis ridge transect. Initial reports of the Deep Sea Drilling Project, LXXIV, Washington, 739-754.

Richardson S.H., Erlank A.J., Duncan A.R. and Reid D.L. (1982). Correlated Nd, Sr and Pb isotope variation in Walvis Ridge basalts and implications for the resolution of their mantle source. Earth and Planet. Sci. Letters 59, 327-342.

Richardson S.H., Gurney J.J., Erlank A.J. and Harris J.W. (1984) Origins of diamonds in old enriched mantle. Nature 310, 198-202.

Richter F.M. and McKenzie D.P. (1981). On some consequences and possible causes of layered mantle convection. J. Geophys. Res. 86, 6124-6133.

Rimann E. (1917). A kimberlita no Brazil. Escola de Minas de Ouro Preto. Anais, 15, 27-32. Not seen; extracted from Meyer H.O.A. and Svisero D.P. (1980) Kimberlites and diamonds in

Brazil:windows to the upper-mantle. Academia Brasileira de Ciencias, 52, 819-825.

Ringwood A.E. and Irifune T. (1988). Nature of the 650 km discontinuity: implications for mantle dynamics and differentiation. Nature 331.

Rogers N.W., Hawkesworth, C.J. and Palacz Z.A. (in press). Phlogopite in the generation of olivine melilitites from Namaqualand, South Africa and implications for element fractionation processes in the upper mantle. Geol. Soc. Lond. Spec. Publ.

Romano A.W. (1989). Evolution tectonique de la region Nord-Ouest du Quadrilatere Ferrifere - Minas Gerais - Bresil (Geochronologie du socle - aspects geochimiques et petrographiques des supergroupes Rio das Velhas et Minas. Thesis pour L'obtension de docteur de L'Universite de Nanci I. (unpublished).

Saadi A., Noce C.M. and Quintão N.H. (1989). Neotectônica na região sul de Minas Gerais, primeira hipóteses. V Simp. Geol. Núcl. Minas Gerais/I Simp. Geol. Núcl. Brasília. SBG, 115-119.

Santos S.F., Cupertino J.A.a and Braga J.A.E. (1990). Síntese sobre a geologia das bacias do Recôncavo, Tucano e Jatobá. In: Pederneiras G., Gabaglia R. and Milani E.J. (coords) Origem e evolução de bacias sedimentares. Petróleo Brasileiro S.A. Rio de Janeiro, Brazil, 235-266.

Schorscher H.D., Santana F.C., Polonia J.C. and Moreira J.M.P. (1982). Quadrilátero Ferrífero, Minas Gerais State: Rio das Velhas greenstone belt and Proterozoic rocks. Excursion Annex. ISAP. Salvador, Brazil, 44.

Schrank A. (1982). Petrologie des komatiites et des roches associées de la Ceintures Verte du Massif Précambrien de Piumhi (Minas Gerais, Bresil). These Doctor Ingenieur, Univ. Paris Sud. Orsay (unpublished).

Seer H.J. and Moraes L.C. (1988). Estudo petrográfico das rochas ígneas alkalinas da região de Lagoa Formosa, MG. Rev. Bras. Geociências 18, 134-140.

Seer H.J., Moraes L.C. and Fogaça A.C.C. (1989). Roteiro geológico para a região de Lagoa Formosa - Chumbo - Carmo do Paranaíba, MG. Soc. Bras. Geologia, Núcl. MG, Bol. 9, 58

Seixas L.A.R. (1988). Geologia e Metalotectos de ouro de uma fraçao do lineamento Congonhas, MG. MSc. thesis, Universidade de Brasília, Brasília, Brazil. (unpublished).

Seixas L.A.R. and Baars F.J. (1991). características geoquímicas das rochas ultramáficas do lineamento Congonhas, Minas Gerais, Brasil. 3o. Congresso Bras. Geoquímica/ 1o. Congresso de Geoquímica dos Países de Língua Portuguesa, 185-190.

Shearer P.M. and Masters T.G. (1992). Global mapping of topography on the 660 km discontinuity. Nature 355, 791-796.

Shee S.R., Bristow J.W., Bell D.R., Smith C.B., Allsopp H.L. and Shee P.B. (1989). The petrology of kimberlites, related rocks and associated mantle xenoliths from the AKuruman province, South Africa. Kimberlites and related rocks: their composition, occurrence and emplacement. Geological Society of Australia Special Publication N°14. 1, 60-82.

Shilling J.G. (1991). Fluxes and excess temperatures of mantle plumes inferred from their interaction with migrating mid-ocean ridges. Nature 352, 397-403.

Shilling J.G., Kingsley R.H., Hanan B.B. and McCully B.L. (1992). Nd-Sr-Pb isotopic variations along the Gulf of Aden: evidence for Afar Mantle plume-continental lithosphere interaction. Jour. Geoph. Res. 97, 10927-10966.

Shobbenhaus C., Campos D. de A., Derze G.R. and Asmus H.E. (1981). Mapa geologico do Brasil e da area oceânica adjacente incluindo depositos minerais. Escala 1:2,500,000. Brasilia,

Departamento Nacional da Producao Mineral.

Shobbenhaus C., Campos D. de A., Derze G.R. and Asmus H.E. (1984). Geologia do Brasil; texto explicativo do mapa geologico do Brasil e da area oceânica adjacente incluindo depositos minerais. Escala 1:2,500,000. Book volume, Brasilia, Departamento Nacional da Producao Mineral.

Skinner E.M.W. (1989). Contrasting group I and group II kimberlites: towards a genetic model for kimberlites. In: Kimberlites and related rocks, Ross J. (Ed), 1, 528-544.

Skinner E.M.W., Smith C.B., Viljoen K.S. and Clark T.C. The petrography, tectonic setting and emplacement ages of kimberlites of kimberlites in the south western border region of the Kaapval craton, Prieska area, South Africa.In: Proceedings of the 5th International Kimberlite Conference (in press).

Smith C.B. (1983). Pb, Sr and Nd isotopic evidence for sources of southern African Cretaceous kimberlites. Nature, 304, 51-54.

Smith C.B. (1983). Rubidium-strontium, uranium-lead and samarium-neodymium isotopic studies of kimberlite and selected mantle-derived xenoliths. PhD thesis (unpublished), University of the Witwatersrand.

Smith C.B., Gurney J.J., Skinner E.M.W., Clement C.R. and Ebrainm N. (1985). Geochemical character of southern African kimberlites: a new approach based on isotopic constraints. Trans. Geological Society of South Africa, 88, 267-280.

Sohnge A.P.G. and Halbich I.W (1983). - Geodynamics of the Cape Fold Belt. Spec. Publ. Geol. Soc. S. Africa 12 - Johannesburg. Geol. Soc. South Africa.

Stark et al., (1991) Oil geology off-shore Namibia 1991. Book Volume. Schlumberger.

Svisero D.P. (1979). Piropos cromíferos da mina de diamantes de Romaria: composicão química e origem. Boletin Mineralógico, 6, 7-14.

Svisero D.P. and Meyer H.O.A. (1981). Ilmenitas kimberlíticas da mina de diamantes de Romaria, MG. Revista Brasileira de Geociências, 11, 217-221.

Svisero D.P., Meyer H.O.A., Haralyi N.L.E. and Hasui Y. (1984). A note on the geology of some Brazilian kimberlites. Journal of Geology 92, 331-338.

Sweeney, R.J., Falloon T.J., Green D.H. and Tatsumi Y. (1991). The mantle origin of Karoo picrites. Earth Planet. Sci. Lett. 107, 256-271.

Tainton K.M. and McKenzie D. (1994). The generation of kimberlites, lamproites and their source rocks. Journal of Petrology, Vol. 35, 787-817.

Tankard A.J.,, Jackson M.P.A., Erickson K.A., Hobday D.K., Hunter D.R. and Minter W.E.L. (1982). 3.5 Billion years of Crustal Evolution of Southern Africa. New York, Springer Verlag.

Teixeira W. (1982). Geochronology of southern part of the São Francisco Craton. Revista Brasileira de Geociências, 12, 268-277.

Teixeira W., Cordani U.G., Kawashita K., Taylor P.N. and Van Shmus W.R. (1987). Archean and early Proterozoic crustal evolution in the southern part of the São Francisco craton. Int. Symp. Granites and Ass. Mineralization. Salvador, Brazil. Ext. Abstr. 37-40.

Teixeira W. and Figueiredo M.C.H. (1991). An outline or early Proterozoic crustal evolution in the São Francisco craton, Brazil: a review. Precambrian Research 53, 1-22.

Teixeira W., Fonseca A. do C., Pompeu G., Padilha A.V., Zaparolli L.H., Kawashita K. and

Khouri M.C. (1985). Esbôço da evolução geotectônica da parte sul do craton do São Francisco: uma interpretação com base nos dados Rb-Sr, K-Ar, Pb-Pb e traços de fissão. 3° simpósio de geologia de Minas Gerais, Belo Horizonte, 28-44.

Teixeira W., Evangelista H.J., Kawashita K. and Taylor N.R. (1988). Geochronologia K-Ar do enchame de diques básicos da parte meridional do cráton do São Francisco e implicações no contexto geotectõnico. 35 Congr. Bras. Geol. Belém, Brazil, 6, 2870-2886.

Thirwall M.F. and Jones N.W. (1983). Isotope geochemistry and contamination mechanics of Tertiary lavas from Skye, Northwest Scotland. In: Continental Mantle Xenoliths, Hawkesworth C.J. and Norry C.M.J. (Eds), 186-208.

Thompson R.N. and Gibson S.A. (1991). Subcontinental mantle plumes, hotspots and pre-existing thinspots. Jour. of Geol. Soc. Lond., 148, 973-977.

Thompson R.N., Dickin A.P., Gibson I.L. and Morrison M.A. (1982). Elemental fingerprints of isotopic contamination of Hebridean Paleocene mantle-derived magmas by Archean Sial. Contr. Min. Petrol. 79, 159-168.

Tompkins L.A., and Gonzaga G.M. (1989). Diamonds in Brazil and a proposed model for the origin and distribution of diamonds in the Coromandel region, Minas Gerais, Brazil. Economic Geology 84, 591-602.

Tompkins L.A. (1991). Kimberlite structural environments and diamonds in Brazil. 5th Int. Kimb. Conf. Ext. Abstr. 426-428.

Tompkins L.A. (1991). The Japecanga pipe. Field guide book 5th Int. Kimb. Conf. 45-48.

Toyoda K., Horiuchi H. and Tokonami M. (1994). Dupal anomaly of Brazilian carbonatites: geochemical correlations with hotspots in the South Atlantic and implications for the mantle

source. Earth and Planet. Sci. Letters 126, 315-331.

Tredoux M., Davies G., Lindsay N.M. and Sellshop J.P.F. (1986). The influence of temperature on the geochemistry of the Platinum-group elements and gold. Geol. Soc. S.Afr., Geocongress-86 (ext.Abstr.) 625-628.

Tredoux M. (1990). The platinum-group elements: nuclear methods for their analysis and their behavior in terrestrial rocks and meteorites. PhD thesis (unpublished). Two volumes. University of the Witwatersrand.

Tredoux M., de Wit M.J., Hart R.J., Armstrong R.A., Lindsay N.M. and Sellschop J.P.F. (1989). Platinum-group elements in a 3.5 Ga nickel-iron occurrence:possible evidence of a deep mantle origin. Journal Geophys. Research 94, 795-813.

Uchupi E. (1989). The Tectonic style of the Atlantic Mesozoic rift system. Jour. Afr. Earth Sci. 8, 143-164.

Ulbrich H.H.G.J. and Gomes C.B. (1981). Alkaline rocks from continental Brazil. Earth Sci. Reviews 17, 135-154.

Uliana et al., (1989). In: Tankard A.J. and Balkwill H.R. (Eds). Extensional tectonics and stratigraphy of the North Atlantic margins. AAPG Memoir 46, Tulsa.

Van de Merwe R. and Fouche J. (1992). Inversion tectonics in the Bredasdorp basin off-shore South Africa (Abstract). Abstract Volume, Conference on Inversion Tectonics of the Cape Fold Belt.

Veevers J.J. (1988). Gondwana facies started when Gondwanaland merged in Pangea. Geology 16, 732-734.

Veevers J.J. (1989). Middle/late Triassic (230 ± 5 Ma) singularity in the stratigraphic and magmatic history of the Pangean heat anomaly. Geology 17, 784-787.

Visser J.N.J. (1992). Basin tectonics in southwestern Gondwana during the Carboniferous to Permian. In: de Wit M.J. and Ransome I.G.D. (Eds) Inversion tectonics of the Cape Fold Belt, Karoo and Cretaceous Basins of Southern Africa (in press).

Vollmer (1983). Terrestrial lead evolution and formation time of the Earth's core. Nature 270, 144-147.

White W.M. and Hoffmann A.W. (1982). Sr and Nd isotope geochemistry of oceanic basalts and mantle evolution. Nature 296, 821-825.

White R.S. and McKenzie D.P. (1989). Magmatism at rift zones: the generation of volcanic continental margins and flood basalts. Journal of Geophysical Research, 94, 7685-7730.

Wilsher, W.A., de Wit, M.J., and Marrao E. (1989). A GIS solution for Gondwana geoscientific data. Journal of African Earth Sciences, 9, No. 2, 371-374.

Worsley T.R., Nance D. and Moody J.B. (1984). Global Tectonics and Eustasy for the Past 2 Billion Years. Marine Geology 58, 373-400.

Worsley T.R., Nance D. and Moody J.B. (1986). Tectonic Cycles and the History of the Earth's Biochemical and Paleoceanographic Record. Paleoceanography 1, 233-263.

Zalan P.V., Wolff S., Astolfi M.A.M., Vieira I.S., Conceicao J.C.J., Appi V.T., Neto E.V.S., Cerqueira J.R. and Marques A. (1990). The Paraná Basin, Brazil. In: Leighton, M.W, Kolata D.R., Oltz D.F. and Eidel J.J. (Eds) Interior Cratonic Basins. AAPG Memoir 51, Tulsa, 681-708.

Zindler A. and Hart S.R. (1986) Chemical geodynamics. Ann. Rev. Earth and Planet. Sci. Letters 14, 493-571.

Appendix

Analytical methods

i - Sample preparation

All of the kimberlite samples were prepared at once by the author at the Isotope Geophysics Unit of the Bernard Price Institute of Geophysics of the University of the Witwatersrand. Rock samples were coarsely crushed in a clean steel jaw crusher up to centimeter size. The smaller and more homogeneous samples from Japecanga and from Três Ranchos dolerite were crushed with a mortar and pestle. The centimetric rock fragments which were apparently free of xenolithic fragments at the level of observation employed (x20 binocular microscope) were then crushed to fine powder in a pre-contaminated agate swing mill. All instruments used were cleaned with compressed air and acetone in between rock samples. Two or more samples per locality were prepared according to the homogeneity and freshness of the rocks. Individual dissolutions comprised about 300 milligrams of rock sample.

Phlogopite concentrates handpicked from the crushed samples were hand-cleaned under a binocular microscope and washed in a mixture of distilled water and alcohol or acetone in an ultrasonic bath. Individual samples of fresh, optically distinctive, inclusion-free mica populations comprising of about 300 to 500 milligrams of mica were then leached for about 10 minutes in 10 ml of double-distilled 1N HCl, with about one minute of ultrasonic agitation. A second stage of examination under the binocular microscope then followed the leaching process because altered, chloritized or serpentinized phlogopite grains acquired a distinctive greenish color during the leaching.

Crustal rock samples discussed in Chapter I (results presented in table I.2) were prepared by Mr. Ernest Stout under the supervision of Franciscus Baars at the Isotope Facility Unit of the University of Cape Town using similar procedures. In that case, however, no mineral separates

were prepared.

ii - X-Ray Fluorescence

X-Ray fluorescence (XRF) spectrometry used for the determination of major and trace element elements was carried out by the author at the University of Cape Town using the methodology described by Norrish and Hutton (1969) and Le Roex and Dick (1981). The samples were first dried for four hours at 110°C. The loss of water (H_2O^-) was determined as the mass difference between air dried rock powder and oven dried (110°C) rock powder. To ignite the samples the temperature was increased to 1050°C for further four hours. The loss of ignition (LOI) was determined from the corresponding loss in mass.

Major and minor elements were determined using fusion discs made by quantitatively mixing Lithium Tetraborate flux (Johnson Matthey Spectroflux 105) with the pre-ignited rock powder. The mixtures were then fused and cast into glass discs suitable for the sample holders of the two XRF spectrometers. Trace elements were determined from undiluted pressed powder pellets of a diameter of 30 mm made of mixed rock powder and Mowiol solution (20% Hoechst Wax N 70-88 in distilled water) as a binder, with a surround and base of boric acid powder. A 6 tons hydraulic press was used.

Standard X-ray tubes and programmes of the X-Ray facility of the Department of Geological Sciences of the University of Cape Town were used. The analysis was performed with a Siemens-303AS and a Philips PW1400 XRF Spectrometer. A Hewlett-Packard 9000 computer and the in-house programs NAVAL, SMSAM, MAJOR, AVERG, and the program TRACE (Duncan, 1975) were used to convert the intensity data into elemental concentrations.

ii - Neutron Activation Analysis

Rare Earth Element (REE) concentrations on kimberlite samples were determined at the Schonland Research Centre of the University of the Witwatersrand by instrumental neutron activation analysis (INAA) using a similar procedure to that outlined by Erasmus et al. (1977) and employing the instrumentation and dual detector system described by McDonald (1992).

Rock powders were weighed onto polythene capsules and then onto polythene irradiation cans together with international standards in a pre-designated order. Samples were irradiated within the Pelindaba Reactor Centre for about 30 hours of reactor time. Platinum Group Element (PGE) and gold were determined in separate samples by the nickel sulphide fire-assay and neutron activation analysis procedure described by McDonald et al. (1992). This analytical procedure overcomes the problems of incomplete melting and poor recovery of PGE from silica-poor and carbonate-rich samples during fire-assay. Counting and data processing were performed by Iain McDonald from the Schonland Research Centre of the University of the Witwatersrand using spectroscopy amplifiers and a multichannel analyzer.

Platinum Group Element and gold concentrations reported represent the average of two 100 gram duplicate analysis. The precision of the PGE determinations was similar to that obtained for the routine analysis of an internal komatiite standard (called WITS-1) using 50 gram of sample but the precision for gold was considerably improved by the use of larger sample masses. In comparison with the high coefficients of variation for gold determination from WITS-1 by this method (>30%), the average coefficients of variation obtained in the analysis of the alkaline rocks was 10.3%. For Os the average covariation for WITS-1 (13.2%) compares with that for the alkaline rocks (16.8%). For Ir the coefficients of variation are 12.0% and 5.3%, respectively. For Ru, 11.2% and 12.5%. For Rh, 8.7% and 6.7%. For Pt, 27.3% and 9.5%. And for Pd, 14.3% and 7.9% respectively.

iii - Solid-source mass spectrometry

Solid source mass spectrometry for Sr, Nd, U and Pb isotopes on all of the kimberlite-related and crustal rocks listed in Tables I.2 and II.5 was performed by the author at the Bernard Price Institute for Geophysical Research, University of the Witwatersrand; and at the FRD Radiogenic Isotope Facility of the University of Cape Town. Isotope compositions and concentrations of whole-rock powders and mineral separates were determined by double dissolution of natural samples and isotope dilution as described by Kramers (1977) and Smith (1983).

Natural and accurately multiple-spiked samples were dissolved in clean teflon beakers with six

ml of triple-distilled hydrofluoric acid (HF) and 2 ml of double-distilled 12 normal nitric acid (HNO_3). They were then left on hot-plates for three to five days in laminar flow cupboards until complete dissolution. Samples were then evaporated, taken into solution in double-distilled 6 normal hydrochloric acid (HCl), and evaporated again. A second stage of sample solution into 2.59 normal HCl and centrifuge separation produced about 2.5 ml of solution which was loaded into pre-conditioned ion-exchange columns. Smaller columns (about 2 grams of resin) were used for Rb and Sr separation in mica samples. Bigger columns (about 10 grams of resin) were used for the separation in whole-rock samples.

After Rb and Sr were eluted from the Rb-Sr columns with 2.59 normal HCl, REE were eluted with 6 normal HCl, dried and converted to nitrate before being added onto small (4.5 grams of Bio-rad AG1-X8 resin at BPI and HDEHP at UCT) preconditioned teflon powder columns. REE were eluted from these small columns with nitric acid. Separate spiking and sample dissolution were used for Pb isotope geochemistry, which was performed at the Radiogenic Isotope Facility of the University of Cape Town. Sample dissolutions were carried out following similar procedures to those described above for Sr and Nd geochemistry. Pb is eluted with 6 normal HCl. U is converted to nitrate form and eluted with water. Anodic electrodeposition of Pb was used for final Pb purification. Column sizes and calibration were slightly different in the two laboratories used, but the procedures were basically the same.

Samples were loaded onto outgassed single filaments of rhenium (Pb sample loaded onto silica gel base with 2% HNO_3 and oxidized with H_3PO_4) or tantalum (Sr sample loaded with 2% HNO_3 and oxidized with H_3PO_4), or loaded onto tantalum side filaments (Rb loaded with H_2O; Sm, Nd and U loaded with 2% HNO_3) welded onto pins mounted in glass beads. Rb-Sr determination on phlogopite micas; and Rb-Sr and Sm-Nd determination on whole-rock kimberlite samples were performed using MM30 and VG260 mass spectrometers at the Bernard Price Institute for Geophysical Research, University of the Witwatersrand. Pb-Pb and U-Pb determination on the alkalic ultramafic rock samples; and Rb-Sr and Sm-Nd on crustal rock samples were performed at the FRD Radiogenic Isotope Facility of the University of Cape Town using a VG Sector multi-collector thermal mass spectrometer. All elements were analyzed at $< 10^{-7}$ atmospheres

and accelerating potential of 8 kv. Filament currents were optimized to generate beam intensities of about $2x10^{-10}$ Amperes. Sr beams were generally obtained at a filament current of about 2.5 Amperes. Rb beams were normally obtained at 0.5 Amperes (side filament) with a constant 2.0 Amperes current in the centre filament. Sm and Nd beams were normally obtained at 1.5 to 2.0 Amperes (side filament) with a constant 4.5 Amperes in the centre filament. U and Pb beams were obtained at variable temperatures according to beam sizes and run by the VG Sector computer programs. Determinations using the MM30 were made in a semi-automatic fashion (i.e. manual focusing and setting of running parameters) whereas determinations made using the VG260 and the VG Sector were run automatically. At UCT Sr and Nd were analyzed using triple and quadruple dynamic configurations, respectively. Rb analysis were performed in double collector static mode; and a single collector, peak-jumping routine, was used during the Sm analyses.

Concentrations of Rb, Sr, K, U, Pb, Sm and Nd were determined by isotope dilution using tracer solutions periodically calibrated against gravimetric standards in the two laboratories. Reagent, total method and partial method blanks have been measured throughout the course of this work to monitor contamination effects. Total method blanks were about 100 picograms or less in both laboratories, a level considered negligible for the studied samples. Laboratory contamination, therefore, has not been a serious source of errors for the analysis, and blank corrections have not been applied to the data.

Standards and duplicate sample dissolutions were used to ascertain the effects of both geologic and analytical error. Errors on $^{87}Rb/^{86}Sr$ and $^{147}Sm/^{144}Nd$ ratios are 1.5 and 1.0 relative %, respectively. Errors for $^{87}Sr/^{86}Sr$ ratio are 0.00003 or better and are two standard errors of the running means. True reproducibility on the Rb and Sr isotopic ratios are better than 0.01%. The BPI $^{87}Sr/^{86}Sr$ value for E&A Sr standard is 0.70803. Repeat analysis of the NBS Sr carbonate standard SRM 987 at UCT is $^{87}Sr/^{86}Sr = 0.71005$. Reproducibility on the Sm and Nd ratios is taken as 0.006%, equivalent to an absolute error of better than 0.00003. The BPI value for the $^{143}Nd/^{144}Nd$ ratio in standard BCR-1 is 0.512645. BPI values for the La Jolla and Rhon basalt standards are 0.511837 and 0.512864, respectively. For UCT the $^{143}Nd/^{144}Nd$ value for the La

Jolla Nd isotopic standard is 0.51176. For Pb isotopes reproducibility is better than 0.05%. Repeated analyses of the common Pb NBS isotopic standard SRM981 were used to determine a correction factor (relative to the levels of Catanzaro et al., 1968) to counter the effects of mass fractionation. The mean standard values for the period of analysis (n=121) were: $^{206}Pb/^{204}Pb$ = 16.902 ± 0.016; $^{207}Pb/^{204}Pb$ = 15.449 ± 0.017; and $^{208}Pb/^{204}Pb$ = 36.570 ± 0.052.